Doctorate Program in Molecular Oncology and Endocrinology Doctorate School in Molecular Medicine

XXIII cycle - 2007-2010
Coordinator: Prof. Giancarlo Vecchio

"The emerging role of FKBP51 in melanoma: characterization of a promising molecular target for innovative therapies"

Simona Romano

University of Naples Federico II
Dipartimento di Biologia e Patologia Cellulare e Molecolare
"L. Califano"

Administrative Location

Dipartimento di Biologia e Patologia Cellulare e Molecolare "L. Califano"
Università degli Studi di Napoli Federico II

Partner Institutions

Italian Institutions
Università degli Studi di Napoli "Federico II", Naples, Italy
Istituto di Endocrinologia ed Oncologia Sperimentale "G. Salvatore", CNR, Naples, Italy
Seconda Università di Napoli, Naples, Italy
Università degli Studi di Napoli "Parthenope", Naples, Italy
Università del Sannio, Benevento, Italy
Università di Genova, Genoa, Italy
Università di Padova, Padua, Italy
Università degli Studi "Magna Graecia", Catanzaro, Italy
Università degli Studi di Firenze, Florence, Italy
Università degli Studi di Bologna, Bologna, Italy
Università degli Studi del Molise, Campobasso, Italy
Università degli Studi di Torino, Turin, Italy
Università di Udine, Udine, Italy

Foreign Institutions
Université Libre de Bruxelles, Brussels, Belgium
Universidade Federal de Sao Paulo, Brazil
University of Turku, Turku, Finland
Université Paris Sud XI, Paris, France
University of Madras, Chennai, India
University Pavol Jozef Šafàrik, Kosice, Slovakia
Universidad Autonoma de Madrid, Centro de Investigaciones Oncologicas (CNIO), Spain
Johns Hopkins School of Medicine, Baltimore, MD, USA
Johns Hopkins Krieger School of Arts and Sciences, Baltimore, MD, USA
National Institutes of Health, Bethesda, MD, USA
Ohio State University, Columbus, OH, USA
Albert Einstein College of Medicine of Yeshiwa University, N.Y., USA

Supporting Institutions
Associazione Leonardo di Capua, Naples, Italy
Dipartimento di Biologia e Patologia Cellulare e Molecolare "L. Califano", Università degli Studi di Napoli "Federico II", Naples, Italy
Istituto Superiore di Oncologia (ISO), Genoa, Italy
Istituto di Endocrinologia ed Oncologia Sperimentale "G. Salvatore", CNR, Naples, Italy

Italian Faculty

Giancarlo Vecchio, MD, Co-ordinator

Salvatore Maria Aloj, MD

Francesco Saverio Ambesi Impiombato, MD

Francesco Beguinot, MD

Maria Teresa Berlingieri, MD

Bernadette Biondi, MD

Francesca Carlomagno, MD

Gabriella Castoria, MD

Angela Celetti, MD

Lorenzo Chiariotti, MD

Vincenzo Ciminale, MD

Annamaria Cirafici, PhD

Annamaria Colao, MD

Sabino De Placido, MD

Gabriella De Vita, MD

Monica Fedele, PhD

Pietro Formisano, MD

Alfredo Fusco, MD

Michele Grieco, MD

Massimo Imbriaco, MD

Paolo Laccetti, PhD

Antonio Leonardi, MD

Paolo Emidio Macchia, MD

Barbara Majello, PhD

Rosa Marina Melillo, MD

Claudia Miele, PhD

Roberto Pacelli, MD

Giuseppe Palumbo, PhD

Silvio Parodi, MD

Nicola Perrotti, MD

Giuseppe Portella, MD

Giorgio Punzo, MD

Antonio Rosato, MD

Guido Rossi, MD

Giuliana Salvatore MD

Massimo Santoro, MD

Giampaolo Tortora, MD

Donatella Tramontano, PhD

Giancarlo Troncone, MD

Giuseppe Viglietto, MD

Mario Vitale, MD

Foreign Faculty

Université Libre de Bruxelles, Belgium
Gilbert Vassart, MD
Jacques E. Dumont, MD

Universidade Federal de Sao Paulo, Brazil
Janete Maria Cerutti, PhD
Rui Monteiro de Barros Maciel, MD PhD

University of Turku, Turku, Finland
Mikko Laukkanen, PhD

Université Paris Sud XI, Paris, France
Martin Schlumberger, MD
Jean Michel Bidart, MD

University of Madras, Chennai, India
Arasambattu K. Munirajan, PhD

University Pavol Jozef Šafàrik, Kosice, Slovakia
Eva Cellárová, PhD
Peter Fedoročko, PhD

Universidad Autonoma de Madrid - Instituto de Investigaciones Biomedicas, Spain
Juan Bernal, MD, PhD
Pilar Santisteban, PhD

Centro de Investigaciones Oncologicas, Spain
Mariano Barbacid, MD

Johns Hopkins School of Medicine, USA
Vincenzo Casolaro, MD
Pierre A. Coulombe, PhD
James G. Herman MD
Robert P. Schleimer, PhD

Johns Hopkins Krieger School of Arts and Sciences, USA
Eaton E. Lattman, MD

National Institutes of Health, Bethesda, MD, USA
Michael M. Gottesman, MD
J. Silvio Gutkind, PhD
Genoveffa Franchini, MD
Stephen J. Marx, MD
Ira Pastan, MD
Phillip Gorden, MD

Ohio State University, Columbus, OH, USA
Carlo M. Croce, MD
Ginny L. Bumgardner, MD PhD

Albert Einstein College of Medicine of Yeshiwa University, N.Y., USA
Luciano D'Adamio, MD
Nancy Carrasco, MD

"The emerging role of FKBP51 in melanoma: characterization of a promising molecular target for innovative therapies"

TABLE OF CONTENTS

LIST OF PUBLICATIONS

This dissertation is based upon the following publications:

Romano MF, Avellino R, Petrella A, Bisogni R, **Romano S**, Venuta S. *Rapamycin inhibits doxorubicin-induced NF-kappaB/Rel nuclear activity and enhances the apoptosis of melanoma cells.* **Eur J Cancer** 2004; 40: 2829-2836.

Avellino R, **Romano S**, Parasole R, Bisogni R, Lamberti A, Poggi V, Venuta S, Romano MF. *Rapamycin stimulates apoptosis of Childhood acute lymphoblastic leukemia cells.* **Blood** 2005; 106:1400-1406.

Giordano A, Avellino R, Ferraro P, **Romano S**, Corcione N, Romano MF. *Rapamycin antagonizes NF-kappaB nuclear translocation activated by TNF-alpha in primary vascular smooth muscle cells and enhances apoptosis.* **Am J Physiol Heart Circ Physiol** 2006; 290:H2459-65.

Romano MF, **Romano S**, Mallardo M, Bisogni R, Venuta S. *Rapamycin Controls Multiple Signalling Pathways Involved in Cancer Cell Survival.* **Trends in Cell Apoptosis Research**, ISBN 1-60021-424-X, Editor: Herold C. Figgins, 2006 Nova Science Publishers, Inc.

Giordano A, **Romano S**, Mallardo M, D'Angelillo A, Calì G, Corcione N, Ferraro P, Romano MF. *FK506 can activate transforming growth factor-beta signalling in vascular smooth muscle cells and promote proliferation.* **Cardiovasc Res** 2008; 79:519-26.

Romano S, Mallardo M, Chiurazzi F, Bisogni R, D'Angelillo A, Liuzzi R, Compare G, Romano MF. *The effect of FK506 on transforming growth factor beta signaling and apoptosis in chronic lymphocytic leukemia B cells.* **Haematologica** 2008; 93:1039-48.

Romano S, D'Angelillo A, Pacelli R, Staibano S, De Luna E, Bisogni R, Eskelinen EL, Mascolo M, Calì G, Arra C, Romano MF. *Role of FK506-binding protein 51 in the control of apoptosis of irradiated melanoma cells.* **Cell Death Differ** 2010; 17:145-57.

Romano S, D'Angelillo A, Staibano S, Ilardi G, Romano MF. *FK506-binding protein 51 is a possible novel tumoral marker.* **Cell Death Disease** 2010, 1, e55; doi:10.1038/cddis.2010.32; published online 15 July 2010.

Romano S, Di Pace AL, Sorrentino A, Bisogni R, Sivero L, Romano MF. *FK506 Binding Proteins as Targets in Anticancer Therapy*. **Anticancer Agents Med Chem.** Invited review, in press.

Romano S, Romano MF. *The emerging role of FK506 binding protein 51 in cancer.* **Curr Opin Drug Discov Devel.** Invited review, submitted.

ABSTRACT

Melanoma is a malignant skin cancer with high metastatic potential. The number of melanoma cases worldwide is increasing faster than any other cancer. The prognosis is bad in the advanced stages of the disease due to resistance to conventional anti-cancer treatments. Patients diagnosed with advanced stage melanoma continue to pose a significant challenge for clinicians. Although many therapeutic regimens for metastatic melanoma have been tested, very few achieve response rates greater than 25%. There is much hope for targeted therapies and promising agents include those that act on apoptosis-regulating molecules. Very recently, we have identified that an immunophilin, namely FK506 binding protein (FKBP) 51 controls response of melanoma to DNA damaging agents, such as anthracyclines compounds. The aim of this study was to investigate the possible role of FKBP51 in the control of response to ionizing radiation (IR) in malignant melanoma. FKBP51-silenced cells showed reduced clonogenic potential after irradiation compared with non-silenced cells. After IR, we observed apoptosis in FKBP51-silenced cells and autophagy in non-silenced cells. FKBP51 was required for the activation of Rx-induced NF-κB, which in turn inhibited apoptosis by stimulating X-linked inhibitor of apoptosis protein and promoting authophagy-mediated Bax degradation. Using a tumor-xenograft mouse model, the *in vivo* pretreatment of tumors with FKBP51-siRNA provoked massive apoptosis after irradiation. Immunohistochemical analysis of 10 normal skin samples and 80 malignant cutaneous melanomas showed that FKBP51 is a marker of melanocyte malignancy, correlating with vertical growth phase and lesion thickness. Moreover, we provided evidence that FKBP51 targeting radiosensitizes cancer stem/initiating cells. Finally, we expanded the study to other types of cancer, including ovarian, pancreatic, prostate, colon, breast and lung cancer and found a strong correlation between the protein expression and malignity of the tumoral lesions. In conclusion, our study identifies a possible molecular target for radiosensitizing therapeutic strategies against malignant melanoma and a potential novel tumoral biomarker.

BACKGROUND

FK506 Binding Proteins (FKBPs)

FKBP51 is a member of the FK506 binding proteins (FKBP), these proteins, together with cyclophilins (Cyp), belong to the family protein of immunophilins (Dornan J et al. 2003). FKBP derive their name by the ability to bind immunosuppressant agents like rapamycin and FK506 (Fischer G et Aumüller T. 2003). In addition to the capacity to bind to immunosuppressant drugs, immunophilins have another distinguishing property, namely peptidyl-prolyl cis-trans isomerase activity (PPIase) catalyzing the isomerization of peptidylprolyl imide bonds, from cis to trans, in protein substrates (Dornan J et al. 2003; Fischer G et al.2003) (Fig.1).
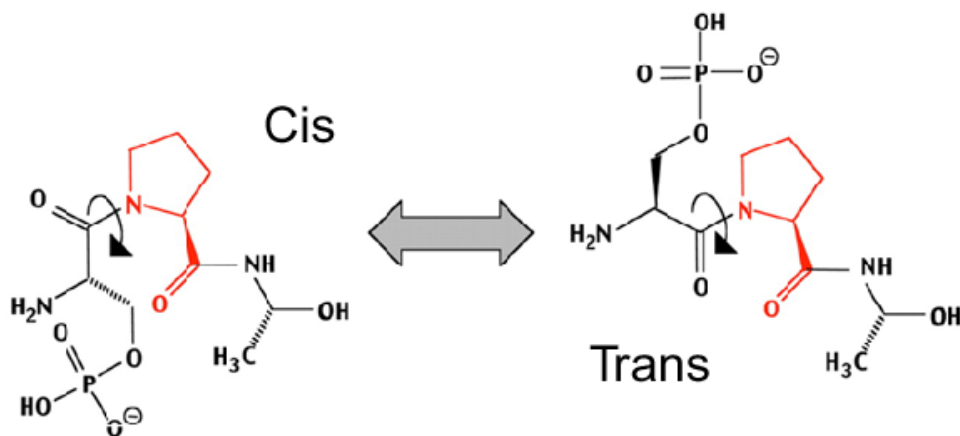
Fig.1. Peptidyl-prolyl cis-trans isomerase activity (PPIase). Immunophilins catalyze the isomerization of peptidyl-prolyl imide bonds, from cis to trans, in protein substrate. This activity can influence the function of different proteins, especially some kinases, making them more stable and improving their activity. Indeed, the straighter shape of the trans isomer leads to hydrogen intermolecular forces that make the isomer more stable, than the cis isomers.

In humans, at least 15 FKBPs have been identified and named to reflect their molecular weights (Somarelli JA et al. 2008). Family members of this ubiquitous enzyme class are found in abundance in virtually all organisms and subcellular compartments. Their amino acid sequences are highly conserved phylogenetically (Fischer G and Aumüller T. 2003). Organisms express many members of each family that encompass one or more PPIase domain, complemented with other functional polypeptide segments (Fig.2).

Fig.2. FKBPs domains. FKBP12 is the prototype FKBP containing only a single FK506-binding domain (FKBD) comprising 108 amino acids. FKBPs show structural similarity to that of FKBP12, but possess further domains involved in protein-protein interaction or tetratrico peptide repeat (TPR) motifs, nuclear signaling, calcium binding, protein trafficking, and ATP/GTP-binding sequences, explaining the wide variety of cellular functions these proteins exhibit.

These domains include tetratricopeptide repeat motifs involved in protein-protein interaction, EF-hand calcium-binding domain containing helix-loop-helix topology in which Ca^{2+} ions are coordinated within the loop, nucleic acid binding regions, transmembrane domain, and nuclear localization and endoplasmic reticulum signal sequences. These domains enable such proteins to perform a wide variety of cellular functions, including protein folding, improvement of kinase performance, receptor signaling, protein trafficking, and transcription (Dornan J et al. 2003; Fischer G and Aumüller T. 2003; Somarelli JA et al. 2008).

FKBP51 and its functions

Immune system

FKBP51 is an immunophilin physiologically expressed in T lymphocytes. This protein is capable of immunosuppression, mediated by calcineurin (CaN) inhibition, when complexed to FK506 (Baughman G et al. 1995). CaN is a Ca^{2+}/calmodulin-dependent serine-threonine phosphatase that regulates the clonal expansion of T cells, after stimulation by an antigen, through activation of the nuclear factors of activated T lymphocytes (NFAT). NFAT proteins are phosphorylated and reside in the cytoplasm in resting cells; upon stimulation, they are dephosphorylated by CaN, translocated to the nucleus, and become transcriptionally active (Hogan PG et al. 2003). The NFAT group of transcription factors regulates production of interleukin (IL) 2 and a number of T cell specific activators, leading to immune response.

Glucocorticoid response

FKBP51 is also part of the glucocorticoid receptor (GR) complex and regulates the response to these hormones. Glucocorticoids up-regulate the FKBP51 gene, whose product in turn reduces response to glucocorticoids, thereby providing a mechanism for desensitization of cells after an initial exposure to the hormone (Cheung J and Smith DF. 2000). Indeed, cortisol insensitivity is facilitated by a constitutive overexpression of FKBP51 (Cheung J and Smith DF. 2000). Increased intracellular FKBP51 protein expression is associated with particular single nucleotide mutations of the FKBP51 gene (Binder EB et al. 2004). This condition triggers adaptive changes in the glucocorticoid receptor and provokes alteration of the stress hormone-regulating hypothalamic-pituitary-adrenal axis, with implications for the psychic sphere (Binder EB et al. 2004). Genetic mutations leading to FKBP51

hyperexpression have been correlated with major depressive disorders (Binder EB et al. 2004).

Nervous system

In the nervous system, FKBP51 prevents clearance of tau protein by regulating its phosphorylation status (Jinwal UK et al. 2010). Tau is a highly soluble microtubule-associated protein, particularly abundant in neurons, that is important for the stability of axonal microtubules (Goedert M et al. 2000). FKBP51-mediated isomerization of tau reduces its phosphorylation pattern and prevents its clearance, which results in microtubule stabilization (Jinwal UK et al. 2010). By contrast, tau hyperphosphorylation leads to its abnormal buildup, with self-assembly of tangles of paired helical filaments and straight filaments (Alonso A et al. 2001). Accumulation of these aggregates, which have a neurotoxic effect, is a common feature for a group of diseases termed tauopathies, the most common being Alzheimer's disease (Goedert M et al. 2000; Alonso A et al. 2001).

NF-κB activation

FKBP51 isomerase activity is important for the enzymatic function of the inhibitor κB kinase (IKK) α (Boumeester T et al. 2004). The NF-κB transcription complex belongs to the Rel family, which comprises five mammalian Rel/NF-κB proteins: RelA (p65), c-Rel, RelB, NF-κB1 (p50/p105), and NF-κB2 (p52/100) (Ghosh S et al. 1998). The activity of NF-κB is controlled by cytoplasmic shuttling to the nucleus in response to cell stimulation. The NF-κB dimers containing RelA or c-Rel are retained in the cytoplasm through interaction with inhibitors (IκBs) (Baldwin AS Jr. 1996). In the canonical pathway of NF-κB activation, IKKα forms with IKKβ and a regulatory subunit of IKKα, namely NEMO, the IKK kinase complex, that mediates the phosphorylation of IκB proteins in response to various stimuli (Baldwin AS Jr. 1996). Phosphorylated IκBs create a recognition signal for ubiquitinating enzymes, which mark IκBs for rapid 26S proteasomal degradation (Baldwin AS Jr. 1996). This process allows p50/RelA dimers to translocate to the nucleus, where they stimulate the expression of multiple target genes involved in immune response, inflammation, cell survival, anti-apoptosis, and cancerogenesis (Ghosh S et al.1998; Karin M et al. 2002). IKKα also works independent of the IKK complex. This occurs, for instance, in the alternative NF-κB pathway, which results in activation of p52/RelB heterodimers (Xiao G et al. 2001). In this pathway, IKKα requires an

upstream kinase, namely NF-κB-inducing kinase (NIK), and induces phosphorylation of p100 to produce mature p52 (Xiao G et al. 2001). Furthermore, active IKKα phosphorylates CREB-binding protein (CBP) at serine 1482 and serine 1386. Such phosphorylation enhances NF-κB-mediated gene expression and suppresses p53-mediated gene expression, thereby promoting cell proliferation and tumor growth (Huang WC et al. 2007) (Fig.3).
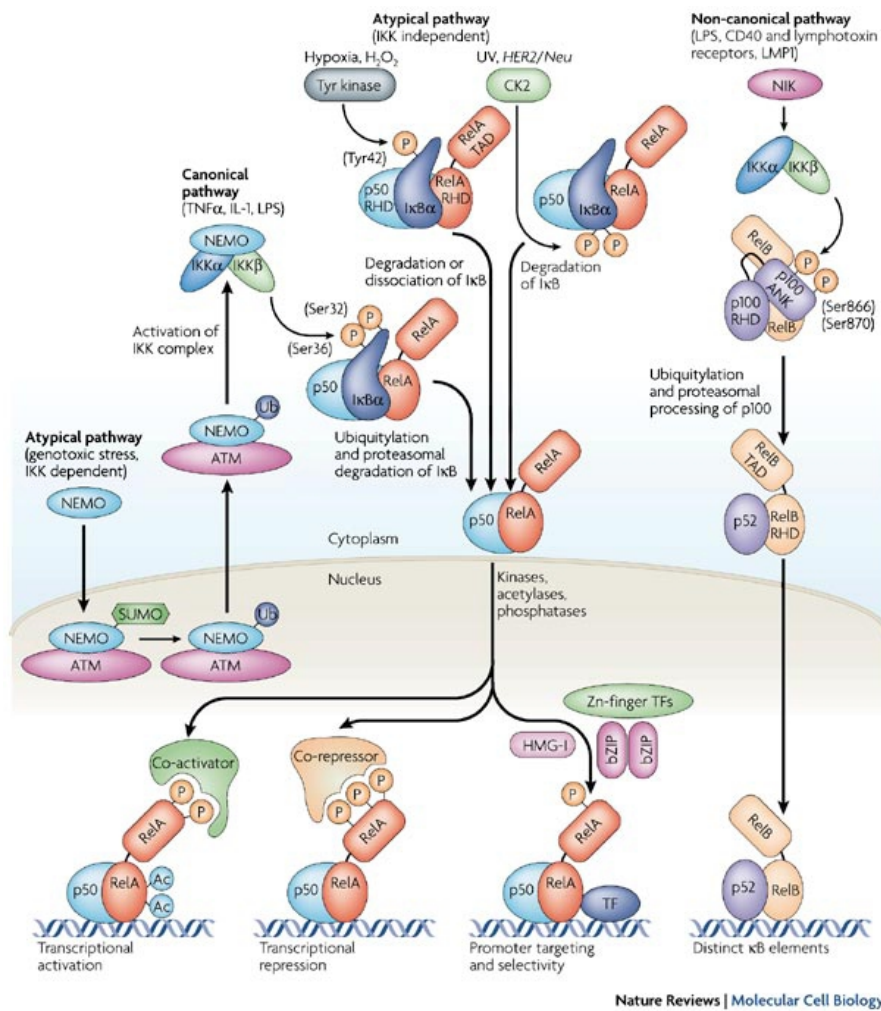
Fig.3. Schematic representation of the NF-κB activation pathways, namely canonical-, atypical- and non canonical- pathway (see text).

Role of FKBP51 in cell growth and malignant transformation

FKBP51 was first cloned in the mouse where it appeared to be restricted to T lymphocytes (Baugman G et al. 1995). Subsequent studies in humans confirmed that FKBP51 is abundantly expressed in T lymphocytes and is also expressed in several other tissues; although, it is not a uniform distribution (Baugman G et al. 1997). There is increasing evidence that enhanced expression of FKBP51 sustains cell survival and growth in both non neoplastic and neoplastic conditions. The FKBP51 homolog in Arabidopsis, PAS-1, plays a critical role in the growth and development of this organism (Vittorioso P et al. 1998). In mammals, FKBP51 has a specialized role during cell division and is preferentially expressed in mitotically active cells, in the very early phases of differentiation (Liu TM et al. 2007; Menicanin et al. 2009; Yeh WC et al. 1995). FKBP51 is among the top candidates genes expressed during early mesenchymal differentiation into the three mesodermal lineages namely osteogenesis/chondrogenesis/adipogenesis (Menicanin et al. 2009). At this stage, FKBP51 is co-expressed with ZNF145 (Menicanin et al. 2009). ZNF145 is a member of the Krueppel C2H2-type zinc-finger protein family, it encodes a zinc finger transcription factor that interacts with a histone deacetylase and is involved in cell cycle progression (Menicanin et al. 2009; Yeh WC et al. 1995; Zhang et al. 1999). Abnormal rearrangement of ZNF145, due chromosomal translocation t(11;17), causes acute promyelocytic leukemia (Zhang et al. 1999).

Myeloproliferative disorders

The concept that FKBP51 is an essential factor for cell proliferation is also supported by studies on myeloproliferative disorders (Komura E et al. 2003; Komura E et al. 2005; Giraudier S et al. 2002). FKBP51 is overexpressed in idiopathic myelofibrosis (Komura E et al. 2003), a chronic myeloproliferative disorder characterized by megakaryocyte hyperplasia and bone marrow fibrosis. Overexpression of FKBP51 in this disorder regulates the growth factor independence of megakaryocyte progenitors and induces an apoptotic resistance to cytokine deprivation mediated by the JAK/STAT5 pathway (Komura E et al. 2003). It has been shown that STAT5 is dephosphorylated on tyrosine residues more slowly in an FKBP51-overexpressing cell line. This condition sustains cell survival mechanisms, as suggested by the pro-apoptotic effect of a dominant negative variant of STAT5. The high pSTAT5 levels are, in turn, sustained by persistent JAK2 phosphorylation. The spontaneously megakaryocyte growth was abolished by the JAK2 inhibitor AG490.

Furthermore, FKBP51 overexpression promotes fibrosis, that is mediated by upregulation of TGF-α synthesis (Komura E et al. 2005).

Glioma

Enhanced FKBP51 expression is associated with apoptosis resistance and enhanced proliferation in gliomas (Jiang W et al. 2008). A study of specimens from 192 patients, including glioblastoma multiforme, oligodendrogliomas, astrocytomas, and mixed gliomas, showed the FKBP51 expression level correlated with grading (Jiang W et al. 2008). The study of patient survival showed that the expression of FKBP51 correlated with overall glioblastoma patient survival rates; that is, the glioblastoma patients with high levels of FKBP51 had shorter survival than those with intermediate levels (Jiang W et al. 2008). Moreover, using both hyperexpression and knock-down approaches, it was shown that FKBP51 proliferative and anti-apoptotic properties in gliomas were mediated by NF-κB activation (Jiang W et al. 2008).

Prostate cancer

In prostate cancer, FKBP51 is upregulated in association with cyclophilin Cyp40 (Periyasamy S et al. 2010). In androgen-dependent tumor cell lines of prostate cancer, FKBP51 hyperexpression increased androgen receptor transcriptional activity in the presence and absence of androgens; whereas, knockdown of FKBP51 dramatically decreased androgen dependent gene transcription and proliferation. In androgen-independent prostate cancer, FKBP51 was also hyperexpressed (Periyasamy S et al. 2010). Most intriguingly, a very recent paper implicates IKKα in the androgen independent growth of prostate cancer (Ammirante M et al. 2010).

FKBP51 is an important molecular determinant in the anticancer activity of rapamycin

In a previous study our laboratory provided evidence supporting the involvement of FKBP51 in the resistance to cancer therapies through mechanistic studies of the antitumor activity of rapamycin (Avellino R et al. 2005; Romano MF et al. 2004). Rapamycin is a conventional immunosuppressant agent with anticancer properties (Sabatini DM. 2006). Both immunosuppression and anticancer effects of rapamycin are classically ascribed to inhibition of the mammalian target of rapamycin (mTOR) (Sabatini DM 2006), which is the core of an evolutionarily conserved signaling pathway

that controls the cell cycle in response to changing nutrient levels (Schmelzle T and Hall MN. 2000). The rapamycin/FKBP complex interacts with the FKBP-rapamycin binding domain in mTOR, adjacent to the catalytic kinase domain, and blocks its function (Choi J et al. 1994). mTOR is a member of the ataxia-telangiectasia-mutated (ATM) family of kinases that functions as a checkpoint for nutritional status in G1 (Brown EJ et al. 1994). It is a downstream protein in the phosphatidylinositol 3 kinase (PI3k), protein kinase B (PkB or Akt) signaling pathway (Burgering BM and Coffer PJ. 1995; Gao X and Pan D. 2001). Many genomic aberrations in human cancers result in activation of this pathway, which alters the control of survival and leads to defective apoptosis (Hennessy BT et al. 2005). Generally, such genomic aberrations involve deletions of the tumor suppressor gene PTEN, the inositol 3-phosphatase and tensin homologue, which dephosphorylates phosphoinositides at the D3 position, thereby terminating the PI3k/Akt cascade (Wu X et al. 1998). A number of rapamycin analogs have been developed over recent years and have shown antitumor activity across a variety of human cancers in clinical trials (Sabatini DM. 2006).

However, our recent studies identify FKBP51 as an additional important molecular determinant of the drug's anticancer activity (Avellino R et al. 2005; Romano MF et al. 2004; Jiang W et al. 2008). In a study conducted in melanoma, a tumor in which PTEN is often mutated (Wu H et al. 2003), we found that rapamycin markedly enhanced doxorubicin-induced apoptosis (Avellino R et al. 2005). However, contrary to expectations, the apoptosis sensitizing effect of rapamycin appeared to be independent of blockage of the PI3k/Akt/mTOR pathway and was instead associated with inhibition of NF-κB signalling. Rapamycin, but not wortmannin, a PI3k inhibitor, induced a block of the IKK kinase phosphorylating ability (Avellino R et al. 2005). The effect of rapamycin on NF-κB was reproduced using FKBP51 siRNA, which depleted the cell of this protein. In accordance, the NF-κB regulated genes, Bcl-2 (Catz SD and Johnson JL. 2001) and c-IAP1 (Wu MX et al. 1998), were decreased; these genes have been implicated in tumor cell resistance to doxorubicin (Lopez de Menezes DE et al. 2003; Vaziri SA et al. 2003). The finding that rapamycin can sensitize cancer cells to apoptosis, independent of mTOR inhibition, was confirmed by our laboratory in childhood acute lymphoblastic leukemia (ALL) (Avellino R et al. 2005). This cancer comprises a heterogeneous variety of subtypes. In most of these leukemias, blasts are sensitive to the apoptosis-inducing effect of rapamycin because of constitutive activation of the PI3k/Akt pathway, which sustains blast survival (Watowich SS et al. 1996). Rapamycin increased doxorubicin-induced cell death, even in samples that did not respond to PI3k inhibition, while wortmannin was unable to cooperate with the anthracycline drug. The apoptosis sensitizing effect of

rapamycin was counteracted by hyperexpression of the NF-κB RelA subunit in leukemic cells (Avellino R et al. 2005). Increased cytotoxicity to doxorubicin was observed in leukemic cells depleted of FKBP51 (Romano MF et al. 2004). These results support the conclusion that rapamycin may also be effective against neoplasias that express the tumor suppressor PTEN. Consistent with this conclusion, we found rapamycin retained the capacity to cooperate with NF-κB-inducing chemotherapeutics in PTEN reconstituted tumors (Romano MF et al. 2004).

Melanoma

Melanocytes exert a protective role against UV radiation for the skin, by distributing pigment from melanosomes to keratinocytes. Cutaneous melanoma arises from uncontrolled proliferation of melanocytes, melanin-producing cells, located in the basal layer of the epidermis (Chin L. 2003). Melanoma can also occur in the eye (ocular), meninges and digestive tract and is the most aggressive form of skin cancer, surpassing most solid tumors in terms of metastatic potential. The incidence of this tumor is increasing. Melanoma pathogenesis is driven by both genetic and environmental risk factors. Its incidence is influenced by skin pigmentation, sun-exposure history and geographical location. Melanoma progression can begin with the development of either dysplastic or benign nevi (common acquired or congenital) (Chin L. 2003). These can then progress to the radial growth phase, in which the growth expands laterally, but remains localized to the epidermis. At this phase, cells are still dependent on growth factors, and are not anchorage independent or tumorigenic. Progression to the vertical growth phase is hallmarked by invasion into the dermis, subcutaneous tissue and upper epidermis. In the vertical growth phase, cells are no longer growth factor dependent, are anchorage independent and presage distal metastasis (Fig.4).
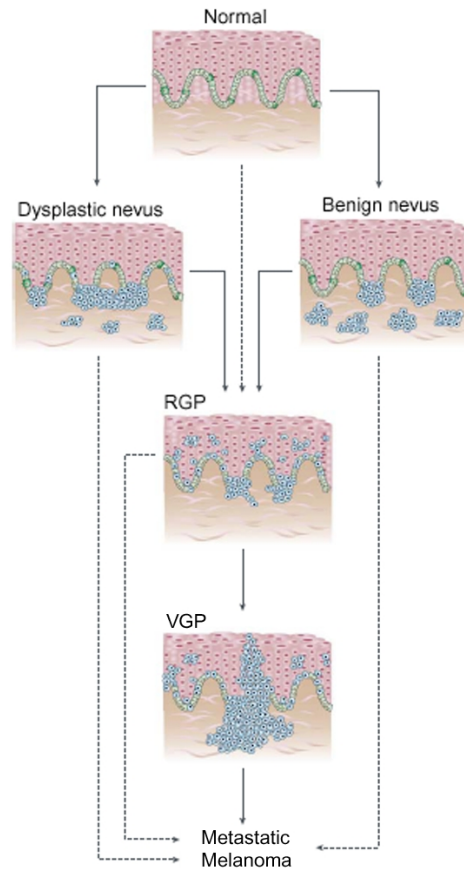
Fig.4. Schematic representation of melanoma progression stages. Melanocytes are pigment-synthesizing cells that are normally confined to the basal layer of the epidermis. These cells, by sending out arborizing dendritic processes, contact keratinocytes in basal and superficial layers of the skin, thus forming an epidermal melanin unit. Once within the keratinocytes, the pigment protects the skin by absorbing and scattering harmful solar radiation. Five distinct stages have been proposed in the evolution of melanoma on the basis of its histological location and stage of progression: common acquired and congenital nevi without dysplastic changes; dysplastic nevi with structural and architectural atypia; radial-growth phase (RGP) melanoma; vertical-growth phase (VGP) melanoma; and metastatic melanoma. Both benign and dysplastic nevi are characterized by disruption of the epidermal melanin unit, leading to increased numbers of melanocytes in relation to keratinocytes. These precursor lesions progress to in situ melanoma, which grow laterally and remain largely confined to the epidermis, so this stage is defined as the RGP melanoma. This is in contrast to the VGPmelanoma, which both invades the upper layer of the epidermis and beyond, and penetrates into the underlying dermis and subcutaneous tissue through the basement membrane, forming expansile nodules of malignant cells. The transition from RGP toVGP is the crucial step in the evolution of melanoma that presages the acquisition of metastatic potential and poor clinical outcome. Consistent with that, the total thickness/height of a primary melanoma lesion is still one of the most predictive parameters for metastatic disease and adverse clinical outcome (Chin L. 2003).

Clinical staging of melanoma progresses from an *in situ* growth to one increasing in thickness and vertical invasion, to regional lymph-node spread and, finally, to distal metastasis. Vertical invasion may be representative of the degree of progression and is often measured by the Breslow thickness, a measure of the thickness of the tumor from the upper layer of the epidermis to the innermost depth of invasion (Balch CM et al. 2001). The prognosis is bad in advanced stages of melanoma because of resistance to conventional anticancer treatments and the high metastatic potential of this tumor. Moreover, melanoma can remain quiescent for years after resection of primary tumor and then recur; recurrences are due both to local persistence of malignant cells, after surgical resection, and to micro metastases derived from lymphatic or hematogenous dissemination (Norris LB and Beam S. 2008). Currently, no efficient therapeutic strategies are available to control the advanced disease.

The use of radiotherapy, the most common antitumor treatment, is controversial for advanced melanoma; it serves mainly as a palliative treatment because of the tumor's radioresistance. The response to ionizing radiation involves DNA damage recognition, repair, and the induction of signaling cascades leading to cell cycle checkpoint activation and stress-related responses. (Dewey WC et al. 1995; Wallace SS. 1994). Apoptosis is a common biological mechanism for eliminating damaged cells involving the activation of enzymes known as caspases, and leading to endonuclease-mediated internucleosomal fragmentation of DNA (Hengartner MO. 2000) (Fig.5).
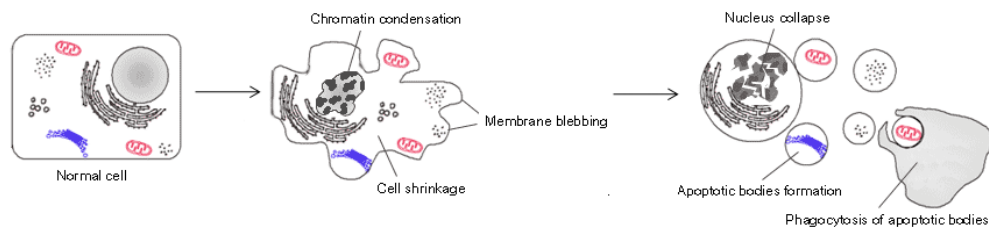
Fig.5. Apoptosis. Apoptosis is a common biological mechanism for eliminating damaged cells involving the activation of enzymes known as caspases, and leading to endonuclease-mediated internucleosomal fragmentation of DNA.

Stress-inducing agents are able to activate also autophagy, namely type II cell death (Elliott A and Reiners Jr JJ. 2008; Ogata M et al. 2006). Autophagy is a process of intracellular bulk degradation in which cytoplasmic components, including organelles, are sequestered within double-membrane vesicles that deliver the contents to the lysosome/vacuole for degradation (Eskelinen EL. 2008) (Fig.6).
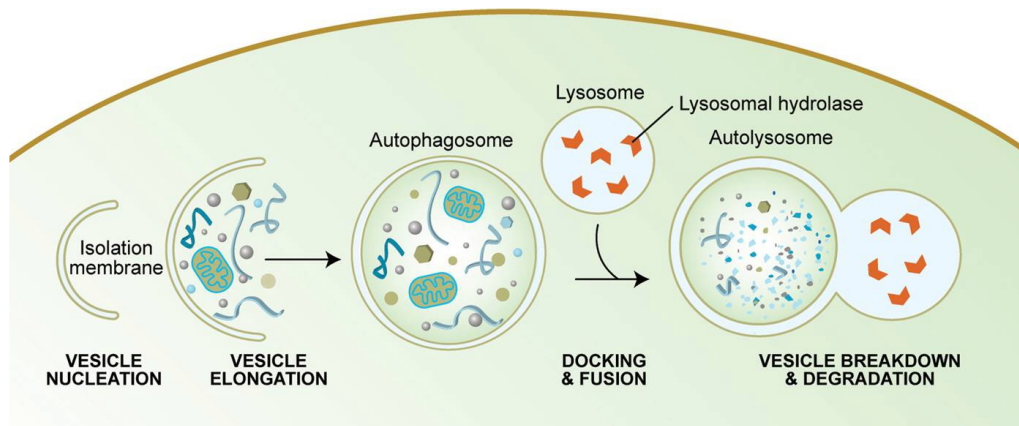
Fig.6. Autophagy. Autophagy is a process of intracellular bulk degradation in which cytoplasmic components, including organelles, are sequestered within double-membrane vesicles that deliver the contents to the lysosome/vacuole for degradation.

It is controversial whether this recently discovered process causes death or, instead, protects cells (Baehrecke EH. 2005). Indeed, the products derived from autophagy are recycled to maintain essential cellular processes. However, there are several lines of evidence that support a role for autophagy in increasing the threshold for apoptosis, thereby sustaining cell survival under conditions of stress (Mathew R et al. 2007).

Activated NF-κB is one of the pathways responsible for the radioresistance of melanoma cells and strategies for inhibiting its influence are proven to be useful in restoring the radio-response of melanomas (Munshi A et al. 2004). FKBP51 involvment in control of NF-κB activation supports a role for this protein in promoting radio-resistance.

AIM OF THE STUDY

Aim of this study was to investigate the role of FKBP51 in the control of response to ionizing radiation (IR) of malignant melanoma. In this regard, the present study was focussed on characterization of the role of FKBP51 in IR-activation of NF-κB signaling, and cell death pathways termed apoptosis, or programmed cell death type 1 and autophagy, or programmed cell death type 2. A further purpose was to investigate expression, in primary melanoma samples, of FKBP51, whose expression is highly increased in melanoma cell lines, to find out eventual association with prognostic factors. Finally, study of FKBP51 expression was extended to a variety of human tumors, to find out eventual protein deregulation. Results from this study identify a candidate target for radio-sensitizing strategies against malignant melanoma and a potential novel tumoral biomarker.

MATERIALS AND METHODS

Cell culture

The melanoma cell line SAN (Romano MF et al. 2004; Benassi B et al. 2007) was established from a patient's tumor lymphonodal metastasis and was provided by Dr. Gabriella Zupi (Experimental Preclinic Laboratory, Regina Elena Institute for Cancer Research, Roma, Italy). Cells were cultured in RPMI 1640 medium (Lonza, Belgium) supplemented with 10% heat-inactivated fetal bovine serum (FBS), 200mM glutamine, and 100 U/ml penicillin-streptomycin (Lonza) at 37°C in a 5% CO_2 humidified atmosphere. The melanoma cell lines G361 and SK-MEL-3 (Trotta PP et al. 1987) (derived from a primary tumor and a lymphonodal metastasis, respectively) were cultured in McCoy's modified medium (Sigma Aldrich, Saint Louis, MO, USA) supplemented with 10% heat-inactivated FBS, 200mM glutamine and 100 U/ml penicillin-streptomycin at 37°C in a 5% CO_2 humidified atmosphere. The melanoma cell line A375 (Giard DJ et al. 1973) derived from a metastatic tumor, was cultured in Dulbecco's Modified Eagle's Medium (Lonza) supplemented with 15% heat-inactivated FBS, 200mM glutamine, and 100 U/ml penicillinstreptomycin at 37°C in a 5% CO_2 humidified atmosphere. G361, SK-MEL-3, and A375 were kindly provided by Dr. Rosella Di Noto (CEINGE, Naples, Italy).

Cell transfection

At 24 h before transfection, cells were seeded into six-well plates at a concentration of $2x10^5$ cells/ml to obtain 30-60% confluence at the time of transfection. Then, the cells were transfected with specific short interfering oligoribonucleotide (siRNA) or with a non-silencing oligoribonucleotide (NS RNA) as control, at a final concentration of 50 nM using Metafectene (Biontex, Munich, Germany) according to the manufacturer's recommendations. NS RNAs and siRNAs corresponding to human cDNA sequences for FKBP51, FKBP12, RelA, xIAP, and Becn-1 were purchased from Qiagen (Germantown, Philadelphia, PA, USA) (Romano S et al. 2010). For over-expressing Becn-1, cells were transfected with a pEGFP-N1 vector carrying Becn-1 (kind gift of Dr. Sharon Tooze, London Research Institute, Lincoln's Inn Fields Laboratories, London, UK), and with a pEGFP-N1 vector as control. At 48 h after transfection, cells were irradiated with a 6 MV X-ray

of a linear accelerator (Primus, Siemens, München, Deutschland) and processed according to the different experimental procedures.

Clonogenic assay

This assay was performed as described earlier (Franken NAP et al. 2006) Briefly, melanoma cells, not transfected and transfected with FKBP51 siRNA or with NS RNA, were irradiated at IR doses between 1 and 8 Gy, harvested and plated in triplicate at a density of 500 cells/plate. After 10 days, the formed colonies were stained with crystal violet and counted. The mean colony count was calculated for each treatment (both IR dose and type of cell transfection). The number of colonies in the irradiated dishes was divided by the number of colonies in the non-irradiated dishes and expressed as a percentage. The graph of percent survival (y axis) against IR dose (x axis) was performed in semilogarithmic scale.

Cell lysates, western blot and immunoprecipitation assay

Whole cell lysates were prepared by homogenization in modified RIPA buffer. For phospho-IκBα, IκBα and IκBβ detection, cytosolic extracts were obtained from cells resuspended in a different lysing buffer (Romano S et al. 2010). Cell debris was removed by centrifugation. Protein concentration was determined using the Bradford protein assay. Cell lysates were equalized for total protein, run in 10–14% SDS in polyacrylamide gel electrophoresis (PAGE) and transferred onto a methanol-activated polyvinylidene difluoride membrane (Millipore, Tokyo, Japan), which was incubated with the primary antibody. The goat polyclonal antibodies against FKBP51, FKBP12, and Actin (Santa Cruz Biotechnology, Santa Cruz, CA, USA); the rabbit polyclonal antibodies against Becn-1, phospho-IκBα (Ser 32) IκBα, IκBβ (Santa Cruz Biotechnology), LC3 (Novus Biologicals, Littleton, CO, USA), caspase-7 (Sigma, Saint Louis, MO, USA), and cleaved caspase-3 (Cell Signaling, Danvers, MA, USA) were used diluted 1:500. The mouse monoclonal antibodies against caspase-3 (specific for both pro-caspase and cleaved caspase-3) (Sigma Aldrich), xIAP (Stressgene, San Diego, CA, USA) and Bax (Santa Cruz Biotechnology) were used diluted 1:1000. The blots were developed with an electrochemiluminescence system (ECL) (GE Healthcare-Amersham, Buckinghamshire, UK). For immunoprecipitation assay, whole cell lysates were prepared by melanoma cells not irradiated and 3h after irradiation with 4 Gy. After obtaining a homogeneous suspension, protein concentration was determined using the Bradford method and 500 μg of protein extract were precleared for 1 h. For immunoprecipitation, 15 μg anti-

FKBP51 (rabbit polyclonal, H100) or anti-IKKα/β (rabbit polyclonal, N-19) (Santa Cruz Biotechnology, CA, USA) were added together with 25 µl of protein A/G-Sepharose (Santa Cruz Biotechnology) and precipitation took place overnight with rotation at 4°C. Immunoprecipitated and whole cell lysates were then separated by 14% SDS-PAGE and subjected to immuno-blot with goat polyclonal anti-FKBP51 (F-13), or the rabbit anti-IKKα/β.

Transmission electron microscopy

Melanoma cells, not transfected or transfected with Becn-1 siRNA, or with NS RNA, were irradiated at 4Gy, harvested after 6 h from IR and plated on 60 mm dishes. At 30-50% confluence, the cells were fixed with 2% glutaraldehyde in 0.2M Hepes, pH 7.4, at room temperature for 30 min. The cells were scraped and pelleted, and the fixation was continued for 2 h. The cells were then dehydrated in ethanol and embedded in epoxy resin. Thin sections were cut and stained with uranyl acetate and lead citrate, and examined under a Jeol JEM1200 EX2 Transmission Electron Microscope (Jeol, Tokyo, Japan).

Nuclear exstracts, EMSA and oligonucleotides

Cell nuclear extracts were prepared following the procedure thoroughly described (Romano S et al., 2010). Protein concentrations were determined using the Bradford method. The NF-κB oligonucleotide (Wallace SS. 1994) was end-labeled with [γ^{32}P] ATP using a polynucleotide kinase (Roche, Basel, Switzerland). End labeled DNA fragments were incubated at room temperature for 20 min with 5 µg of nuclear protein, in the presence of an incubation mixture (Romano S, 2010). In supershifting experiments, rabbit antibodies against p105/p50, p65, cRel, RelB (Santa Cruz Biotechnology), and against p52 (kindly provided by Professor Shao-Cong Sun, Department of Microbiology and Immunology, Pennsylvania State University College of Medicine, Hershey, PA, USA) were added to the incubation mixture. In competition assays, a 50x molar excess of NF-κB, or NFAT cold oligo, was added to the incubation mixture. Protein-DNA complexes were separated from the free probe on a 6% polyacrylamide (w/v) gel run in 0.25x Tris Borate EDTA buffer at 200 mV for 3 h at room temperature. The gels were dried and exposed to X-ray film (Fuji film, L.E.P., Naples, Italy).

Analysis of apoptosis

Caspase-3 and -9 activity was determined using the Carboxyfluorescein Fluorochrome Inhibitor of Caspases Assay (FLICA) Kits (B-Bridge International, San Jose, USA,) according to the instructions of the manufacturer. Cells are permeable to the fluorochrome inhibitor that binds covalently to the activated caspase, thereby inhibiting enzymatic activity. Cells were analyzed by flow cytometry and the green fluorescent signal was a direct measure of the number of active caspases (Romano S et al. 2010). Phosphatidylserine externalization, investigated by annexin V staining, and analysis of DNA content by propidium iodide incorporation were performed by flow cytometry. The peptide caspase-3 inhibitor Z-Asp-Glu-Val-Asp fluoromethyl ketone (Z-DEVD-fmk) was purchased by Sigma Aldrich.

Real-time PCR

Total RNA was isolated by Trizol (Invitrogen, Carlsbad, CA, USA) from melanoma cells harvested 6 h after IR, and from peripheral blood lymphocytes (PBLs), according to the instructions of the manufacturer. From paraffinized tumors RNA was isolated using the High Pure RNA Paraffin Kit (Roche Diagnostics GmbH, Mannheim, Germany) according to the manufacturer's instructions. In all samples, a total of 1 µg of each RNA was used for cDNA synthesis with Moloney Murine Leukemia Virus Reverse Transcriptase (Invitrogen). Gene expression was quantified by real-time PCR using the iQSYBR Green Supermix (Biorad, Hercules, CA, USA) and specific real-time-validated QuantiTect primers for Bax, Becn-1, and XIAP (Qiagen) and specific primers for β-actin (Fw 5'CGACAGGATGCAGAAGGAGA3';Rev5'CGTCATACTCCTGCTTGCTT GCTG3') and FKBP51 (Fw 5'GTGGGGAATGGTGAGGAAACGC3'; Rev 5'CATGGTAGCCACCCCAATGTCC3'). Relative quantitation of each transcript across multiple samples was performed by using a coamplified β-actin internal control for sample normalization. For paraffinized tumors RNA the values of each sample were compared to PBL (expression=1) for an estimate of the relative expression change fold of FKBP51.

Confocal microscopy

Cells were fixed, permeabilized and incubated with mouse monoclonal anti-Bax (Santa Cruz Biotechnology) and rabbit polyclonal LC3 (Novus Biologicals), diluted 1:40 in PBS 0.5% BSA for 1 h in a humidified atmosphere. The cells were then extensively washed in PBS before staining

with secondary goat anti-mouse Alexa Fluor 546 and anti-rabbit Alexa Fluor 488 (Molecular Probe, Invitrogen Corporation, Carlsbad, CA, USA). Nuclei were counterstained with Hoechst 33258 and the cells were mounted on glass slides with PBS containing 50% glycerol. The analysis of immunofluorescence was performed with a confocal laser scanner microscopy Zeiss 510 LSM (Carl Zeiss Microimaging GmbH, München, Germany), equipped with Argon ionic laser (Carl Zeiss Microimaging GmbH, München, Germany) (Romano S et al. 2010). Images for the double-staining immunofluorescence were acquired by sequential scanning to eliminate the cross talk of chromophores in the green and red channels and then saved in TIFF format to prevent the loss of information. They had been acquired with a resolution of 1024x1024 pixel with the confocal pinhole set to one Airey unit.

Cell sorting and immunostaining of ABCG2$^+$cells

SAN melanoma cells were incubated with a monoclonal antibody against human ABCG2-pycoerythrin (PE) conjugated (R&D Systems, Minneapolis, MN, USA). Briefly, cells were fixed, and intracellular indirect immunostaining was performed with anti-FKBP51 (H-100) (Santa Cruz Biotechnology) and a secondary fluorescein isothiocyanate (FITC)-conjugated antibody. Expression of FKBP51 in both ABCG2$^+$ and ABCG2$^-$ cells was analyzed in flow cytometry by using the ABCG2-PE/SSc gating strategy. For the immunohistochemistry of ABCG2$^+$ cells, these were sorted from the whole cells of the melanoma cell line SAN with a BD FACSAria (BD Biosciences). The ABCG2$^+$ population was >77% in purified cells. The sorted cells were immediately fixed, deposited on a slide (Cytoslide Shandon, Waltham, MA, USA) by spinning in a cytocentrifuge (Cytospin 3, Shandon) and subjected to FKBP51 immunohistochemical staining.

Immuhistochemistry

Serial sections of 4-mm thickness from routinely formalin-fixed, paraffin-embedded blocks were cut for each case of cutaneous malignant melanoma (CMM), breast, lung, prostate, ovary, pancreas and colon cancer and relative normal tisuues. Section were then mounted on poly-l-lysine-coated glass slides, as described earlier (Giard DJ et al. 1973). Briefly, deparaffinized sections were incubated with the anti-FKBP51 primary antibody (F-13; Santa Cruz Biotechnology) diluted 1:50 overnight at 4°C. The standard streptavidin-biotin-peroxidase complex technique was performed. Hematoxylin was used for nuclear counterstaining. Only cells with a definite brown cytoplasmatic immunostaining were judged as positive for FKBP51 antibody. The

immunohistochemical expression of FKBP51 in CMM was evaluated semiquantitatively as the percentage of positive tumor cells among the total melanoma cells present in at least 10 representative fields and scored according to an arbitrary scale (Staibano et al. 2005) as follows: 0 (no immunopositive cells); + (<5% of positive cells); ++ (5<25% of positive cells); +++ (>25% of positive cells).

Animal studies

SAN melanoma cells, 3×10^6 in a volume of 100 µl PBS, were injected s.c. into one flank of 24 6-week-old athymic nu/nu mice (Charles RiverLaboratory, Wilmington, MA, USA). Mice were maintained under specific pathogen free conditions in the Laboratory Animal Facility of the National Cancer Institute, G Pascale Foundation, Naples, Italy. All studies were conducted in accordance with Italian regulations for experimentations on animals. Mice were observed daily for the visual appearance of tumors at the injection sites. Tumor diameters were measured using calipers and calculated as the mean value between the shortest and the longest diameters. When tumors reached ~10mm in mean diameter, mice were subjected to a single intratumor injection of FKBP51 siRNA, or NS RNA, subjected to tumor irradiation and killed 24 or 48 h after irradiation (Romano S et al. 2010). Each tumor was divided into two parts: one portion was formalin-fixed and paraffinembedded for immunohistochemistry and the other was processed for the preparation of whole cell lysates. For immunohistochemical assays, 5-mm-thick paraffin-embedded sections were incubated with a rabbit polyclonal antibody against cleaved caspase-3 (Asp175) (Cell Signaling) or isotype-matched control antibody. Lysates of excised tumors were prepared by homogenization in modified RIPA buffer in a Dounce Homogenizer (Romano S et al. 2010). Samples were equalized for total protein and run in SDS-PAGE electrophoresis. Western blot filter was incubated with the rabbit polyclonal antibody for cleaved caspase-3 (Asp175) (Cell Signaling).
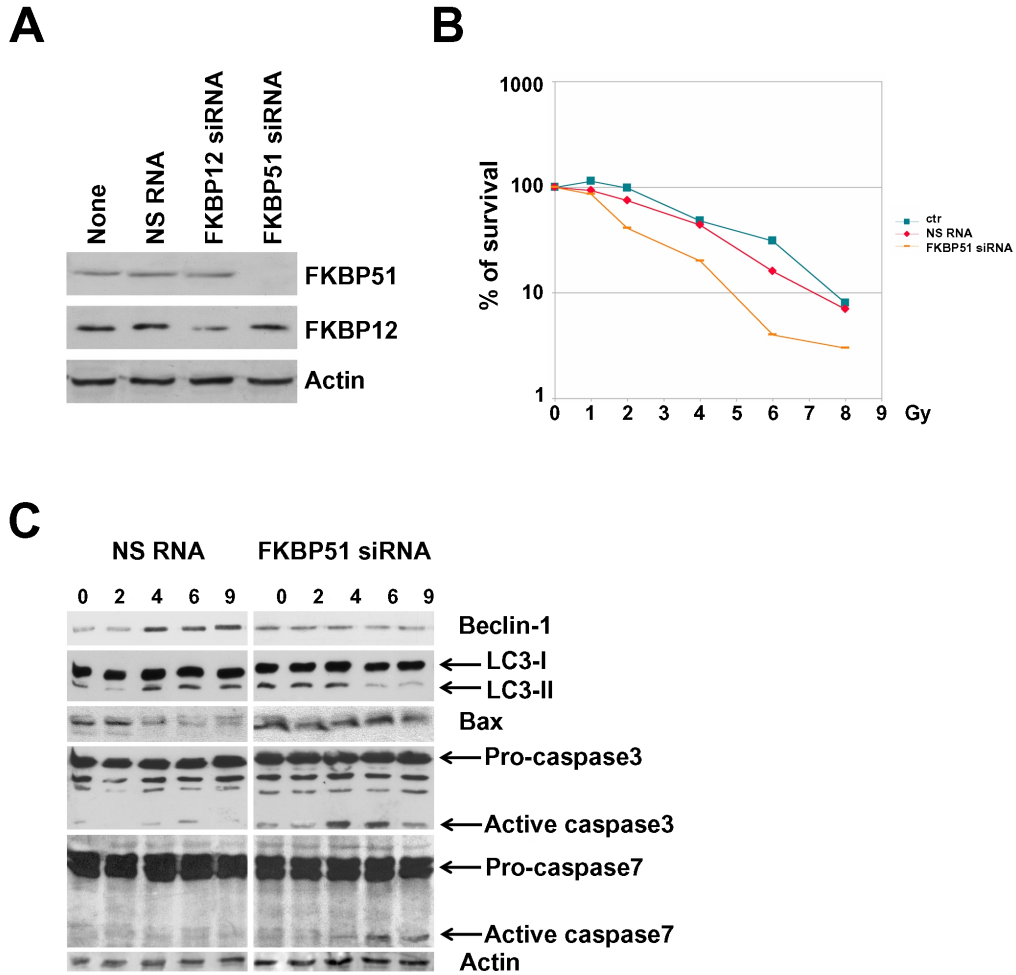
Statistical analysis

The results reported are the mean and standard deviation of independent experiments. The statistical significance of differences between means was estimated using Student's t-test. The χ^2-test was used to assess the difference between categorical variables. The Spearman's rank correlation coefficient was used for non-parametric data. Values of $P \leq 0.05$ were considered statistically significant. The statistical analysis was performed using the SPSS statistical package (SPSS Inc., Chicago, IL, USA).

RESULTS

FKBP51 downmodulation sensitizes melanoma cells to IR-induced apoptosis

In order to investigate the role of FKBP51 in the cellular response to ionizing radiations (IR), melanoma cells were transfected with a short interfering (si) RNA. Such siRNA was previously (Romano MF. 2004) shown to efficiently downmodulate the protein and to be specific for FKBP51, since other FKBP expression levels were not affected (Romano S et al. 2008). In Figure 7, representative results of the effect of FKBP51 gene silencing in the SAN melanoma cell line are shown. The specificity of the downmodulating effect of FKBP51 siRNA was also shown (Fig.7A). A clonogenic assay was performed using cells transfected with FKBP51 siRNA, non-silencing (NS) RNA, or nothing. Melanoma cells, knocked down for FKBP51, showed a sensitizing enhancement ratio (Chen AY et al. 1997) of 1.5 (7.2 Gy/4.8 Gy). This ratio was calculated on the basis of the radiation dose necessary to obtain the end point of a 90% inhibition of colony formation. As shown in figure 7B, the line corresponding to 10% survival intercepts the dose response curve of control cells (not transfected or transfected with NS RNA) at 7.2 Gy, whereas that of FKBP51-depleted cells occurred at 4.8 Gy. This result suggests that decreased levels of FKBP51 remarkably increase the cytotoxic effect of radiation in melanoma cells. To investigate the cellular response to Rx in cells depleted of FKBP51, we investigated by western blot hallmarks of autophagy (Kabeya Y et al. 2000) and apoptosis (Hengartner MO. 2000), in particular the autophagic protein Beclin-1 (Becn-1), the light chain 3 (LC3)-I to LC3-II conversion, the pro-apoptotic protein Bax and the active fragments of caspase 3 and 7. Whole cell lysates were prepared from cells transfected with the specific siRNA or NS RNA. At 48 h after transfection, cells were exposed to 4Gy dose of IR and harvested at 0, 2, 4, 6, and 9 h. Figure 7C shows the presence of the autophagosome membrane recruited LC3-II isoform in non-irradiated cells, both transfected and not transfected with FKBP51 siRNA, which is consistent with a basal level of autophagy. The isoform disappeared 6 h after IR exposure in FKBP51-depleted cells, but not in NS RNA-transfected cells. An increase in Becn-1 levels was detected in non-silenced cells after 4 h, suggesting that this increase had a role in sustaining the LC3-I to LC3-II conversion. In contrast, the appearance of the active fragment of the execution caspases-3 and -7 (Chandler JM et al. 1998) in FKBP51-depleted cells, as early as 4 h after IR exposure, suggests the activation of apoptosis. Interestingly,
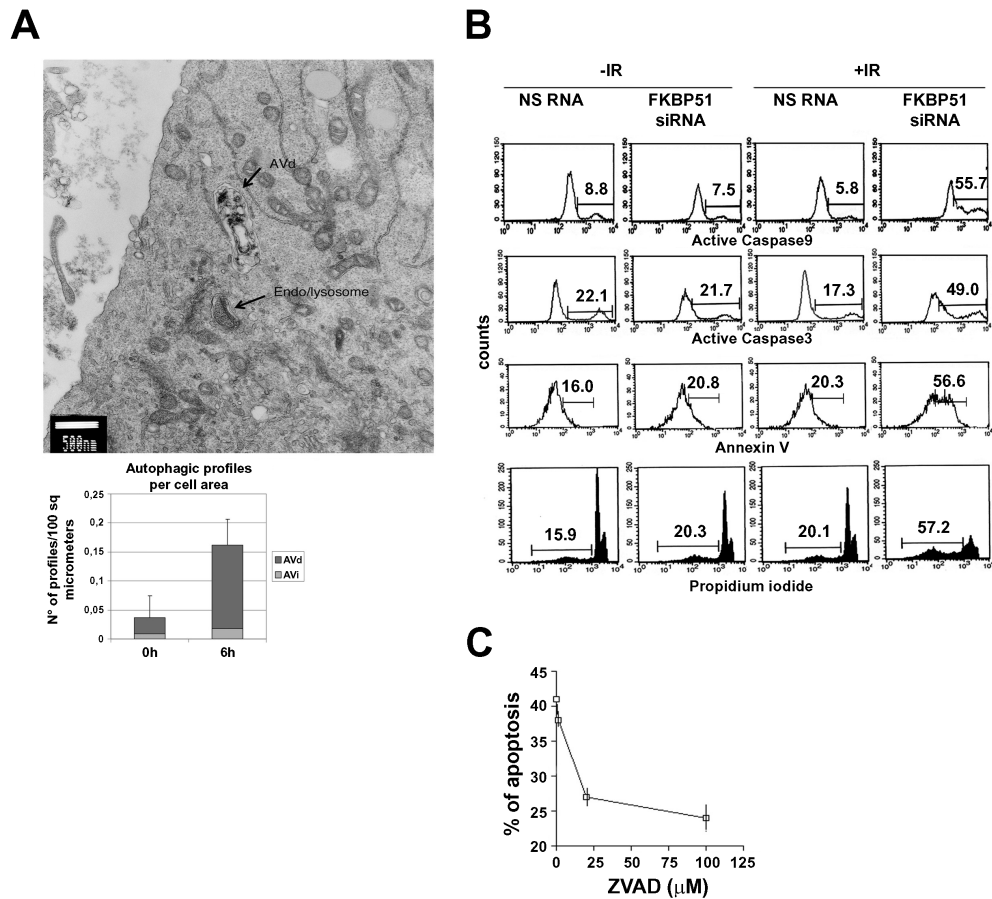
Bax levels decreased in irradiated non-silenced cells, concomitant to increase of Becn-1 levels and LC3-I to LC3-II conversion.


Fig.7. Activation of apoptosis in irradiated melanoma cells depleted of FKBP51. (A) Western blot assay of FKBP51 in cell lysates obtained from the melanoma cell line SAN transfected with FKBP51 siRNA, FKBP12 siRNA, or a non-silencing (NS) oligoribonucleotide as control. (B) Clonogenic assay of irradiated cells transfected with FKBP51 siRNA, NS RNA, or not transfected. Cells were irradiated with the indicated doses of ionizing radiation (Rx), harvested, and plated in triplicate. After 10 days, the colonies were stained with crystal violet and counted. (C) Western blot assay of Becn-1, LC3-II, Bax, caspase-3 and -7 in cell lysates prepared from melanoma cells transfected with FKBP51 siRNA or NS RNA. Cells were irradiated with 4 Gy IR and harvested at the indicated times.

Autophagy was confirmed by transmission electron microscopy; a quantitation analysis of autophagic profiles/cell area showed a clear increase in autophagosomes 6 h after IR exposure (Fig.8A).

Apoptosis was confirmed by flow cytometry. Figure 8B shows the flow cytometric histograms of caspase-9 and -3 activation, annexin V binding, and propidium iodide incorporation in irradiated cells. A measure of cell death by annexin V binding in 15 independent experiments clearly showed that IR induced a remarkable increase in the cell death of FKBP51-depleted cells (48.7 ± 11.8) compared with that of non-silenced cells (26.7 ± 8.1) (P=0.000). The mean values of cell death for non-irradiated, non-silenced or silenced cells were 18.0 ± 4.4 and 27.9 ± 8.5, respectively (P=0.022). This finding suggests that knocking down of FKBP51 reduces the threshold for cell death. The induction of apoptosis in FKBP51-depleted cells was confirmed using the pan-caspase inhibitor z-Valine-Alanine-Aspartic Acid (zVAD), which clearly inhibited IR-induced cell death (Fig.8C). The sensitizing effect of FKBP51 siRNA on IR-induced apoptosis was observed also in G361, A375, and SK-MEL-3 melanoma cell lines (Figure 9). These data showed that FKBP51 plays a relevant role in counteracting apoptotic processes stimulated by IR. Cellular events consistent with autophagy, such as an increase in Becn-1 levels and the autophagosome membrane associated LC3-II isoform, but very few with cell death were observed in irradiated melanoma cells, suggesting that autophagy supports the survival of the tumor cells. Transmission electron microscopy showed an increased number of autophagic vacuoles in irradiated cells. In contrast, typical biochemical markers of apoptosis, such as cleaved caspase-9 and -3, phosphatidylserine externalization on the plasma membrane, and hypodiploid DNA in melanoma cell nuclei, were observed in irradiated melanoma cells pre-treated with FKBP51 siRNA. These data suggested that FKBP51 plays a relevant role in counteracting apoptotic processes stimulated by IR. In particular it promotes an autophagic response in irradiated melanoma cells, which enhances the treshold for apoptosis and most probably sustains cell survival.

A

AVd

Endo/lysosome

Autophagic profiles per cell area

N° of profiles/100 sq micrometers

0,25
0,2
0,15
0,1
0,05
0

0h   6h

AVd
AVi

B

-IR

NS RNA   FKBP51 siRNA

+IR

NS RNA   FKBP51 siRNA

counts

8.8   7.5   5.8   55.7

Active Caspase9

22.1   21.7   17.3   49.0

Active Caspase3

16.0   20.8   20.3   56.6

Annexin V

15.9   20.3   20.1   57.2

Propidium iodide

C

% of apoptosis

45
40
35
30
25
20

0   25   50   75   100   125

ZVAD (μM)

Fig.8. IR induces autophagy in melanoma but apoptosis in condition of FKBP51 knockdown. (A) Transmission electron microscopy image of an irradiated melanoma cell, 6 h after exposure at a 4 Gy dose of ionizing radiation. Scale bar, 500 nm. Graphic representation of autophagic profiles/cell area in non-irradiated (0 h) and irradiated (6 h) cells. AVd, degradative autophagic compartment; AVi, initial autophagosome. (B) Flow cytometric histograms of active caspases-9 and -3, annexin V binding, and the propidium iodide incorporation of SAN melanoma cells transfected with NS RNA or FKBP51 siRNA. Cells were irradiated with 4 Gy and harvested after 6, 48, and 72 h to measure caspase activity, annexinV binding, and propidium iodide incorporation, respectively. (C) Graphic representation of the apoptosis of melanoma cells transfected with FKBP51 siRNA. At 48 h after transfection, cells were incubated with the indicated doses of zVAD and irradiated with 4 Gy of IR. After another 48 h, cells were harvested and apoptosis was determined by annexin V staining.
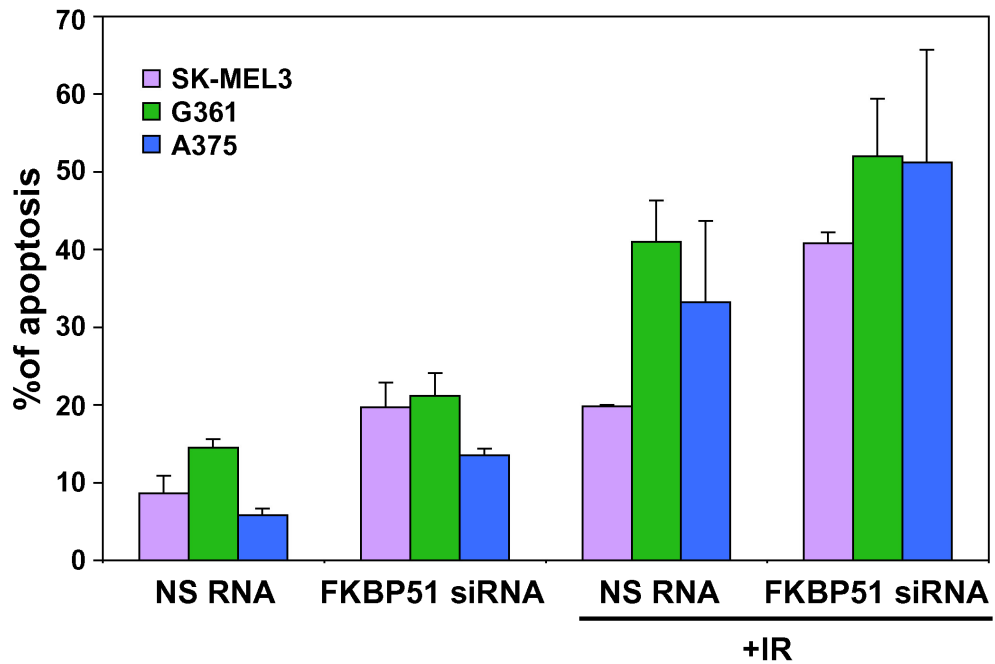
Fig.9. FKBP51 knock-down sensitizes different melanoma cell line to apoptosis. Graphic representation of the apoptosis of SK-MEL3, G361 and A375 melanoma cell transfected with NS RNA or FKBP51 siRNA. Forty-eight hours after transfection, cells were irradiated at 4Gy of IR and harvested after further 48 h. Apoptosis was analyzed by annexin V staining in flow cytometry; in figure are shown averages and standard deviations of five different experiments.

FKBP51 is essential for IR-induced activation of NF-κB

IR induces NF-κB activation (HabrakenY et al. 2006). The kinetics of IκB degradation showed a decrease in IκBα levels and the complete disappearance of IκBβ, as early as 4 h after irradiation, with a return to the basal level after 20 h (Fig.10A). The activation of NF-κB was confirmed by electrophoretic gel mobility shift assay (EMSA) (Fig.10B). FKBP51 is an important co-factor of IKK kinase complex (Boumwester T. 2004). Figure 10C shows that a molecular interaction between FKBP51 and IKK occurs during IR, in fact, IKK co-immunoprecipitated with FKBP51 in irradiated cells. The relevant role of FKBP51 in IKK kinase function was confirmed by measuring IκBα degradation and the levels of phospho-IκBα (Ser 32) in irradiated FKBP51-silenced cells, in comparison with irradiated non-silenced cells. Increased levels of phospho-IκBα could be detected in irradiated melanoma cells, but not when FKBP51 was downmodulated (Fig.10D).
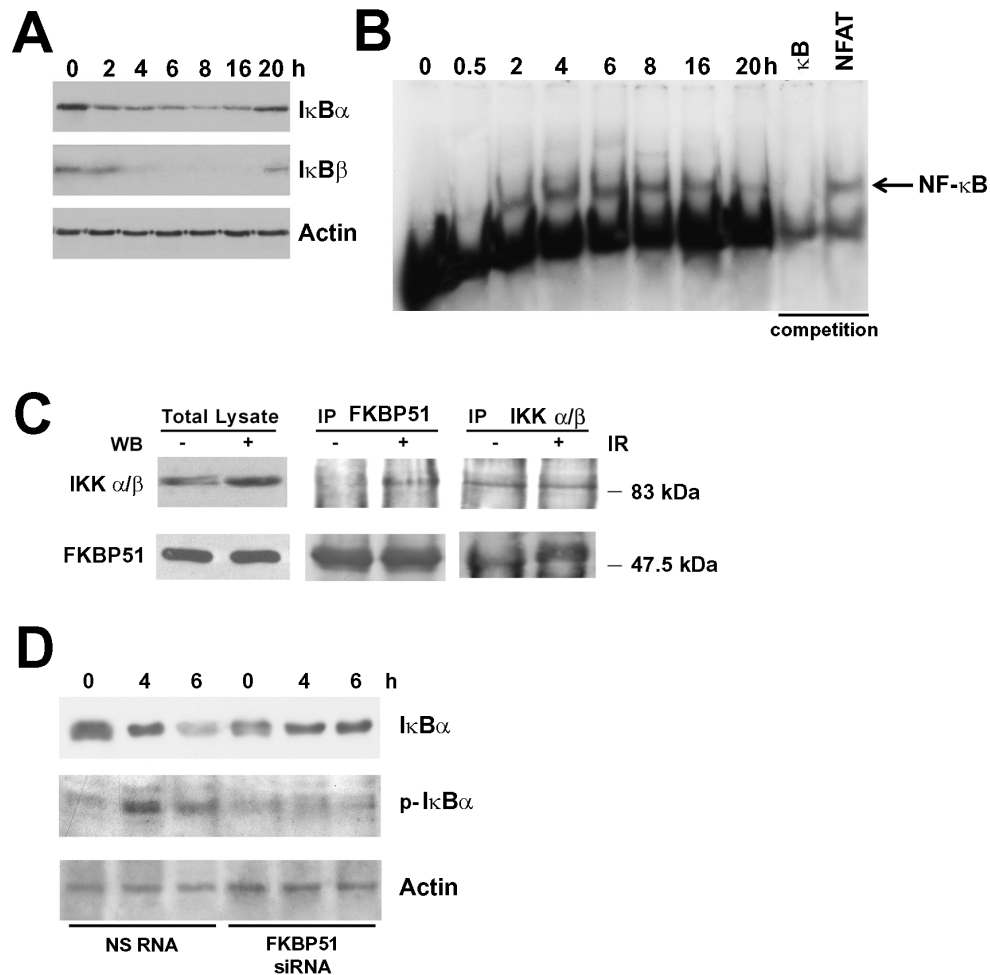
Fig.10. IR induces NF-κB activation and FKBP51/IKK interaction. (A) Western blot assay of IkBα and IkBβ levels in cytoplasmic extracts prepared from irradiated SAN melanoma cells harvested at the indicated times. (B) An electrophoretic mobility shift assay (EMSA) using nuclear extracts prepared from irradiated melanoma cells harvested at the indicated times. The last two lanes show a competition assay performed with the same κB cold oligonucleotide or an unrelated cold oligonucleotide (NFAT) that was added to the incubation mixture. (C) Total cell lysates were prepared by melanoma cells not irradiated and 3h after irradiation with 4 Gy. Cell lysates were immunoprecipitated (IP) with FKBP51 antibody, or IKKα/β antibody. Immunoprecipitated and total lysates were then subjected to western blot and FKBP51 and IKKα/β were analyzed. (D) Western blot assay of IκBα and phospho- IκBα (Ser 32) levels in cytoplasmic extracts prepared from melanoma SAN cells transfected with FKBP51 siRNA, or a NS RNA as control. After 48h from transfection cells were irradiated at 4Gy and harvested at the indicated times.

In line with NF-κB activation, an increase in the level of the caspase inhibitor X-linked inhibitor of apoptosis protein (xIAP) was observed. As expected, such an increase was not observed in FKBP51-silenced cells (Fig. 11A). Consistent with the notion that xIAP transcription is under NF-κB control (Karin M et al. 2002), reduced levels of XIAP mRNA, both basal and IR-induced, were found in p65-silenced cells compared with those in non-silenced cells (Fig.11B). The upregulation of xIAP had a role in the inhibition of irradiated melanoma cell apoptosis. In fact, when xIAP expression was silenced with a specific siRNA, the IR stimulated caspase activation and cell death (Fig.11C). Taken together, these findings suggest that FKBP51-silenced cells fail to activate NF-κB-controlled anti-apoptotic genes when irradiated.
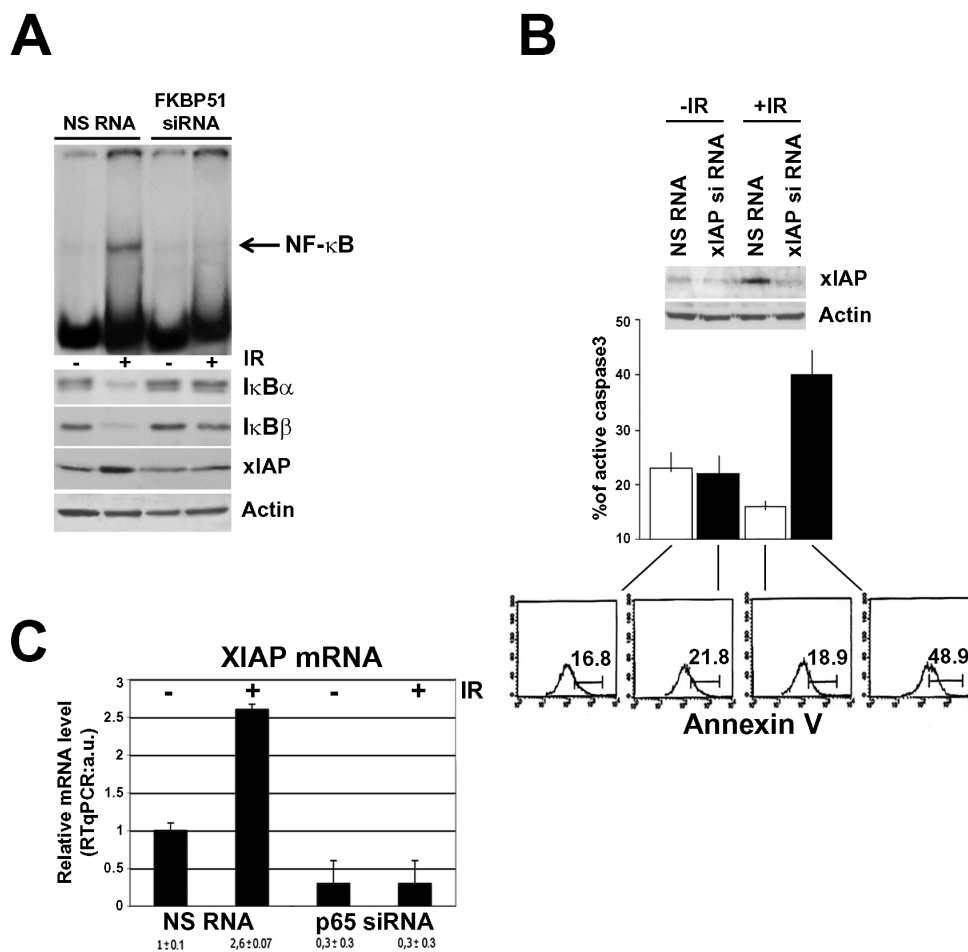
Fig.11. Lack of NF-κB activation and xIAP induction in melanoma cells depleted of FKBP51. (A) EMSA using nuclear extracts and western blot assay of whole cell lysates obtained from melanoma cells transfected with NS RNA or FKBP51 siRNA. At 48 h after transfection, cells were irradiated with 4 Gy of IR and, after an additional 6 h incubation, harvested for the preparation of both nuclear extracts and whole cell lysates. (B) Effect of xIAP downmodulation on IR-induced apoptosis. Western blot assay of xIAP levels in melanoma cells transfected with NS RNA or xIAP siRNA. At 48 h after transfection, cells were irradiated with 4 Gy IR. Cells were harvested after 6 h for whole cell lysate preparation. At the same time, a flow cytometric analysis of caspase-3 activation was performed. The graph represents the mean values and standard deviations of active caspase-3 from three different experiments, each performed in triplicate. Apoptosis was measured 48 h after irradiation by annexin V binding. A representative result of three independent experiments, performed in triplicate, is shown. (C) Normalized expression rates of XIAP mRNA (a.u.: arbitrary units) in melanoma cells SAN, which were transfected with p65 siRNA or a NS RNA, and irradiated or not with a 4 Gy dose. Vertical bars indicate standard deviations. Values were obtained from three independent experiments.

Rx-induced NF-κB sustains autophagy

In order to investigate whether the levels of Becn-1 were enhanced by NF-κB activation, we attempted to downmodulate the p65 subunit of NF-κB. The supershift assay provided evidence that p65 represents the main component of the NF-κB complex activated by IR in our cell system. As shown in figure 12A, the IR-induced NF-κB band was supershifted by anti-p50 and anti-p65 antibodies. Melanoma cells transfected with p65 siRNA, or a NS RNA as control, were irradiated and, after 6 h, total cell lysates were prepared. A western blot assay showed that p65 siRNA, but not NS RNA, downmodulated the protein (Fig.12B). Radiation treatment enhanced the levels of Becn-1 in non-silenced cells, but this was not observed in cells depleted of p65. An increase in the levels of the LC3-II isoform was found in irradiated cells, but not when p65 was downmodulated (Fig.12B). The IR-induced increase in Becn-1 protein was associated to increase in BECN-1 mRNA levels. Such increase was not observed in p65-silenced cells (Fig.12C). This result suggests that p65 was essential for Becn-1 expression. Our finding is in accordance with the very recent demonstration that p65 exerts transcriptional control on BECN-1 gene expression (Copetti T et al. 2009).
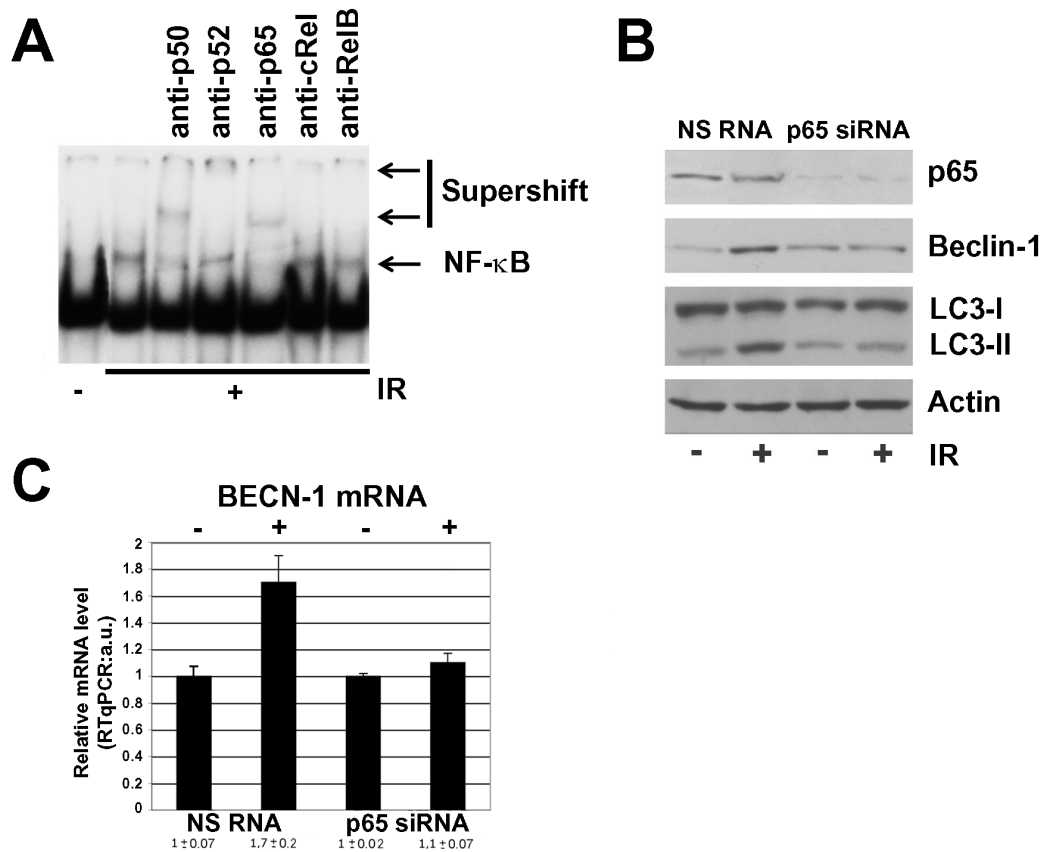
Fig.12. NF-κB promotes cell survival by enhancing the expression of the autophagic protein beclin-1. (A) Supershift assay of a nuclear extract prepared from SAN melanoma cells 6 h after a 4 Gy dose of IR. The extract was incubated with [γ-32P] ATP end-labeled NF-κB consensus oligonucleotide in the absence or presence of the indicated antibodies against NF-κB and run in a 6% acrylamide gel electrophoresis. (B) Western blot assay of p65, Becn-1, and LC3-II levels in melanoma cells transfected with NS RNA or p65 siRNA. At 48 h after transfection, cells were irradiated with 4 Gy Rx. Cells were harvested after 6 h for whole cell lysate preparation. (C) Normalized expression rates of BECN-1 mRNA (a.u., arbitrary units) in melanoma cells SAN, which were transfected with p65 siRNA or a NS RNA, and irradiated or not with a 4 Gy dose. Vertical bars indicate standard deviations. Values were obtained from three independent experiments.

To investigate whether Becn-1, an important component of the autophagic machinery (Eskelinen EL. 2008; Baehrecke EH. 2005; Mathew R et al. 2007), has a role in the apoptosis inhibition of irradiated cells, we used specific siRNA to downmodulate Becn-1. A western blot assay of whole cell extracts prepared from cells 6 h after irradiation showed an increase in the level of LC3-II isoform in cells transfected with NS RNA, but not those depleted of Becn-1 by specific siRNA (Fig.13A). This finding was confirmed by transmission electron microscopy; we performed TEM analysis of Becn-1 silenced cells, at times 0 and 6 h after irradiation. In accordance with previous results, there was no induction of autophagy after irradiation of Becn-1 silenced cells. A quantitation analysis of autophagic profiles/cell area showed a clear decrease in autophagosomes 6 h after IR exposure of Becn-1 silenced cells. Representative images of the cells are shown in figure 13B. These results are in accordance with the concept that Becn-1 is essential for the activation of autophagy (Eskelinen EL. 2008; Baehrecke EH. 2005; Mathew R et al. 2007). An analysis of cell death after an additional 40 h of incubation showed that the percentage of annexin V-positive cells clearly increased in Becn-1-depleted cells (Fig.13A).
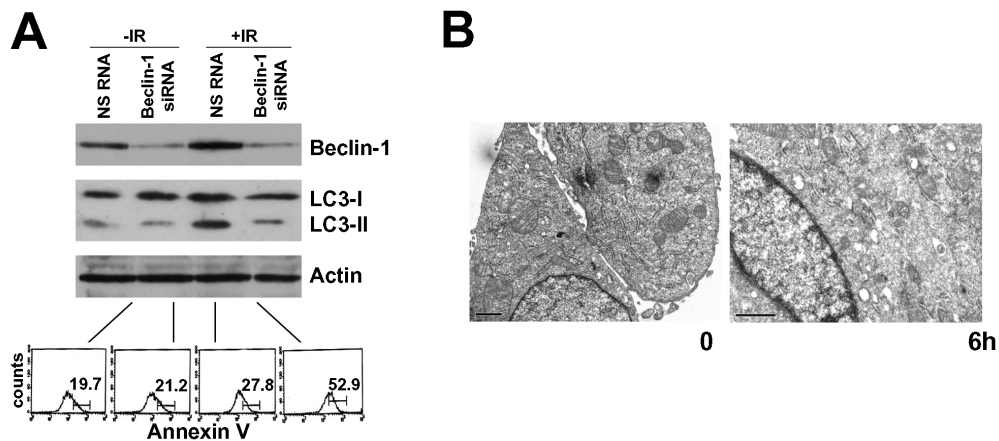
Fig.13. Becn-1 exerts an essential role in apoptosis inhibition in melanoma cell. (A) The effect of Becn-1 depletion on IR-induced apoptosis. A representative western blot of Becn-1 levels in melanoma cells transfected with NS RNA or Becn-1 siRNA is shown. At 48 h after transfection, cells were irradiated with 4 Gy IR. A portion of cells was harvested after 6 h for whole cell lysate preparation. After an additional 42 h, the remaining cells were harvested and apoptosis was measured by annexin V binding. A representative result of three independent experiments, each performed in triplicate, is shown. (B) Representative TEM images of Becn-1 silenced cells, at times 0 and 6h after irradiation with a 4Gy dose. Scale bar, 500nm.

In order to confirm these data, we analyzed apoptosis also in presence of high levels of Beclin-1. Melanoma cells were transfected with a vector carrying EGFP-tagged BECN-1 to over-express beclin-1, or an EGFP vector as control. Transfection efficiency was assessed by both a flow cytometric analysis and a western blot assay of Beclin-1 and LC3 (Fig.14A,B). We found that 35.5% and 29.8% of cells, transfected with EGFP and BECN-1/EGFP, respectively, expressed the exogenous gene. Exogenous beclin-1 was functional, as suggested by increased levels of LC3 II isoform in cells transfected with the fusion protein, compared to cells transfected with control vector, which indicates an increase in basal autophagy. To investigate the effect of Becn-1 over-expression on apoptosis of FKBP51 depleted cells, we co-transfected BECLIN1/EGFP plasmid (or EGFP plasmid as control) and FKBP51 siRNA. Forty-eight h after irradiation, cells were collected, stained with annexin V-PE and analyzed by flow cytometry. Green fluorescent cells were gated as in A, according to FL-1/SSc parameters, and then the percentage of annexin V-PE positive cells was calculated. Beclin-1 over-expression clearly decreased the levels of apoptosis, that were lower than those of cells co-transfected with EGFP and FKBP51 siRNA (Fig.14C). To confirm apoptosis, we measured the levels of active caspase-3 by indirect immunofluorescence. In accordance with apoptosis data, the levels of active caspase-3 were reduced in cells over-expressing beclin1 (Fig.14D). These findings suggest that activation of NF-κB in irradiated melanoma induces autophagy and that this mechanism is, at least in part, responsible for lack of cell death.
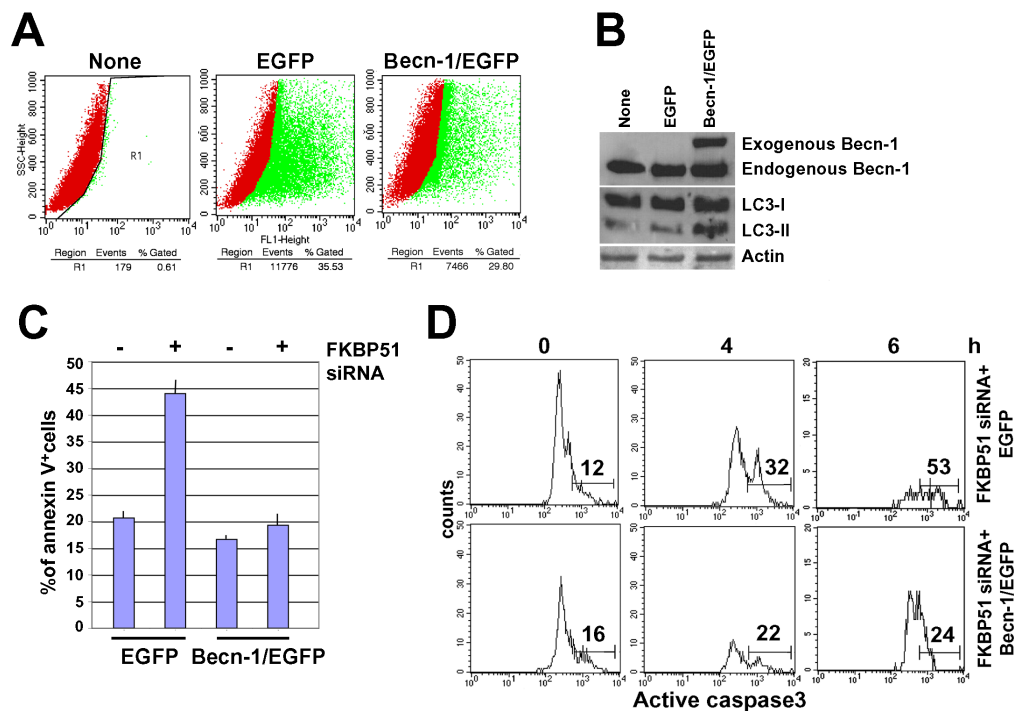
Fig.14. Becn-1 overexpression inhibits apoptosis in melanoma cell. (A) Flow cytometric histograms of melanoma cells transfected with a vector carrying EGFP-tagged BECN-1 or an EGFP vector as control. A gate was placed on EGFP expressing cells based on FL1/SSc parameters. The percentages of EGFP$^+$ cells were: 0.6, 35.5, 29.8 in not transfected, EGFP-transfected and BECN-1/ EGFP-transfected cells, respectively. (B) Western blot assay of Beclin1 and LC3 levels in cell lysates prepared from cells transfected with BECN-1/EGFP or EGFP. (C) Analysis of apoptosis of melanoma cells co-transfected with NS RNA+EGFP, NS RNA+BECN-1/EGFP, FKBP51 siRNA+EGFP and FKBP51 siRNA+ BECN-1/EGFP. Cells were irradiated after 48h from transfection and harvested after a further 48 h incubation. Apoptosis was analyzed by flow cytometry. The percentage of annexin V positive events was calculated in cells gated as in A. Mean values and standard deviations of three independent experiments, each performed in triplicate, are represented. (D) Flow cytometric histograms of cleaved caspase-3. Cells, co-transfected with FKBP51 siRNA+EGFP and FKBP51 siRNA+BECN-1/EGFP, were harvested after 0, 4 and 6h from irradiation at 4Gy. Then, cells were fixed, permeabilized, and incubated with a cleaved caspase-3 antibody. Cells were analyzed by flow cytometry and the percentage of cells expressing cleaved caspase-3 was calculated in a gate performed as in A.

Rx-induced autophagy increases the threshold for apoptosis

To clarify the mechanism by which Becn-1 inhibited apoptosis, we investigated the levels of Bax, which is an important component of the permeability transition pore in mitochondrion-dependent apoptosis (Kim H et al. 2006). Western blot showed reduced Bax levels in irradiated melanoma cells, which is consistent with its degradation. In Becn-1-silenced cells, Bax levels were higher compared with those in non-silenced cells after irradiation (Fig.15A). Normalized expression rates of Bax mRNA in cells transfected with BECN-1 siRNA, or a NS RNA, by Real-time PCR, did not show any relevant increase of Bax transcript after depletion of Becn-1, thus suggesting a post-transcrptional regulation (Fig.15B).
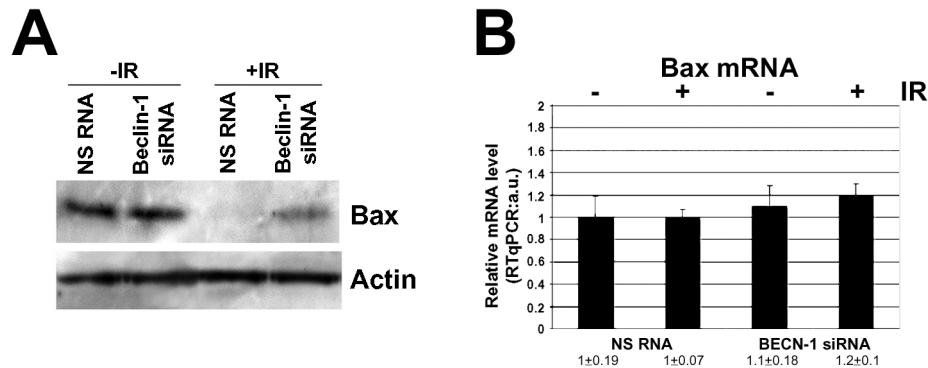
Fig.15. *Becn-1 downregulation counteracts bax degradation in irradiated melanoma cell.* (A) The effect of IR on Bax levels in Becn-1-depleted cells. A representative western blot of Bax levels in melanoma cells transfected with NS RNA or Becn-1 siRNA is shown. At 48 h after transfection, cells were irradiated with 4 Gy IR. Cells were harvested after 4 h for whole cell lysate preparation. (B) Normalized expression rates of Bax mRNA in cells transfected with BECN-1 siRNA or a NS RNA, by Real-time PCR.
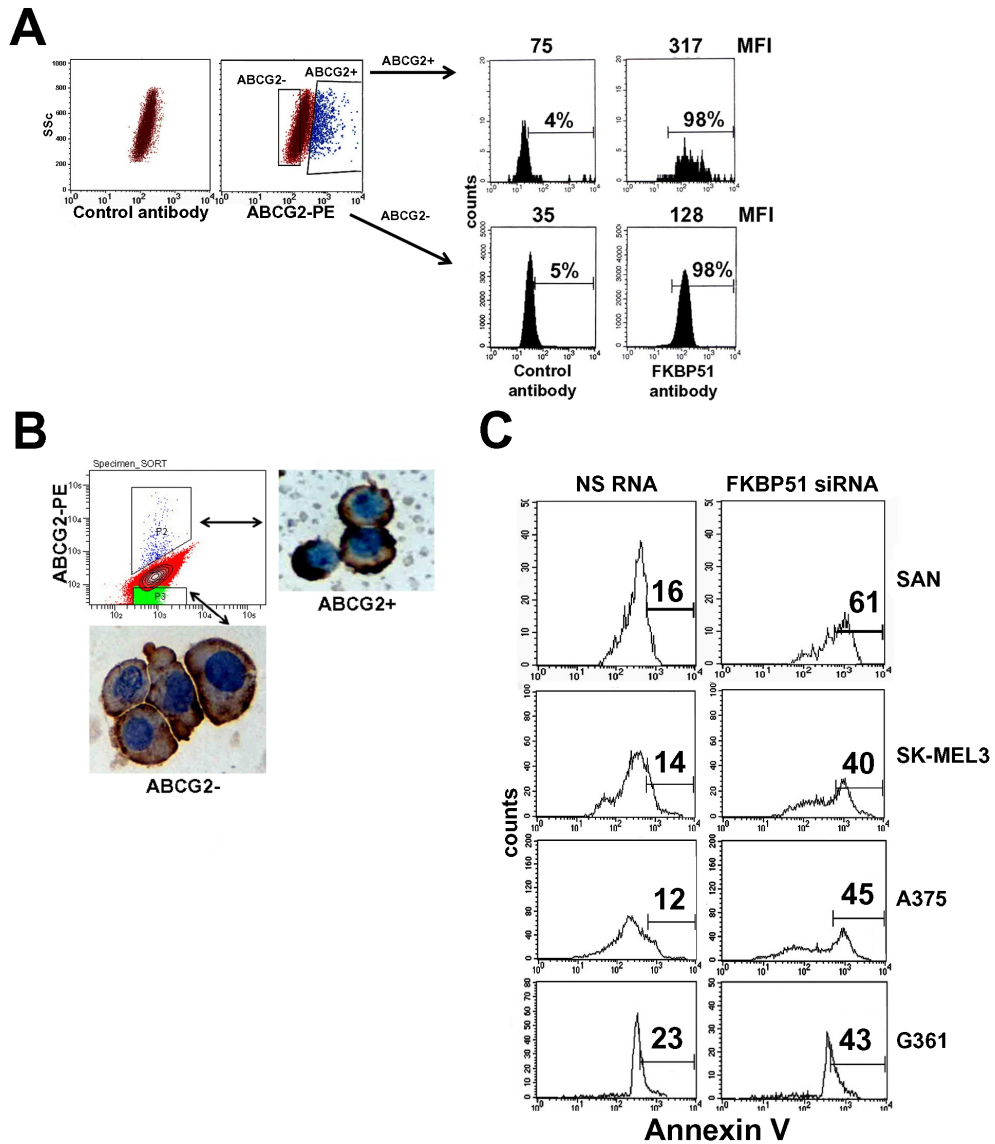
Bax localization was investigated by confocal microscopy, in double fluorescence with LC3 (Fig.16A). Bax was mostly localized in the nucleus, in basal conditions, and to some extent in the cytosol. After irradiation, nuclear Bax apparently translocated to the cytosol. The presence of colocalization areas in LC3 aggregates (see enlarged detail in Fig.16A) suggests a possible inclusion of Bax in autophagic vacuoles (Fig.16A). A semi-quantitative western blot analysis of Bax levels in cells irradiated, in the absence or presence of inhibitors of lysosomal proteolysis, showed a decrease in Bax levels in irradiated cells, but not when inhibitors of lysosomal proteases were added to the cell culture (Fig.16B). These findings confirm that Becn-1 expression is controlled by NF-κB. Moreover, by showing the IR-induced autophagic degradation of Bax, these results provide an explanation through which autophagy represses apoptosis.
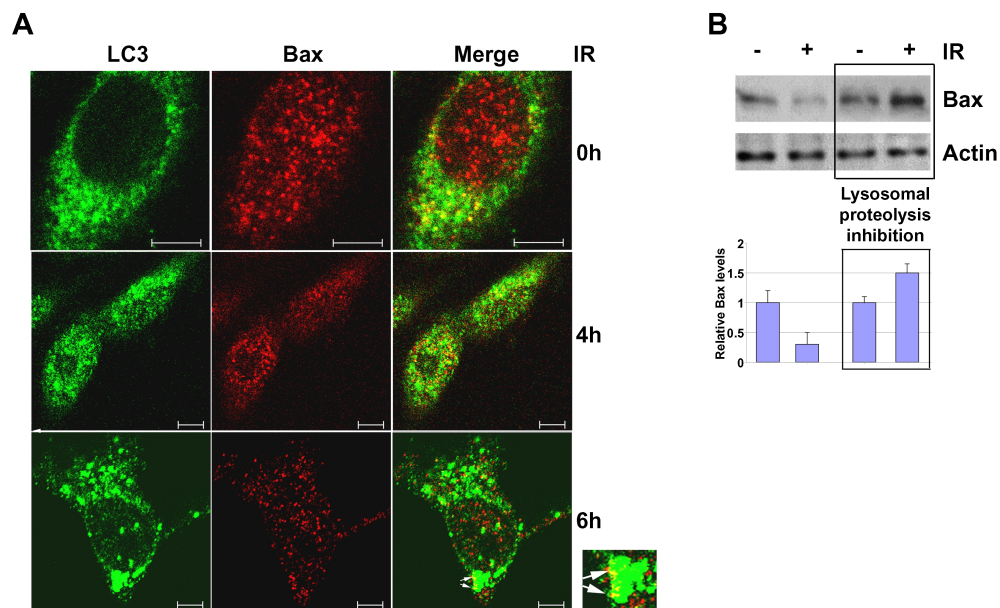
Fig.16. IR induces Bax delocalization and degradation. (A) Confocal images of cells fixed after 0, 4 h, and 6 h from irradiation with 4 Gy and stained with anti-Bax (red fluorescence) and anti-LC3 (green fluorescence). Enlarged detail of colocalization areas. Bar 5 mm. (B) Western blot of Bax levels in melanoma cells irradiated for 6 h with 4 Gy, in the absence or presence of 0.25mM leupeptin and 10 μg/ml pepstatin. Protease inhibitors were added to the culture medium 1 h before cell harvest. Bax expression levels were quantified by densitometry using NIH Image 1.61 for Macintosh. Integrated optical densities, normalized to actin, were expressed versus baseline level.

FKBP51 is expressed in malignant melanoma-stem/initiating cells

Normal stem cells have a high drug efflux capability because of the expression levels of ATP-binding cassette (ABC) transporters, which actively pump drugs out of the cell. The ABC, subfamily G, member 2 (ABCG2) is a member of this superfamily of ABC transporter proteins, and it is known to be not only a member of the membrane transporters implicated in multidrug resistance but also a molecular determinant of cancer stem/initiating cells of melanoma (Monzani E et al. 2007). To find out whether FKBP51 targeting can overcome radioresistance in such cells with enhanced tumorigenic potential, we investigated if they expressed this immunophilin. The FKBP51 expression was determined by flow cytometry and immunohistochemistry. After the acquisition of $1x10^6$ cells with a flow cytometer, a gate was placed for ABCG2$^+$ cells (0.5% of total cells), according to ABCG2-PE/SSc parameters (Fig.17A). The expression of FKBP51 in gated cells was then analyzed in the FL-1 channel. The percentage of FKBP51$^+$ events was comparable in ABCG2$^+$ and ABCG2$^-$ cells, whereas the mean fluorescence intensity (MFI) was clearly higher in ABCG2$^+$ cells, when compared with that in ABCG2$^-$ cells, suggesting an increased production of FKBP51 in cells with enhanced tumorigenic potential. The expression of FKBP51 in ABCG2$^+$ cells was confirmed by immunohistochemistry of cells sorted with the BD FACSAria cell sorting system (BD Biosciences, San Jose, CA USA) (Fig.17B). We then investigated the effect of IR on the apoptosis of ABCG2$^+$ cells. Forty-eight h after irradiation, melanoma cells transfected with NS RNA or FKBP51 RNA were harvested and stained with ABCG2-PE and annexin V-FITC. The enhanced percentage of annexin V-positive events in ABCG2 gated cells clearly indicated a radiosensitizing effect of FKBP51 siRNA on these cells. This biparametric analysis of apoptosis was performed also in other melanoma cell lines called SK-MEL3, G361 and A375. In conclusion, we demonstrated that ABCG2$^+$ melanoma cells contain intracytoplasmic FKBP51 at higher levels than ABCG2$^-$ cells. Moreover, ABCG2$^+$ cells are also killed by IR after pre-treatment with siRNA. Taken together, these findings suggest that FKBP51 may be a suitable target for eliminating cancer-stem cells of melanoma.

Fig.17. FKBP51 is expressed in ABCG2$^+$ cells. (A) Flow cytometric histograms of
the ABCG2 gating strategy and FKBP51 expression in SAN melanoma cells. Cells were
stained with PE-conjugated isotype control antibody or mouse monoclonal ABCG2-PE. The
cells were then fixed, permeabilized, and incubated with or without rabbit anti-FKBP51. After
a second staining with anti-rabbit FITC, cells were analyzed by flow cytometry. ABCG2
marked a subpopulation of melanoma cells. According to ABCG2/SSc parameters, two gates
were placed, one for ABCG2$^+$ cells (red) and another for ABCG2$^-$ cells (blue). The expression
of FKBP51 was measured in the gated populations in the FL1-channel. Bars indicate the
percentage of FL1-positive events, and the values of mean fluorescence intensity (MFI) are
also indicated. (B) Detection of FKBP51 by immunohistochemistry. SAN melanoma cells
expressing ABCG2 were separated from the whole population by BD FACSaria cell sorting,

fixed, and subjected to the immunohistochemical examination of FKBP51. (C) Effect of FKBP51 depletion on IR-induced apoptosis of ABCG2$^+$ melanoma cells. Flow cytometric histograms of the annexin V binding of ABCG2$^+$ melanoma cells gated as in A. Melanoma cells from SAN, SK-MEL3, A375, and G361 cell lines were transfected with NS RNA or FKBP51 siRNA and irradiated with 4 Gy IR. After 48 h, cells were harvested and stained with ABCG2-PE and annexin V-FITC to measure apoptosis.

In vivo targeting of FKBP51 radiosensitizes melanoma xenografts

We confirmed that the downmodulation of FKBP51 radiosensitized melanoma in vivo. We produced human melanoma xenografts in imminocompromised mice. To investigate apoptosis in tumor xenografts, the activation of caspase-3 was determined by the immunohistochemistry of tumor sections and western blot of tumor lysates. Strong immunoreactivity for cleaved caspase-3 was found in the tumor tissues from xenografts pretreated with FKBP51 siRNA before irradiation. Only a few apoptotic cells were detected in both non-irradiated (Fig.18A) and irradiated (Fig.18B) non-silenced tumors, in which most of the melanocytes were viable and considerable mitotic activity was present. Few melanocytes showing the morphological signs of apoptosis and caspase-3 immunoreactivity were found in non-irradiated silenced tumors (Fig.18C). In contrast, a prevalence of apoptotic melanocytes with clear caspase-3 immunopositivity was present in irradiated silenced tumors (Fig.18D). Western blot confirmed the prominent activation of caspase-3 in tumors pretreated with FKBP51 siRNA (Fig.18E). These finding confirm *in vivo* that the double treatment FKBP51 siRNA and IR activates apoptosis in melanoma.
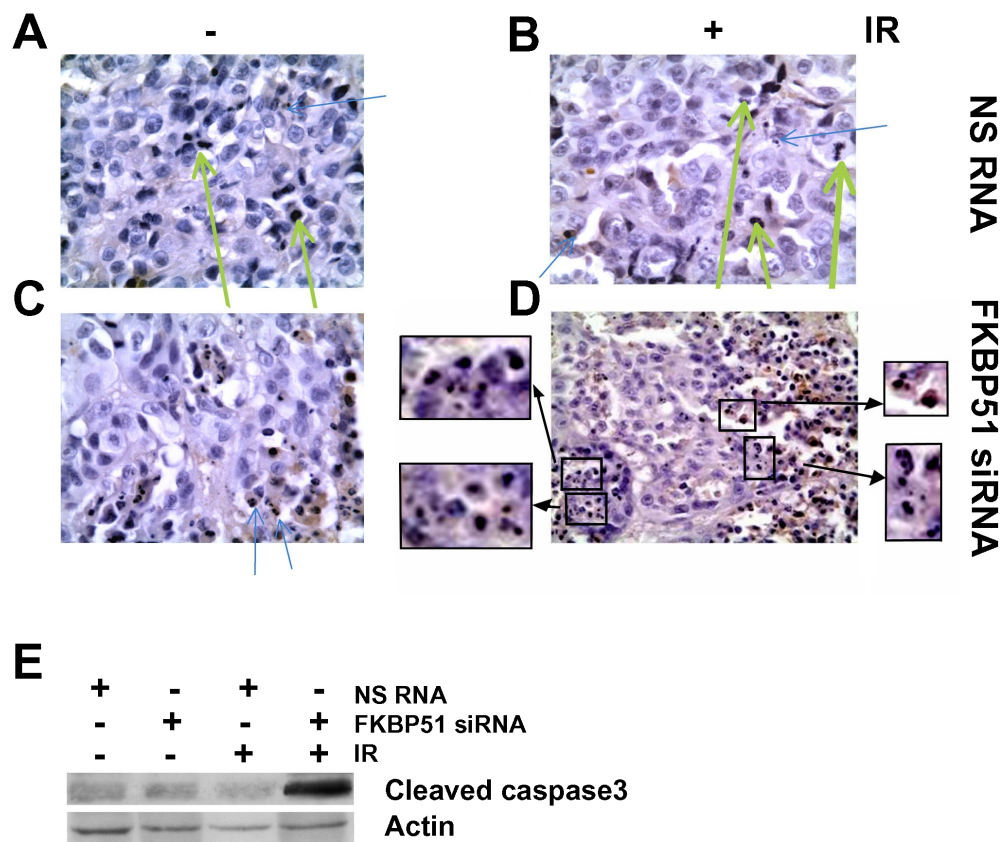
Fig.18. IR-induced apoptosis in tumor xenografts pretreated with FKBP51 siRNA. Immunohistochemistry and western blot assay of cleaved caspase-3 in tumor sections. Tumors were excised 48 h after irradiation. For immunohistochemistry, the avidin-biotin complex technique was used. Original magnification, x250 (A, B, C); x150 (D). The morphology of apoptotic nuclei was indicated by blue arrows; green arrows indicate mitosis. Enlarged details of apoptotic nuclei from panel D. (E) Whole tissue lysates prepared from the same tumors were run in SDS-PAGE for the western blot assay and cleaved caspase3 levels were analyzed.

FKBP51 is a marker of malignant melanocytes

Specimens of cutaneous melanoma from 80 patients and 10 samples of normal skin stored in the archive of the Pathology section (Department of Biomorphological and Functional Sciences, University Federico II of Naples, Italy) were examined for FKBP51 expression. In normal skin, no immunopositive melanocytes were found. Table 1 presents the patient profiles relative to the cases studied. In most patients (58/80, 72%), a low (+) immunopositivity was found in melanocytes during the radial growth phase. Melanocytes in the vertical growth phase displayed a stronger immunopositivity (++) compared with radial melanocytes (P<0.001, Pearson $\chi^2 = 62.082$). A significant correlation was found between FKBP51 expression and the thickness of the tumor lesion (Spearman's $\rho=0.646$, P<0.001). Moreover, metastatic melanoma was associated with the highest immunoreactivity (+++) (Spearman's $\rho=0.538$, P<0.001).
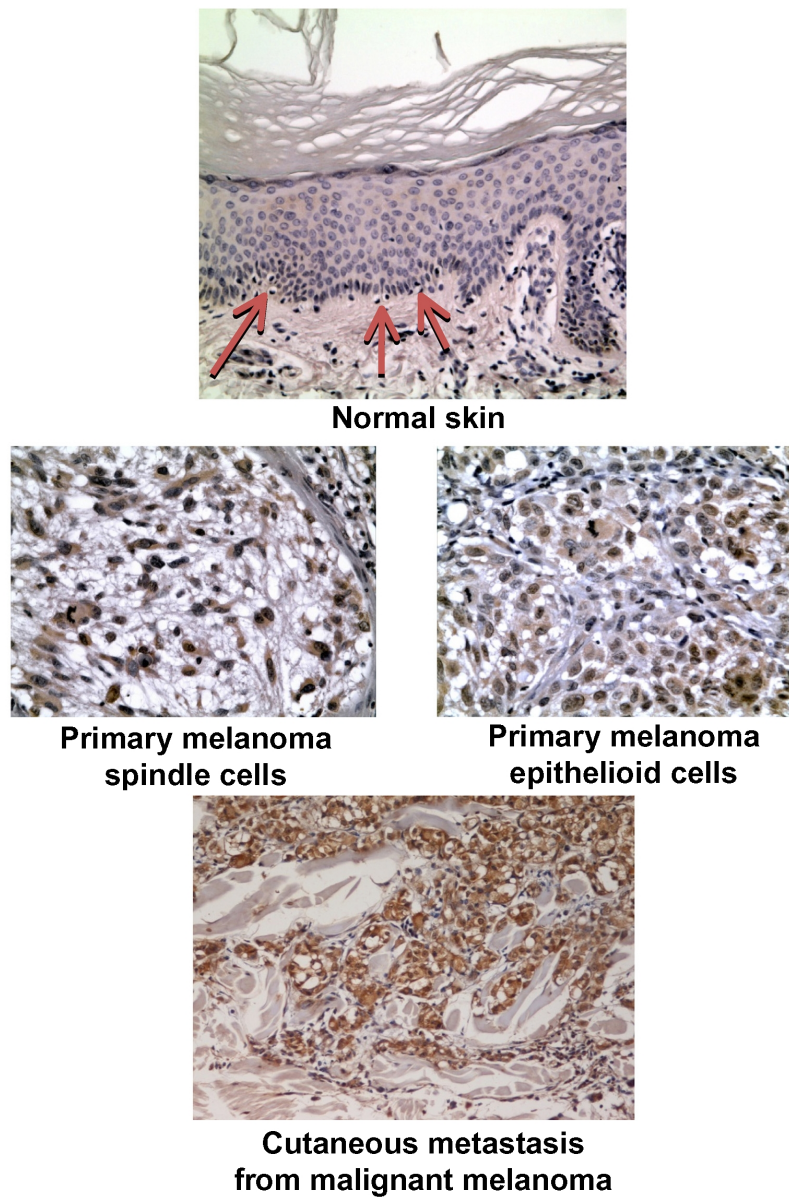
Table 1. FKBP51 expression in cutaneous malignant melanoma (CMM) and patients' profiles.

Case	Age (y)	Sex	Breslow	FKBP51r	FKBP51v	Follow up (y)
1	58	F	≤1.00	+	+	12
2	36	M	≤1.00	+	+	12
3	67	M	≤1.00	+	+	12
4	45	F	≤1.00	+	+	12
5	50	F	≤1.00	++	++	11
6	49	F	≤1.00	+	+	11
7	42	M	≤1.00	+	+	10
8	43	F	≤1.00	+	+	9
9	43	M	≤1.00	+	++	9
10	49	M	≤1.00	+	+	7
11	40	M	≤1.00	++	++	7
12	41	M	≤1.00	+	+	7
13	39	M	≤1.00	+	++	6R
14	37	F	≤1.00	+	+	6
15	66	F	1.01-2.00	++	++	12N
16	65	F	1.01-2.00	+	++	12
17	56	M	1.01-2.00	+	++	12
18	49	M	1.01-2.00	+	++	12
19	48	M	1.01-2.00	+	++	12
20	39	F	1.01-2.00	+	++	12
21	47	F	1.01-2.00	++	+++	12N,M,D
22	51	M	1.01-2.00	+	++	11
23	53	M	1.01-2.00	+	++	11
24	56	M	1.01-2.00	+	++	11
25	51	F	1.01-2.00	++	++	10
26	45	F	1.01-2.00	+	++	10
27	53	M	1.01-2.00	+	++	10
28	67	M	1.01-2.00	+	++	10
29	54	M	1.01-2.00	+	++	10
30	34	M	1.01-2.00	+	++	9
31	44	F	1.01-2.00	+	++	9
32	43	F	1.01-2.00	+	++	9
33	71	F	1.01-2.00	++	+++	9
34	34	M	1.01-2.00	++	++	9
35	43	F	1.01-2.00	+	++	9
36	51	F	1.01-2.00	+	++	9
37	50	M	1.01-2.00	+	++	9
38	39	F	1.01-2.00	+	++	9N
39	29	F	1.01-2.00	+	++	9
40	42	M	1.01-2.00	+	++	7
41	37	F	1.01-2.00	++	++	7R,N
42	65	M	1.01-2.00	+	++	7
43	43	M	1.01-2.00	++	++	7N
44	44	F	1.01-2.00	+	++	6
45	18	F	1.01-2.00	+	++	4

46	22	M	1.01-2.00	+	++	4
47	24	M	1.01-2.00	+	++	4
48	32	M	1.01-2.00	++	++	4
49	30	F	1.01-2.00	+	++	4
50	38	F	1.01-2.00	+	++	4
51	37	M	1.01-2.00	+	++	3
52	40	M	1.01-2.00	+	++	3
53	40	M	2.01-4.00	++	+++	12
54	36	M	2.01-4.00	+	++	12
55	39	M	2.01-4.00	+	++	11
56	50	F	2.01-4.00	+	+++	11
57	48	F	2.01-4.00	++	++	11
58	45	M	2.01-4.00	++	+++	11N,M,D
59	43	F	2.01-4.00	+	++	10
60	53	F	2.01-4.00	+	++	10
61	47	M	2.01-4.00	++	+++	10N
62	54	M	2.01-4.00	++	+++	10
63	50	M	2.01-4.00	+	++	10
64	69	F	2.01-4.00	+	++	10
65	54	M	2.01-4.00	+	++	10
66	53	M	2.01-4.00	+	++	9
67	42	F	2.01-4.00	++	+++	9N,M,D
68	37	F	2.01-4.00	++	++	9N,M
69	45	F	2.01-4.00	+	++	9
70	49	F	2.01-4.00	++	+++	9N,M,D
71	32	M	2.01-4.00	+	++	7N
72	38	F	2.01-4.00	+	++	6N
73	38	M	2.01-4.00	+	++	3
74	32	M	2.01-4.00	++	+++	3N,M
75	40	M	2.01-4.00	++	+++	3
76	46	F	2.01-4.00	++	+++	3N
77	50	M	2.01-4.00	+	++	2
78	24	F	2.01-4.00	+	++	2
79	30	M	2.01-4.00	++	++	2
80	32	F	2.01-4.00	+	++	2

FKBP51r, FKBP51 radial growth; FKBP51v, FKBP51 vertical growth; R, recidivation; N, lymph node; M, metastasis; D, tumor death.

Figure 19 shows representative immunohistochemical stains for FKBP51 in skin specimens from patients with primitive and metastatic lesions. A definite brown cytoplasmic immunostaining for FKBP51 is visible in tumor, but not normal, melanocytes. The immunoreactivity of the metastatic cutaneous lesion was impressive. In conclusion, our findings unequivocally show that FKBP51 is overexpressed in melanoma lesions of all the patients studied and that FKBP51 expression correlates with malignity of the lesions. Data obtained from this study on 80 melanoma patients reinforce the translational implication our previous findings. The relevant data from this analysis is that FKBP51 i) was expressed in all cutaneous malignant melanomas analyzed but not in normal skin; ii) expression was higher in melanocytes during the vertical growth phase compared to the radial growth phase; iii) expression correlated with the thickness of the tumor lesion; iv) expression was maximal in metastatic melanoma.

Normal skin

**Primary melanoma
spindle cells**

**Primary melanoma
epithelioid cells**

**Cutaneous metastasis
from malignant melanoma**

Fig.19. FKBP51 expression in normal skin and cutaneous malignant melanoma (CMM). FKBP51 immunochemical staining of normal skin (red arrows indicate melanocytes, original magnification, x200); primary malignant melanoma spindle cells (original magnification, x250); primary malignant melanoma epithelioid cells (magnification, x250); and dermal metastasis from malignant melanoma (original magnification, x150), using the avidin–biotin complex technique.

FKBP51 is a possible novel tumoral marker

Data provided so far support the conclusion that FKBP51, a protein with important biological roles in normal cells (Sinars CR et al. 2003; Bouwmeester T et al. 2004; Baughman G et al. 1995), acquires a pro-oncogenic potential when its expression is deregulated, which is what occurs in melanoma. Such deregulation might sustain survival networks that protect the melanoma against killing. Therefore we asked if FKBP51 could play a role in tumor progression of other cancers. We performed an immunohistochemistry study of expression of FKBP51 in fifty tumoral samples, acquired from our pathology section, including breast, lung, pancreas, ovary, and prostate (10 samples for each tumor), and a comparable number of normal tissue samples. At the same time, a quantitative measure of FKBP51 mRNA was performed in RNAs exctracted by deparaffinized tissues. An intense FKBP51 signal was found in 38 out of 50 tumors analyzed, whereas normal tissues of the same histotypes showed a weak/absent immunohistochemical signal. The 12 tumor samples with low/negative immunohistochemistry were the 10 breast cancer samples and 2 out of 10 pancreatic tumors. Interestingly, these two pancreatic tumors belonged to the well-differentiated histotype (G1). Figure 20A shows representative immunohistochemical findings. Measurement of FKBP51 mRNA levels in deparaffinized tissues using real-time PCR confirmed the immunohistochemistry results (Fig.20B).
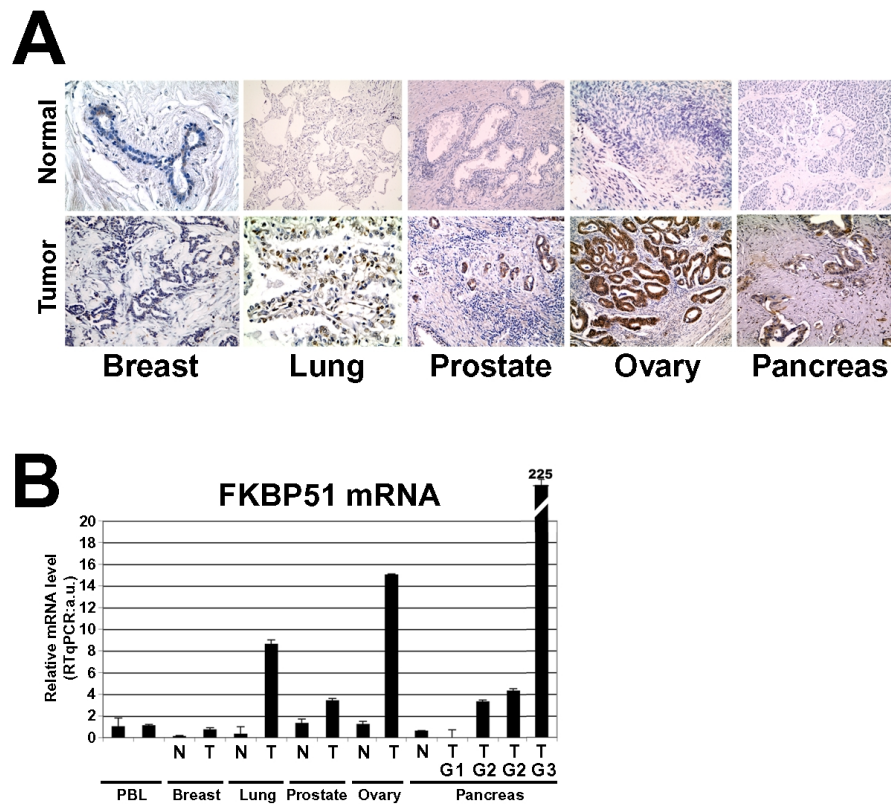
Fig.20. FKBP51 immunochemical staining of normal and neoplastic tissues.
(A) FKBP51 immunochemical staining of different tumoral tissues and normal counterpart, using the avidin–biotin complex technique. Hematoxylin was used for nuclear counterstaining. (B) Normalized expression rates of FKBP51 mRNA (a.u., arbitrary units) in PBL and deparaffinized tissues; each histogram is referred to a representative normal or tumoral sample. Values represent means and standard deviations of arbitrary units from three different real-time experiments, each performed in triplicate. The values of each sample were compared to PBL (expression=1) for an estimate of the relative expression change fold of FKBP51.

Moreover, we performed a wide immunohistochemistry study of FKBP51 expression in 21 colon tumoral samples. FKBP51 was found expressed in normal colonic mucosa, particularly in proliferative basal zone of normal glands. An increased expression of the protein was found in 15 out of 21 tumor analyzed (Fig.21A). Interestingly, FKBP51 cellular compartimentalization in colon carcinoma changed with grading. FKBP51 was mostly cytosolic in well-differentiated colon cancer (G1), whereas it was nuclear in undifferentiated histotype (G3) (Fig.21B). Immunohistochemistry data were confirmed by

Realtime-PCR. FKBP51 mRNA transcription rates were found higher in colon cancer, compared to normal colon (Fig.21C). Taken together, these findings suggest that FKBP51 plays a relevant role in cancer biology and can become in the near future a novel tumor biomarker.
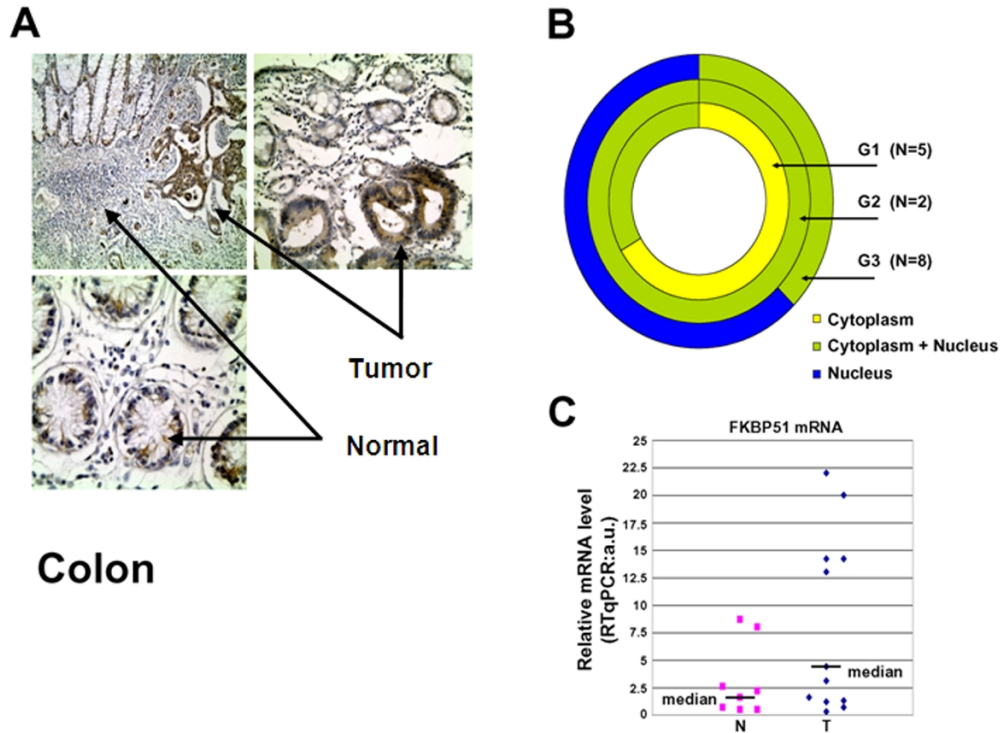
Fig.21. FKBP51 immunochemical staining of normal and neoplastic colon tissue. (A) FKBP51 immunochemical staining of 21 colon tumoral and normal tissues, using the avidin–biotin complex technique. Hematoxylin was used for nuclear counterstaining. (B) FKBP51 compartimentalization in colon cancer. FKBP51 cellular compartimentalization in colon carcinoma changed with grading. FKBP51 was mostly cytosolic in G1 (yellow), whereas it was nuclear in G3 (blu) and both nuclear and cytoplasmic in G2 (green). (C) Normalized expression rates of FKBP51 mRNA (a.u., arbitrary units) in colon deparaffinized tissues. Values represent median of arbitrary units from different real-time experiments, each performed in triplicate.

CONCLUSIONS

Among cancers, malignant melanoma is one of the most resistant to treatment. Patients diagnosed with advanced stage melanoma have a very poor prognosis and relatively few treatment options. Given the rising incidence of melanoma and the paucity of effective treatments, there is much hope for targeted therapies and promising agents, including those that act on apoptosis regulating molecules. Herein, we showed a novel role for FKBP51 as a marker of melanocyte malignancy and its involvement in the protection of melanoma against IR-induced apoptosis. Our data showed that FKBP51 counteracts apoptotic processes stimulated by IR by sustaining autophagy, which supports the survival of the tumor cells. FKBP51 is required for NF-κB activation; in fact, FKBP51 silencing prevented the IR-induced nuclear translocation of this transcription factor and activated apoptosis. FKBP51 knocking-down provoked extensive apoptosis also *in vivo*, as showed by the study of tumor sections from melanoma xenografts. Furthermore, we provide evidence that FKBP51 is espressed at high levels in cancer stem/initiating cell of melanoma and that also these cells are killed by IR, after pretreatment with siRNA. This finding suggests that FKBP51 is a suitable target for eliminating such cells responsible for tumor self-renewal and generate the heterogeneous cancer cells that comprise the tumor. The translational implication of our findings was reinforced by the correlation of FKBP51 expression levels with the thickness of the tumor lesion and with prognostic factors.

FKBP51 is a protein with important biological roles in normal cells that acquires a pro-oncogenic potential when its expression is deregulated, which is what occurs in melanoma. Such deregulation sustains survival networks that protect the melanoma against killing. Besides melanoma, FKBP51 is expressed in several other cancers; this opens the door to the development of a novel tumoral biomarker.

ACKNOWLEDGEMENTS

REFERENCES

Alonso A, Zaidi T, Novak M, Grundke-Iqbal I, Iqbal K. Hyperphosphorylation induces self-assembly of tau into tangles of paired helical filaments/straight filaments. Proc Natl Acad Sci USA 2001; 98:6923-28.

Ammirante M, Luo JL, Grivennikov S, Nedospasov S and Karin M. B-cell-derived lymphotoxin promotes castration-resistant prostate cancer. Nature 2010; 464:302-5.

Avellino R, Romano S, Parasole R, Bisogni R, Lamberti A, Poggi V, Venuta S, Romano MF. Rapamycin stimulates apoptosis of childhood acute lymphoblastic leukemia cells. Blood 2005; 106:1400-6.

Baehrecke EH. Autophagy: dual roles in life and death? Nat Rev Mol Cell Biol 2005; 6:505-10. Review.

Balch CM, Soong SJ, Gershenwald JE, Thompson JF, Reintgen DS, Cascinelli N, Urist M, McMasters KM, Ross MI, Kirkwood JM, Atkins MB, Thompson JA, Coit DG, Byrd D, Desmond R, Zhang Y, Liu PY, Lyman GH, Morabito A. Prognostic factors analysis of 17,600 melanoma patients: validation of the American Joint Committee on Cancer melanoma staging system. J Clin Oncol 2001; 19:3622-34.

Baldwin AS Jr. The NF-κB and IκB proteins: new discoveries and insights. Annu Rev Immunol 1996; 14:649-83. Review.

Baughman G, Wiederrecht GJ, Faith Campbell N, Martin MM, Bourgeois S. FKBP51, a novel T-cell specific immunophilin capable of calcineurin inhibition. Mol Cell Biol 1995; 15:4395-4402.

Baughman G, Wiederrecht GJ, Chang F, Martin MM, Bourgeois S. Tissue distribution and abundance of human FKBP51, and FK506-binding protein that can mediate calcineurin inhibition. Biochem Biophys Res Commun 1997. 232:437-443.

Benassi B, Zupi G, Biroccio A. Gamma-glutamylcysteine synthetase mediates the c-Myc dependent response to antineoplastic agents in melanoma cells. Mol Pharmacol 2007; 72:1015-23.

Binder EB, Salyakina D, Lichtner P, Wochnik GM, Ising M, Pütz B, Papiol S, Seaman S, Lucae S, Kohli MA, Nickel T, Künzel HE, Fuchs B, Majer M, Pfennig A, Kern N, Brunner J, Modell S, Baghai T, Deiml T, Zill P, Bondy B, Rupprecht R, Messer T, Köhnlein O, Dabitz H, Brückl T, Müller N, Pfister H, Lieb R, Mueller JC, Lõhmussaar E, Strom TM, Bettecken T, Meitinger T, Uhr M, Rein T, Holsboer F, Muller-Myhsok B. Polymorphisms in FKBP5 are associated with increased recurrence of depressive episodes and rapid response to antidepressant treatment. Nat Genet 2004; 36:1319-25.

Bouwmeester T, Bauch A, Ruffner H, Angrand PO, Bergamini G, Croughton K, Cruciat C, Eberhard D, Gagneur J, Ghidelli S, Hopf C, Huhse B, Mangano R, Michon AM, Schirle M, Schlegl J, Schwab M, Stein MA, Bauer A, Casari G, Drewes G, Gavin AC, Jackson DB, Joberty G, Neubauer G, Rick J, Kuster B, Superti-Furga G. A physical and functional map of the human TNF-alpha/NF-kappaB signal transduction pathway. Nat Cell Biol 2004; 6:97-105.

Brown EJ, Albers MW, Shin TB, Ichikawa K, Keith CT, Lane WS, Schreiber SL. A mammalian protein targeted by G1-arresting rapamycin-receptor complex. Nature 1994; 369:756-58.

Burgering BM, Coffer PJ. Protein kinase B (c-Akt) in phosphatidylinositol-3-OH kinase signal transduction. Nature 1995; 376:599-602.

Catz SD, Johnson JL. Transcriptional regulation of bcl-2 by nuclear factor kappa B and its significance in prostate cancer. Oncogene 2001; 20:7342-51.

Chandler JM, Cohen GM, MacFarlane M. Different subcellular distribution of caspase-3 and caspase-7 following Fas-induced apoptosis in mouse liver. J Biol Chem 1998; 273:10815-818.

Chen AY, Okunieff P, Pommier Y, Mitchell JB. Mammalian DNA topoisomerase I mediates the enhancement of radiation cytotoxicity by camptothecin derivatives. Cancer Res 1997; 57:1529-36.

Cheung J, Smith DF. Molecular chaperone interactions with steroid receptors: an update. Mol Endocrinol 2000; 14:939-46.

Chin L. The genetics of malignant melanoma: lessons from mouse and man. Nat Rev Cancer 2003; 3:559-70.

Choi J, Chen J, Schreiber SL, Clardy J. Structure of the FKBP12-rapamycin complex interacting with the binding domain of human FRAP. Science 1996; 273:239-42.

Copetti T, Bertoli C, Dalla E, Demarchi F, Schneider C. p65/RelA modulates BECN1 transcription and autophagy. Mol Cell Biol 2009; 29:2594-2608.

Dewey WC, Ling CC, Meyn RE. Radiation-induced apoptosis: relevance to radiotherapy. Int J Radiat Oncol Biol Phys 1995; 33:781-796.

Dornan J, Taylor P, Walkinshaw MD. Structures of Immunophilins and their ligand complexes. Curr Top Med Chem 2003; 3:1392-1409. Review.

Elliott A, Reiners Jr JJ. Suppression of autophagy enhances the cytotoxicity of the DNAdamaging aromatic amine p-anilinoaniline. Toxicol Appl Pharmacol 2008; 232:169-179.

Eskelinen EL. New insights into the mechanisms of macroautophagy in mammalian cells. Int Rev Cell Mol Biol 2008; 266:207-47. Review.

Fischer G, Aumüller T. Regulation of peptide bond cis/trans isomerization by enzyme catalysis and its implication in physiological processes. Rev Physiol Biochem Pharmacol 2003; 148:105-50. Review.

Franken NAP, Rodermond HM, Stap J, Haveman J, van Bree C. Clonogenic assay of cells in vitro. Nat Protoc 2006; 1:2315-19.

Gao X, Pan D. TSC1 and TSC2 tumor suppressors antagonize insulin signaling in cell growth. Genes Dev 2001; 15:1383-92.

Giard DJ, Aaronson SA, Todaro GJ, Arnstein P, Kersey JH, Dosik H, Parks WP. In vitro cultivation of human tumors: establishment of cell lines derived from a series of solid tumors. J Natl Cancer Inst 1973; 51:1417-23.

Ghosh S, May MJ, and Kopp EB. NF-κB and Rel proteins: evolutionarily conserved mediators of immune response. Annu Rev Immunol 1998; 16:225-60.

Goedert M, Wischik CM, Crowther RA, Walker JE, Klug A. Cloning and sequencing of the cDNA encoding a core protein of the paired helical filament

of Alzheimer disease: identification as the microtubule-associated protein tau. Proc Natl Acad Sci USA 2000; 85:4051-55.

Habraken Y, Piette J. NF-kappaB activation by double-strand breaks. Biochem Pharmacol 2006; 72:1132-41. Review.

Hengartner MO. The biochemistry of apoptosis. Nature 2000; 407:770-76.

Hennessy BT, Smith DL, Ram PT, Lu Y, Mills GB. Exploiting the PI3K/AKT pathway for cancer drug discovery. Nature Reviews Drug Discovery 2005. 4:988-1004.

Hogan PG, Chen L, Nardone J, Rao A. Trascriptional regulation by calcium, calcineurin and NFAT. Genes Dev 2003; 17:2205-32. Review.

Huang WC, Ju TK, Hung MC, Chen CC. Phosphorylation of CBP by IKKα promotes cell growth by switching the binding preference of CBP from p53 to NF-κB. Molecular Cell. (2007) 26(1):75–87.

Kabeya Y, Mizushima N, Ueno T, Yamamoto A, Kirisako T, Noda T Kominami E, Ohsumi Y, Yoshimori T. LC3, a mammalian homologue of yeast Apg8p, is localized in autophagosome membranes after processing. EMBO J 2000; 19:5720-28.

Karin M, Cao X, Greten FR, Li Z-W. NF-kappaB in cancer: from innocent bystander to major culprit. Nat Rev Cancer 2002; 2:301-10.

Kim H, Rafiuddin-Shah M, Tu HC, Jeffers JR, Zambetti GP, Hsieh JJ, Cheng EH. Hierarchical regulation of mitochondrion-dependent apoptosis by BCL-2 subfamilies. Nat Cell Biol 2006; 8:1348-58.

Komura E, Tonetti C, Penard-Lacronique V, Chagraoui H, Lacout C, Lecouédic JP, Rameau P, Debili N, Vainchenker W and Giraudier S. Role for the nuclear factor kappaB pathway in transforming growth factor-beta1 production in idiopathic myelofibrosis: possible relationship with FK506 binding protein 51 overexpression. Cancer Res 2005; 65:3281-89.

Jiang W, Cazacu S, Xiang C, Zenklusen JC, Fine HA, Berens M, Armstrong B, Brodie C, Mikkelsen T. FK506 binding protein mediates glioma cell growth

and sensitivity to rapamycin treatment by regulating NF-kappaB signaling pathway. Neoplasia 2008; 10:235-43.

Jinwal UK, Koren J 3rd, Borysov SI, Schmid AB, Abisambra JF, Blair LJ, Johnson AG, Jones JR, Shults CL, O'Leary JC 3rd, Jin Y, Buchner J, Cox MB, Dickey CA. The Hsp90 cochaperone, FKBP51, increases Tau stability and polymerizes microtubules. J Neurosci 2010; 30:591-99.
Liu TM, Martina M, Hutmacher DW, Hui JH, Lee EH, Lim B. Identification of common pathways mediating differentiation of bone marrow- and adipose tissue- derived human mesenchymal stem cells into three mesenchymal lineages. Stem cells 2007; 25:750-60.

Lopes de Menezes DE, Hu Y, Mayer LD. Combined treatment of Bcl-2 antisense oligodeoxynucleotides (G3139), p-glycoprotein inhibitor (PSC833), and sterically stabilized liposomal doxorubicin suppresses growth of drug-resistant growth of drug-resistant breast cancer in severely combined immunodeficient mice. J Exp Ther Oncol 2003; 3:72-82.

Mathew R, Karantza-Wadsworth V, White E. Role of autophagy in cancer. Nat Rev Cancer 2007; 7:961-67.

Menicanin D, Bartold PM, Zannettino AC, Gronthos S. Genomic profiling of mesenchymal stem cells. Stem Cell Rev 2009; 5:36-50. Review.

Monzani E, Facchetti F, Galmozzi E, Corsini E, Benetti A, Cavazzin C, Gritti A, Piccinini A, Porro D, Santinami M, Invernici G, Parati E, Alessandri G, La Porta CA. Melanoma contains CD133 and ABCG2 positive cells with enhanced tumourigenic potential. Eur J Cancer 2007; 43:93546.

Munshi A, Kurland JF, Nishikaw T, Chiao PJ, Andreeff M, Meyn RE. Inhibition of constitutively activated nuclear factor-kappaB radiosensitizes human melanoma cells. Mol Cancer Ther 2004; 3:98592.

Norris LB, Beam S. Multidisciplinary perspectives on melanoma treatment. Updates from the 44th Annual Meeting of the American Society of Clinical Oncology, The Oncology Nurse 2008; 1:1-7.

Ogata M, Hino S, Saito A, Morikawa K, Kondo S, Kanemoto S, Murakami T, Taniguchi M, Tanii I, Yoshinaga K, Shiosaka S, Hammarback JA, Urano F, Imaizumi K. Autophagy is activated for cell survival after endoplasmic reticulum stress. Mol Cell Biol 2006; 26:9220-31.

Periyasamy S, Hinds T Jr, Shemshedini L, Shou W, Sanchez ER. FKBP51 and Cyp40 are positive regulators of androgen-dependent prostate cancer cell growth and the targets of FK506 and cyclosporin A. Oncogene 2010; 29:1691-1701.

Romano MF, Avellino R, Petrella A, Bisogni R, Romano S, Venuta S. Rapamycin inhibits doxorubicin-induced NF-kappaB/Rel nuclear activity and enhances the apoptosis of melanoma cells. Eur J Cancer 2004; 40:2829-36.

Romano MF, Romano S, Mallardo M, Bisogni R, Venuta S. Rapamycin Controls Multiple Signalling Pathways Involved in Cancer Cell Survival. Trends in Cell Apoptosis Research, ISBN 1-60021-424-X, Editor: Herold C. Figgins, 2006 Nova Science Publishers, Inc.

Romano S, D'Angelillo A, Pacelli R, Staibano S, De Luna E, Bisogni R, Eskelinen EL, Mascolo M, Calì G, Arra C, Romano MF. Role of FK506-binding protein 51 in the control of apoptosis of irradiated melanoma cells. Cell Death Differ 2010; 17:145-57

Sabatini DM. mTOR and cancer: insights into a complex relationship. Nat Rev Cancer 2006; 6:729-34. Review.

Sinars CR, Cheung-Flynn J, Rimerman RA, Scammell JG, Smith DF, Clardy J. Structure of the large FK506-binding protein FKBP51, an Hsp90-binding protein and a component of steroid receptor complexes. Proc Natl Acad Sci USA 2003; 100:868-73.

Schmelzle T, Hall MN. TOR, a central controller of cell growth. Cell 2000; 103:253-62.

Somarelli JA, Lee SY, Skolnick J, Herrera RJ. Structure-based classification of 45 FK506-binding proteins. Proteins 2008; 72:197-208.

Staibano S, Pepe S, Lo Muzio L, Somma P, Mascolo M, Argenziano G. Poly(adenosine diphosphate-ribose) polymerase 1 expression in malignant melanomas from photoexposed areas of the head and neck region. Hum Pathol 2005; 36:724-31.

Trotta PP, Harrison Jr SD. Evaluation of the antitumor activity of recombinant human gamma-interferon employing human melanoma xenografts in athymic nude mice. Cancer Res 1987; 47:5347-53.

Vaziri SA, Grabowski DR, Tabata M, Holmes KA, Sterk J, Takigawa N, Bukowski RM, Ganapathi MK, Ganapathi R. c-IAP1 is overexpressed in HL-60 cells selected for doxorubicin resistance: effects on etoposide-induced apoptosis. Anticancer Res 2003. 23:3657-61.

Vittorioso P, Cowling, R, Faure JD, Caboche M, Bellini C. Mutation in the Arabidopsis PASTICCINO1 gene, which encodes a new FK506-binding protein-like protein, has a dramatic effect on plant development. Molecular and Cellular biology 1998; 18:3034-43.

Wallace SS. DNA damages processed by base excision repair: biological consequences. Int J Radiat Biol 1994; 66:579-89.

Watowich SS, Wu H, Socolovsky M, Klingmuller U, Constantinescu SN, Lodish HF. Cytokine receptor signal transduction and the control of hematopoietic cell development. Ann Rev Cell Develop Biol 1996; 12:91-128. Review.

Wu MX, Ao Z, Prasad KVS, Wu R, Schlossman SF: IEX-1L, an apoptosis inhibitor involved in NF-kappaB-mediated cell survival. Science 1998; 281:998-99.

Wu H, Goel V and Haluska FG. PTEN signaling pathways in melanoma. Oncogene 2003; 22:3113-22. Review.

Wu X, Senechal K, Neshat MS, Whang YE; Sawyers CL. The PTEN/MMAC1 tumor suppressor phosphatase functions as a negative regulator of the phosphoinositide 3-kinase/Akt pathway. Proc Natl Acad Sci U S A 1998; 95:15587-91.

Xiao G, Harhaj EW, Sun SC. NF-kappaB-inducing kinase regulates the processing of NF-kappaB2 p100. Mol Cell 2001; 7:401-9.

Yeh WC, Bierer BE, McKnight SL. Rapamycin inhibits clonal expansion and adipogenic differentiation of 3T3-L1 cells. Proc Natl Acad Sci U S A 1995; 92:11086-190.

Yeh WC, Li TK, Bierer BE, McKnight SL. Identification and characterization of an immunophilin expressed during the clonal expansion phase of adipocyte differentiation. Proc Natl Acad Sci U S A 1995; 92:11081-5.

Zhang T, Xiong H, Kan LX, Zhang CK, Jiao XF, Fu G, Zhang QH, Lu L, Tong JH, Gu BW, Yu M, Liu JX, Licht J, Waxman S, Zelent A, Chen E, Chen J. Genomic sequence, structural organization, molecular evolution and abberrant rearrangement of promyelocytic leukemia zinc finger gene. Proc Natl Acad Sci U S A 1999; 96:11422-27.

Rapamycin inhibits doxorubicin-induced NF-κB/Rel nuclear activity and enhances the apoptosis of melanoma cells[☆]

Maria Fiammetta Romano [a,*], Raffaella Avellino [a], Antonello Petrella [b], Rita Bisogni [a], Simona Romano [a], Salvatore Venuta [c]

[a] *Department of Biochemistry and Medical Biotechnologies, Federico II University,Via S. Pansini, 5, 80131 Naples, Italy*
[b] *DIFARMA, University of Fisciano, Via Ponte don Melillo, 84084 Fisciano, Salerno, Italy*
[c] *Department of Clinical and Experimental Medicine, Magna Graecia University, 88100 Catanzaro, Italy*

Abstract

Inhibition of nuclear factor (NF)-κB/Rel can sensitise many tumour cells to death-inducing stimuli, including chemotherapeutic agents, and there are data suggesting that disruption of NF-κB may be of therapeutic interest in melanoma. We found that rapamycin sensitised a human melanoma cell line, established from a patient, to the cytolytic effects of doxorubicin. Doxorubicin is a striking NF-κB/Rel-inducer, we therefore investigated if rapamycin interfered with the pathway of NF-κB/Rel activation, i.e. IκBα-phosphorylation, -degradation and NF-κB/Rel nuclear translocation, and found that the macrolide agent caused a block of IKK kinase activity that was responsible for a reduced nuclear translocation of transcription factors. Western blots for Bcl-2 and c-IAP1 showed increased levels of these anti-apoptotic proteins in cells incubated with doxorubicin, in accordance with NF-κB/Rel activation, while rapamycin clearly downmodulated these proteins, in line with its pro-apoptotic ability. The effect of the macrolide on NF-κ B/Rel induction appeared to be independent of the block in the PI3k/Akt pathway, because it could not be reproduced by the phosphatidyl inositol 3 kinase (PI3k) inhibitor, wortmannin. Recently, the immunophilin, FKBP51, has been shown to be essential for the function of IKK kinase. We found high expression levels of FKBP51 in melanoma cells. Moreover, we confirmed the involvement of this immunophilin in the control of IKK activity. Indeed, IκBα could not be degraded when FKBP51 was downmodulated by short-interfering RNAs (siRNAs). These findings provide a possible mechanism for the downmodulation of NF-κB by rapamycin, since the macrolide agent specifically inhibits FKBP51 isomerase activity. In conclusion, our study demonstrates that rapamycin blocked NF-κB/Rel activation independently of PI3k/Akt inhibition suggesting that the macrolide agent could synergise with NF-κB-inducing anti-cancer drugs in PTEN-positive tumours.
© 2004 Elsevier Ltd. All rights reserved.

Keywords: NF-κB/Rel; Apoptosis; Rapamycin; Melanoma

1. Introduction

Rapamycin, a conventional immunosuppressant agent that is used to prevent immunological rejection in organ transplantations, has recently been shown to have anti-cancer effects, decreasing cell proliferation and increasing apoptosis [1–3]. Its anti-cancer activity is classically ascribed to its binding to FKBP12 [4] and forming a complex that inhibits the serine/threonine kinase – mammalian target of rapamycin (mTOR) [5–7]. mTOR, in response to growth factors, hormones, [8,9] mitogens and amino acids [9–11] is activated through the phosphatidyl inositol 3 kinase (PI3k) (PI3k)/Akt cascade [8,9] and regulates protein translation, cell cycle progression and cellular proliferation

[9–11]. Rapamycin was found to inhibit the oncogenic transformation of human cells induced by either PI3k or Akt [12]. Thus, it is expected to act as an anti-cancer agent, in neoplasias that lack the tumour suppressor gene, PTEN [13]. This gene encodes a lipid and protein phosphatase that, by reducing the cellular levels of phosphatidylinositol triphosphate, antagonises the action of PI3k [14–17]. Nevertheless, data suggests rapamycin inhibits the induction of NF-κB/Rel after different stimuli in various cell types [18–20]. In addition, these findings have recently been strongly supported by the discovery that the rapamycin-binding immunophilin, FKBP51, is an important cofactor of the IKK-α subunit of the IκB-kinase (IKK) complex [21]. NF-κB transcriptional activity is normally inhibited by IκB proteins that sequester it in the cytoplasm [22]. The 700–900 kD IKK complex phosphorylates two critical serine residues (S32 and S36) in IκBs, triggering events that lead to the proteolytic degradation of these inhibitors [23,24], and thereby allowing nuclear translocation of NF-κB/Rel proteins. Active NF-κB factors modulate the expression of a number of genes that sustain cell survival [25–28] and it is widely described that inhibition of this transcriptional activity sensitises many tumour cells to death-inducing stimuli, including chemotherapeutic agents [26,29,30]. Data suggesting that rapamycin was able to inhibit the NF-κB/Rel nuclear activity induced by CD28 in Jurkat cells [18], by insulin in myoblasts [19] and by lipopolysaccharide (LPS) in rat hepatocytes [20], prompted us to investigate if this macrolide agent might, also inhibit chemotherapy induced-NF-κB and overcome drug resistance in aggressive tumours, such as melanoma. Indeed, melanomas are known to be poorly responsive to current anti-cancer drugs, but disruption of NF-κB has been shown to be of therapeutic utility [30]. To this end, we utilised the anthracycline drug, doxorubicin, that activates NF-κB/Rel transcription factors [31] and studied whether rapamycin was able to inhibit the induction of NF-κB/Rel and promote apoptosis in a human melanoma cell line established from a patient.

2. Materials and methods

2.1. Cells and reagents

A melanoma cell line was established from a patient's primary tumour and was provided by Dr. Gabriella Zupi (Experimental Preclinic Laboratory, Regina Elena Institute for Cancer Research, Roma, Italy). Cells were cultured in Roswell Park Memorial Institute (RPMI) 1640 medium (ICN Biomedicals, Ohio, USA) supplemented with 10% heat-inactivated foetal calf serum (FCS) (v/v), glutamine and antibiotics at 37 °C in a 5% CO_2 humified atmosphere. Purified primary T lymphocytes were ob-

tained from heparinised fresh peripheral blood of healthy donors by a two step-centrifugation, first through a Ficoll–Hipaque (ICN Biomedicals, Ohio, USA) and second 50% Percoll (v/v) (ICN Biomedicals, Ohio, USA) density gradient. The purified cells were >93% $CD3^+$. Rapamycin (Rapamune, Wyeth Ayerst Laboratories. Marietta, PA), doxorubicin hydrochloride (Sigma–Aldrich. St. Louis, Missouri) and wortmannin (Sigma–Aldrich) were used at the concentrations indicated. Cells were preincubated for 20 h with rapamycin or wortmannin before adding doxorubicin.

2.2. Analysis of cell death

For analysis of cell viability, the MTT (methylthiazoletetrazolium) test was performed as described in [32]. Absorbance was measured at 550 nm using a microplate spectrophotometer. The mean of the absolute absorbance values of the treated samples was divided by the absolute absorbance of the control samples and expressed as the % of cell viability. Caspase 3 activity was analysed using the Caspase-3 Fluorometric Assay Kit (Perbio Science, Belgium) according to the manufacturer's instructions. Cells (2×10^5) were lysed in a buffer containing 10 mM Tris (pH 7.5), 130 mM NaCl, 1% Triton X-100 (v/v), 10 mM NaPi, 10 mM NaPPi; then 50 μg of protein was analysed. Analysis of apoptosis by propidium iodide incorporation was performed using permeabilised cells by flow cytometric analysis. Cells (2×10^4) were harvested 24 h after the addition of doxorubicin to the cultures, washed in phosphate-buffered solution (PBS) and resuspended in 500 μl of a solution containing 0.1% sodium citrate (w/v), 0.1% Triton X-100 (v/v) and 50 μg/ml propidium iodide (Sigma Chemical Co., Gallarate, Italy). Following incubation at 4 °C for 30 min in the dark, cell nuclei were analysed using a Becton Dickinson FACScan flow cytometer. Cellular debris was excluded from the analysis by raising the forward scatter threshold, and the DNA content of the nuclei was registered on a logarithmic scale. The percentage of the elements in the hypodiploid region was calculated.

2.3. IKK immunoprecipitation and kinase assay

Melanoma cells (1×10^6), preincubated or not with rapamycin (100 ng/ml), were cultured in the absence or presence of doxorubicin (10 μM). After a 5-h incubation, cells were harvested, washed and lysed in a buffer containing 20 mM HEPES, pH 7.4, 150 mM NaCl, 10% glycerol (v/v), 1% Triton X-100 (v/v), 1 mM Na3V04, 20 mM β-glycerophosphate, 1 mM NaF and a complete protease inhibitor mixture (Roche). After a 30-min incubation on ice, the lysates were cleared by centrifugation for 15 min at 4 °C at 14 000 rotations per minute (rpm). Endogenous IKK was immunoprecipitated using an anti-IKK antibody H470 (Santa Cruz Biotechnology) plus protein A-

agarose and the kinase activity was assayed using gluta-thione-*S*-transferase (GST)–IκB (Santa Cruz Biotechnology) as a substrate, as described in [33]. Briefly, 500 μg of immunoprecipitate was incubated with kinase buffer (20mM HEPES, pH 7.4, 10 mM MgCl$_2$, 25 mM β-glycerophosphate, 1 mM dithiothreitol (DTT), 1 mM Na3V04) in the presence of 0.1 mM adenosine triphosphate (ATP), [γ-^{32}P]ATP and GST–IκB. After a 10-min incubation at 37 °C, the reactions were terminated by boiling in sodium dodecylsulphate (SDS) sample buffer, and the products were resolved by 10% SDS–polyacrylamide (w/v) gel electrophoresis. Phosphorylated proteins were detected by autoradiography.

2.4. Cell lysates and Western blotting analysis

For detection of IkBα, cytosolic extracts were obtained from 1×10^6 cells resuspended in 100 μl of lysis buffer (10 mM HEPES, pH 7.9, 1 mM ethylene diamine tetra acetic acid (EDTA), 60 mM KCl, 1 mM DTT, 1 mM phenyl methyl sulphonyl fluoride (PMSF), 50 μg/ml antipain, 40 μg/ml bestatin, 20 μg/ml chymostatin, 0.2% (v/v) Nonidet P-40) for 15 min in ice. For detection of Bcl-2, c-IAP1 and FKBP51, whole cell lysates were prepared by homogenisation in modified RIPA buffer (150 mM sodium chloride, 50 mM Tris–HCl, pH 7.4, 1 mM EDTA, 1 mM PMSF, 1% Triton X-100 (v/v), 1% sodium deoxycholic acid (w/v), 0.1% SDS (w/v), 5 μg/ml of aprotinin and 5 μg/ml of leupeptin). Cell debris was removed by centrifugation. Protein concentrations were determined using the Bio-Rad protein assay. The cell lysate was boiled for 5 min in 1× SDS sample buffer (50 mM Tris–HCl pH 6.8, 12.5% glycerol, 1% SDS (w/v), 0.01% bromophenol blue (w/v)) containing 5% β-mercaptoethanol, run on 10% SDS (w/v) polyacrylamide gel, transferred onto a membrane filter (Cellulosenitrate, Schleider and Schuell) and finally incubated with the primary antibody. Anti-human-antibodies against IκB α (a rabbit polyclonal antibody from Santa Cruz Biotechnology), Bcl-2 (a mouse monoclonal antibody from Santa Cruz Biotechnology), c-IAP1 (a mouse monoclonal antibody from BD Pharmingen), FKBP51 (a rabbit polyclonal antibody from Abcam Limited, UK) were used at a dilution of 1:500. After a second incubation with peroxidase-conjugated goat anti-rabbit IgG (Santa Cruz Biotechnology) or anti-mouse IgG (Santa Cruz Biotechnology), the blots were developed using the enhanced chemiluminescence (ECL) system (Amersham Pharmacia Biotech).

2.5. Nuclear extracts, electrophoretic mobility shift assay (EMSA), and oligonucleotides

Cell nuclear extracts were prepared from 1×10^6 cells by homogenisation of the cell pellet in two volumes of 10 mM HEPES, pH 7.9, 10 mM KCl, 1.5 mM MgCl$_2$, 1 mM EDTA, 0.5 mM DTT, 0.5 mM PMSF and 10% glyc-

erol (v/v). Nuclei were centrifuged at 1000*g* for 5 min, washed and resuspended in two volumes of the above specified solution. KCl (3M) was added until the concentration reached 0.39 M KCl. Nuclei were extracted at 4 °C for 1 h and centrifuged at 10 000*g* for 30 min. The supernatants were clarified by centrifugation and stored at −80 °C. Protein concentrations were determined using the Bradford method. The NF-κB consensus 5′-CAACGG-CAGGGGAATCTCCCTCTCCTT-3′ oligonucleotide [34] was end-labelled with [γ-^{32}P] adenosine triphosphate (ATP) (Amersham) using a polynucleotide kinase (Roche). End-labelled DNA fragments were incubated at room temperature for 20 min with 5 μg of nuclear protein, in the presence of 1 μg poly(dI–dC), in 20 μl of a buffer consisting of 10 mM Tris–HCl, pH 7.5, 50 mM NaCl, 1 mM EDTA, 1 mM DTT and 5% glycerol (v/v). In supershifting experiments, rabbit antibodies against the C-terminal peptide (529–551) of human p65 or against the N-terminal peptide (1–21) of p105/p50 (kindly provided by Dr. Warner C. Greene, Gladstone Institute of Virology and Immunology, San Francisco, CA) were added to the incubation mixture. Protein–DNA complexes were separated from the free probe on a 6% polyacrylamide (w/v) gel run in 0.25× Tris borate buffer at 200 mV for 3 h at room temperature. The gels were dried and exposed to X-ray film (Kodak AR).

2.6. Transfection of siRNA

Twenty-four hours before transfection with short-interfering RNA (siRNA) oligonucleotide corresponding to the target sequence 5′-ACCUAAUGCUGAGCU-DAU-3′ of the sense-strand of human FKBP51 (Dharmacon Research Inc.) or a scrambled duplex as a control (Dharmacon Research Inc.), cells were seeded into six-well plates in medium without antibiotics at a concentration of 2.5×10^5/ml, to obtain 30–50% confluence at the time of transfection. The siRNA or the scrambled oligo were transfected at a final concentration of 50 nM using Oligofectamine (Invitrogen) according to the manufacturer's recommendations. After 3 days, the cells were processed for Western blotting analysis.

2.7. Statistical analysis

Statistical analysis of the results was performed by the Student's *t* test.

3. Results

3.1. Rapamycin enhanced doxorubicin-induced apoptosis in human melanoma cells

Melanoma tumours are poorly responsive to the cytotoxic effects of doxorubicin [30]. We found that

rapamycin greatly enhanced the amount of cell death induced by the anthracycline in melanoma cells. Analysis of cell viability by the MTT assay showed that $84.4 \pm 6.1\%$ of doxorubicin-treated cells were still alive after 16 h of incubation. As shown in Fig. 1, Panel (a), rapamycin alone did not substantially affect melanoma cell survival, while in the presence of doxorubicin, the macrolide agent reduced cell viability to $56.3 \pm 0.1\%$. Analysis of caspase 3 activity confirmed that rapamycin alone did not activate the apoptotic process in melanoma cells. Indeed, the levels of active caspase 3 in cells

cultured in RPMI with or without rapamycin were comparable and <6 U/ml. Fig. 1, Panel (b) shows the kinetics of caspase 3 activation in cells cultured with doxorubicin, with or without rapamycin. We found that the anthracycline drug alone produced an eightfold increase in the basal caspase 3 activity, while the addition of rapamycin produced a further 25% increase after a 8-h incubation. Analysis of apoptosis by propidium iodide incorporation and flow cytometry, revealed that doxorubicin induced $34.3\% \pm 8.2$ apoptosis after 24 h in the absence of rapamycin and $55.9\% \pm 9.3$ when the macro-
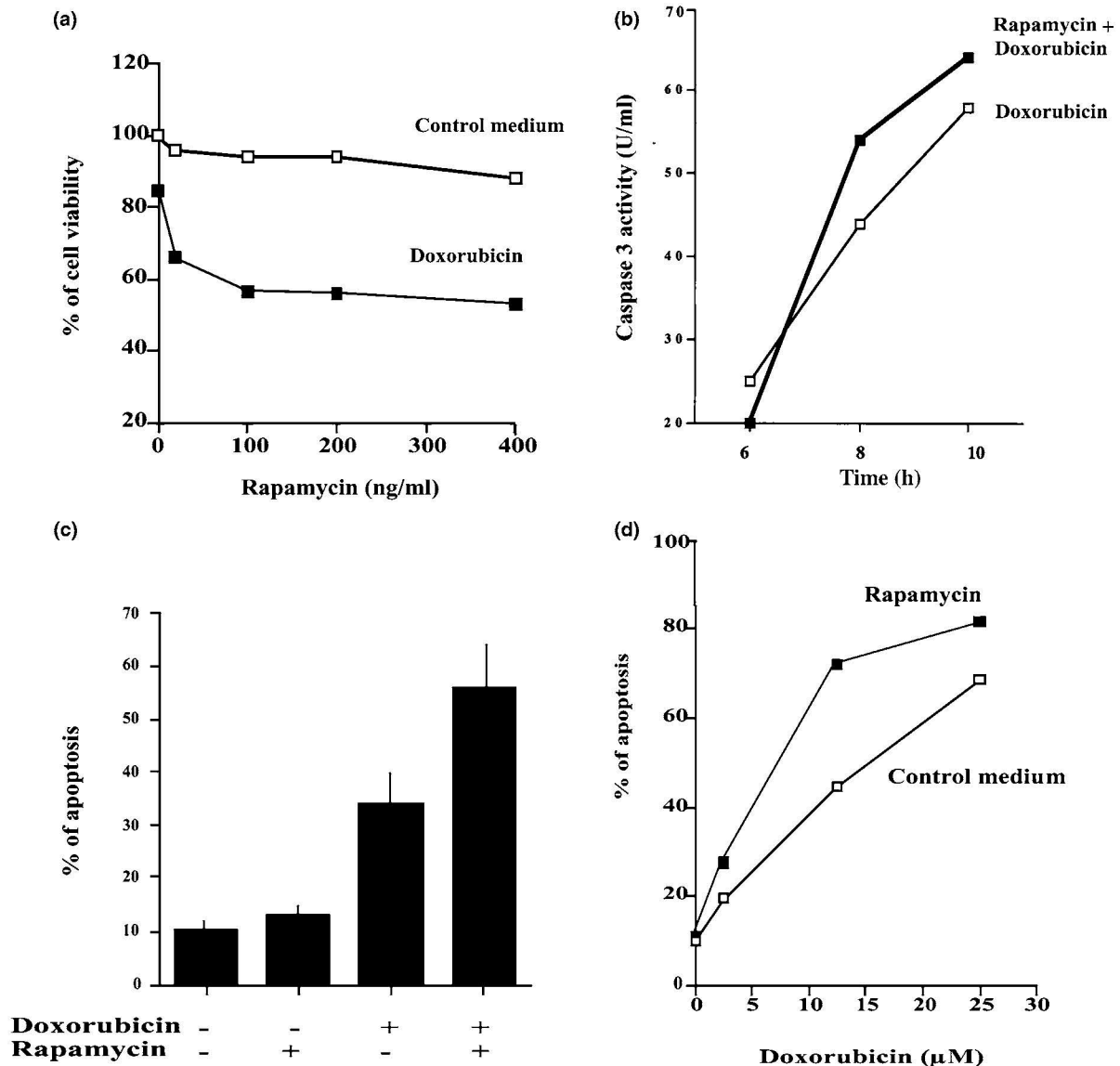

Fig. 1. Rapamycin enhances doxorubicin-induced apoptosis in human melanoma cells. (Panel (a)) Cells, preincubated or not with rapamycin at the indicated doses, were cultured in the absence or the presence of 10 μM doxorubicin. After a 16-h incubation, cell viability was analysed by the methylthiazoletetrazolium (MTT) assay. (Panel (b)) Cells, preincubated or not with rapamycin (100 ng/ml), were cultured with 10 μM doxorubicin. After 6, 8 and 10 h, cells were harvested and the lysates obtained were analysed using a fluorometric assay to detect caspase 3 activation. (Panel (c)) Cells, preincubated or not with rapamycin (100 ng/ml), were cultured in the absence or the presence of 10 μM doxorubicin. After a 24-h incubation, cells were harvested and an analysis of the amount of apoptosis was performed by propidium iodide incorporation and flow cytometry. (Panel (d)) Cells, preincubated or not with rapamycin (100 ng/ml), were cultured in the absence or the presence of doxorubicin at the indicated doses. After 24 h of incubation, cells were harvested and an analysis of apoptosis was performed by propidium iodide incorporation and flow cytometry.

lide was added to the cultures ($P = 0.042$) (Fig. 1, panel (c)). A dose–response curve of doxorubicin-induced apoptosis and its modulation by rapamycin is shown in Fig. 1, panel (d). Results represented in Fig. 1, were obtained in four different experiments, each performed in triplicate.

3.2. Doxorubicin induced NF-κB/Rel nuclear activation in human melanoma cells

The response of the cells to anthracyclines is modulated by activation of NF-κB/Rel transcription factors [31]. Western blots and EMSA verified that doxorubicin induced, IκB α degradation and NF-κB/Rel nuclear translocation, in the melanoma cells (Fig. 2, panels (a) and (b)). IκBα degradation was detected after a 3-h incubation and was complete after 5 h. Analysis of the NF-κB/Rel complexes by supershifting showed mainly p50/p65 heterodimers (Fig. 2, panel (b)).

3.3. Rapamycin inhibited doxorubicin-induced NF-κB/Rel activation in human melanoma cells

To investigate if the pro-apoptotic effect of rapamycin on doxorubicin-induced apoptosis could be related to the inhibition of cell survival pathways governed by
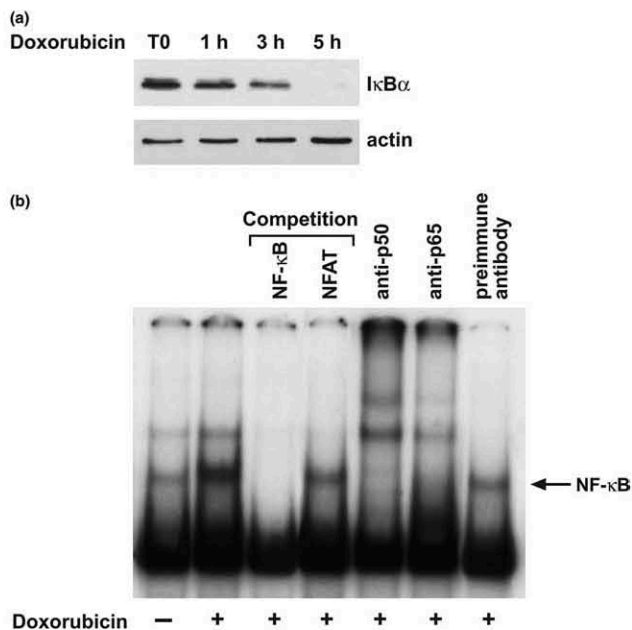

Fig. 2. Doxorubicin induces NF-κB/Rel activation in human melanoma cells. (Panel (a)) Western blotting analysis of IκB α protein. Cells were cultured in the presence of 10 μM doxorubicin and after 1-, 3-, 5-h of incubation were harvested and cytosolic extracts were obtained. (Panel (b)) electrophoretic mobility shift assay (EMSA) analysis of nuclear extracts obtained from human melanoma cells cultured in the absence or the presence of 10 μM doxorubicin for 5 h. A competition assay with the indicated cold oligos demonstrated the specificity of NF-κB band. Supershifting analysis showed the presence of p50/p65 heterodimers.
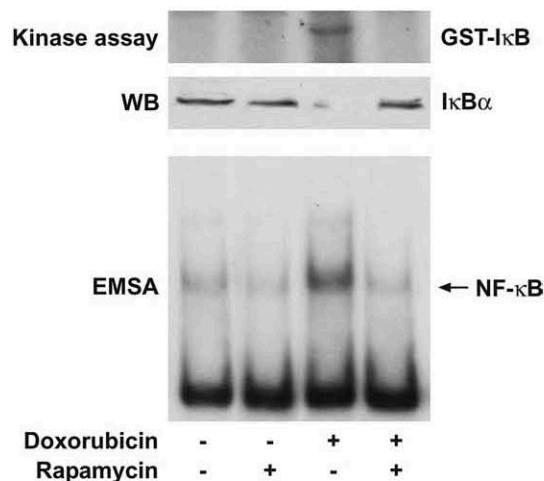

Fig. 3. Rapamycin inhibits doxorubicin-induced IκBα phosphorylation and degradation and NF-κB/Rel nuclear translocation. Melanoma cells, preincubated or not with rapamycin (100 ng/ml), were cultured in the absence or presence of 10 μM doxorubicin. After a 5-h incubation, cells were harvested and lysates were analysed using a IKK kinase assay to detect phosphorylated-IκBα, or by Western blotting to verify IkBα degradation. Nuclear extracts were also analysed by EMSA to detect NF-κB/Rel nuclear translocation.

NF-κB/Rel transcription factors, we first analysed the effect of rapamycin on the NF-κB/Rel nuclear activity induced by doxorubicin. We incubated cells, pretreated or not with rapamycin, in the absence or the presence of doxorubicin and after 5 h obtained nuclear- and cytosolic-extracts. Then, we analysed the catalytic activity of the IKK kinase complex using a kinase assay and, at the same time, investigated IκBα degradation and NF-κB/Rel nuclear translocation by Western blotting analysis and EMSA, respectively. Fig. 3 shows that rapamycin inhibited the phosphorylation of the IκB substrate, the degradation of IkB α and the nuclear translocation of NF-κB/Rel complexes induced by doxorubicin.

3.4. Rapamycin downmodulated the levels of Bcl-2 and c-IAP1

Among the NF-κB/Rel-regulated genes, Bcl-2 [24] and c-IAP1 [25] have been implicated in the resistance of tumour cells to the cytotoxic effects of doxorubicin [35,36]. For this reason, we investigated if rapamycin could sensitise melanoma cells to anthracycline-cytotoxicity through a decrease in the levels of these anti-apoptotic proteins. Western blotting analysis of cell lysates obtained after 6 h of culturing showed that doxorubicin upregulated Bcl-2 and c-IAP1 expression levels in melanoma cells, but to a lesser extent in the presence of rapamycin (Fig. 4). Although several reports suggest that anti-apoptotic members of Bcl-2-family could be stimulated through PI3k/Akt activation [37], analysis of phosphorylated-Akt at Thr308 or Ser473 did not reveal an increase of Akt activation following doxorubicin
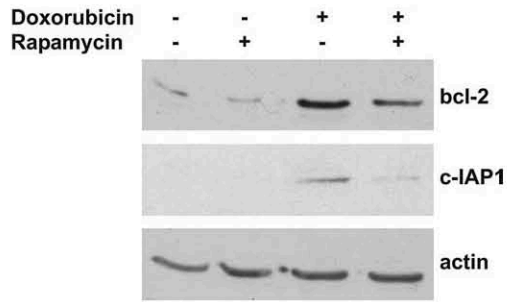
Fig. 4. Rapamycin counteracts the doxorubicin-induced increase in Bcl-2 and c-IAP1 expression levels Melanoma cells, preincubated or not with rapamycin (100 ng/ml), were cultured in the absence or presence of 10 μM doxorubicin. After a 6-h incubation, whole cell lysates were obtained and subjected to Western blotting for the detection of Bcl-2 and c-IAP1.
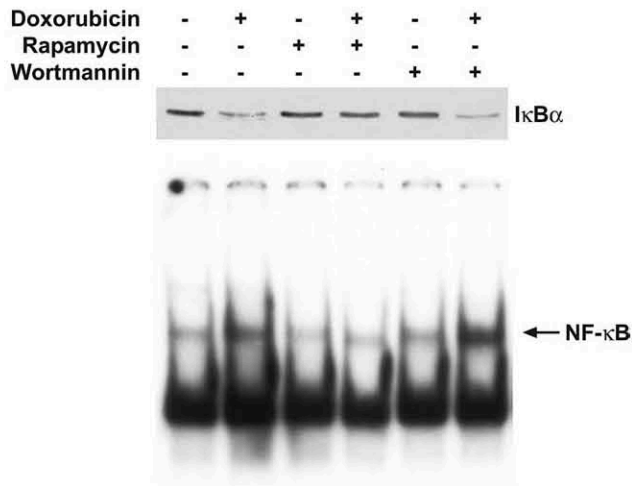

Fig. 5. Wortmannin does not inhibit doxorubicin-induced NF-κB/Rel activation. Melanoma cells, preincubated or not with rapamycin (100 ng/ml) or wortmannin (10 μM), were cultured in the absence or the presence of 10 μM doxorubicin. After a 5-h incubation, cells were harvested and cytosolic or nuclear extracts for Western blotting and EMSA analysis respectively, were obtained.

treatment (data not shown). Thus, their upregulation was apparently related to NF-κB/Rel activation. These results suggest that the doxorubicin-induced NF-κB/Rel activation in melanoma cells resulted in an increase in the expression of anti-apoptotic genes, namely Bcl-2 and c-IAP1, and this was responsible for the poor cytotoxic effects of the drug. By contrast, rapamycin, by counteracting the NF-κB/Rel nuclear translocation, decreased the levels of these proteins, thereby enhancing apoptosis, in these cells.

3.5. PI3K/Akt pathway inhibition was not involved in the NF-κB/Rel downmodulation produced by rapamycin

To verify if the inhibition of NF-κB/Rel activation was due to inhibition of the PI3K/Akt/mTOR pathway, we investigated if the PI3K inhibitor wortmannin was able to antagonise IκB α degradation and NF-κB/Rel nuclear translocation in response to doxorubicin. Fig. 5 shows that wortmannin could not inhibit doxorubicin-induced NF-κB/Rel nuclear translocation and IkB α degradation. Thus, we conclude that the downmodulation of NF-κB/Rel activity is independent of the inhibition of the phosphatidylinositol triphosphate kinase pathway. These findings suggest that rapamycin could synergise with anti-cancer drugs that activate NF-κB/Rel transcription factors in PTEN-positive tumours.

3.6. The rapamycin-binding protein FKBP51, is expressed at high levels in melanoma cells and is involved in the NF-κB signalling pathway

FKBP51 has been cloned in T lymphocytes, where it appears to be particularly abundant [39]. This immunophilin displays a peptidyl-prolyl-isomerase activity that has been shown to be essential for the function of IKK-α [21]. Rapamycin binds very specifically to this protein and inhibits the isomerase activity [39]. Fig. 6,
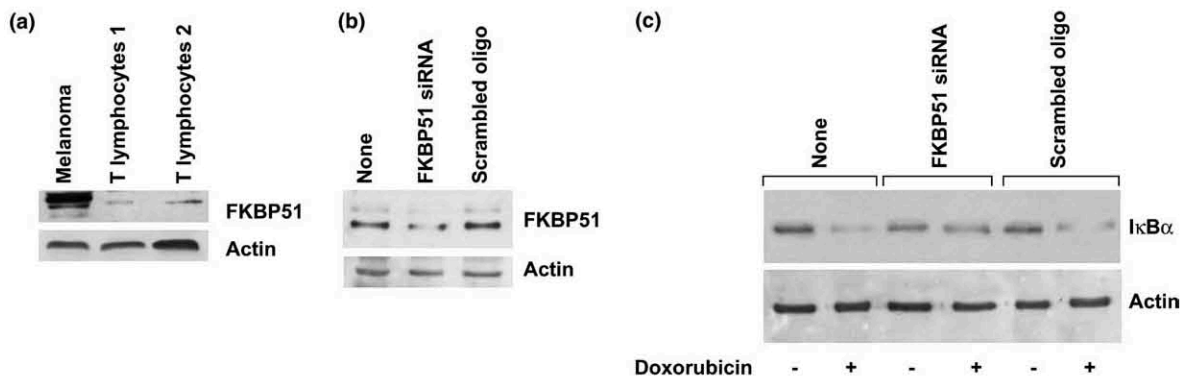

Fig. 6. FKBP51 is expressed at high levels in melanoma cells and is involved in the NF-κB signalling pathway (Panel (a)) Western blotting analysis of FKBP51 expression levels in cell lysates (20 μg) obtained from the melanoma cell line and two different preparations of purified primary T lymphocytes. (Panel (b)) Western blotting analysis of FKBP51 expression levels of cell lysates (2.5 μg) obtained from the melanoma cell line transfected or not with FKBP51 short interfering RNA (siRNA) or the scrambled oligo as a control. (Panel (c)) Western blotting analysis of IκB α expression levels of cells transfected with FKBP51 siRNA and cultured with or without doxorubicin (10 μM).

panel (a) shows that FKBP51 is expressed at high levels in melanoma cells in comparison to two different preparations of purified primary T lymphocytes. To investigate the role of FKBP51 in the NF-κB activation pathway, we downmodulated the immunophilin using a siRNA approach. As is shown in Fig. 6, panel (b), cells transfected with FKBP51 siRNA displayed a striking decrease in their protein expression levels, compared with cells incubated with control medium or transfected with a scrambled oligo. We then verified if doxorubicin was still able to induce IκBα degradation in the presence of low FKBP51 levels. Fig. 6, panel (c) shows that IκBα disappeared in control- or scrambled-oligo-transfected cells cultured with doxorubicin, according to its degradation, while it did not in the FKBP51 siRNA-transfected cells. These experiments suggest that FKBP51 is synthesised in melanoma cells and controls IKK activity in this tumour.

4. Discussion

Both the PI3k/Akt- and NF-κB/Rel pathways are involved in oncogenic processes and promote cell survival following stimuli which lead to cell death [12–14,25–29]. The inhibitory effect of rapamycin on the downstream effectors of the phosphatidylinositol triphosphate pathway is well known [1–13]. Herein, we demonstrated that rapamycin downregulated the NF-κB/Rel activation induced by doxorubicin, independently of PI3k/Akt inhibition. Furthermore, we showed that the macrolide agent was able to sensitise poorly responsive human melanoma cells [30] to anthracycline-triggered apoptosis, apparently by antagonising the induction of the anti-apoptotic genes, Bcl-2 and c-IAP1, that are under NF-κB control. Several reports suggest that anti-apoptotic members of the Bcl-2-family can be upregulated by PI3k/Akt [37]. However, analysis of phosphorylated-Akt at Thr308 or Ser473 did not reveal an increase of phospho-Akt following doxorubicin stimuli (data not shown), thus the increased Bcl-2 and c-IAP1 protein expression levels appeared to be related to NF-κB/Rel activation. A critical step in the activation of NF-κB is the phosphorylation of IκB proteins by the IKK complex targeting them for degradation by the proteasome [38]. We analysed the pathway of doxorubicin-induced NF-κB activation, from I κBα phosphorylation to nuclear translocation of the transcription factors and found that rapamycin inhibited IKK kinase activity. Recently, an integrated approach of proteomic NF-κB pathway mapping detected new components involved in this signal transduction pathway [21]. Among them, FKBP51, with peptidyl-prolyl-isomerase activity, was identified as an important IKK-α cofactor. Furthermore, functional analysis with RNA interference re-

vealed that the immunophilin was essential for the overall signalling process leading to NF-κB nuclear translocation [21]. We found high levels of expression of FKBP51 in melanoma cells. In addition, we confirmed the involvement of this immunophilin in the control of IKK activity. Since rapamycin binds with high affinity to FKBP51 [39], and specifically inhibits its isomerase activity [39], it is reasonable to assume that it can affect IKK catalytic function through this mechanism. The IKK complex is an important target for therapeutic intervention, since it represents the converging point for the activation of NF-κB by a broad spectrum of stimuli that sustain cell survival and tumour progression. Indeed, a new class of drugs, based on molecules that inhibit the NF-κB signalling pathway have now been developed for the treatment of diseases which result from abnormal cell proliferation and cell death, including cancer [40]. Our findings suggest that rapamycin, when associated with drugs that induce NF-κB activation, could improve the effectiveness of treatments, even for aggressive tumours, such as melanoma, that are often resistant to standard anti-cancer therapies. Our observation that rapamycin acts through IKK is a novel mechanism that should increase interest in this molecule as an anti-cancer agent. Furthermore, our findings that the effect on NF-κB was independent of PI3k/Akt inhibition suggests that the drug could synergise with chemotherapeutic drugs in PTEN-positive tumours.

Conflict of Interest Statement

Acknowledgements

References

1. Fingar DC, Salama S, Tsou C, Harlow E, Blenis J. Mammalian cell size is controlled by mTOR and its downstream targets S6K1 and 4EBP1/eIF4E. *Genes Dev* 2002, **16**, 1472 1487.
2. Guba M, von Breitenbuch P, Steinbauer M, Koehl G, Flegel M, Hornung M, *et al.* Rapamycin inhibits primary and metastatic tumor growth by antiangiogenesis: involvement of vascular endothelial growth factor. *Nature Med* 2002, **8**, 128 135.
3. Geoerger B, Kerr K, Tang CB, Fung KM, Powell B, Sutton LN, *et al.* Antitumor activity of the rapamycin analog CCI-779 in human primitive neuroectodermal tumor/medulloblastoma models as single agent and in combination chemotherapy. *Cancer Res* 2001, **61**, 1527 1532.

4. Siekierka JJ, Hung SH, Poe M, Lin CS, Sigal NH. A cytosolic binding protein for the immunosuppressant FK506 has peptidyl-prolyl isomerase activity but is distinct from cyclophilin. *Nature* 1989, **341**, 755 757.

5. Brown EJ, Albers MW, Shin TB, Ichikawa K, Keith CT, Lane WS, et al. A mammalian protein targeted by G1-arresting rapamycin-receptor complex. *Nature* 1994, **369**, 756 758.

6. Chiu MI, Katz H, Berlin V. RAPT1, a mammalian homolog of yeast Tor, interacts with the FKBP12/rapamycin complex. *Proc Natl Acad Sci USA* 1994, **91**, 12574 12578.

7. Sabatini DM, Erdjument-Bromage H, Lui M, Tempst P, Snyder SH. RAFT1: a mammalian protein that binds to FKBP12 in a rapamycin-dependent fashion and is homologous to yeast TORs. *Cell* 1994, **78**, 35 43.

8. Gingras AC, Raught B, Gygi SP, Niedzwiecka A, Miron M, Burley SK, et al. Hierarchical phosphorylation of the translation inhibitor 4E-BP1. *Genes Dev* 2001, **15**, 2852 2864.

9. Schmelzle T, Hall MN. TOR, a central controller of cell growth. *Cell* 2000, **103**, 253 262., [Review].

10. Abraham RT, Wiederrecht GJ. Immunopharmacology of rapamycin. *Annu Rev Immunol* 1996, **14**, 483 510., [Review].

11. Gingras AC, Raught B, Sonenberg N. Regulation of translation initiation by FRAP/mTOR. *Genes Dev* 2001, **15**, 807 826., [Review].

12. Furnari FB, Huang HJ, Cavenee WK. The phosphoinositol phosphatase activity of PTEN mediates a serum-sensitive G1 growth arrest in glioma cells. *Cancer Res* 1998, **58**, 5002 5008.

13. Neshat MS, Mellinghoff IK, Tran C, Stiles B, Thomas G, Petersen R, et al. Sensitivity of PTEN-deficient tumors to inhibition of FRAP/mTOR. *Proc Natl Acad Sci USA* 2001, **98**, 10314 10319.

14. Steck PA, Pershouse MA, Jasser SA, Yung WK, Lin H, Ligon AH, et al. Identification of a candidate tumour suppressor gene, MMAC1, at chromosome10q23.3 that is mutated in multiple advanced cancers. *Nature Genet* 1997, **15**, 356 362.

15. Comer FI, Parent CA. PI 3-kinases and PTEN: how opposites chemoattract. *Cell* 2002, **109**, 541 544.

16. Birle D, Bottini N, Williams S, Huynh H, deBelle I, Adamson E, et al. Negative feedback regulation of the tumor suppressor PTEN by phosphoinositide-induced serine phosphorylation. *J Immunol* 2002, **169**, 286 291.

17. Lewis C, Neel C, Neel BG. New insights into tumor suppression: PTEN suppresses tumor formation by restraining the phosphoinositide 3-kinase/AKT pathway. *Proc Natl Acad Sci USA* 1999, **96**, 4240 4245., [Review].

18. Lai JH, Tan TH. CD28 signaling causes a sustained down-regulation of I kappa B alpha which can be prevented by the immunosuppressant rapamycin. *J Biol Chem* 1994, **269**, 30077 30080.

19. Conejo R, Valverde AM, Benito M, Lorenzo M. Insulin produces myogenesis in C2C12 myoblasts by induction of NF-kappaB and downregulation of AP-1 activities. *J Cell Physiol* 2001, **186**, 82 94.

20. Tunon MJ, Sanchez-Campos S, Gutierrez B, Culebras JM, Gonzalez-Gallego J. Effects of FK506 and rapamycin on generation of reactive oxygen species, nitric oxide production and nuclear factor kappa B activation in rat hepatocytes. *Biochem Pharmacol* 2003, **66**, 439 445.

21. Bouwmeester T, Bauch A, Ruffner H, Angrand PO, Bergamini G, Croughton K, et al. A physical and functional map of the human TNF-alpha/NF-kappaB signal transduction pathway. *Nature Cell Biol* 2004, **6**, 97 105.

22. Karin M, Delhase M. The I kappa B kinase (IKK) and NF-kappa B: key elements of proinflammatory signalling. *Semin Immunol* 2000, **12**, 85 98., [Review].

23. Regnier CH, Song HY, Gao X, Goeddel DV, Cao Z, Rothe M. Identification and characterization of an IkappaB kinase. *Cell* 1997, **90**, 373 383.

24. Mercurio F, Zhu H, Murray BW, Shevchenko A, Bennett BL, Li J, et al. IKK-1 and IKK-2: cytokine-activated IkappaB kinases essential for NF-kappaB activation. *Science* 1997, **278**, 860 866.

25. Wu MX, Ao Z, Prasad KVS, Wu R, Schlossman SF. IEX-1L, an apoptosis inhibitor involved in NF-kappaB-mediated cell survival. *Science* 1998, **281**, 998 999.

26. Wang CY, Guttridge DC, Mayo MW, Baldwin Jr AS. NF-kappaB induces expression of the Bcl-2 homologue A1/Bfl-1 to preferentially suppress chemotherapy-induced apoptosis. *Mol Cell Biol* 1999, **19**, 5923 5929.

27. Catz SD, Johnson JL. Transcriptional regulation of bcl-2 by nuclear factor kappa B and its significance in prostate cancer. *Oncogene* 2001, **20**, 7342 7351.

28. LaCasse EC, Baird S, Korneluk RG, MacKenzie AE. *The inhibitors of apoptosis (IAPs) and their emerging role in cancer* *Oncogene* 1998, **17**, 3247 3259.

29. Wang CY, Cusak JC, Liu R, Baldwin AS. Control of inducible chemoresistance: enhanced anti-tumor therapy through increased apoptosis by inhibition of NF-kappaB. *Nature Med* 1999, **5**, 412 417.

30. Soengas MS, Lowe SW. Apoptosis and melanoma chemoresistance. *Oncogene* 2003, **22**, 3138 3151., [Review].

31. Laurent G, Jaffrezou J-P. Signaling pathways activated by daunorubicin. *Blood* 2001, **98**, 913 924.

32. Mosmann T. Rapid colorimetric assay for cellular growth and survival: application to proliferation and cytotoxicity assays. *J Immunol Methods* 1983, **65**, 55 63.

33. Leonardi A, Chariot A, Claudio E, Cunningham K, Siebenlist U. CIKS, a connection to Ikappa B kinase and stress-activated protein kinase. *Proc Natl Acad Sci USA* 2000, **97**, 10494 10499.

34. Romano MF, Lamberti A, Tassone P, Alfinito F, Costantini S, Chiurazzi F, et al. Triggering of CD40 antigen inhibits fludarabine-induced apoptosis in B chronic lymphocytic leukemia cells. *Blood* 1998, **92**, 990 995.

35. Lopes de Menezes DE, Hu Y, Mayer LD. Combined treatment of Bcl-2 antisense oligodeoxynucleotides (G3139), p-glycoprotein inhibitor (PSC833), and sterically stabilized liposomal doxorubicin suppresses growth of drug-resistant growth of drug-resistant breast cancer in severely combined immunodeficient mice. *J Exp Ther Oncol* 2003, **3**, 72 82.

36. Vaziri SA, Grabowski DR, Tabata M, Holmes KA, Sterk J, Takigawa N, et al. c-IAP1 is overexpressed in HL-60 cells selected for doxorubicin resistance: effects on etoposide-induced apoptosis. *Anticancer Res* 2003, **23**(5A), 3657 3661.

37. Sade H, Krishna S, Sarin A. The anti-apoptotic effect of Notch-1 requires p56lck-dependent, Akt/PKB-mediated signaling in T cells. *J Biol Chem* 2004, **279**, 2937 2944.

38. Huxford T, Malek S, Ghosh G. Structure and mechanism in NF-kappa B/I kappa B signaling. *Cold Spring Harb Symp Quant Biol* 1999, **64**, 533 540., [Review].

39. Baughman G, Wiederrecht GJ, Faith Campbell N, Martin MM, Bourgeois S. FKBP51, a novel T-cell specific immunophilin capable of calcineurin inhibition. *Mol Cell Biol* 1995, **15**, 4395 4402.

40. Bayon Y, Ortiz MA, Lopez-Hernandez FJ, Gao F, Karin M, Pfahl M, et al. Inhibition of IkappaB kinase by a new class of retinoid-related anticancer agents that induce apoptosis. *Mol Cell Biol* 2003, **23**, 1061 1074.

Rapamycin stimulates apoptosis of childhood acute lymphoblastic leukemia cells

Raffaella Avellino, Simona Romano, Rosanna Parasole, Rita Bisogni, Annalisa Lamberti, Vincenzo Poggi, Salvatore Venuta, and Maria Fiammetta Romano

The phosphatidyl-inositol 3 kinase (PI3k)/Akt pathway has been implicated in childhood acute lymphoblastic leukemia (ALL). Because rapamycin suppresses the oncogenic processes sustained by PI3k/Akt, we investigated whether rapamycin affects blast survival. We found that rapamycin induces apoptosis of blasts in 56% of the bone marrow samples analyzed. Using the PI3k inhibitor wortmannin, we show that the PI3k/Akt pathway is involved in blast survival. Moreover, rapamycin increased doxorubicin-induced apoptosis even in nonresponder samples. Anthracyclines activate nuclear factor κB (NF-κB), and disruption of this signaling pathway increases the efficacy of apoptogenic stimuli. Rapamycin inhibited doxorubicin-induced NF-κB in ALL samples. Using a short interfering (si) RNA approach, we demonstrate that FKBP51, a large immunophilin inhibited by rapamycin, is essential for drug-induced NF-κB activation in human leukemia. Furthermore, rapamycin did not increase doxorubicin-induced apoptosis when NF-κB was overexpressed. In conclusion, rapamycin targets 2 pathways that are crucial for cell survival and chemoresistance of malignant lymphoblasts—PI3k/Akt through the mammalian target of rapamycin and NF-κB through FKBP51—suggesting that the drug could be beneficial in the treatment of childhood ALL. (Blood. 2005;106:1400-1406)

© 2005 by The American Society of Hematology

Introduction

In recent decades, conventional chemotherapy has produced a dramatic improvement in survival of childhood acute lymphoblastic leukemia (cALL)[1]; however, refractory or relapsed disease remains a problem. Anticancer drug research is aimed at developing new compounds directed against inappropriately activated cell-signaling pathways that stimulate the uncontrolled growth of neoplastic cells.[2] A deregulated cytokine circuitry has been proposed in the malignant transformation of lymphoid precursors in primary B- and T-lineage ALL.[3] Other reports suggest that the insulin-like growth factor system plays a pathogenetic role in cALL.[4,5] Phosphorylation of cytokine[6,7] or growth factor receptors[4,5] generate docking sites for signaling molecules, thereby activating the phosphatidyl-inositol 3 kinase (PI3k)/Akt-protein kinase B survival pathway,[4-7] which promotes blast growth.[4,5]

The carbocyclic lactone-lactum antibiotic rapamycin, which has been approved by the Food and Drug Administration for the prevention of allograft rejection,[8] exerts an anticancer effect by decreasing cell proliferation and increasing apoptosis.[9,10] Therefore, rapamycin is expected to suppress cytokine responses[11] and tumor-cell survival.[12] The mammalian target of rapamycin (mTOR) is a serine-threonine kinase that regulates protein translation, cell-cycle progression, and cellular proliferation.[13-16] In response to growth factors, hormones, mitogens, and amino acids,[15-17] mTOR is activated through phosphorylation by Akt[18] and in turn activates 2 key translational regulators: the initiation factor 4E binding protein (4E-BPI),[16] and p70-kDa S6 ribosomal protein kinase (p70S6k).[14] The pathways governed by mTOR and p70S6k are involved in the survival of malignant lymphoblasts,[19] which explains the antileukemic activity of rapamycin detected in human cell lines and in a murine model.[19] Taken together, these findings prompted us to investigate whether rapamycin induces apoptosis of ALL blasts.

We recently demonstrated that rapamycin sensitized a poorly responsive human melanoma cell line to doxorubicin-induced apoptosis.[20] Anthracycline compounds activate nuclear factor κB (NF-κB)/Rel nuclear translocation,[21] and disruption of this signaling pathway increases the efficacy of apoptogenic stimuli.[22] We showed that the immunophilin FKBP51 is required for IκBα degradation after stimulation with doxorubicin.[20] FKBP51, which is specifically inhibited by rapamycin binding,[23] exerts peptidyl-prolyl-isomerase activity that catalyzes the isomerization of peptidyl-prolyl-imide bonds in subunit α of the IKK kinase complex, and is required for IKK function.[24] Given the foregoing, we investigated whether rapamycin inhibits anthracycline-induced NF-κB/Rel activity in blasts from cALL, and increases sensitivity to chemotherapy.

Finally, to assess the role of FKBP51 in NF-κB/Rel activation in lymphoid cells, we down-modulated FKBP51 levels in the Jurkat leukemic cell line using a short interfering (si) RNA approach, and investigated whether IκBα degradation and NF-κB/Rel nuclear translocation occurred in the absence of the IKKα cofactor.

Patients, materials, and methods

Cells and culture conditions

Bone marrow samples were obtained between April 2002 and October 2004 from 15 children affected by B-ALL and from 10 children affected by

Table 1. Patient profiles

Patient no.	Sex	Age, y.mo	% Blasts	Lineage	WBC count, 10^9/L	Immunophenotype	Genetic rearrangement	GR*	RR†
1	F	11.3	100	B	111.680	CD10, CD19, CD34	T(12;21)	Good	Yes
2	M	6.11	100	T	15.760	CD10, CD7, CD2, CD3cy, CD4, CD8	—	Good	Yes
3	M	2.10	84	T	118.740	CD7, CD4, CD8, CD10, CD2, CD3$^{+/-}$	—	Good	Yes
4	F	11.10	100	T	198.510	CD7, CD34, CD3cy, CD2, CD5, TdT	Partial deletion chromosome 1	Poor	No
5	M	14.5	100	B	40.600	CD10, CD34, CD19, DR, CD33, CD13	—	Good	No
6	M	13.10	95	B	56.130	CD19, CD79a-cy CD22, CD24, DR,	—	Good	Yes
7	M	3.3	100	B	5.790	CD10, CD19, CD24, TdT, CD34, CD38	NT	Good	No
8	M	9.4	20	T	3.650	CD5, CD7, CD3cy, CD1a	—	Poor	Yes
9	M	3.9	90	B	98.100	CD34, CD19, CD10, DR, CD13, CD33, TdT	t(9;22)	Poor	No
10	M	7.4	100	T	314.950	CD3cy, CD4, CD8, CD10, CD7, CD5, TdT	—	Poor	Yes
11	F	12.3	90	T	334.900	CD2, CD3, CD4, CD8, CD7	Partial deletion chromosome 4	Good	Yes
12	M	4.0	100	B	45.500	CD19, CD34, CD10	—	Poor	No
13	M	14.8	100	B	20.240	CD10, CD19, CD20, DR, CD34$^{+/-}$, TdT	—	Good	Yes
14	M	1.8	100	B	17.810	CD10, CD19, DR, TdT	—	Good	Yes
15	F	3.7	100	B	108.700	CD34, CD19, CD10, DR	Hyperdiploid	Poor	No
16	F	2.7	100	B	196.000	CD10, CD19, CD20, DR, CD34	Hyperdiploid	Poor	No
17	M	2.0	98	T	92.500	CD5, CD2, CD7, CD3cy, CD10, CD4, CD8	—	Poor	No
18	F	1.9	98	B	124.560	CD34, CD19, DR	t(4;11)	Poor	Yes
19	M	5.7	100	T	16.800	CD2, CD5, CD7, TdT, CD10$^{+/-}$	—	Good	Yes
20	F	3.5	98	B	78.400	Tdt, CD10, CD19, CD20, DR	t(12;21)	Good	No
21	M	8.11	98	T	21.990	CD3cy, CD7, CD5, TdT, CD34, TCR	—	Good	Yes
22	M	10.7	60	B	3.630	CD10, CD19, CD22, CD34, TγδT	NT	Good	Yes
23	F	9.10	99	B	34.190	CD19, CD34, TdT	—	Poor	No
24	M	11.1	99	T	310.000	CD7, CD2, CD5, CD8, cyCD3, TdT	—	Poor	No
25	F	9.3	90	B	6.970	CD10, CD19, CD33, CD34, TdT	—	Good	Yes

— indicates not found; NT, not tested.

*GR: an in vivo response to glucocorticoids after a 7-day prednisone prophase.

†RR: an in vitro response to rapamycin.

T-ALL (Table 1). Twenty-two samples were collected at diagnosis, 2 at relapse (patients 18 and 22), and 1 from a patient who partially responded to therapy (patient 8). It is declared that informed consent was provided by the patients' parents in accordance with the Declaration of Helsinki for these studies, conducted in the departments of Biochemistry and Medical Biotechnologies, University of Naples Federico II (Naples, Italy); Pediatric Onco-Hematology, AORN Pausilipon (Naples, Italy); and Clinical and Experimental Medicine, "Magna Graecia" University (Catanzaro, Italy).

Mononuclear cells from the 25 bone marrow samples were separated through Ficoll-Hypaque gradient (ICN Biomedicals, Aurora, OH). The percentage of blasts in mononuclear-cell specimens was more than 90%, except for refractory ALL, in which it was 59.1%. Cells (1×10^6 cells/mL) were cultured in 10% fetal calf serum (FCS; Biochrom KG, Berlin, Germany) RPMI 1640 (Cambrex Bio Science, Verviers, Belgium), supplemented with antibiotic and glutamine (Cambrex Bio Science) at 37°C in a 5% CO_2 humidified atmosphere, with and without rapamycin (Rapamune; Wyeth Ayerst Laboratories, Marietta, PA).

Cell transfection, plasmids, and siRNA

Jurkat cells (2×10^7) in the logarithmic growth phase were resuspended in 400 μL serum-free RPMI 1640 and transfected with 20 μg plasmid DNA by electroporation at 250 V and 960 mF using the Gene Pulser (Bio-Rad Laboratories, Hercules, CA). The cells were transferred to culture flasks and incubated in complete medium supplemented with 1 mg/mL G418 (Roche,

Basel, Switzerland) to obtain stable lines. The cDNA coding for p65 (RelA), cloned in a pCMV4 vector carrying resistance for G418, was kindly donated by Dr Shao-Cong Sun (Pennsylvania State University College of Medicine).

For siRNA transfection, cells at a concentration of 5×10^5/mL were incubated for 24 hours in 6-well plates in medium without antibiotics. This was followed by transfection of the oligonucleotide 5'-ACCUAAUGCU-GAGCUUAUAdTdT-3' corresponding to the sense strand of the target sequence 5'-AAACCUAAUGCUGAGCUUAUA-3' of human *FKBP51* (Dharmacon Research, Chicago, IL) or of a scrambled duplex as control (Dharmacon Research). The siRNA or the scrambled oligo was transfected at the final concentration of 50 nM using Metafectene (Biontex, Munich, Germany) according to the manufacturer's recommendations. Two days later, 5 μM doxorubicin was added to the culture medium and cells were harvested 5 hours later and processed for Western blot analysis or electrophoretic mobility shift assay (EMSA).

Analysis of apoptosis

We used the lipophylic cation 5,5',6,6' tetrachloro-1,1',3,3'-tetraethylben-zimidazol-carbocyanine iodide (JC-1) and flow cytometry to analyze the mitochondria membrane potential. In this procedure, the color of the dye changes from orange to green as the membrane potential decreases.[25] Briefly, 5×10^5 cells were incubated for 10 minutes at 37°C with 10 μg/mL JC-1 (Molecular Probes, Leiden, The Netherlands), washed, and analyzed

by flow cytometry. Phosphatidylserine externalization was investigated by annexin V staining in double or single fluorescence. Next, 5×10^5 cells were incubated with annexin V–fluorescein isothiocyanate (FITC) (Pharmingen/Becton Dickinson, San Diego, CA) or phycoerythrin (PE; Alexis, San Diego, CA) conjugated in 100 µL binding buffer containing 10 mM HEPES (N-2-hydroxyethylpiperazine-N'-2-ethanesulfonic acid)/NaOH pH 7.5, 140 mM NaCl, 2.5 mM CaCl$_2$ for 15 minutes at room temperature in the dark. Subsequently, 400 µL of the same buffer was added to each sample and the cells were analyzed in the Becton Dickinson FACScan flow cytometer. The mouse monoclonal antibody, anti–CD7-FITC, –CD3-PE, or –CD20-PE (Pharmingen/Becton Dickinson), was added in double fluorescence tests. Caspase-3 activity was detected with the caspase-3 fluorometric assay kit (Perbio Science, Erembodegem, Belgium) according to the manufacturer's instructions. The cells (2×10^6) were lysed in a buffer containing 10 mM Tris (pH 7.5), 130 mM NaCl, 1% Triton X-100, 10 mM NaPi, and 10 mM NaPPi, and 50 µg protein was analyzed.

Cell lysates and Western blot analysis

For IκBα detection, cytosolic extracts were obtained by resuspending the cells in lysing buffer (10 mM HEPES, pH 7.9, 1 mM EDTA [ethylenediaminetetraacetic acid], 60 mM KCl, 1 mM dithiothreitol [DTT], 1 mM PMSF [phenylmethylsulfonyl fluoride], 50 µg/mL antipain, 40 µg/mL bestatin, 20 µg/mL chymostatin, 0.2% vol/vol Nonidet P-40) for 15 minutes in ice. For Akt, phospho-Akt, p65, and FKBP51 detection, whole-cell lysates were prepared by homogenization in modified RIPA buffer (150 mM sodium chloride, 50 mM Tris-HCl, pH 7.4, 1 mM EDTA, 1 mM PMSF, 1% Triton X-100, 1% sodium deoxycholic acid, 0.1% sodium dodecyl sulfate [SDS], 5 µg/mL aprotinin, 5 µg/mL leupeptin). Cell debris was removed by centrifugation. Protein concentration was determined with the Bio-Rad protein assay. The cell lysate was boiled for 5 minutes in 1x SDS sample buffer (50 mM Tris-HCl pH 6.8, 12.5% glycerol, 1% SDS, 0.01% bromophenol blue) containing 5% beta-mercaptoethanol, run on 10% SDS–polyacrylamide gel electrophoresis, transferred onto a membrane filter (Cellulosenitrate; Schleider and Schuell, Keene, NH), and incubated with the primary antibody. The anti-IκBα and -p65(RelA) were rabbit polyclonal antibodies from Santa Cruz Biotechnology (Santa Cruz, CA); anti-Akt, anti–phospho-Akt (Thr308), and anti–phospho-Akt (Ser473) were rabbit polyclonal antibodies purchased from Cell Signaling (Beverly, MA). Anti-FKBP51 was a rabbit polyclonal antibody purchased from Abcam (Cambridge, United Kingdom). After a second incubation with peroxidase-conjugated goat anti–rabbit IgG or anti–mouse IgG (both from Santa Cruz Biotechnology), the blots were developed with the enhanced chemiluminescence (ECL) system (Amersham Pharmacia Biotech, Piscataway, NJ).

Nuclear extracts, EMSA, and oligonucleotides

Cell nuclear extracts were prepared by cell-pellet homogenization in 2 volumes of 10 mM HEPES, pH 7.9, 10 mM KCl, 1.5 mM MgCl$_2$, 1 mM EDTA, 0.5 mM DTT, 0.5 mM PMSF, and 10% glycerol vol/vol. Nuclei were centrifuged at 1000g for 5 minutes, washed, and resuspended in 2 volumes of the same solution. KCl was added to reach 0.39 M KCl. Nuclei were extracted at 4°C for 1 hour and centrifuged at 10 000g for 30 minutes. The supernatant was clarified by centrifugation and stored at −80°C. Protein concentration was determined with the Bio-Rad protein assay. The NF-κB consensus 5'-CAACGGCAGGGGAATCTCCCTCTCCTT-3' oligonucleotide was end-labeled with γ-[^{32}P] adenosine triphosphate (ATP; Amersham Pharmacia Biotech) using a polynucleotide kinase (Roche). End-labeled DNA fragments were incubated at room temperature for 15 minutes with 5 µg nuclear protein, in the presence of 1 µg poly(dI-dC), in 20 µL of a buffer consisting of 10 mM Tris-HCl, pH 7.5, 50 mM NaCl, 1 mM EDTA, 1 mM DTT, and 5% glycerol vol/vol. In competition assays, a 50× molar excess of NF-κB or nuclear factor of activated T cells (NFAT) cold oligonucleotide was added to the incubation mixture. Protein-DNA complexes were separated from free probe on a 6% polyacrylamide wt/vol gel run in 0.25× Tris borate buffer at 200 mV for 3 hours at room temperature. The gels were dried and exposed to x-ray film (Kodak AR).
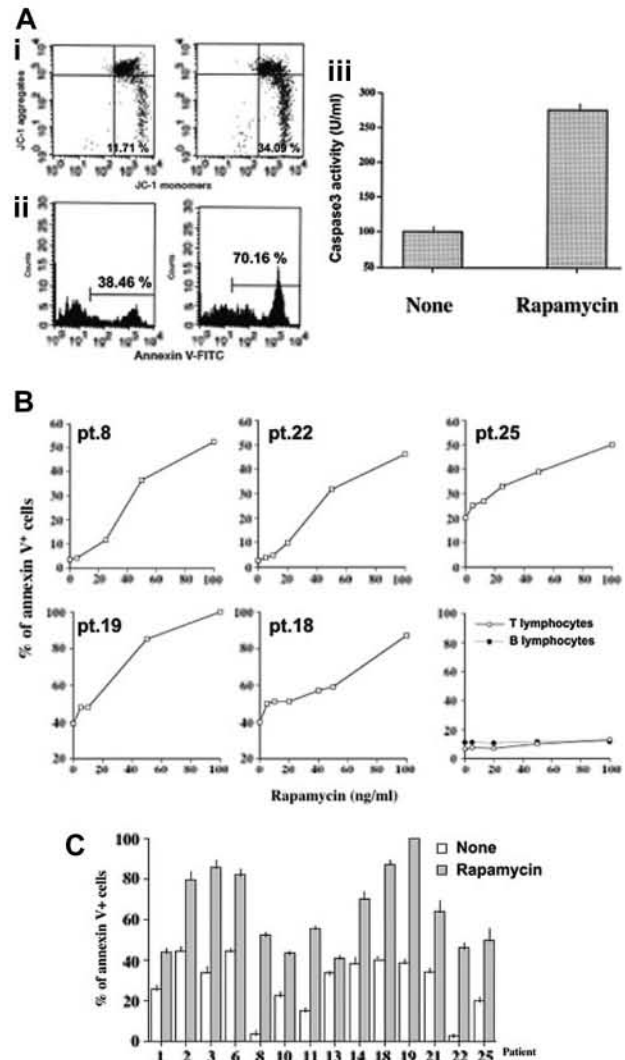
Statistical analysis

Statistical analysis of the apoptosis data was performed by means of the paired Student t test. The chi square test was used to compare categorical data.

Results

Rapamycin-induced apoptosis of cALL blasts

We evaluated apoptosis in cultured mononuclear cells from 25 bone marrow samples obtained from patients with cALL (15
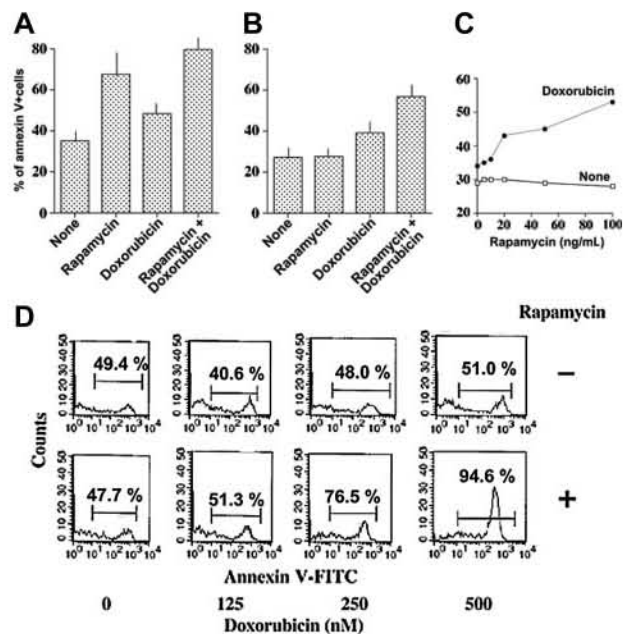

Figure 1. Rapamycin induces apoptosis of primary malignant lymphoblasts. (A) Analysis of mitochondrial membrane potential (i), phosphatidyl-serine externalization (ii), and caspase 3 catalytic activity (iii) of cALL blasts cultured with rapamycin (50 ng/mL). After 6 hours of incubation, mitochondrial potential was analyzed by calculating the amount of JC-1 monomers by flow cytometry. Annexin V binding and caspase 3 activity were measured by flow cytometry and fluorometric assay, respectively, after 24 hours of incubation. The percentages on the bars indicate the amount of annexin V–positive cells. (B) Dose/response curve to rapamycin. Malignant lymphocytes from 5 different samples and peripheral B or T lymphocytes from a healthy donor were incubated with rapamycin at different concentrations. After 24 hours, the cells were harvested and apoptosis was evaluated by annexin V staining and flow cytometry. For B and T lymphocyte analysis, the whole PBMCs were acquired in flow cytometry, after which B or T cells were gated on the basis of CD3/SSc or CD20/SSc parameters, and the percentage of annexin V+ cells was calculated. Pt. indicates patient number. (C) Mean values ± standard deviation (SD) of rapamycin-induced apoptosis in responder samples. Apoptosis was evaluated by annexin V staining of ALL blasts, from the indicated patients, after 24 hours of incubation with or without rapamycin (100 ng/mL).
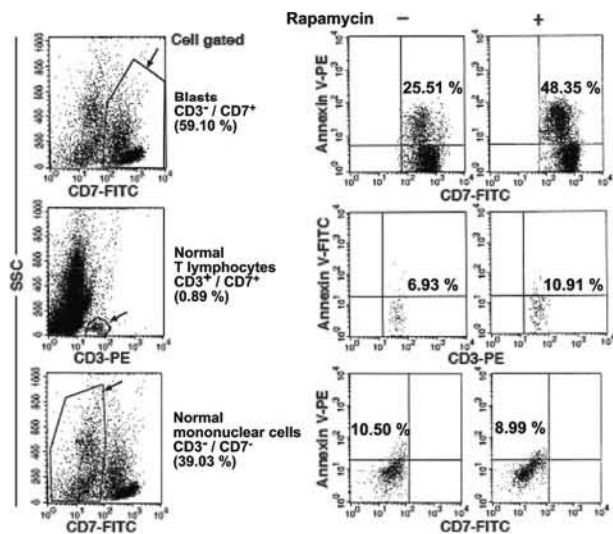
Figure 2. Normal bone marrow mononuclear cells display low sensitivity to cell-death stimuli compared with blasts. Flow cytometry evaluation of apoptosis of leukemic (CD3−/CD7+) or normal (CD3+/CD7+, CD3−/CD7−) mononuclear-cell populations (patient 8), incubated for 24 hours with 25 ng/mL rapamycin. The cells were gated on the basis of FL1 (CD7-FITC)/side scatter (SSc) or FL2(CD3-PE)/SSc parameters and the percentage of annexin-positive cells was measured.

Figure 4. Rapamycin enhances doxorubicin-induced apoptosis of ALL cells. Mean values ± SD of apoptosis of ALL blasts, from 8 responder samples (A; patients 1, 2, 3, 6, 11, 14, 18, 19) and 7 nonresponder samples (B; patients 4, 5, 7, 9, 12, 15, 20), incubated for 24 hours with and without rapamycin (100 ng/mL) or doxorubicin (0.5 μM). (C) Dose/response effect of rapamycin on doxorubicin-induced apoptosis. ALL cells (patient 7) were cultured with and without 0.5 μM doxorubicin and with or without rapamycin at the indicated concentrations; 24 hours later, apoptosis was measured by annexin V staining. (D) Flow cytometry diagrams of apoptosis of blasts, from patient 20, cultured with doxorubicin at the indicated concentrations, with and without rapamycin (100 ng/mL). The percentages on the bars indicate the amount of annexin V–positive cells.

B-cALL and 10 T-cALL) and exposed to rapamycin. We found that rapamycin significantly ($P = .004$) increased basal-cell death in 14 (7 B-cALL and 7 T-cALL) of the 25 leukemia samples (56%; Table 1). Thus, 46.6% of B-cALL and 70.0% of T-cALL samples responded to the drug (responder group). Interestingly, the response of blasts to rapamycin in vitro correlated with prednisone response in vivo ($P = .01$). Indeed, 11 of the 14 patients who responded to prednisone in vivo responded to rapamycin in vitro. Similarly, 8 of the 11 poor responders to prednisone in vivo, including the 2 hyperdiploid patients, did not respond to rapamycin in vitro. It is noteworthy that the patient with the t(4;11) rearrangement (patient 18) was among the 3 poor responders to glucocorticoids who responded to rapamycin. Rapamycin caused mitochondrial depolarization after 6 hours of incubation (Figure 1A). After an additional 19 hours, the proportion of annexin V+ cells was increased more than 80% with an enhancement of caspase 3 catalytic activity of more than 100%. Figure 1B shows dose/response curves relating to 5 donors. At 20 ng/mL, rapamycin increased basal-cell death by at least 25%. The apoptotic effect increased as the rapamycin dose increased. The active doses of rapamycin were within the range considered to be therapeutically achievable.[26] Indeed, although the maximum serum level should

not exceed 15 ng/mL, it must be taken into account that approximately 95% of rapamycin is vehicled by red blood cells because of its high lipophilicity.[26] Rapamycin did not appear to affect the survival of normal peripheral T and B lymphocytes (Figure 1B). The mean values of apoptosis in the rapamycin-responsive samples are shown in Figure 1C; each experiment was in triplicate.

Normal bone marrow cells were less sensitive than cALL blasts to rapamycin-induced apoptosis

We next evaluated if rapamycin is cytotoxic for the normal hematopoietic counterpart of cALL cells. To this aim, we used annexin V in double fluorescence and flow cytometry to examine the effect of rapamycin in diverse bone marrow cell subpopulations from a patient with refractory cALL (patient 8). Figure 2 shows the flow cytometry diagrams of rapamycin-induced apoptosis of normal mononuclear cells (CD3+ or
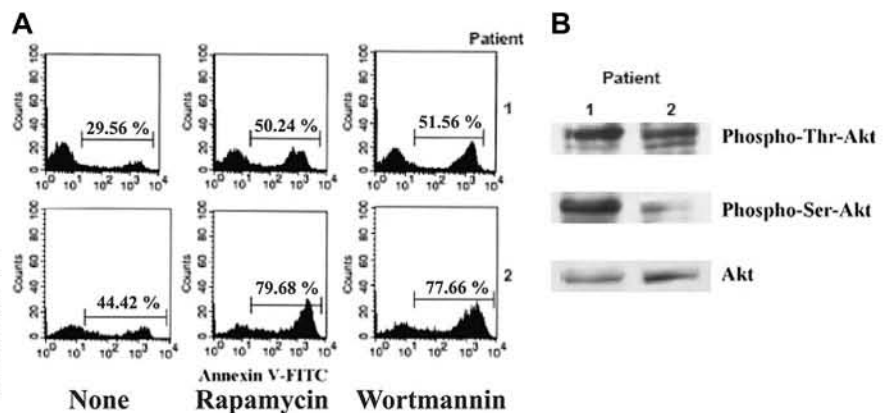
Figure 3. The PI3k/Akt pathway plays a role in ALL blast apoptosis. (A) Flow cytometry analysis of apoptosis, by annexin V–FITC staining, of ALL blasts incubated for 24 hours with and without rapamycin (100 ng/mL) or wortmannin (1 μM). The percentages over the bars indicate the amount of annexin V–positive cells. (B) Western blotting assay of phospho-Akt, at Ser 473 or Thr 308, in cell lysates from the same samples.
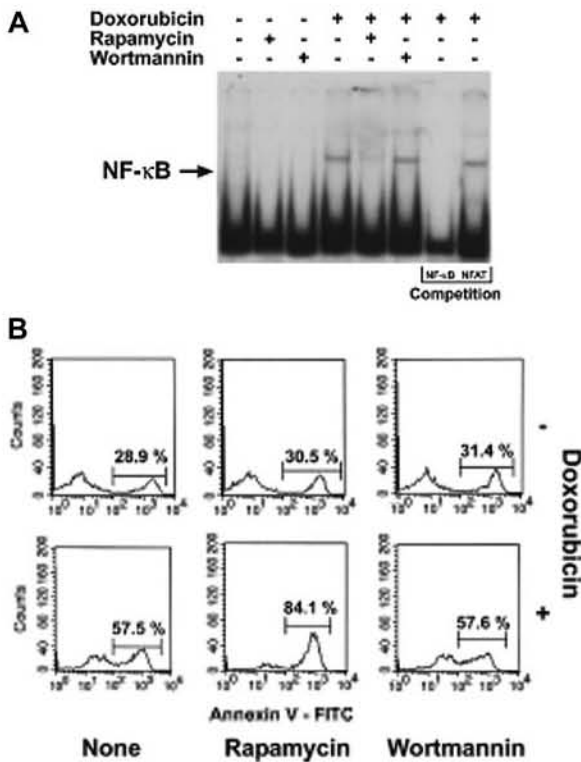
CD7⁻) compared with that of CD3⁻/CD7⁺ blasts. At a rapamycin concentration between 20 ng/mL and 100 ng/mL, the extent of apoptosis of normal bone marrow mononuclear cells was less than 15%. These results suggested that rapamycin counteracted a cell signaling pathway that is deregulated in cALL blasts.

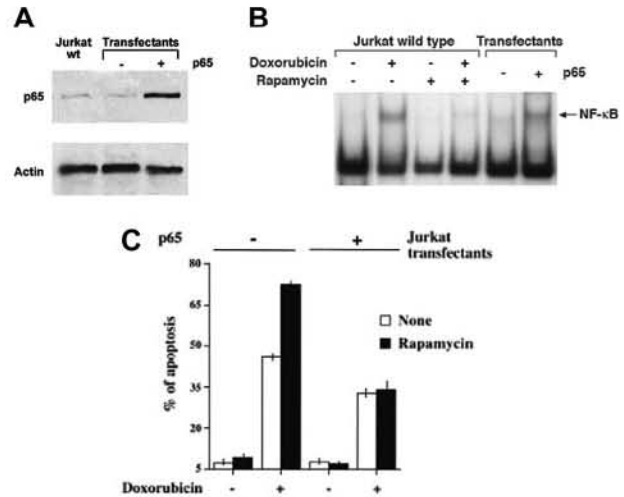### Akt was activated in rapamycin-sensitive samples

To determine if the phosphatidyl-inositol pathway is involved in blast survival, we investigated the effect of the PI3k inhibitor wortmannin[27] on cALL-cell death. Our data show that wortmannin induced levels of apoptosis comparable to those induced by rapamycin in 11 of the 15 samples from the responder group, whereas none of the samples from nonresponder patients underwent apoptosis when stimulated with wortmannin. Figure 3A shows the flow cytometry diagrams of annexin V binding to cALL blasts from 2 samples, cultured for 24 hours with rapamycin (100 ng/mL) or wortmannin (1 μM). Analysis of phospho-Akt by Western blotting assay revealed high expression of both Ser473- and Thr301-phospho-Akt in patient 1 and of Thr301-phospho-Akt in patient 2 (Figure 3B). These findings suggest that the PI3k/Akt pathway is involved in the survival of malignant lymphoblasts.

Rapamycin enhanced doxorubicin-induced apoptosis

Anthracycline compounds are widely used to treat leukemias. We investigated if rapamycin could enhance doxorubin-induced cALL blast apoptosis. To this end, we cultured primary leukemic cells from 15 bone marrow samples (8 samples responding and 7

Figure 6. Rapamycin does not enhance doxorubicin-induced apoptosis in RelA-hyperexpressing transfectants. (A) Western blotting analysis of p65 (RelA) expression levels in cell lysates obtained from wild-type Jurkat cells and void vector– or RelA-stable transfectants. (B) EMSA analysis of nuclear extracts obtained from Jurkat wild-type cells cultured for 5 hours with and without 5 μM doxorubicin and with or without rapamycin (100 ng/mL), and RelA- or void vector–stable transfectants. (C) Analysis of apoptosis of RelA- or void vector–stable transfectants cultured with and without 5 μM doxorubicin and with and without rapamycin (100 ng/mL). After 24 hours of incubation, cells were harvested and cell death was analyzed by propidium iodide incorporation in flow cytometry. Results are from 4 different experiments, each of which was in triplicate. Error bars indicate standard deviations.

nonresponding to rapamycin) for 24 hours with 500 nM doxorubicin, in the presence and absence of rapamycin (100 ng/mL), and then evaluated apoptosis by measuring annexin V staining in flow cytometry. In responder samples (Figure 4A), both rapamycin and doxorubicin significantly increased cell death over basal levels ($P < .001$ and .005, respectively). The addition of rapamycin to doxorubicin-exposed cells increased apoptosis versus cells exposed to doxorubicin alone, in both responder (Figure 4A; $P = .001$)
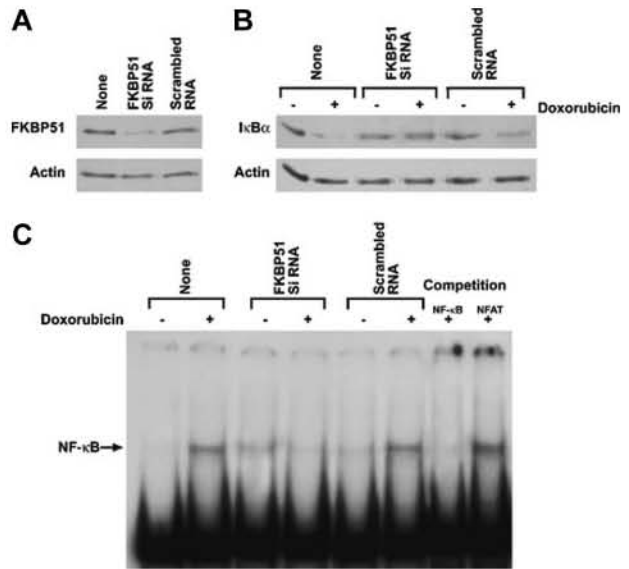

Figure 5. Rapamycin inhibits doxorubicin-induced NF-κB activation in ALL blasts. (A) EMSA analysis of nuclear extracts from ALL cells (patient 5) cultured for 5 hours with 0.5 μM doxorubicin, with and without rapamycin (100 ng/mL) or wortmannin (1 μM). A competition assay performed with the same NF-κB cold oligo or an unrelated oligo (see "Materials and methods") indicated the specificity of the NF-κB band. (B) Flow cytometry diagrams of apoptosis of ALL blasts, from the same patient, cultured for 24 hours with 0.5 μM doxorubicin, with and without rapamycin (100 ng/mL) or wortmannin (1 μM). The percentages over the bars indicate the amount of annexin V–positive cells.

Figure 7. FKBP51 controls drug-induced NF-κB activation in human leukemia. (A) Western blotting analysis of FKBP51 expression levels in cell lysates obtained from transfected or nontransfected Jurkat cells, with FKBP51 siRNA or the scrambled oligo as control. (B) Western blotting analysis of IκBα expression levels in cells transfected with FKBP51 siRNA and cultured with or without doxorubicin (5 μM) for 5 hours. (C) EMSA analysis of nuclear extracts from Jurkat cells transfected with FKBP51 siRNA and cultured with or without doxorubin (5 μM) for 5 hours. A competition assay, with the same –κB cold oligo or an unrelated oligo (see "Materials and methods"), indicated the specificity of the NF-κB band.

and nonresponder samples (Figure 4B; $P = .001$). Therefore, rapamycin exerts a proapoptotic effect even when it is unable to directly activate cell death. As is shown in Figure 4C, the cooperative effect of rapamycin plus doxorubicin was detected at doses more than or equal to 20 ng/mL. Figure 4D shows a sample in which rapamycin or doxorubicin alone did not induce cell death, whereas the 2 drugs together enhanced basal apoptosis by more than 90%.

Rapamycin inhibited doxorubicin-induced NF-κB/Rel activation in cALL cells

To identify the mechanism by which rapamycin enhanced doxorubicin-induced apoptosis in cALL blasts, we investigated if rapamycin was able to counteract the induction of NF-κB/Rel transcription factors[20] in cALL blasts. In fact, anthracycline compounds activate transcription factors that play an important role in chemoresistance.[21] As shown in Figure 5A, rapamycin, but not wortmannin, inhibited the translocation of NF-κB/Rel complexes in blast nuclei. Furthermore, rapamycin, but not wortmannin, enhanced doxorubicin-induced apoptosis (Figure 5B). These results suggest that rapamycin can sensitize cALL blasts to anthracycline drugs by inhibiting activation of NF-κB/Rel transcription factors through a mechanism independent of PI3k/Akt inhibition.

The enhancement of apoptosis by rapamycin was antagonized by p65(RelA) hyperexpression

To determine if rapamycin-induced enhancement of apoptosis was related to NF-κB down-modulation, we investigated whether rapamycin increased apoptosis when NF-κB was overexpressed. In these experiments we used the Jurkat leukemic cell line in which we transfected PCMV4 vector carrying the p65 subunit of NF-κB and resistance to genetycin, thus obtaining stable transfectants (Figure 6A). As shown in Figure 6B, doxorubicin activated NF-κB in Jurkat cells, whereas rapamycin antagonized this effect. Moreover, as expected, p65 transfectants constitutively expressed NF-κB in nuclei, but control cells did not. We subsequently incubated p65- and void vector–stable transfectants both with and without doxorubicin for 24 hours, and analyzed apoptosis by propidium iodide incorporation. Rapamycin did not enhance apoptosis in cells hyperexpressing p65. In fact, it increased apoptosis by 59.4% in control cells ($P = .032$) and by only 3.9% in RelA hyperexpressing Jurkat cells (Figure 6C). We therefore conclude that down-modulation of NF-κB/Rel transcription factors is a mechanism by which rapamycin enhances apoptosis and that rapamycin can cooperate with NF-κB–inducing drugs.

The rapamycin-binding protein FKBP51 controls NF-κB activation in leukemia

The immunophilin FKBP51 is required for IKK-α functioning.[24] Rapamycin specifically binds to FKBP51 and inhibits its peptidyl-prolyl-isomerase activity.[23] FKBP51 was first cloned in lymphocytes in which it was abundant.[23] To assess the role of FKBP51 in the NF-κB activation pathway in human leukemia, we down-modulated immunophilin levels in Jurkat cells using the siRNA technique. As shown in Figure 7A, the expression levels of FKB51 were remarkably decreased in Jurkat cells transfected with FKBP51 siRNA than in cells incubated with control medium or transfected with a scrambled oligonucleotide. We then investigated the ability of doxorubicin to induce IκBα degradation and NF-κB nuclear

translocation when FKBP51 was down-modulated. Figure 7B shows that IκBα levels decreased in control- or scrambled-oligo–transfected cells cultured with doxorubicin, but not when FKBP51 was down-modulated. Accordingly, NF-κB complexes were not detected by EMSA in nuclear extracts from FKBP51 siRNA-transfected cells (Figure 7C). These findings suggest that FKBP51 controls NF-κB activation in human leukemia.

Discussion

mTOR mediates PI3k/Akt-driven cell proliferation and survival.[12,15-18] In line with this finding, rapamycin has been reported to exert its major anticancer effect in neoplasias that lack the PI3k antagonist, phosphatase and tensin homolog (PTEN).[12,28] mTOR controls the synthesis of proteins essential for cell-cycle progression and cellular proliferation[14-17] by phosphorylating 2 key translational regulators: the initiation factor 4E binding protein (4E-BPI),[16] and the 70-kDa S6 ribosomal protein kinase (p70S6k).[14] Several lines of evidence support the view that abnormal survival signals from the phosphatidyl-inositol cascade lead to neoplastic transformation of lymphoid precursors.[5-7,19] The finding that rapamycin exerts antiproliferative and apoptotic effects on B-precursor leukemia, in vitro and in vivo, by mechanisms involving the inhibition of mTOR and p70S6k,[19] provided the rationale for new therapeutic strategies against acute lymphoblastic leukemia. In agreement with these findings, we show that rapamycin induces apoptosis of blasts in 56% of bone marrow samples from patients with cALL. Moreover, we found that apoptosis can be induced, in responder samples, also by inhibiting PI3k using the specific inhibitor wortmannin.[27] These findings, together with the detection of constitutive activation of Akt in 2 different cALL bone marrow samples, support previous evidence[5-7,19] that the phosphatidyl-inositol pathway is involved in blast survival.

We also found that rapamycin increased doxorubicin-induced cell death, even in nonresponder samples, whereas the PI3k inhibitor wortmannin did not act in concert with doxorubin. These findings suggest that rapamycin may also exert a proapoptotic activity by mechanisms independent of PI3k/Akt/mTOR inhibition. We demonstrate that the immunophilin FKBP51 controls drug-induced NF-κB activation in human leukemia, which explains the proapoptotic effect of rapamycin. Immunophilins are the first target of the drug[23,29] and, in fact, the binding of rapamycin to FKBP12 is crucial for mTOR inhibition.[29] Immunophilins are abundant cytosolic proteins endowed with inherent peptidyl-prolyl cis-trans isomerase activity that is inhibited by drug ligand binding.[23,29] Given the biologic relevance of this class of proteins,[24,30-32] it is not surprising that rapamycin induces effects independent of PI3k/Akt/mTOR inhibition.

In conclusion, our findings suggest that rapamycin might be effective in the treatment of cALL, despite the biologic heterogeneity of the disease. Finally, our study, in agreement with other reports showing that immunophilins are involved in a host of diseases that do not necessarily involve the same signaling pathway,[33-34] opens the way to the development of a range of new drugs specifically targeting immunophilins.[34]

References

1. Winick NJ, Carroll WL, Hunger SP. Childhood leukemia: new advances and challenges. N Engl J Med. 2004;351:601-603.

2. Lin TS, Mahajan S, Frank DA. STAT signaling in the pathogenesis and treatment of leukemias. Oncogene. 2000;19:2496-2504.

3. Weber-Nordt RM, Egan C, Wehinger J, et al. Constitutive activation of STAT proteins in primary lymphoid and myeloid leukemia cells and in Epstein-Barr virus (EBV)-related lymphoma cell lines. Blood. 1996;88:809-816.

4. Vorwerk P, Wex H, Hohmann B, et al. Expression

of components of the IGF signalling system in childhood acute lymphoblastic leukaemia. Mol Pathol. 2002;55:40-45.

5. Zumkeller W, Burdach S. The insulin-like growth factor system in normal and malignant hematopoietic cells. Blood. 1999;94:3653-3657.

6. Gaffen SL. Signaling domains of the interleukin 2 receptor. Cytokine. 2001;14:63-77.

7. Watowich SS, Wu H, Socolovsky M, Klingmuller U, Constantinescu SN, Lodish HF. Cytokine receptor signal transduction and the control of hematopoietic cell development. Ann Rev Cell Develop Biol. 1996;12:91-128.

8. MacDonald AS, The RAPAMUNE Global Study Group. A worldwide, phase III, randomized, controlled, safety and efficacy study of a sirolimus/cyclosporine regimen for prevention of acute rejection in recipients of primary mismatched renal allografts. Transplantation. 2001;71:271-280.

9. Guba M, von Breitenbuch P, Steinbauer M, et al. Rapamycin inhibits primary and metastatic tumor growth by antiangiogenesis: involvement of vascular endothelial growth factor. Nat Med. 2002;8: 128-135.

10. Geoerger B, Kerr K, Tang CB, et al. Antitumor activity of the rapamycin analog CCI-779 in human primitive neuroectodermal tumor/medulloblastoma models as single agent and in combination chemotherapy. Cancer Res. 2001;61:1527-1532.

11. Blazar BR, Taylor PA, Panoskaltsis-Mortari A, Vallera DA. Rapamycin inhibits the generation of graft-versus-host disease- and graft-versus-leukemia-causing T cells by interfering with the production of Th1 or Th1 cytotoxic cytokines. J Immunol. 1998;160:5355-5365.

12. Neshat MS, Mellinghoff IK, Tran C, et al. Sensitivity of PTEN-deficient tumors to inhibition of FRAP/mTOR. Proc Natl Acad Sci U S A. 2001;98: 10314-10319.

13. Abraham RT, Wiederrecht GJ. Immunopharmacology of rapamycin. Annu Rev Immunol. 1996; 14:483-510.

14. Price DJ, Grove JR, Calvo V, Avruch J, Bierer BE. Rapamycin-induced inhibition of the 70-kilodalton S6 protein kinase. Science. 1992;257:973-977.

15. Schmelzle T, Hall MN. TOR, a central controller of cell growth. Cell. 2000;103:253-262.

16. Gingras AC, Raught B, Gygi SP, et al. Hierarchical phosphorylation of the translation inhibitor 4E-BP1. Genes Dev. 2001;15:2852-2864.

17. Gingras AC, Raught B, Sonenberg N. Regulation of translation initiation by FRAP/mTOR. Genes Dev. 2001,15:807-826.

18. Gao X, Pan D. TSC1 and TSC2 tumor suppressors antagonize insulin signaling in cell growth. Genes Dev. 2001;15:1383-1392.

19. Brown VI, Fang J, Alcorn K, et al. Rapamycin is active against B-precursor leukemia in vitro and in vivo, an effect that is modulated by IL-7-mediated signaling. Proc Natl Acad Sci U S A. 2003; 100:15113-15118.

20. Romano MF, Avellino R, Petrella A, Bisogni R, Romano S, Venuta S. Rapamycin inhibits doxorubicin-induced NF-κB/Rel nuclear activity and enhances apoptosis in melanoma. Eur J Cancer. 2004;40:2829-2836.

21. Laurent G, Jaffrezou J-P. Signaling pathways activated by daunorubicin. Blood. 2001;98:913-924.

22. Wang CY, Cusak JC, Liu R, Baldwin AS. Control of inducible chemoresistance: enhanced antitumor therapy through increased apoptosis by inhibition of NF-kappaB. Nat Med. 1999;5:412-417.

23. Baughman G, Wiederrecht GJ, Faith Campbell N, Martin MM, Bourgeois S. FKBP51, a novel T-cell specific immunophilin capable of calcineurin inhibition. Mol Cell Biol. 1995;15:4395-4402.

24. Bouwmeester T, Bauch A, Ruffner H, et al. A physical and functional map of the human TNF-alpha/NF-kappaB signal transduction pathway. Nat Cell Biol. 2004;6:97-105.

25. Cossarizza A, Baccarani-Contri M, Kalashnikova G, Franceschi C. A new method for the cytofluorimetric analysis of mitochondrial membrane potential using the J-aggregate forming lipophilic cation 5,5',6,6'-tetrachloro-1,1',3,3'-tetraethylbenzimidazolcarbocyanine iodide (JC-1). Biochem Biophys Res Commun. 1993;197:40-45.

26. National PBM Drug Monograph. Sirolimus (Rapamune). VHA Pharmacy Benefits Management Strategic Healthcare Group and Medical Advisory Panel. January 2003.

27. Akagi T, Shishido T, Murata K, Hanafusa H. v-Crk activates the phosphoinositide 3-kinase/AKT pathway in transformation. Proc Natl Acad Sci U S A. 2000;97:7290-7295.

28. Furnari FB, Huang HJ, Cavenee WK. The phosphoinositol phosphatase activity of PTEN mediates a serum-sensitive G1 growth arrest in glioma cells. Cancer Res. 1998;58:5002-5008.

29. Choi J, Chen J, Schreiber SL, Clardy J. Structure of the FKBP12-rapamycin complex interacting with the binding domain of human FRAP. Science. 1996;27:239-242.

30. Sinars CR, Cheung-Flynn J, Rimerman RA, Scammell JG, Smith DF, Clardy J. Structure of the large FK506-binding protein FKBP51, an Hsp90-binding protein and a component of steroid receptor complexes. Proc Natl Acad Sci U S A. 2003;100:868-873.

31. Charng MJ, Zhang D, Kinnunen P, Schneider MD. A novel protein distinguishes between quiescent and activated forms of the type I transforming growth factor beta receptor. J Biol Chem. 1998; 273:9365-9368.

32. Shou W, Aghdasi B, Armstrong DL, et al. Cardiac defects and altered ryanodine receptor function in mice lacking FKBP12. Nature. 1998;391:489-492.

33. Khatua S, Peterson KM, Brown KM, et al. Overexpression of the EGFR/FKBP12/HIF-2alpha pathway identified in childhood astrocytomas by angiogenesis gene profiling. Cancer Res. 2003; 63:1865-1870.

34. Steiner JP, Hamilton GS, Ross DT, et al. Neurotrophic immunophilin ligands stimulate structural and functional recovery in neurodegenerative animal models. Proc Natl Acad Sci U S A. 1997;94: 2019-2024.

Rapamycin antagonizes NF-κB nuclear translocation activated by TNF-α in primary vascular smooth muscle cells and enhances apoptosis

Arturo Giordano,[1] Raffaella Avellino,[2] Paolo Ferraro,[1] Simona Romano,[2] Nicola Corcione,[1] and Maria Fiammetta Romano[2]
[1]*Invasive Cardiology Unit, Clinica Pineta Grande, Castelvolturno; and* [2]*Department of Biochemistry and Medical Biotechnology, University of Naples "Federico II," Naples, Italy*

Giordano, Arturo, Raffaella Avellino, Paolo Ferraro, Simona Romano, Nicola Corcione, and Maria Fiammetta Romano. Rapamycin antagonizes NF-κB nuclear translocation activated by TNF-α in primary vascular smooth muscle cells and enhances apoptosis. *Am J Physiol Heart Circ Physiol* 290: H2459–H2465, 2006. First published January 20, 2006; doi:10.1152/ajpheart.00750.2005.—Several lines of evidence support the view that rapamycin inhibits NF-κB. TNF-α, a potent inducer of NF-κB, is released after artery injury (e.g., balloon angioplasty) and plays an important role in inflammation and restenosis. We investigated the effect of rapamycin on NF-κB activation and apoptosis in vascular smooth muscle cells (VSMCs) stimulated with TNF-α. Using EMSA, we found that TNF-α caused NF-κB nuclear translocation in VSMCs after 1 h of incubation. Rapamycin inhibited IκBα degradation, thereby preventing nuclear translocation. Activation of NF-κB was accompanied by an increase of Bcl-xL and Bfl-1/A1 proteins, detected by Western blot assay, whereas rapamycin prevented the TNF-α-induced enhancement of these antiapoptotic proteins. The extent of apoptosis of VSMCs exposed to TNF-α was significantly enhanced by rapamycin. The effect of rapamycin appeared to be independent of the phosphatidylinositol 3-kinase/Akt-protein kinase B survival pathway, because the phosphatidylinositol 3-kinase inhibitor wortmannin neither prevented IκBα degradation nor increased apoptosis of cells incubated with TNF-α. Finally, we demonstrate that the large immunophilin FK-506 binding protein FKBP51 is essential for TNF-α-induced NF-κB activation in VSMCs. Our findings show that rapamycin inhibits NF-κB activation and acts in concert with TNF-α in induction of VSMC apoptosis.

inflammation; restenosis; vascular injury

BALLOON ANGIOPLASTY IS A POTENT stimulus for smooth muscle cell proliferation (43). Rapamycin is a potent inhibitor of neointimal formation after artery injury. Indeed, the implantation of stents coated with a rapamycin-containing biopolymer has dramatically decreased the incidence of in-stent restenosis (39, 43). Rapamycin acts by binding to the ubiquitous cytosolic FK-506 binding protein FKBP12 to form a complex that inhibits the serine/threonine kinase function of the mammalian target of rapamycin (mTOR) (9, 15, 35, 38). mTOR is activated through the phosphatidylinositol 3-kinase/Akt-protein kinase B survival pathway (13) and controls the synthesis of proteins essential for cell cycle progression (14, 31) by phosphorylating two key translational regulators: the initiation factor 4E binding protein (4E-BPI) (14) and the 70-kDa S6 ribosomal protein kinase (p70^{S6k}) (31). Rapamycin also increases levels of the cyclin-dependent kinase inhibitor p27^{Kip1} (21) and, reportedly, blocks the cell cycle at the G$_1$-to-S transition in vascular smooth muscle cells (VSMCs) (19). However, the findings that cell cycle progression and proliferation can occur despite 4E-BPI dephosphorylation (22) and that rapamycin inhibited intimal hyperplasia in p27-knockout mice by decreasing proliferation and enhancing apoptosis (34) suggested that other mechanisms are involved in the capacity of rapamycin to prevent poststent restenosis.

Inhibition of NF-κB prevented neointimal formation after balloon injury in a rat carotid artery model (44). NF-κB is an important element in the activation of the inflammatory cytokines and adhesion molecule genes involved in lesion development after vascular injury (25). Moreover, NF-κB factors modulate expression of a number of genes that sustain cell survival (3, 10, 42, 46); among these, Bcl-xL and Bfl-1/A1 play an important role in the pathogenesis of vascular lesion formation (17, 28, 29, 39). Bcl-xL is expressed at high levels after artery injury and is considered a key regulator of VSMC apoptosis (17). Inhibition of Bcl-xL dramatically induces VSMC apoptosis (29), and differences in Bcl-xL expression may account for differences in sensitivity to apoptosis after VSMC injury (28). Also Bfl-1/A1 is involved in resistance to VSMC apoptosis and contributes to development of atherosclerotic lesions in diabetes (37). TNF-α, which is released at high levels after artery injury (45), stimulates expression of Bcl-xl and Bfl-1/A1 by activating NF-κB transcription factors (1, 36), and TNF-α-induced apoptosis, reportedly, is suppressed by these proteins (10, 46).

Rapamycin has been shown to inhibit NF-κB in various cell types (20, 31, 41). We thus investigated whether it antagonizes the induction of Bcl-xl and Bfl-1/A1 in VSMCs stimulated with TNF-α. We also analyzed the effect of rapamycin on apoptosis of cells incubated with TNF-α. It is conceivable that, besides blocking proliferation, this drug limits the accumulation of neointimal cells in injured vessels by enhancing their apoptosis.

We attempted to clarify the role of the large immunophilin FK-506 binding protein FKBP51 (5), which is specifically inhibited by rapamycin (5), in NF-κB/Rel activation in VSMCs. Indeed, mapping of the TNF-α-NF-κB signal transduction pathway showed that FKBP51 is an IKKα cofactor essential for the function of the IKK kinase complex (7).

MATERIALS AND METHODS

Cell culture and reagents. VSMCs from Wistar rat thoracic aorta (kindly provided by Dr. G. Esposito, Dept. of Cardiovascular and

Immunological Sciences, University of Naples Federico II) (18) were cultured in medium 199 (ICN Biomedicals, Aurora, OH) supplemented with 10% heat-inactivated FCS (ICN Biomedicals). The experiments were performed when the cells were at *passage 4–6*. Rapamycin (Rapamune) was obtained from Wyeth Ayerst Laboratories (Marietta, PA), wortmannin from Sigma Aldrich (St. Louis, MO), and TNF-α from Roche Diagnostics (Basel, Switzerland).

Western blot analysis. For IκBα detection, cytoplasmic extracts were obtained from 1×10^6 cells resuspended in 100 μl of lysing buffer [10 mM HEPES, pH 7.9, 1 mM EDTA, 60 mM KCl, 1 mM DTT, 1 mM PMSF, 50 μg/ml antipain, 40 μg/ml bestatin, 20 μg/ml chymostatin, and 0.2% (vol/vol) Nonidet P-40] for 15 min in ice. For Bcl-xL, Bfl-1/A1, p65/RelA, and FKBP51 detection, whole cell lysates were prepared by homogenization in modified RIPA buffer (150 mM NaCl, 50 mM Tris·HCl, pH 7.4, 1 mM EDTA, 1 mM PMSF, 1% Triton X-100, 1% sodium deoxycholic acid, 0.1% SDS, 5 μg/ml aprotinin, and 5 μg/ml leupeptin). Cell debris was removed by centrifugation. Protein concentration was determined by a protein assay (Bio-Rad, Richmond, CA). The cell lysate was boiled for 5 min in 1× SDS sample buffer (50 mM Tris·HCl, pH 6.8, 12.5% glycerol, 1% SDS, and 0.01% bromphenol blue) containing 5% β-mercaptoethanol, run on a 10% SDS-polyacrylamide gel, transferred to a membrane filter (Cellulosenitrate, Schleicher and Schuell, Keene, NH), and incubated with the primary antibody. The antibodies against IκBα (a rabbit polyclonal antibody; Santa Cruz Biotechnology, Santa Cruz, CA), Bcl-xL (a mouse monoclonal antibody; Santa Cruz Biotechnology), Bfl-1/A1 (a rabbit polyclonal antibody; Santa Cruz Biotechnology), FKBP51 (a rabbit polyclonal antibody; Abcam, Cambridge, UK), and p65/RelA [a rabbit polyclonal antibody against COOH-terminal peptide (529–551) kindly provided by Dr. Shao-Cong Sun, Pennsylvania State University College of Medicine] were added to the incubation mixture at a dilution of 1:500. After a second incubation with peroxidase-conjugated goat anti-rabbit IgG (Santa Cruz Biotechnology) or anti-mouse IgG (Santa Cruz Biotechnology), the blots were developed with the enhanced chemiluminescence system (ECL, Amersham Pharmacia Biotech, Piscataway, NJ).

EMSA. Cell nuclear extracts were prepared from 1×10^6 cells by cell pellet homogenization in two volumes of 10 mM HEPES, pH 7.9, 10 mM KCl, 1.5 mM MgCl₂, 1 mM EDTA, 0.5 mM DTT, 0.5 mM PMSF, and 10% glycerol. Nuclei were centrifuged at 1,000 g for 5 min, washed, and resuspended in two volumes of the above-specified solution. KCl (3 M) was added to reach 0.39 M KCl. Nuclei were lysed at 4°C for 1 h and centrifuged at 10,000 g for 30 min. The supernatants clarified by centrifugation were collected and stored at −80°C. Protein concentration was determined with a protein assay (Bio-Rad). The NF-κB consensus 5'-CAACGGCAGGGGAATCTC-CCTCTCCTT-3' (32) oligonucleotide was end-labeled with [γ-³²P]ATP (Amersham Pharmacia Biotech) using a polynucleotide kinase (Roche). End-labeled DNA fragments were incubated at room temperature for 20 min with 5 μg of nuclear protein in the presence of 1 μg of poly(dI-dC) in 20 μl of a buffer consisting of 10 mM Tris·HCl, pH 7.5, 50 mM NaCl, 1 mM EDTA, 1 mM DTT, and 5% glycerol. In competition assays, a 50× molar excess of NF-κB or nuclear factor of activated T cells (NF-AT) cold oligonucleotide was added to the incubation mixture. The rabbit antibody against p65 (see above) or a preimmune antibody was used in the supershift assay. Protein-DNA complexes were separated from free probe on a 6% polyacrylamide gel run in 0.25× Tris-borate buffer at 200 mV for 3 h at room temperature. The gels were dried and exposed to X-ray film (Kodak AR).

Cell transfection and small interfering RNA. A small interfering (si) RNA was designed for the rat FKBP51 gene [5'-AGGCGAGAU-CUGCCACUUA-3' (sense); Dharmacon Research, Boulder, CO]. The siRNA for the human p65 gene [5-GCCCUAUCCCU-UUACGU-3 (sense)] (40), which shares 77% homology with the rat gene, was kindly provided by Prof. M. C. Turco (DIFARMA, Fisciano, Italy). Scrambled duplexes were used as controls (Dharma-

con Research). At 24 h before transfection of the oligonucleotide, the cells were incubated in six-well plates in medium without antibiotics at 5×10^5 cells/ml. The siRNA or the scrambled oligonucleotide was transfected at the final concentration of 50 nM using Metafectene (Biontex, Munich, Germany) according to the manufacturer's instructions. After 2 days, 20 ng/ml of TNF-α were added to the culture medium, and 1 or 2 h later, the cells were harvested and processed by Western blot assay or EMSA.

Analysis of apoptosis. Phosphatidylserine externalization was investigated by annexin V staining. Briefly, 1×10^5 cells were resuspended in 100 μl of binding buffer (10 mM HEPES-NaOH, pH 7.5, 140 mM NaCl, and 2.5 mM CaCl₂) containing 5 μl of annexin V-FITC (Pharmigen/Becton Dickinson, San Diego, CA) for 15 min at room temperature in the dark. Then 400 μl of the same buffer were added to each sample, and the cells were analyzed with a flow cytometer (FACScan, Becton Dickinson). A TdT-mediated dUTP nick end-labeling assay was performed with the In Situ Cell Death Detection Kit (Roche) using TMR red according to the manufacturer's instructions. Briefly, 1×10^6 cells were fixed with 2% (vol/vol) paraformaldehyde in PBS for 15 min at room temperature, washed, and permeabilized with 0.1% Triton X-100 in PBS for 2 min in ice. After a second wash, the cells were incubated with TMR red labeling solution for 1 h at 37°C and analyzed by flow cytometry.

Statistical analysis. Values are means and SD of independent experiments. The statistical significance of differences between means was estimated using the paired Student's *t*-test, because the two series of samples compared were the same and differed only in the treatment applied. $P < 0.05$ was considered statistically significant.

RESULTS

Rapamycin inhibits TNF-α-induced NF-κB/Rel activity in VSMCs. High levels of TNF-α have been detected after balloon angioplasty (45). To investigate whether neointimal cells were sensitive to signals induced by TNF-α receptor triggering, we evaluated the induction of NF-κB/Rel nuclear activity by EMSA in VSMCs incubated with TNF-α for 30, 60, and 90 min. NF-κB proteins appeared in VSMC nuclei after 60 min of incubation with TNF-α (Fig. 1A). The band indicated by the arrow in Fig. 1 corresponds to specific NF-κB complexes, because it was supershifted by anti-p65 (RelA) antibodies. This finding suggests that the band consists of RelA dimers. On the contrary, incubation with the preimmune antibody did not change the migration pattern of the band (Fig. 1B). To investigate whether rapamycin inhibited NF-κB/Rel nuclear activity induced by TNF-α, we incubated VSMCs with and without TNF-α and with and without rapamycin for 1 h and then analyzed the nuclear extracts by EMSA. Addition of rapamycin to TNF-α-stimulated VSMCs caused a decrease in NF-κB/Rel nuclear levels compared with cells stimulated with TNF-α alone (Fig. 1C).

NF-κB nuclear translocation is preceded by IκBα degradation (3). We therefore investigated whether rapamycin prevented this process by measuring IκBα cytoplasmic levels in Western blot. TNF-α induced IκBα degradation after 45 min, and IκBα levels were restored after 120 min (Fig. 2A). Rapamycin did not cause the disappearance of IκBα, which indicates that the NF-κB inhibitor was not degraded. In contrast to rapamycin, wortmannin, a specific phosphatidylinositol 3-kinase inhibitor, did not prevent TNF-α-induced IκBα degradation (Fig. 2B). Thus our findings suggest that rapamycin inhibits NF-κB independently of blockage of the phosphatidylinositol 3-kinase/Akt pathway.
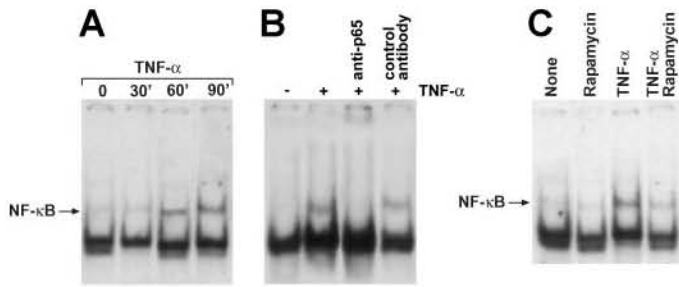
Fig. 1. Rapamycin inhibits TNF-α-induced NF-κB/Rel activity in vascular smooth muscle cells (VSMCs). *A*: effect of TNF-α on NF-κB/Rel nuclear translocation in VSMCs. Nuclear extracts prepared from VSMCs cultured for 30–90 min with 20 ng/ml TNF-α were incubated with [γ-^{32}P]ATP-end-labeled NF-κB consensus and subjected to EMSA. *B*: supershift analysis of nuclear complexes induced by TNF-α in rat VSMCs. Nuclear extracts prepared from VSMCs cultured for 1 h with 20 ng/ml TNF-α were incubated with [γ-^{32}P]ATP-end-labeled NF-κB consensus with and without anti-p65 or pre-immune antibody and subjected to EMSA. *C*: effect of rapamycin on TNF-α-induced NF-κB/Rel nuclear translocation in VSMCs. Nuclear extracts prepared from VSMCs cultured for 1 h with and without 20 ng/ml TNF-α and with and without 100 ng/ml rapamycin were incubated with [γ-^{32}P]ATP-end-labeled NF-κB consensus and subjected to EMSA. Results from 3 different experiments show that intensity of the NF-κB band, expressed as integrated optical density and determined using NIH Image 1.61 for Macintosh, was significantly increased in TNF-α samples compared with control ($P = 0.006$) or rapamycin + TNF-α specimens ($P = 0.02$).

Rapamycin counteracts the TNF-α-induced increase of anti-apoptotic proteins. NF-κB/Rel transcription factors regulate the expression of genes that protect cells against death. Among these genes, Bcl-xL (10) and Bfl-1/A1 (46) are induced by TNF-α and are responsible for resistance to TNF-α-triggered cell death. Furthermore, both genes are involved in the control of smooth muscle cell apoptosis (17, 29, 30, 37). We therefore evaluated the effect of TNF-α and rapamycin on Bcl-xL and Bfl-1/A1 expression in VSMCs by Western blot assay. Representative results of two different experiments are shown in Fig. 3. TNF-α enhanced the basal expression of Bcl-xL by twofold, whereas it induced the expression of Bfl-1/A1, which was negligible in control cells. Coincubation of rapamycin and TNF-α caused a ≥50% decrease in Bcl-xL and Bfl-1/A1 protein levels compared with samples incubated with TNF-α alone. This finding is in agreement with inhibition of NF-κB.
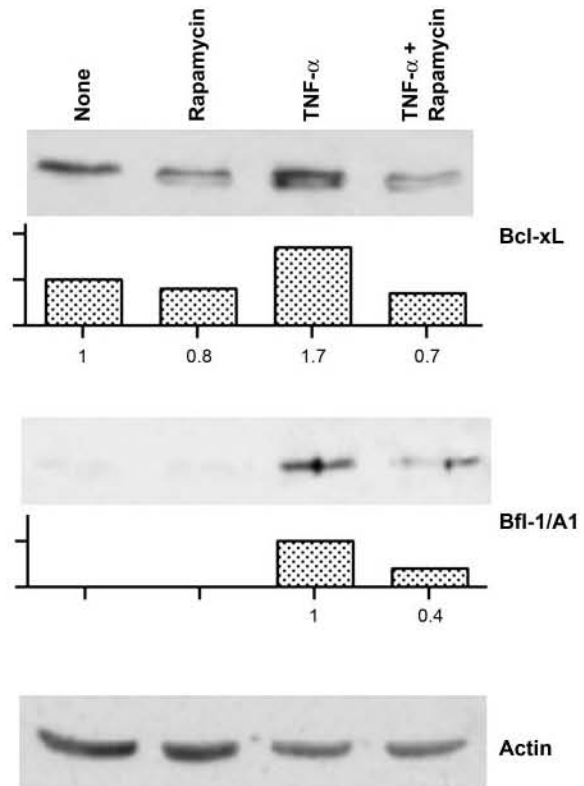

Fig. 3. Effect of TNF-α and rapamycin on induction of Bcl-xL and Bfl-1/A1 in VSMCs. Bcl-xL and Bfl-1/A1 expression levels in whole cell lysates prepared from cells cultured for 2 h with and without 20 ng/ml TNF-α and with and without 100 ng/ml rapamycin were analyzed by Western blot. Expression levels were quantified by densitometry and expressed vs. baseline (Bcl-X$_L$) or TNF-α-induced level (Bfl-1/A1).

Rapamycin enhances apoptosis of VSMCs stimulated with TNF-α. NF-κB inhibition sensitizes many cell types to TNF-α-induced apoptosis (10, 42). Consequently, it is feasible that rapamycin, which inhibited NF-κB, modulates apoptosis of VSMCs stimulated with TNF-α. To address this issue, we cultured VSMCs with TNF-α in the presence and absence of rapamycin and analyzed cell death. Furthermore, because rapamycin also inhibits phosphatidylinositol 3-kinase/Akt through
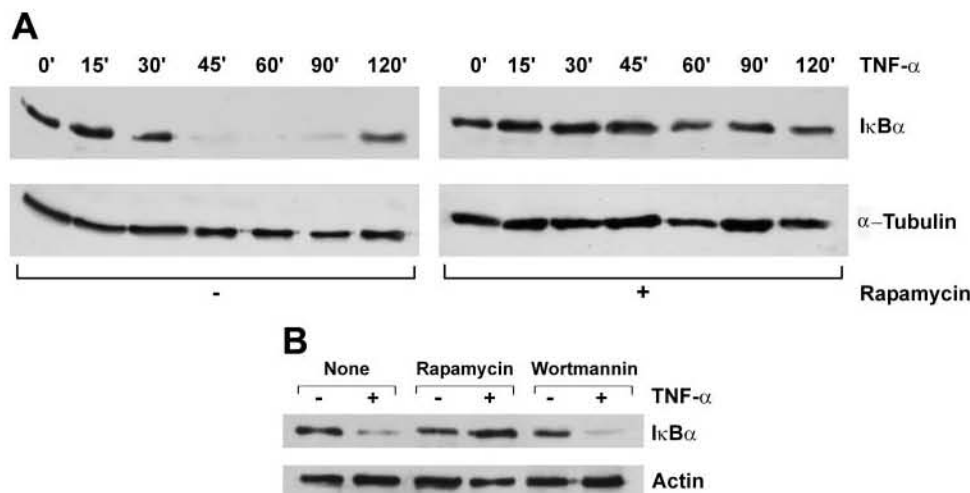
Fig. 2. Effect of rapamycin on TNF-α-induced IκBα degradation in VSMCs. *A*: Western blot analysis of IκBα levels in cytoplasmic lysates prepared from cells cultured for 0–120 min with 20 ng/ml TNF-α and with and without 100 ng/ml rapamycin. *B*: Western blot analysis of IκBα levels in cytoplasmic lysates prepared from cells cultured for 1 h with and without 20 ng/ml TNF-α and with and without 100 ng/ml rapamycin or 1 μM wortmannin. Densitometry analysis of IκBα levels in 3 different experiments, determined by NIH Image 1.61 for Macintosh, show decreased levels in TNF-α specimens compared with control ($P = 0.05$) or rapamycin + TNF-α samples ($P = 0.02$). No difference was detected between samples treated with TNF-α alone and those treated with TNF-α + wortmannin.

blockage of mTOR kinase activity, we examined the effect of the specific phosphatidylinositol 3-kinase inhibitor wortmannin on apoptosis of VSMCs incubated with TNF-α. Annexin V stained 31.5% (SD 6.2) of cells cultured in 10% FCS-medium 199 and 40.0% (SD 6.6) of cells cultured in the presence of TNF-α ($P = 0.1$; Fig. 4A). Addition of rapamycin (100 ng/ml) to TNF-α-stimulated cells significantly increased cell death [60.1% (SD 1.1), $P < 0.03$; Fig. 4A]. Rapamycin alone at ≤200 ng/ml caused a slight increase of basal apoptosis ($P > 0.09$). Wortmannin also slightly increased basal apoptosis ($P = 0.1$) but did not act in concert with TNF-α. Indeed, the extent of apoptosis of VSMCs cultured with wortmannin + TNF-α was similar to that of cells cultured with the cytokine alone (Fig. 4A). These findings suggest that the cooperative effect of rapamycin and TNF-α on VSMC apoptosis involved mechanisms unrelated to phosphatidylinositol 3-kinase/Akt inhibition. This cooperative effect was confirmed by TdT-mediated dUTP nick end-labeling assay. The percentage of cells that incorporated dUTP in their DNA increased after addition of rapamycin to TNF-α-stimulated cells (Fig. 4B).

FKBP51 controls TNF-α-induced NF-κB activation in VSMCs. Components of the FKBP family are the first target of rapamycin (5, 11, 12). These abundant cytosolic proteins are endowed with peptidyl-prolyl-isomerase activity, which is required for many cellular processes and is specifically inhibited by rapamycin (5). Among these, FKBP51 catalyzes the isomerization of peptidyl-prolyl-imide bonds in the α-subunit of the IKK kinase complex and is essential for IKK function (7). To assess the role of FKBP51 in the NF-κB activation pathway in VSMCs, using the siRNA approach, we downmodulated immunophilin levels in primary rat VSMCs. FKBP51 protein levels were clearly lower in VSMCs transfected with FKBP51 siRNA than in cells incubated with control medium or transfected with a scrambled oligonucleotide (Fig. 5A). We then

investigated the ability of TNF-α to induce IκB degradation and NF-κB nuclear translocation when FKBP51 was downmodulated. IκB levels decreased in control cells and in scrambled-oligonucleotide-transfected cells cultured with TNF-α (Fig. 5B), which indicated IκB degradation. On the contrary, the levels of the inhibitor did not decrease when FKBP51 was downmodulated. Accordingly, EMSA showed the absence of NF-κB complexes in nuclear extracts from FKBP51 siRNA-transfected cells stimulated with TNF-α (Fig. 5C). These findings suggest that FKBP51 controls NF-κB activation in VSMCs. A competition assay showed the specificity of the NF-κB band. This band disappeared when the extract was incubated with the ^{32}P-labeled NF-κB oligonucleotide in the presence of a 50× molar excess of unlabeled NF-κB oligonucleotide, but not in the presence of unlabeled NF-AT.

Lack of induction of Bcl-xL in p65- or FKBP51-depleted cells. To verify that the induction of antiapoptotic proteins by TNF-α depended on NF-κB activation, we used the siRNA technique to downmodulate the levels of p65 and used Western blot to analyze the expression levels of Bcl-xL in VSMCs stimulated with TNF-α. TNF-α caused a twofold increase in Bcl-xL basal levels in cells transfected with the control oligonucleotide, but not when p65 was downmodulated (Fig. 6A). This result suggests that the *trans*-activating property of p65/RelA is essential for the induction of Bcl-xL stimulated by TNF-α. Similar results were obtained in FKBP51-depleted cells, notwithstanding the stable levels of p65. These findings support the concept that FKBP51 is important in NF-κB signaling (7).

DISCUSSION

Various signaling pathways, activated during vascular injury by a number of cytokines (6), concur in determining postangioplasty restenosis (43). NF-κB contributes to angioplasty-
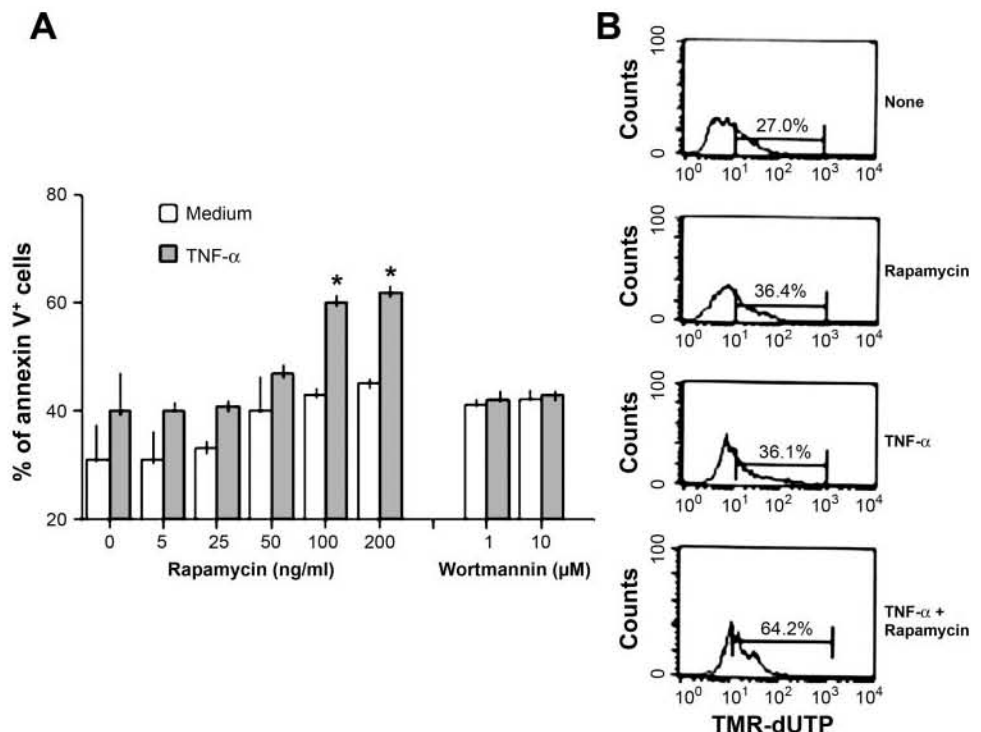
Fig. 4. Rapamycin enhances apoptosis of VSMCs stimulated with TNF-α. A: effect of rapamycin and wortmannin on apoptosis of VSMCs cultured in the absence and presence of TNF-α. Cell death values (means ± SD) were measured by annexin V staining and flow cytometry. VSMCs were cultured for 24 h in 10% FCS-medium 199 with and without 20 ng/ml TNF-α and with and without rapamycin or wortmannin. Data are from 4 different experiments, each done in triplicate. *Significantly different ($P < 0.03$): rapamycin (≥100 ng/ml) + TNF-α vs. TNF-α alone. B: effect of rapamycin on apoptosis of VSMCs cultured with TNF-α. Flow cytometry diagrams show tetramethylrhodamine (TMR)-dUTP incorporation in VSMCs cultured for 24 h with 20 ng/ml TNF-α and/or 100 ng/ml rapamycin.
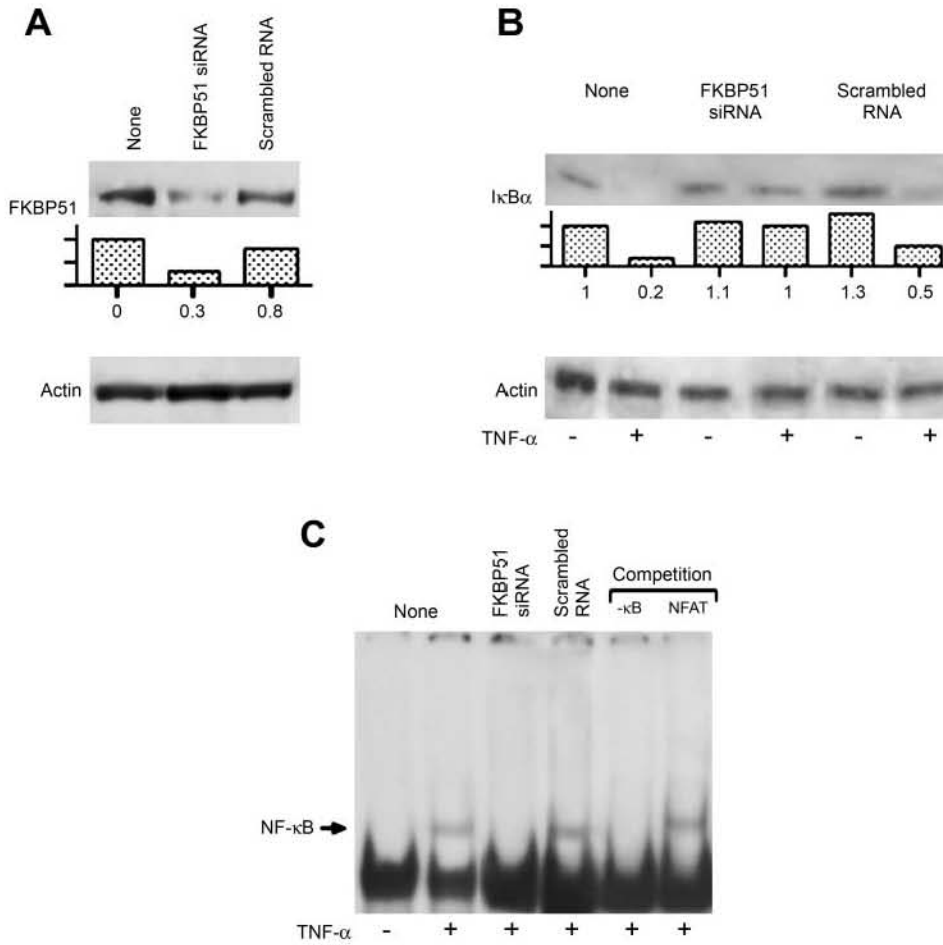
Fig. 5. FK-506 binding protein (FKBP51) controls TNF-α-induced NF-κB activation in VSMCs. *A*: effect of small interfering RNA (siRNA) transfection on FKBP51 levels in VSMCs. FKBP51 expression levels in cell lysates obtained from nontransfected VSMCs and VSMCs transfected with specific siRNA or scrambled oligonucleotide as control were assayed by Western blot. Expression levels were quantified by densitometry and expressed vs. baseline level. *B*: effect of FKBP51 depletion on TNF-α-induced IκBα degradation in VSMCs. IκBα levels in cytoplasmic lysates prepared from nontransfected VSMCs and VSMCs transfected with FKBP51 siRNA or scrambled oligonucleotide as control and cultured for 1 h with and without 20 ng/ml TNF-α were assayed by Western blot. Expression levels were quantified by densitometry and expressed vs. baseline level. *C*: effect of FKBP51 depletion on TNF-α-induced NF-κB/Rel nuclear translocation in VSMCs. Nuclear extracts prepared from VSMCs cultured for 1 h with 20 ng/ml TNF-α were incubated with [γ-^{32}P]ATP-end-labeled NF-κB consensus and subjected to EMSA. A competition assay, performed with the same NF-κB cold oligonucleotide or an unrelated oligonucleotide, demonstrated specificity of the NF-κB band (arrow). Results are representative of 2 different experiments. NF-AT, nuclear factor of activated T cells.

induced lumen loss by inducing an inflammatory response (23, 25, 44) and a decreased rate of apoptosis (23), whereas the phosphatidylinositol 3-OH-kinase cascade controls VSMC proliferation (23). Among the cytokines released at the site of artery injury, TNF-α, which is mainly produced by infiltrating monocytes/macrophages (24), is particularly intriguing. TNF-α is a pleiotropic cytokine (4), and its receptor binding leads to activation of apoptosis, mitogen-activated protein kinase (MAPK), phosphatidylinositol 3-OH-kinase, and IKK (16), thereby eliciting a broad spectrum of cellular responses.
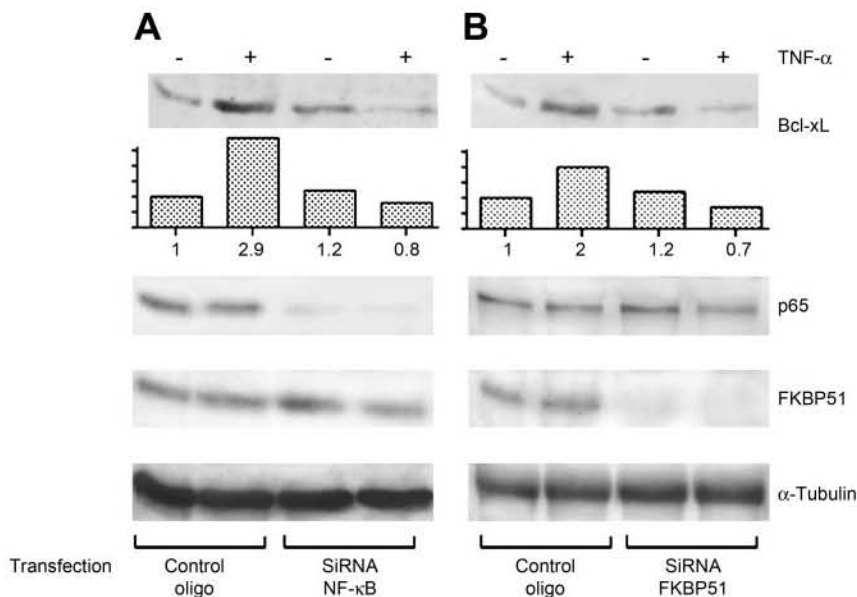
Fig. 6. Effect of TNF-α on induction of Bcl-xL in VSMCs depleted of p65 or FKBP51. *A*: Western blot assay of Bcl-xL, p65, and FKBP51 expression levels in whole cell lysates from VSMCs transfected with specific p65 siRNA or scrambled oligonucleotide (oligo) as control and cultured for 2 h with and without 20 ng/ml TNF-α. *B*: Western blot assay of Bcl-xL, p65, and FKBP51 expression levels in whole cell lysates from VSMCs transfected with specific FKBP51 siRNA or scrambled oligonucleotide as control and cultured for 2 h with and without 20 ng/ml TNF-α.

Suppression of apoptosis, which is NF-κB dependent (4, 23, 42, 46), augments the inflammatory response to TNF-α (23). We investigated the effects of TNF-α on NF-κB activation and apoptosis in VSMCs and their modulation by rapamycin. Our study suggests that rapamycin interferes with IKK function and, hence, prevents TNF-α-induced NF-κB activation. This notion is supported by the finding that rapamycin exerted an anti-inflammatory effect in a human model of angioplasty (27). Accordingly, we found that induction of the prosurvival Bcl-2 homologs Bcl-X$_L$ and Bfl-1/A1, which are transcriptional targets of NF-κB (10, 46), was inhibited by rapamycin, and, as expected, the extent of apoptosis of VSMCs cultured with rapamycin + TNF-α was greater than that of cells cultured with the cytokine alone. Taken together, these findings suggest that, besides blocking cell proliferation, rapamycin controls neointimal hyperplasia by cooperating with endogenous TNF-α to induce VSMC apoptosis. This concept is consistent with the finding of apoptosis in a porcine coronary angioplasty model treated with rapamycin (33).

Although TNF-α through TNF-α receptor type 1 (TNFR1) induces tyrosine phosphorylation of the p85 subunit of phosphatidylinositol 3-OH-kinase (16), thereby activating the phosphatidylinositol 3-kinase/Akt pathway, the effect of rapamycin on NF-κB activation and apoptosis seemed to be independent of this signaling pathway, because the phosphatidylinositol 3-kinase inhibitor wortmannin neither prevented IκBα degradation nor increased apoptosis of VSMCs cultured with TNF-α. In contrast, we demonstrate that the large immunophilin FKBP51 (5) is required for TNF-α-induced NF-κB activation in VSMCs. Rapamycin very specifically binds to FKBP51 and inhibits its isomerase activity (5), which is required for function of the IKK kinase complex (7). Therefore, it is reasonable to assume that it counteracts NF-κB activation by affecting the IKKα cofactor (7). The finding that rapamycin reduces the phosphorylating activity of IKK on its IκB substrate (31) supports this hypothesis.

Data from our present study may have an impact on the synthesis of natural-product derivatives, in particular small molecules that are able to modulate the action of the target and improve the bioavailability of a drug (2). Indeed, a low tissue distribution of the drug has been cited as a cause of the unsuccessful outcome of oral rapamycin therapy for recalcitrant restenosis (8). Thus far, the rapamycin derivatives used in clinical trials have been tested for their ability to inhibit mTOR (26). Our finding that IKK is also a target of rapamycin raises the possibility that molecules specifically targeting IKK may improve clinical outcome after balloon dilatation.

In conclusion, our study shows that rapamycin inhibits NF-κB activity in VSMCs and downmodulates antiapoptotic proteins possibly responsible for reduced sensitivity to death signals that might counteract smooth muscle cell growth after artery injury.

REFERENCES

1. **Abbas S and Abu-Amer Y.** Dominant-negative IκB facilitates apoptosis of osteoclasts by tumor necrosis factor-α. *J Biol Chem* 278: 20077–20082, 2003.
2. **Arya P and Baek MG.** Natural-product-like chiral derivatives by solid-phase synthesis. *Curr Opin Chem Biol* 5: 292–301, 2001.
3. **Baldwin AS Jr.** The NF-κB and IκB proteins: new discoveries and insights. *Annu Rev Immunol* 14: 649–681, 1996.
4. **Baud V and Karin M.** Signal transduction by tumor necrosis factor and its relatives. *Trends Cell Biol* 11: 372–377, 2001.
5. **Baughman G, Wiederrecht GJ, Campbell NF, Martin MM, and Bourgeois S.** FKBP51, a novel T-cell-specific immunophilin capable of calcineurin inhibition. *Mol Cell Biol* 15: 4395–4402, 1995.
6. **Biasucci LM.** CDC/AHA Workshop on Markers of Inflammation and Cardiovascular Disease: Application to Clinical and Public Health Practice: clinical use of inflammatory markers in patients with cardiovascular diseases. *Circulation* 110: 560–567, 2004.
7. **Bouwmeester T, Bauch A, Ruffner H, Angrand PO, Bergamini G, Croughton K, Cruciat C, Eberhard D, Gagneur J, Ghidelli S, Hopf C, Huhse B, Mangano M, Michon AM, Schirle M, Schlegl J, Schwab M, Stein MA, Bauer A, Casari G, Drewes G, Gavin AC, Jackson DB, Joberty G, Neubauer G, Rick J, Kuster B, and Superti-Furga G.** A physical and functional map of the human TNF-α/NF-κB signal transduction pathway. *Nat Cell Biol* 6: 97–105, 2004.
8. **Brara PS, Moussavian M, Grise MA, Reilly JP, Fernandez M, Schatz RA, and Teirstein PS.** Pilot trial of oral rapamycin for recalcitrant restenosis. *Circulation* 107: 1722–1724, 2003.
9. **Brown EJ, Albers MW, Shin TB, Ichikawa K, Keith CT, Lane WS, and Schreiber SL.** A mammalian protein targeted by G$_1$-arresting rapamycin-receptor complex. *Nature* 369: 756–758, 1994.
10. **Cao WJ, Zhang YZ, Zhang DH, Li DJ, and Tang JZ.** Inhibition of NF-κB by mutant IκBα enhances TNF-α-induced apoptosis in HL-60 cells by controlling bcl-xL expression. *Chin Med J (Engl)* 117: 972–977, 2004.
11. **Choi J, Chen J, Schreiber SL, and Clardy J.** Structure of the FKBP12-rapamycin complex interacting with the binding domain of human FRAP. *Science* 27: 239–242, 1996.
12. **Dornan J, Taylor P, and Walkinshaw MD.** Structures of immunophilins and their ligand complexes. *Curr Top Med Chem* 3: 1392–1409, 2003.
13. **Gao X and Pan D.** TSC1 and TSC2 tumor suppressors antagonize insulin signaling in cell growth. *Genes Dev* 15: 1383–1392, 2001.
14. **Gingras AC, Raught B, Gygi SP, Niedzwiecka A, Miron M, Burley SK, Polakiewicz RD, Wyslouch-Cieszynska A, Aebersold R, and Sonenberg N.** Hierarchical phosphorylation of the translation inhibitor 4E-BP1. *Genes Dev* 15: 2852–2864, 2001.
15. **Gingras AC, Raught B, and Sonenberg N.** Regulation of translation initiation by FRAP/mTOR. *Genes Dev* 15: 807–826, 2001.
16. **Guo D and Donner DB.** Tumour necrosis factor promotes phosphorylation and binding of IRS-1 to phosphatidylinositol 3-kinase in 3T3-L1 adipocytes. *J Biol Chem* 271: 615–618, 1996.
17. **Igase M, Okura T, Kitami Y, and Hiwada K.** Apoptosis and Bcl-xs in the intimal thickening of balloon-injured carotid arteries. *Clin Sci (Lond)* 96: 605–612, 1999.
18. **Indolfi C, Avvedimento EV, Di Lorenzo E, Esposito G, Rapacciuolo A, Giuliano P, Grieco D, Cavuto L, Stingone AM, Ciullo I, Condorelli G, and Chiariello M.** Activation of cAMP-PKA signaling in vivo inhibits smooth muscle cell proliferation induced by vascular injury. *Nat Med* 3: 775–779, 1997.
19. **Jayaraman T and Marks AR.** Rapamycin-FKBP12 blocks proliferation, induces differentiation, and inhibits cdc2 kinase activity in a myogenic cell line. *J Biol Chem* 268: 25385–25388, 1993.
20. **Lai JH and Tan TH.** CD28 signaling causes a sustained down-regulation of IκBα which can be prevented by the immunosuppressant rapamycin. *J Biol Chem* 269: 30077–30080, 1994.
21. **Luo Y, Marx SO, Kiyokawa H, Koff A, Massague J, and Marks AR.** Rapamycin resistance tied to defective regulation of p27^{Kip1}. *Mol Cell Biol* 16: 6744–6751, 1996.
22. **Marx SO and Marks AR.** Cell cycle progression and proliferation despite 4BP-1 dephosphorylation. *Mol Cell Biol* 19: 6041–6047, 1999.
23. **Mehrhof FB, Schmidt-Ullrich R, Dietz R, and Scheidereit C.** Regulation of vascular smooth muscle cell proliferation: role of NF-κB revisited. *Circ Res* 96: 958–964, 2005.

24. **Meiners S, Laule M, Rother W, Guenther C, Prauka I, Muschick P, Baumann G, Kloetzel PM, and Stangl K.** Ubiquitin-proteasome pathway as a new target for the prevention of restenosis. *Circulation* 105: 483–489, 2002.

25. **Monaco C and Paleolog E.** Nuclear factor κB: a potential therapeutic target in atherosclerosis and thrombosis. *Cardiovasc Res* 61: 671–682, 2004.

26. **Neshat MS, Mellinghoff IK, Tran C, Stiles B, Thomas G, Petersen R, Frost P, Gibbons JJ, Wu H, and Sawyers CL.** Enhanced sensitivity of PTEN-deficient tumors to inhibition of FRAP/mTOR. *Proc Natl Acad Sci USA* 98: 10314–10319, 2001.

27. **Nuhrenberg TG, Voisard R, Fahlisch F, Rudelius M, Braun J, Gschwend J, Kountides M, Herter T, Baur R, Hombach V, Baeuerle PA, and Zohlnhofer D.** Rapamycin attenuates vascular wall inflammation and progenitor cell promoters after angioplasty. *FASEB J* 19: 246–248, 2005.

28. **Pollman MJ, Hall JL, and Gibbons GH.** Determinants of vascular smooth muscle cell apoptosis after balloon angioplasty injury. Influence of redox state and cell phenotype. *Circ Res* 84: 113–121, 1999.

29. **Pollman MJ, Hall JL, Mann MJ, Zhang LN, and Gibbons GH.** Inhibition of neointimal cell bcl-x expression induces apoptosis and regression of vascular disease. *Nat Med* 4: 222–227, 1998.

30. **Price DJ, Grove JR, Calvo V, Avruch J, and Bierer BE.** Rapamycin-induced inhibition of the 70-kilodalton S6 protein kinase. *Science* 257: 973–977, 1992.

31. **Romano MF, Avellino R, Petrella A, Bisogni R, Romano S, and Venuta S.** Rapamycin inhibits doxorubicin-induced NF-κB/Rel nuclear activity and enhances apoptosis in melanoma. *Eur J Cancer* 40: 2829–2836, 2004.

32. **Romano MF, Lamberti A, Tassone P, Alfinito F, Costantini S, Chiurazzi F, Defrance T, Bonelli P, Tuccillo F, Turco MC, and Venuta S.** Triggering of CD40 antigen inhibits fludarabine-induced apoptosis in B chronic lymphocytic leukemia cells. *Blood* 92: 990–995, 1998.

33. **Roque M, Cordon-Cardo C, Fuster V, Reis ED, Drobnjak M, and Badimon JJ.** Modulation of apoptosis, proliferation, and p27 expression in a porcine coronary angioplasty model. *Atherosclerosis* 153: 315–322, 2000.

34. **Roque M, Reis ED, Cordon-Cardo C, Taubman MB, Fallon JT, Fuster V, and Badimon JJ.** Effect of p27 deficiency and rapamycin on intimal hyperplasia: in vivo and in vitro studies using a p27 knockout mouse model. *Lab Invest* 81: 895–903, 2001.

35. **Sabatini DM, Erdjument-Bromage H, Lui M, Tempst P, and Snyder SH.** RAFT1: a mammalian protein that binds to FKBP12 in a rapamycin-dependent fashion and is homologous to yeast TORs. *Cell* 78: 35–43, 1994.

36. **Saile B, Matthes N, El Armouche H, Neubauer K, and Ramadori G.** The bcl, NFκB and p53/p21WAF1 systems are involved in spontaneous apoptosis and in the anti-apoptotic effect of TGF-β or TNF-α on activated hepatic stellate cells. *Eur J Cell Biol* 80: 554–561, 2001.

37. **Sakuma H, Yamamoto M, Okumura M, Kojima T, Maruyama T, and Yasuda K.** High glucose inhibits apoptosis in human coronary artery smooth muscle cells by increasing Bcl-xL and Bfl-1/A1. *Am J Physiol Cell Physiol* 283: C422–C428, 2002.

38. **Schmelzle T and Hall MN.** TOR, a central controller of cell growth. *Cell* 103: 253–262, 2000.

39. **Sousa JE, Costa MA, Abizaid A, Abizaid AS, Feres F, Pinto IM, Seixas AC, Staico R, Mattos LA, Sousa AG, Falotico R, Jaeger J, Popma JJ, and Serruys PW.** Lack of neointimal proliferation after implantation of sirolimus-coated stents in human coronary arteries: a quantitative coronary angiography and three-dimensional intravascular ultrasound study. *Circulation* 103: 192–195, 2001.

40. **Todaro M, Zerilli M, Triolo G, Iovino F, Patti M, Accardo-Palumbo A, di Gaudio F, Turco MC, Petrella A, de Maria R, and Stassi G.** NF-κB protects Behcet's disease T cells against CD95-induced apoptosis up-regulating antiapoptotic proteins. *Arthritis Rheum* 52: 2179–2191, 2005.

41. **Tsukamoto N, Kobayashi N, Azuma S, Yamamoto T, and Inoue J.** Two differently regulated nuclear factor κB activation pathways triggered by the cytoplasmic tail of CD40. *Proc Natl Acad Sci USA* 96: 1234–1239, 1999.

42. **Van Antwerp DJ, Martin SJ, Kafri T, Green DR, and Verma IM.** Suppression of TNF-α-induced apoptosis by NF-κB. *Science* 274: 787–789, 1996.

43. **Woods TC and Marks AR.** Drug-eluting stents. *Annu Rev Med* 55: 169–178, 2004.

44. **Yoshimura S, Morishita R, Hayashi K, Yamamoto K, Nakagami H, Kaneda Y, Sakai N, and Ogihara T.** Inhibition of intimal hyperplasia after balloon injury in rat carotid artery model using *cis*-element "decoy" of nuclear factor-κB binding site as a novel molecular strategy. *Gene Ther* 8: 1635–1642, 2001.

45. **Zhou Z, Lauer MA, Wang K, Forudi F, Zhou X, Song X, Solowski N, Kapadia SR, Nakada MT, Topol EJ, and Lincoff AM.** Effect of anti-tumor necrosis factor-α polyclonal antibody on restenosis after balloon angioplasty in a rabbit atherosclerotic model. *Atherosclerosis* 16: 153–159, 2002.

46. **Zong WX, Edelstein LC, Chen C, Bash J, and Gelinas C.** The prosurvival Bcl-2 homolog Bfl-1/A1 is a direct transcriptional target of NF-κB that blocks TNFα-induced apoptosis. *Genes Dev* 13: 382–387, 1999.

Chapter X

Rapamycin Controls Multiple Signalling Pathways Involved in Cancer Cell Survival

Maria Fiammetta Romano, Simona Romano, Maria Mallardo,
Rita Bisogni and Salvatore Venuta

Department of Biochemistry and Medical Biotechnology,
University Federico II, Naples, Italy.
Department of Clinical and Experimental Medicine, University Magna Graecia,
Catanzaro, Italy.

Abstract

Suppression of apoptosis by survival signals is considered a hallmark of malignant transformation and resistance to anti-cancer therapy. The phosphoinositide-3 kinase (PI3k)/Akt pathway and NF-κB transcription factors are potent mediators of tumour cell survival. The carbocyclic lactone-lactam antibiotic rapamycin, a widely used immunosuppressant, inhibits the oncogenic transformation of human cells induced by PI3k or Akt by blocking the downstream mTOR kinase. However, inhibition of the PI3k/Akt/mTOR cascade may not be the only mechanism whereby rapamycin exerts anticancer effects. We previously demonstrated that rapamycin inhibits NF-κB by acting on FKBP51, a large immunophilin whose isomerase activity is essential for the functioning of the IKK kinase complex. This suggested that rapamycin may be effective also against neoplasias that express the tumour suppressor PTEN, which, by reducing cellular levels of phosphatidyl-inositol triphosphate, antagonizes the action of PI3k. To address this issue, we over-expressed PTEN in a human melanoma cell line characterized by high phospho-Akt and phospho-mTOR levels, and examined the effect of rapamycin on the apoptotic response to the NF-κB inducer doxorubicin versus cisplatin, which does not activate NF-κB. Rapamycin increased both cisplatin- and doxorubicin-induced apoptosis. Transient transfection of PTEN remarkably decreased phospho-mTOR levels and increased sensitivity to cisplatin's cytotoxic effect. Under these conditions, rapamycin failed to enhance cisplatin-induced apoptosis. This finding supports the notion

that inhibition of a survival pathway increases the efficacy of cytotoxic drugs, and suggests that the pro-apoptotic effect of the rapamycin-cisplatin association requires activated mTOR. Rapamycin retained the capacity to enhance doxorubicin-induced apoptosis in cells over-expressing PTEN, which confirms our earlier observation that inhibition of the PI3k/Akt/mTOR pathway is not involved in the effect exerted by the rapamycin-doxorubicin association. These findings indicate that constitutive activation of mTOR is sufficient but not necessary for rapamycin's anti-cancer effect. Finally, we show that a decrease in FKBP51 expression levels, obtained with the small interfering RNA technique in the leukemic cell line Jurkat, increased doxorubicin-induced apoptosis, suggesting that this rapamycin ligand is involved in resistance to chemotherapy-induced apoptosis.

In conclusion, rapamycin affects more than one signalling survival pathway and more than one target. Our data may impact on the synthesis of rapamycin derivatives. Thus far, rapamycin derivatives used in clinical trials have been tested for their mTOR-inhibiting effect. Our study opens the door to a novel class of anti-cancer drugs that specifically target immunophilins.

Introduction

Apoptosis is the predominant mechanism by which cancer cells die when subjected to chemotherapy [1,2]. The resistance of tumour cells to anticancer agents can result from the development of survival signals [3]. Signalling pathways responsible for cell survival can be constitutively activated in cancer cells due to mutation or loss of tumour-suppressor genes [4] and may even be induced by chemotherapy itself [5]. Understanding how tumour cells evade apoptotic events may provide a new paradigm for cancer therapy [6]. The phosphoinositide-3 kinase (PI3k)/Akt pathway and NF-κB transcription factors are considered potent mediators of cell survival in cancer [7-9].

The PI3k/Akt pathway plays an important role in regulating glucose metabolism in normal cells [10], it is inactive in resting cells and often deregulated in cancer cells [4,7]. Extracellular survival signals, delivered as soluble factors or through cell attachment, can inhibit apoptosis by activating this pathway [10-12]. Upon growth factor binding, transmembrane receptor tyrosine kinases undergo auto- or trans-phosphorylation, which creates binding sites for PI3k in their cytoplasmic domains. This, in turn, enables recruitment of active PI3k to the inner surface of the plasma membrane [10-12], where PI3k causes membrane phosphoinositides to generate phosphatidylinositol 3,4-bisphosphate and phosphatidylinositol 3,4,5-trisphosphate (PIP3), and activates the serine/threonine kinase Akt [10-12]. Termination of the PIP3 signal occurs through the action of PTEN, the inositol 3-phosphatase and tensin homologue deleted on chromosome 10 in many tumours [4]. Essentially, PTEN dephosphorylates phosphoinositides at the D3 position.

Akt controls a host of signalling molecules, including tuberin, the product of the TSC2 gene [13]. Phosphorylation of tuberin inactivates the tuberous sclerosis complex formed by hamartin (produced by the TSC1 gene) and tuberin, thereby activating the mammalian target of rapamycin (mTOR) [13]. mTOR is a serine-threonine kinase, whose effector molecules are the ribosomal protein S6 kinase [14] and the eukaryotic initiation factor 4E binding protein 1 (4E-BPI) [15], which regulate ribosome biogenesis and the translation of proteins involved in cell cycle progression and proliferation [14-16]. In many human cancers, the PI3k/Akt pathway is targeted by genomic aberrations including mutations, amplifications and rearrangements [4,7,17]. Whatever the mechanism, activation of this pathway results in disturbance of the control of cell

growth and survival and defective apoptosis, which contributes to a competitive growth advantage, metastatic competence and therapy resistance [7].

Another important factor involved in oncogenesis and chemoresistance is NF-κB [5,9,18]. The NF-κB transcription complex belongs to the Rel family, which is constituted by five mammalian Rel/NF-κB proteins that exert transcriptional activity: RelA (p65), c-Rel, RelB, NF-κB1 (p50/p105) and NF-κB2 (p52/100) [18,19]. RelA, c-Rel and RelB are synthesized as mature proteins, whereas p50 and p52 are first synthesized as large precursors (p105 and p100) that are processed by the proteosome [18,19]. The activity of NF-κB is controlled by shuttling from the cytoplasm to the nucleus in response to cell stimulation. NF-κB dimers containing RelA or c-Rel are retained in the cytoplasm through interaction with inhibitors of NF-κB (IκBs) [15-17]. In response to a variety of stimuli, IκBs are phosphorylated by the activated IκB kinase (IKK) complex, a ~900-kDa multiprotein complex responsible for signal-dependent phosphorylation of IκB [18-20]. This complex contains two catalytic subunits, IKKα and IKKβ, and an essential regulatory subunit NEMO or IKKγ. IκB phosphorylation is followed by rapid ubiquitin-dependent degradation by the 26S proteosome [18-20]. This allows NF-κB dimers to translocate to the nucleus, where they stimulate the expression of target genes. Once in the nucleus, NF-κB dimers are further modified, mostly through phosphorylation of Rel proteins, to optimize their transcriptional activity [6]. NF-κB's oncogenic activity is closely linked to its anti-apoptotic function [9,18,19,21]. Activation of NF-κB has proved to be a pivotal mechanism of tumour chemoresistance [5,9,18]. This is supported by the observation that inhibition of NF-κB sensitizes cancer cell lines to chemotherapy [9,21]. NF-κB induces resistance to cancer therapies by modulating the regulation of various antiapoptotic genes [18], including the inhibitors of apoptosis (IAPs) [22], the caspase 8 inhibitory protein (cFLIP) [23], A1/Bfl1 [24], and TNF-receptor-associated factor (TRAF) 1 and 2 [25].

Rapamycin, the product of *Streptomyces hygroscopicus*, targets the PI3k/Akt [26,27] and NF-κB signaling pathways [28,29]. Although conventionally used as an immunosuppressant agent, rapamycin is an effective anticancer agent that both decreases cell proliferation and increases apopotosis [14,30]. Rapamycin is associated with a much lower risk of cancer recurrence versus other immunosuppressant agents because it controls the growth of primary and metastatic tumours and angiogenesis [30]. Its anti-cancer activity is classically ascribed to binding to FK506 binding protein (FKBP)12 [31]. This results in a complex that, in turn, binds to mTOR and inhibits its kinase activity [26].

Rapamycin inhibits the oncogenic transformation of human cells induced by PI3k or Akt [27]. Consequently, its major therapeutic indication is neoplasias that lack the tumour suppressor gene PTEN [17]. However, we recently reported data suggesting that rapamycin can exert anticancer effects also by inhibiting NF-κB [28,29]. We demonstrated that rapamycin reduces the phosphorylating activity of IKK on its IκB substrate [28] by blocking FKBP51, which is an important cofactor of the IKK-α subunit [32]. Because of its effect on NF-κB, rapamycin sensitizes melanoma [28] and leukemic cells [29] to the action of anthracyclins. Thus, it is conceivable that rapamycin may be effective also in PTEN-positive tumours when associated with NF-κB-inducing chemotherapeutic drugs. To address this issue, we transfected PTEN in a human melanoma cell line characterized by high levels of phospho-Akt and -mTOR, and investigated the pro-apoptotic effect of rapamycin in association with cytotoxic agents that either induce or do not induce NF-κB. We also attempted to determine the role of FKBP51 as a factor of resistance to chemotherapy by down-modulating the protein level using the small interfering (si) RNA technique [33].

Effect of Rapamycin on Cancer Cell Apoptosis

Rapamycin Enhances Apoptosis of Cancer Cells Expressing Activated MTor

A loss of PTEN protein and function has been implicated in the early stages of melanomagenesis [34]. Therefore, the PI3k/Akt survival pathway is likely to be constitutively activated in this tumour. In accordance with this concept, we found the active form of both Akt and mTOR in our human melanoma cell line [28], as demonstrated by the decrease of phospho-protein levels after incubation with the PI3k inhibitor wortmannin (Fig.1). Survival pathways can be activated also by anti-cancer agents [35]. As shown in Figure 2, the anthracyclin doxorubicin, but not the alkylating cisplatin, induced NF-κB transcription factors in melanoma cells. Treatment of tumour cells with rapamycin did not stimulate apoptosis per se, but strikingly enhanced apoptosis induced by both chemotherapeutics (Figs 3 and 4).
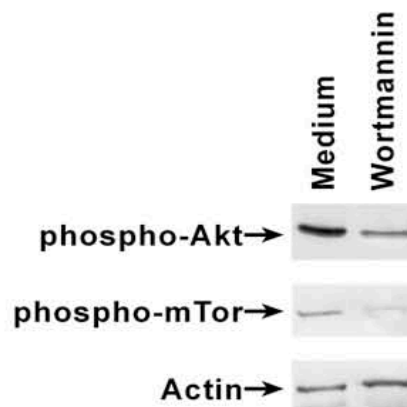
Fig. 1. *Akt and mTOR are melanoma cells.* Western constitutively activated in blot assay of phospho-Akt (Ser 473) and phospho-mTOR (Ser2448) expression levels of lysates from melanoma cells incubated with and without wortmannin (1 μM), for 3 hrs. Whole cell lysates were prepared by homogenization in modified RIPA buffer (150 mM sodium-chloride, 50 mM Tris-HCl, pH 7.4, 1 mM ethylenediamine tetraacetic acid, 1 mM phenylmethylsulfonyl fluoride, 1% Triton X-100, 1% sodium deoxycholic acid, 0.1% sodium dodecylsulfate, 5 μg/ml of aprotinin, 5 μg/ml of leupeptin). Cell debris was removed by centrifugation. The cell lysate was boiled for 5 min in 1x SDS sample buffer (50 mM Tris-HCl pH 6.8, 12.5% glycerol, 1% sodium dodecylsulfate, 0.01% bromophenol blue) containing 5% beta-mercaptoethanol, run on 10% SDS polyacrylamide gel electrophoresis, transferred onto a membrane filter (Cellulosenitrate, Schleider and Schuell, Keene, NH) and incubated with the primary antibody. Anti-phospho-Akt (Ser473) and anti-phospho-mTOR (Ser2448) were rabbit polyclonal antibodies (Cell Signaling Technology, Beverly, MA). After a second incubation with peroxidase-conjugated goat anti-rabbit IgG (Santa Cruz Biotechnology, Santa Cruz, CA) the blots were developed with the ECL system (Amersham Pharmacia Biotech, Piscataway, NJ). Actin was used as the control for loading.
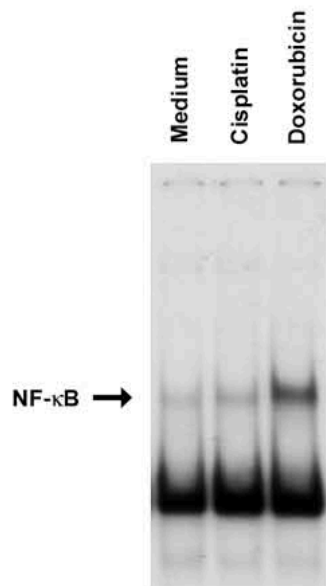
Fig. 2. *Effect of cisplatin and doxorubicin on NF-κB activation.* Electrophoretic mobility shift assay of nuclear extracts from melanoma cells cultured with or without cisplatin (25 μM) or doxorubicin (3 μM) for 5 hrs. The band indicated by the arrow corresponds to NF-κB complexes. Nuclear extracts were prepared by cell pellet homogenization in two volumes of 10 mM Hepes, pH 7.9, 10 mM KCl, 1.5 mM MgCl$_2$, 1 mM EDTA, 0.5 mM DTT, 0.5 mM PMSF and 10% glycerol v/v. Nuclei were centrifuged at 1,000 g for 5 min, washed and resuspended in two volumes of the above-specified solution. KCl was added to reach 0.39 M KCl. Nuclei were extracted at 4°C for 1 h and centrifuged at 10,000 g for 30 min. The supernatant was clarified by centrifugation and stored at –80°C. The NF-κB consensus 5'-CAACGGCAGGGGAATCTCCCTCTCCTT-3' oligonucleotide was end-labeled with [$_\gamma$-^{32}P] ATP (Amersham Pharmacia Biotech) using a polynucleotide kinase (Roche, Basel Switzerland). End-labeled DNA fragments were incubated at room temperature for 15 min with 5 μg of nuclear protein, in the presence of 1 μg poly(dI-dC), in 20 μl of a buffer consisting of 10 mM Tris-HCl, pH 7.5, 50 mM NaCl, 1 mM EDTA, 1 mM DTT and 5% glycerol v/v. Protein-DNA complexes were separated from free probe on a 6% polyacrylamide w/v gel run in 0.25X Tris borate buffer at 200 mV for 3 hrs at room temperature. The gels were dried and exposed to X-ray film (Kodak AR).

Rapamycin Enhances Apoptosis of Cancer Cells Reconstituted with PTEN

To investigate the effect of rapamycin on chemotherapy-induced apoptosis in the context of PTEN over-expression, we transiently co-transfected PTEN and green fluorescent protein (GFP) in melanoma cells, and measured apoptosis induced by doxorubicin and cisplatin in the absence and in the presence of rapamycin. As shown in Figure 5, phospho-mTOR levels, determined in GFP-gated cells by flow cytometry, were clearly lower in PTEN-transfected cells than in both control cells and cells transfected with mutated PTEN.
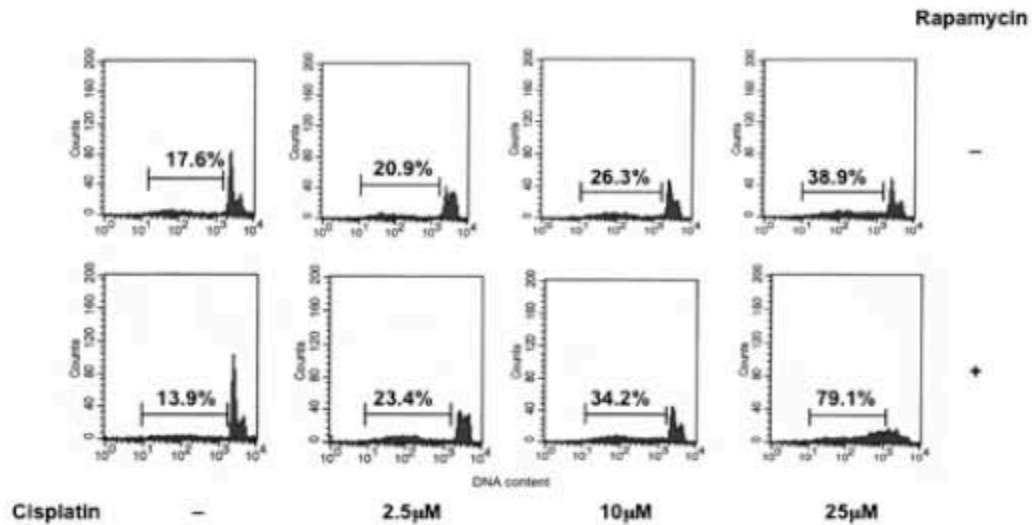
Fig. 3. *Rapamycin enhances cisplatin-induced apoptosis.* Measurement of apoptosis of melanoma cells cultured with cisplatin at different doses, in the absence or the presence of 100 ng/ml rapamycin. Apoptosis, using the propidium iodide incorporation assay, was evaluated in permeabilized cells by flow cytometry. The cells were harvested after 24 hrs of culture, washed in PBS and resuspended in 500 μl of a solution containing 0.1% sodium citrate, 0.1 % Triton X-100 and 50 μg/mL propidium iodide (Sigma Aldrich, Italy). After incubation at 4°C for 30 min in the dark, cell nuclei were examined with flow cytometry. DNA content was recorded on a logarithmic scale. The percentage of the elements in the hypodiploid region was calculated.
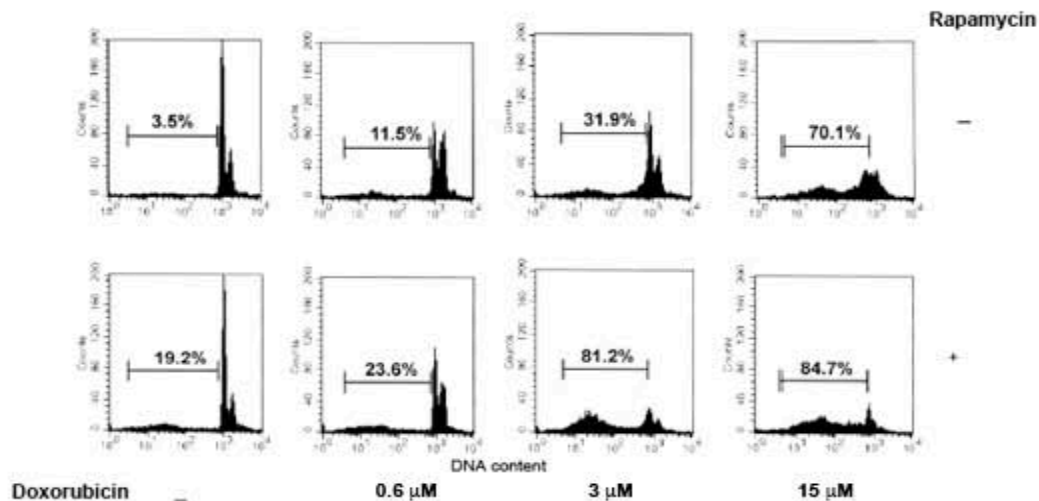
Fig. 4. *Rapamycin enhances doxorubicin-induced apoptosis.* Measurement of apoptosis of melanoma cells cultured with different doses of doxorubicin, in the absence or the presence of 100 ng/ml rapamycin. Apoptosis, using the propidium iodide incorporation assay, was evaluated in permeabilized cells by flow cytometry. Cells were harvested after 24 hrs of culture, washed in PBS and resuspended in 500 μl of a solution containing 0.1% sodium citrate, 0.1% Triton X-100 and 50 μg/mL propidium iodide (Sigma Aldrich, Italy). After incubation at 4°C for 30 min in the dark, cell nuclei were examined

by flow cytometry. DNA content was recorded on a logarithmic scale. The percentage of the elements in the hypodiploid region was calculated.
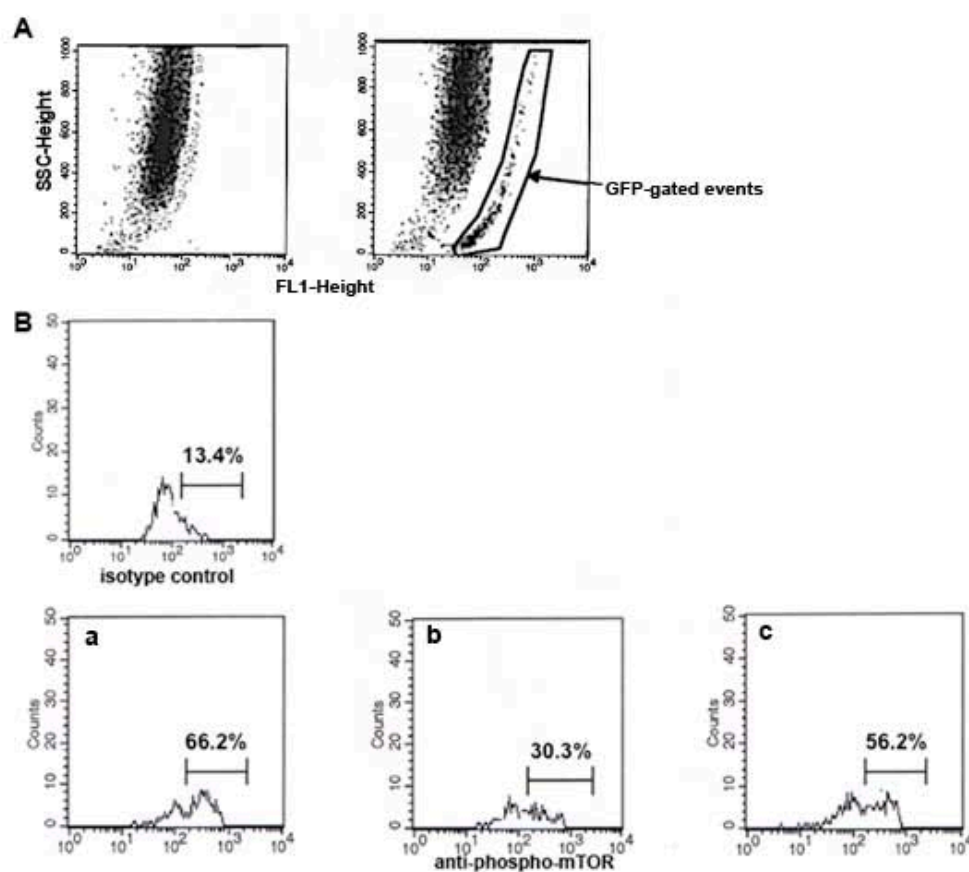

Fig. 5. *PTEN-transfection decreases phospho-mTOR levels*. **A** Flow cytometric dot plots of melanoma cells non-encoding or encoding GFP. A gate was placed on GFP$^+$ cells. **B** Flow cytometric histograms of phospho-mTOR expression in GFP-gated cells. (**a**), cells transfected with GFP; (**b**), cells co-transfected with GFP+ PTEN; (**c**), cells co-transfected with GFP+mutated PTEN. Staining of GFP-gated cells with isotype control Ig is also shown. Melanoma cells in the logarithmic growth phase were resuspended in serum-free RPMI 1640 and transfected with 5 μg of plasmid encoding GFP plus 15 μg of plasmid encoding PTEN or mutated PTEN, by electroporation at 250 mV and 960 μF using the Gene Pulser (Bio-Rad Laboratories, Hercules, CA, USA). The cells were transferred to six-well plates in 10% FCS RPMI 1640 supplemented with antibiotic and glutamine at 37°C in a 5% CO_2 humidified atmosphere. The cDNA encoding for PTEN or mutated PTEN [48] was kindly provided by Dr. David Stokoe (Cancer Research Institute, UCSF, CA). Three days later, the cells were collected, fixed, permeabilized and an indirect immunofluorescence with anti-phospho-mTOR antibody (Cell Signaling Technology, Beverly, MA) was performed using a PE-conjugated secondary antibody.

This demonstrates that the protein encoded by the plasmid was functional. Subsequently, we incubated the cells with cisplatin or doxorubicin, in the absence and in the presence of rapamycin, and measured apoptosis using the TdT-mediated dUTP nick end-labelling (TUNEL) assay [36].

GFP-positive cells were gated (Fig. 5A), and we evaluated the percentage of cells incorporating dUTP (apoptotic cells) using flow cytometry. As shown in Figure 6, rapamycin significantly enhanced cisplatin-induced apoptosis in both control cells (p=0.006) and cells transfected with mutated PTEN (p=0.03), but not in cells transfected with PTEN (p=0.2). Moreover, cisplatin-induced apoptosis was greater (p=0.04) in PTEN-transfected cells than in control cells. There was no difference in cisplatin-induced apoptosis between control cells and cells transfected with mutated PTEN. This result indicated that inhibition of mTOR increases the efficacy of cisplatin, and that the pro-apoptotic effect of the rapamycin-cisplatin association depended on the presence of activated mTOR. Unlike cisplatin-treated cells, doxorubicin cultures were sensitive to rapamycin pro-apoptotic effect also under conditions of PTEN over-expression. Indeed, rapamycin significantly (p=0.02) enhanced anthracyclin-induced apoptosis in PTEN-transfected cells (Fig. 7). These findings support our previous studies [26,27] that the cooperative effect between rapamycin and NF-κB-inducing drugs occurs irrespective of mTOR inhibition.

Fig. 6. *Effect of rapamycin on cisplatin-induced apoptosis in PTEN-transfected cells.* Graphic representation of apoptosis percentages determined in flow cytometry; error bars indicate standard deviations. Melanoma cells in the logarithmic growth phase were resuspended in serum-free RPMI 1640 and transfected (see legend to Fig. 5). Three days later, rapamycin (100 ng/ml) and or cisplatin (25 μM) was added to the cultures and after incubation for a further 9 hrs, TUNEL was performed with the In Situ Cell Death Detection Kit TMR red (Roche, Basel, Switzerland), according to the manufacturer's instructions. Briefly, cells were fixed with 2% paraformaldehyde in PBS v/v, for 15 min at room temperature, washed and permeabilized with 0.1% TRITON x-100 in PBS, for 2 min in ice. After a second wash, the cells were incubated with TMR red labelling solution for 1 hr at 37°C and examined by flow cytometry. The percentage of GFP-gated cells incorporating dUTP was calculated.
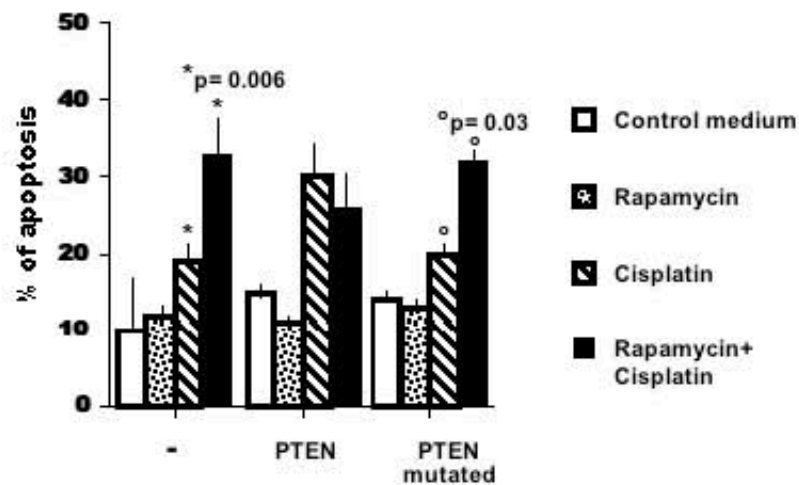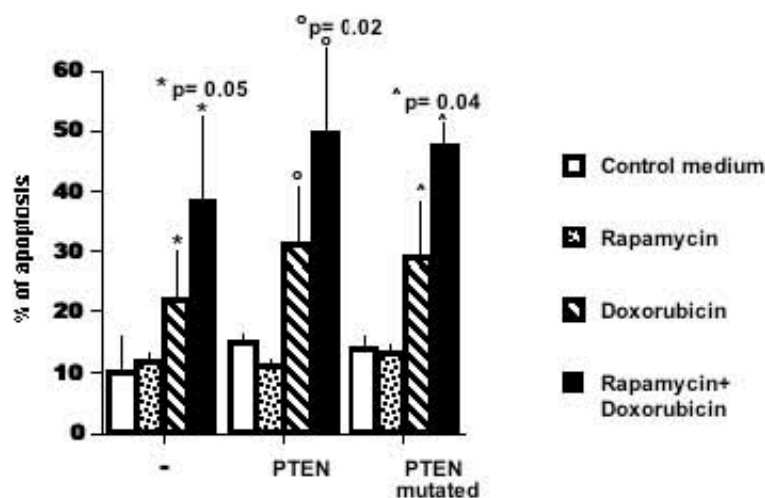
Fig. 7. *Effect of rapamycin on doxorubicin-induced apoptosis in PTEN-transfected cells.* Graphic representation of apoptosis percentages determined by flow cytometry; error bars indicate standard deviations. Melanoma cells in the logarithmic growth phase were resuspended in serum-free RPMI 1640 and transfected (see legend to Fig.5). Three days later, rapamycin (100 ng/ml) and or doxorubicin (3 μM) was added to the cultures and after incubation for a further 9 hrs, TUNEL was performed with the In Situ Cell Death Detection Kit TMR red (Roche, Basel, Switzerland), according to the manufacturer's instructions. Briefly, cells were fixed with 2% paraformaldehyde in PBS v/v, for 15 min at room temperature, washed and permeabilized with 0.1% TRITON x-100 in PBS, for 2 min in ice. After a second wash, the cells were incubated with TMR red labelling solution for 1 hr at 37°C and examined with flow cytometry. The percentage of GFP-gated cells incorporating dUTP was calculated.

The Rapamycin-Binding Protein FKBP51 is Responsible for Chemoresistance

FKBPs are the first cellular target of rapamycin and FKBP51 controls chemotherapy-induced NF-κB activation [28,29]. We recently reported that rapamycin did not increase doxorubicin-induced apoptosis in the leukemic cell line Jurkat, which hyper-expresses the p65 subunit of NF-κB [29]. This illustrated the importance of inactivation of this transcription factor in rapamycin regulation of apoptosis. To verify whether FKBP51 was involved in resistance to doxorubicin, we down-modulated FKBP51 expression levels using the siRNA technique in Jurkat cells, and investigated doxorubicin-induced apoptosis by propidium iodide incorporation by flow cytometry. Treatment of the cells with FKBP51 siRNA efficiently reduced the expression levels of this protein (Fig. 8A) and enhanced doxorubicin-induced apoptosis by more than 60% (Fig. 8B).
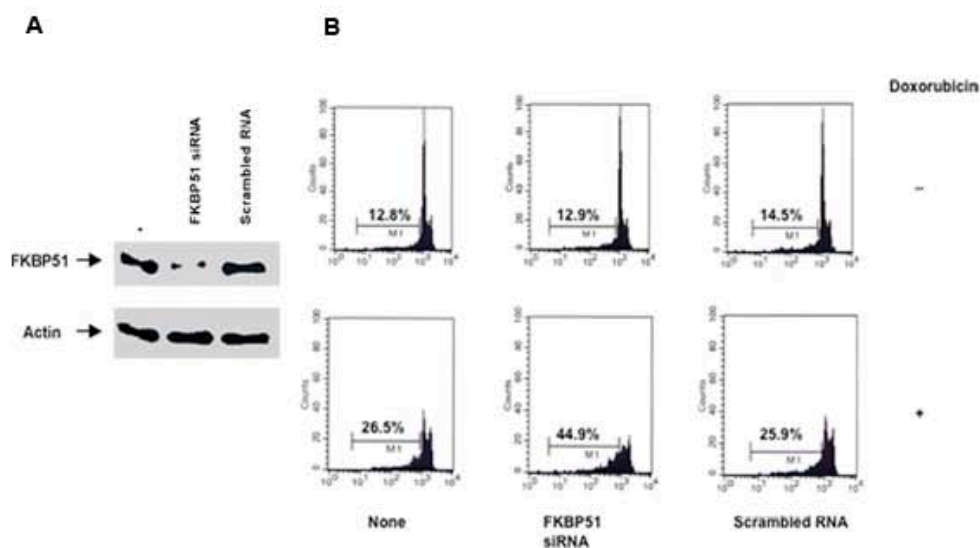
Fig. 8. *Downmodulation of FKBP51 increases doxorubicin-induced apoptosis.* **A** Western blot assay of FKBP51 expression levels in cell lysates obtained from non-transfected Jurkat cells and from Jurkat cells transfected with specific siRNA or the scrambled oligonucleotide as control. Cells were incubated for 24 hrs in six-well plates in medium without antibiotics before transfection of the oligonucleotide 5'-ACCUAAUGCUGAGCUUAUAdTdT-3' corresponding to the sense strand of the target sequence 5'-AAACCUAAUGCUGAGCUUAUA-3' of human FKBP51 (Dharmacon Research Inc., Boulder, CO) or of a scrambled duplex as control (Dharmacon Research Inc.). The siRNA or the scrambled oligo was transfected at the final concentration of 50 nM using Metafectene (Biontex, Munich, Germany) according to the manufacturer's recommendations. Three days later, whole cell lysates were prepared by homogenization in modified RIPA buffer and assayed in Western blot to determine FKBP51 expression levels. Anti-FKBP51 was a goat polyclonal antibody (Sigma Aldrich, Italy). Actin was used as the control for loading. **B** Flow cytometric histograms of DNA content, bar indicates hypodiploid region (apoptosis). Cells transfected as described in **A** were cultured with rapamycin (100 ng/ml) and/or doxorubicin (3 μM). Twenty-four hrs later, cells were harvested, washed in PBS and resuspended in 500 μl of a solution containing 0.1% sodium citrate, 0.1% Triton X-100 and 50 μg/mL propidium iodide (Sigma Aldrich, Italy). After incubation at 4°C for 30 min in the dark, cell nuclei were analyzed in flow cytometry. DNA content was recorded on a logarithmic scale, and he percentage of the elements in the hypodiploid region was calculated.

Conclusion

Modern anti-cancer therapy is based on the use of innovative agents able to antagonize signalling pathways that are deregulated in cancer. A number of rapamycin analogs have been developed over recent years, the most notable being the cell cycle inhibitor 779 (CCI-779), RAD-001 and AP23573 [37]. Rapamycin and its analogs are the most promising candidates for the treatment of tumours that lack the suppressor function of PTEN [8,17]. However, our data suggest

that constitutive activation of mTOR is sufficient but not necessary for the anti-cancer effect of rapamycin [28,29]. Several lines of evidence support the view that rapamycin inhibits NF-κB [38-40] and, as a consequence, it inhibits the expression of anti-apoptotic genes that are under NF-κB transcriptional control [28,29] and that are involved in the resistance of cancer cells to chemotherapy.

In the present study, we transfected PTEN in a human melanoma cell line to abate the expression of activated mTOR, and investigated the apoptosis-enhancing effect which rapamycin exerts in association with two cytotoxic drugs: doxorubicin, which induces NF-κB, and cisplatin that does not. We found that rapamycin retains the ability to enhance apoptosis in PTEN-transfected cells cultured with doxorubicin but not in the same cells cultured with cisplatin. Consequently, it appears that the cooperative effect between rapamycin and cisplatin requires the presence of activated mTOR. This is in agreement with reports that inhibition of mTOR enhances the cytotoxic effect of cisplatin [41]. Indeed, resistance to cisplatin treatment was attributed to overexpression of elongation factor alpha and of genes involved in ribosomal biogenesis that leads to the production of repair and/or survival proteins [42]. Differently, the cytotoxicity of the NF-κB-inducer doxorubicin was enhanced by rapamycin even in the context of PTEN reconstitution. Our previous finding that the large immunophilin FKBP51 is involved in the control of chemotherapy-induced NF-κB activation [28,29] provided a mechanism for NF-κB down-modulation by rapamycin. In agreement with these findings, we now show that FKBP51 down-modulation increases doxorubicin-induced apoptosis, an observation that implicates FKBP51 in resistance to anthracyclin compounds.

As mentioned above, FKBPs are the first target of rapamycin and, in fact, binding to FKBP12 is crucial for mTOR inhibition. FKBPs are immunophilins, which are abundant, cytosolic proteins endowed with inherent peptidyl-prolyl cis-trans isomerase activity. Rapamycin very specifically binds to FKBPs and inhibits their isomerase activity, which is important for several biological functions of the cell, namely, response to transforming growth factor (TGF)-β [43], control of intracellular calcium release [44], sensitivity to glucocorticoids [45], and IKK kinase complex function [32]. FKBP12 interacts with the cytoplasmic domain of TGF-β type I receptor [43] and acts as a molecular guardian of this receptor to prevent it from leaky signalling under sub-optimal ligand concentrations [43]. Moreover, FKBP12 interacts stoichiometrically with multiple intracellular calcium release channels thereby controlling cellular calcium influx [44]. FKBP51 and FKBP52 regulate the affinity of glucocorticoid receptors that form complexes with Hsp-90 and Hsp-binding co-chaperones [45]. Finally, FKBP51 is a co-factor of IKKα [32]. Given the biological relevance of this class of proteins, it is not surprising that rapamycin exerts effects independent of PI3k/Akt/mTOR inhibition.

The identification of increased FKBP12 expression in high-grade childhood astrocytoma [46] and of FKBP51 in idiopathic myelofibrosis, which is responsible for growth factor independence of bone marrow progenitor proliferation [47], suggest that FKBPs are involved in cancerogenesis. In line with these findings, our studies implicate FKBP51 in resistance to apoptosis, thus opening the door to the development of a new class of anti-cancer drugs that specifically target immunophilins.

Our research provides the first demonstration that FKBPs are involved in the control of apoptosis. FKBP rotamase activity is essential for several biological processes in mammalian cells. Therefore, it cannot be excluded that, besides affecting NF-κB, FKBPs act on other regulatory steps of the apoptotic machinery. There is a need for studies designed to elucidate the role of immunophilins in apoptosis regulation.

References

[1]   Brown, JM; Attardi LD. (2005). The role of apoptosis in cancer development and treatment response. *Nature Reviews Cancer, 5,* 231-237.

[2]   Fridman, JS; Lowe, SW. *(2003).* Control of apoptosis by p53. *Oncogene, 22,* 9030-9040.

[3]   Green, DR; Evan, GI. (2002). A matter of life and death. *Cancer Cell, 1,* 19-30.

[4]   Wu, X; Senechal, K; Neshat, MS; Whang, YE; Sawyers, CL. (1998). The PTEN/MMAC1 tumor suppressor phosphatase functions as a negative regulator of the phosphoinositide 3-kinase/Akt pathway. *Proc Natl Acad Sci U S A, 95,* 15587-91.

[5]   Cusack, JC; Liu, R; Baldwin, AS. (1999). NF-kappa B and chemoresistance: potentiation of cancer drugs via inhibition of NF-kappa B. *Drug Resist Update, 2,* 271-73.

[6]   Petak, I; Houghton, JA, and Kopper, L. (2006). Molecular targeting of cell death signal transduction pathways in cancer. *Current Signal Transduction Therapy, 1,* 113-131.

[7]   Hennessy, BT; Smith, DL; Ram, PT; Lu, Y; and Mills GB. (2005). Exploiting the PI3K/AKT pathway for cancer drug discovery. *Nature Reviews Drug Discovery, 4,* 988-1004.

[8]   Bjornsti, M-A; Houghton, PJ. (2004). The Tor pathway: a target for cancer therapy. *Nature Cancer Reviews, 4,* 335-48.

[9]   Nakanishi, C; Toi, M. (2005). Nuclear factor-kappaB inhibitors as sensitizers to anticancer drugs. *Nat Rev Cancer, 5,* 297-309.

[10]   Roques, M; Vidal, H. (1999). A phosphatidylinositol 3-Kinase/p70 ribosomal S6 protein kinase pathway is required for the regulation by insulin of the p85alpha regulatory subunit of phosphatidylinositol 3-kinase gene expression in human muscle cells. *J Biol Chem, 274,* 34005-10.

[11]   Burgering, BM; Coffer, PJ. (1995). Protein kinase B (c-Akt) in phosphatidylinositol-3-OH kinase signal transduction. *Nature, 376,* 599-602.

[12]   Varticovski, L; Harrison-Findik, D; Keeler, ML; Susa, M. (1994). Role of PI 3-kinase in mitogenesis. *Biochim Biophys Acta, 1226,* 1-11. Review.

[13]   Tee, AR; Fingar, DC; Manning, BD; Kwiatkowski, DJ; Cantley, LC; Blenis, J. (2002). Tuberous sclerosis complex-1 and -2 gene products function together to inhibit mammalian target of rapamycin (mTOR)-mediated downstream signaling. *Proc Natl Acad Sci USA, 99,* 13571-6.

[14]   Fingar, DC; Salama, S; Tsou, C; Harlow, E; Blenis, J. (2002). Mammalian cell size is controlled by mTOR and its downstream targets S6K1 and 4EBP1/eIF4E. *Genes Dev, 16,* 1472-1487.

[15]   Gingras, AC; Raught, B; Gygi, SP; Niedzwiecka, A; Miron, M; Burley, SK; Polakiewicz, RD; Wyslouch-Cieszynska, A; Aebersold, R; Sonenberg, N. (2001). Hierarchical phosphorylation of the translation inhibitor 4E-BP1. *Genes Dev, 15,* 2852-64.

[16]   Gingras, AC; Raught, B; Sonenberg, N. (2001). Regulation of translation initiation by FRAP/mTOR. *Genes De 15,* 807-26.

[17]   Neshat, MS; Mellinghoff, IK; Tran, C; Stiles, B; Thomas, G; Petersen, R; Frost, P; Gibbons, JJ; Wu, H; Sawyers, CL. (2001). Enhanced sensitivity of PTEN-deficient tumors to inhibition of FRAP/mTOR. *Proc Natl Acad Sci USA, 98,* 10314-9.

[18]   Karin, M; Cao, X; Greten, FR; Li, Z-W. (2002). NF-kappaB in cancer: from innocent bystander to major culprit. *Nature Reviews Cancer, 2,* 301-310.

[19] Ghosh, S; May, MJ; and Kopp, EB. (1998). NF-κB and Rel proteins: evolutionarily conserved mediators of immune response. *Annu Rev Immunol, 16,* 225-260.

[20] Baldwin, AS Jr. (1996). The NF-kB and IkB proteins: new discoveries and insights. *Annu Rev Immunol, 14,* 649-81.

[21] Wang, CY; Cusack, JC Jr; Liu, R; Baldwin, AS Jr. (1999). Control of inducible chemoresistance: enhanced anti-tumor therapy through increased apoptosis by inhibition of NF-kappaB. *Nat Med, 5,* 412-7.

[22] Roy, N; Deveraux, QL; Takahashi, R; Salvesen, GS; and Reed, JC. (1997). The c-IAP-1 and c-IAP-2 proteins are direct inhibitors of specific caspases. *The EMBO Journal*, 16, 6914–6925.

[23] Thome, M; Schneider, P; Hofmann, K; Fickenscher, H; Meinl, E; Neipel, F; Mattmann, C; Burns, K; Bodmer, JL; Schroter. M; Scaffidi, C; Krammer, PH; Peter ME; Tschopp, J. (1997). Viral FLICE-inhibitory proteins (FLIPs) prevent apoptosis induced by death receptors. *Nature* 386, 517–520.

[24] Wang, C-Y; Guttridge, DC; Mayo, MW; and Baldwin, AS Jr. (1999). NF-κB Induces Expression of the Bcl-2 Homologue A1/Bfl-1 To Preferentially Suppress Chemotherapy-Induced Apoptosis. *Mol Cell Biol. 19,* 5923–5929.

[25] Rothe, M., Wong, S.C., Henzel, W.J., Goeddel, D.V. (1994). A novel family of putative signal transducers associated with the cytoplasmic domain fo the 75 kDa tumor necrosis factor receptor. *Cell. 78,* 681-692.

[26] Brown, EJ; Albers, MW; Shin, TB; Ichikawa, K; Keith, CT; Lane, WS; Schreiber, SL. (1994). A mammalian protein targeted by G1-arresting rapamycin-receptor complex. *Nature, 369,* 756-758.

[27] Aoki, M; Blazek, E; Vogt, PK. (2001). A role of the kinase mTOR in cellular transformation induced by the oncoproteins P3k and Akt. *Proc Natl Acad Sci USA, 98,* 136-41.

[28] Romano, MF; Avellino, R; Petrella, A; Bisogni, R; Romano, S; Venuta, S. (2004). Rapamycin inhibits doxorubicin-induced NF-kB/Rel nuclear activity and enhances apoptosis in melanoma. *Eur J Cancer, 40,* 2829-36.

[29] Avellino, R; Romano, S; Parasole, R; Bisogni, R; Lamberti, A; Poggi, V; Venuta, S; and Romano, MF. (2005). Rapamycin stimulates apoptosis of childhood acute lymphoblastic leukemia cells. *Blood, 106,* 1400-6.

[30] Guba, M; von Breitenbuch, P; Steinbauer, M; Koehl, G; Flegel, S; Hornung, M; Bruns, CJ; Zuelke, C; Farkas, S; Anthuber, M; Jauch, KW; Geissler, EK. (2002). Rapamycin inhibits primary and metastatic tumor growth by antiangiogenesis: involvement of vascular endothelial growth factor. *Nat Med, 8,* 128-135.

[31] Siekierka JJ, Hung SH, Poe M, Lin CS, Sigal NH. (1989). A cytosolic binding protein for the immunosuppressant FK506 has peptidyl-prolyl isomerase activity but is distinct from cyclophilin. *Nature, 341,* 755-757.

[32] Bouwmeester T, Bauch A, Ruffner H, Angrand PO, Bergamini G, Croughton K, Cruciat C, Eberhard D, Gagneur J, Ghidelli S, Hopf C, Huhse B, Mangano R, Michon AM, Schirle M, Schlegl J, Schwab M, Stein MA, Bauer A, Casari G, Drewes G, Gavin AC, Jackson DB, Joberty G, Neubauer G, Rick J, Kuster B, Superti-Furga G. (2004). A physical and functional map of the human TNF-alpha/NF-kappaB signal transduction pathway. *Nat Cell Biol, 6,* 97-105.

[33]   Chi J-T, Chang HI, Wang NN, Chang DS, Dunphy N, and O. Brown P. (2003). Genomewide view of gene silencing by small interfering RNAs. *Proc Natl Acad Sci USA*, *100*, 6343–6346.

[34]   Wu H, Goel V, Haluska FG. (2003). PTEN signaling pathways in melanoma. *Oncogene, 22*, 3113-22. Review.

[35]   Laurent G, Jaffrezou J-P. (2001). Signaling pathways activated by daunorubicin. *Blood, 98*, 913-924.

[36]   Li, X; Traganos, F; Melamed, MR, et al. (1995). Single-step procedure for labeling DNA strand breaks with fluorescein- or BODIPY-conjugated deoxynucleotides: detection of apoptosis and bromodeoxyuridine incorporation. *Cytometry*, 20:172-80.

[37]   Mita MM, Mita A, Rowinsky EK. (2003). The molecular target of rapamycin (mTOR) as a therapeutic target against cancer. *Cancer Biol Ther, 2,* S169-77. Review.

[38]   Lai JH, Tan TH. (1994). CD28 signaling causes a sustained down-regulation of I kappa B alpha which can be prevented by the immunosuppressant rapamycin. *J. Biol. Chem, 269*, 30077-30080.

[39]   Conejo, R., Valverde, A.M., Benito, M., Lorenzo, M. (2001). Insulin produces myogenesis in C2C12 myoblasts by induction of NF-kappaB and downregulation of AP-1 activities. *J. Cell . Physiol, 186*, 82-94.

[40]   Tunon MJ, Sanchez-Campos S, Gutierrez B, Culebras JM, Gonzalez-Gallego J. (2003). Effects of FK506 and rapamycin on generation of reactive oxygen species, nitric oxide production and nuclear factor kappa B activation in rat hepatocytes. *Biochem Pharmacol, 66,* 439-45.

[41]   Wu C, Wangpaichitr M, Feun L, Kuo MT, Robles C, Lampidis T, Savaraj N. (2005). Overcoming cisplatin resistance by mTOR inhibitor in lung cancer. *Mol Cancer. 20,* 4-25.

[42]   Johnsson A, Zeelenberg I, Min Y, Hilinski J, Berry C, Howell SB, Los G. (2000). Identification of genes differentially expressed in association with acquired cisplatin resistance. *Br J Cancer, 83,* 1047-54.

[43]   Wang T, Li BY, Danielson PD, Shah PC, Rockwell S, Lechleider RJ, Martin J, Manganaro T, Donahoe PK. (1996). The Immunophilin FKBP12 Functions as a Common Inhibitor of the TGF Family Type I Receptors. *Cell. 86,* 435- 444 .

[44]   Samso M, Shen X, Allen PD. (2006). Structural characterization of the RyR1-FKBP12 interaction. *J Mol Biol, 356,* 917-27.

[45]   Sinars CR, Cheung-Flynn J, Rimerman RA, Scammell JG, Smith DF, Clardy J. (2003). Structure of the large FK506-binding protein FKBP51, an Hsp90-binding protein and a component of steroid receptor complexes. *Proc Natl Acad Sci USA, 100,* 868-73.

[46]   Khatua S, Peterson KM, Brown KM, et al. (2003). Overexpression of the EGFR/FKBP12/HIF-2alpha pathway identified in childhood astrocytomas by angiogenesis gene profiling. Cancer Res, 63, 1865-1870.

[47]   Giraudier S, Chagraoui H, Komura E, et al. (2002). Overexpression of FKBP51 in idiopathic myelofibrosis regulates the growth factor independence of megakaryocyte progenitors. *Blood, 100,* 2932-2940.

[48]   Xu Z, Stokoe D, Kane LP, Weiss A. (2002). The inducible expression of the tumor suppressor gene PTEN promotes apoptosis and decreases cell size by inhibiting the PI3K/Akt pathway in Jurkat T cells. *Cell Growth Differ,* 285-96.

FK506 can activate transforming growth factor-β signalling in vascular smooth muscle cells and promote proliferation

Arturo Giordano[1], Simona Romano[2], Maria Mallardo[2], Anna D'Angelillo[2], Gaetano Calì[3], Nicola Corcione[1], Paolo Ferraro[1], and Maria Fiammetta Romano[2]*

[1]Invasive Cardiology Unit, Clinica Pineta Grande, Castelvolturno, Italy; [2]Department of Biochemistry and Medical Biotechnology, University of Naples Federico II, via Pansini, 5, 80131 Naples, Italy; and [3]Institute of Endocrinology and Experimental Oncology, Italian National Research Council (CNR), Naples, Italy

Aims FK506-binding protein (FKBP) 12 is an inhibitor of transforming growth factor (TGF)-β type I receptors. Several lines of evidence support the view that TGF-β stimulates vascular smooth muscle cell (VSMC) proliferation and matrix accumulation. We investigated the effect of FK506, also known as tacrolimus, on cellular proliferation and on matrix protein production in human VSMCs.
Methods and results We measured cell proliferation with flow cytometry using BrdU incorporation and fluorimetrically by measuring DNA concentration with Hoechst 33258. Western blot assay of whole-cell lysates was used to measure the levels of signalling proteins involved in proliferative pathways, in particular β-catenin, pErk, pAkt, pmTOR, and cyclin D1. Collagen synthesis was also investigated by Western blotting. The TGF-β signal was studied by both Western blotting and confocal microscopy. We used the SiRNA technique for FKBP12 gene silencing. Our results show that FK506 stimulates VSMC proliferation and collagen type I production. FK506 enhanced β-catenin levels and activated the extracellular signal-regulated kinase, Akt, and mammalian target of rapamycin kinase, which are important effectors of proliferation. Accordingly, cyclin D1 expression was increased. We also demonstrate that FK506 activates the TGF-β signal in VSMCs and that, through this mechanism, it stimulates cell proliferation.
Conclusion FK506 can act as a growth factor for VSMCs.

1. Introduction

A large body of evidence suggests that transforming growth factor (TGF)-β simulates intimal growth in vascular smooth muscle cells (VSMCs) by inducing cellular proliferation and matrix accumulation.[1–6] Direct transfer of the TGF-β gene into arteries stimulates fibrocellular hyperplasia.[3] Systemic infusion of TGF-β protein in animal models of arterial injury[1–4] promotes intimal growth. Moreover, TGF-β antagonists decrease intimal growth in animal models of arterial injury.[5,6]

TGF-β is a pleiotropic cytokine important in the control of cell proliferation and differentiation, embryonic development, angiogenesis, and wound healing.[4,7,8] It can trigger a variety of biological responses by activating Smad transcription factor, depending on the cellular context and nuclear components that recruit Smad to specific target genes.[9] TGF-β signals to the nucleus by binding to a specific pair of membrane receptors, type I (TβR-I) and type II (TβR-II), that contain a cytoplasmic serine–threonine kinase domain.[10] Binding of the ligand to TβR-II results in the formation of a TβR-I/TβR-II heteromeric complex and activation of TβR-II kinase.[10] Activation of TβR-I requires phosphorylation of the glycine–serine (GS) region by TβR-II. Activated TβR-I specifically recognizes and phosphorylates Smad 2 and 3 or R-Smads.[10] This process results in the release of Smad 2 and unmasking of its nuclear import function, thereby leading to rapid accumulation of the activated Smad complex in the nucleus.[10–12] Smad 4 functions as a shared partner or Co-Smad and is required for transcriptional complexes to assemble. Once in the nucleus, activated Smad associates with partner DNA-binding co-factors that contact Smad and a specific DNA sequence, thereby resulting in transcription activation or repression.[9,11]

TGF-β receptor signalling is negatively regulated by FK506-binding protein (FKBP) 12, an abundant and highly conserved 12 kDa cytosolic protein that exerts peptidyl–prolyl isomerase activity.[13] FKBP12 regulates fundamental aspects

* Corresponding author. Tel: +39 0817463125; fax: +39 0817463205.
 E-mail address: romano@dbbm.unina.it

of cell biology, due to specific protein–protein interactions and modulation of partner conformation and activity.[14] Among its multiple biological functions, FKBP12 is a common inhibitor of TGF-β type I receptors.[13,15] Indeed, it binds to the GS region, thereby blocking access to activators. In line with this concept, the TGF-β pathway is overactive in fibroblasts from FKBP12-knock out mice.[16] FK506, the canonical ligand of FKBP12, promoted TGF-β receptor transphosphorylation in a mink epithelial cell line.[15] FK506 is a macrolide compound isolated from *Streptomyces tsukubaensis*[17] and has potent immunosuppressive properties.[18,19] Structurally, FK506 has two domains, a domain bound by FKBP12 and an effector domain that, together with FKBP12, forms a composite surface that interacts with calcineurin, thereby inhibiting its phosphatase activity.[20] Calcineurin is activated by Ca^{2+}-dependent signal transduction events, such as T-lymphocyte activation, and in turn dephosphorylates the cytoplasmic subunit of the nuclear factor of activated T (NFAT) cells, thereby allowing its translocation to the nucleus where it associates with a nuclear subunit to form the fully active NFAT complex.[21] NFAT is an essential component of the transcriptional apparatus required for the expression of IL-2 and other cytokine genes, including interleukin-3, interferon γ, and tumour necrosis factor α.[22] As an immunosuppressive agent, FK506 is approximately 100 times more potent than cyclosporine.[23] Cytokines released in the site of arterial injury, as occurs, for example, after balloon angioplasty, play an important role in inflammation and restenosis.[24] Because some anti-restenosis devices used in interventional cardiology release FK506,[25] the aim of our study was to investigate whether such compound can activate the TGF-β signal in VSMCs and affect cell proliferation. This *in vitro* study can provide possible mechanisms governing vascular remodelling, after FK506-eluting stent implantation.

2. Methods

2.1 Cell culture and reagents

VSMCs were human aortic smooth muscle cells purchased from Cambrex Bio Science (Cambrex Profarmaco, Milan, Italy). The cells were cultured in Clonetics SmGM-3 BulletKit medium, according to the manufacturer's instructions. They were starved of supplement growth factors for 48 h, after which FK506 or TGF-β was added to the medium. The experiments were performed when cells were at the 6–10 passage. FK506, TGF-β, and cyclosporin (Sigma Aldrich, St Louis, MO, USA) were used at the doses indicated under the Results section. SB 431542,[8] which inhibits receptors of the TGF-β superfamily type I activin receptor-like kinase (ALK), was purchased from Sigma Aldrich and used at the concentration of 5 μM.

2.2 Cell lysates and Western blot assay

Whole-cell lysates were prepared by homogenization in the modified RIPA buffer. The lysate was cleared by centrifugation at 14 000 rpm for 20 min. The lysate was run on SDS–polyacrylamide gel electrophoresis, transferred onto a membrane filter (Cellulose-nitrate, Schleider and Schuell, Keene, NH, USA), and incubated with the primary antibody.

The antibody against phospho (p) Smad2 (Ser 465/467) (rabbit polyclonal; Chemicon, Temecula, CA, USA), Smad4, and pErk (mouse monoclonal; Santa Cruz Biotechnology, Santa Cruz, CA, USA), cyclin D1 and Smad 2/3 (rabbit polyclonal; Santa Cruz Biotechnology), pAkt, pmTOR, and extracellular signal-regulated kinase (Erk) 1/2 (rabbit polyclonal, Cell Signaling Technology,

Danvers, MA, USA), FKBP12 (rabbit polycolonal; Santa Cruz Biotechnology) collagen type I (mouse monoclonal, clone SP1D8, Developmental Studies Hybridoma Bank, Iowa City, IA, USA) were all used diluted 1:200. After a second incubation with peroxidase-conjugated anti-rabbit IgG or anti-mouse IgG (Santa Cruz Biotechnology), the blots were developed with the ECL system (Supersignal West Pico, Celbio, Pierce, Rockford, IL, USA).

2.3 Immunofluorescence and microscopy

To investigate VSMC growth on bare stents, cells were plated onto 35 mm plastic dishes together with a stent in the absence or presence of 100 ng/mL FK506. After 9 days of culture, the stents were removed from the dishes, fixed in 4% paraformaldehyde in PBS for 20 min and cells were permeabilized for 5 min in 0.1% Triton X-100 in PBS. Cells were then washed twice in PBS and nuclei were stained with 2′-(4-hydroxyphenyl)5-(4-methyl-1-piperazynyl)-2,5′-bi(1H-benzimidazoil)-6-(1-methyl-4piperazyl) benzimidazole trihydrochloride (Hoechst) 33258 fluorescent reagent (0.5 μg/mL in PBS) (Sigma Aldrich) for 10 min. Stents were mounted on glass slides with PBS containing 50% glycerol. Stained fluorescent nuclei were visualized on a Zeiss Axioscop 2 microscope (Zeiss, Gottingen, Germany) and images were taken with a Zeiss Axiocam.

To investigate Smad nuclear translocation, VSMCs were plated onto 12 mm glass coverslips. Cells were treated with 10 ng/mL TGF-β or with 100 ng/mL FK506 for 60 min. Cells used as control were treated with the medium alone. Cells were fixed in 4% paraformaldehyde in PBS for 20 min, washed twice for 5 min each time, with 50 mM NH4Cl in PBS permeabilized for 5 min in 0.1% Triton X-100 in PBS. Cells were then blocked in 1% BSA in PBS for 1 h and washed twice in PBS. A mouse monoclonal anti-Smad4 diluted 1:100 in PBS 0.5% BSA for 1 h in a humidified atmosphere served as primary antibody. Cells were then extensively washed in PBS before staining with secondary goat anti-mouse Alexa Fluor 488 conjugated (Molecular Probe, Invitrogen Corporation, Carlsbad, CA, USA). Nuclei were counterstained with Hoechst 33258 (0.5 μg/mL in PBS) (Sigma Aldrich) for 10 min. Finally, cells were washed in PBS and mounted on glass slides with PBS containing 50% glycerol.

Immunofluorescence analysis was performed using a confocal laser scanner microscope (LSM 510 Meta; Zeiss). The lambda of the argon ion laser was set at 488 nm. Fluorescence emission was revealed by BP 505–530 band pass filter for Alexa Fluor 488. Nuclear Hoechst 33258-stained cells were excited with mercury lamps and images acquired in a single channel using a 460–489 band pass filter. Double-staining immunofluorescence images were acquired in the green and blue channels at a resolution of 1024 × 1024 pixels.

2.4 Proliferative assays

To measure the concentration of DNA in VSMCs that were grown on stents, cells were seeded onto six-well plates with a stent in each well, in the absence or presence of 100 ng/mL FK506. The stents were removed from wells after 9 days of culture and introduced in a tube with 1 mL of a permeabilizing solution containing Hoechst 33258 (0.5 μg/mL in 0.1% sodium citrate, w/v; 0.1% Triton X-100, v/v). After 30 min incubation at room temperature, tubes were vortexed and centrifuged at 400g for 10 min to collect cells. The supernatant was discarded, stents were examined using a microscope to verify the absence of cells, and the pellets were resuspended in 500 μL of RIPA buffer. The DNA in lysates was read with a fluorimeter at an excitation wavelength of 354 nm and at an emission of 461 nm.

Cell proliferation was measured with 5-bromo-2′-deoxy-uridine labelling and with a detection kit (Detection Kit II, Roche Diagnostics Corporation, Indianapolis, IN, USA) following the manufacturer's instructions. Briefly, cells were plated onto 24-well plates in the
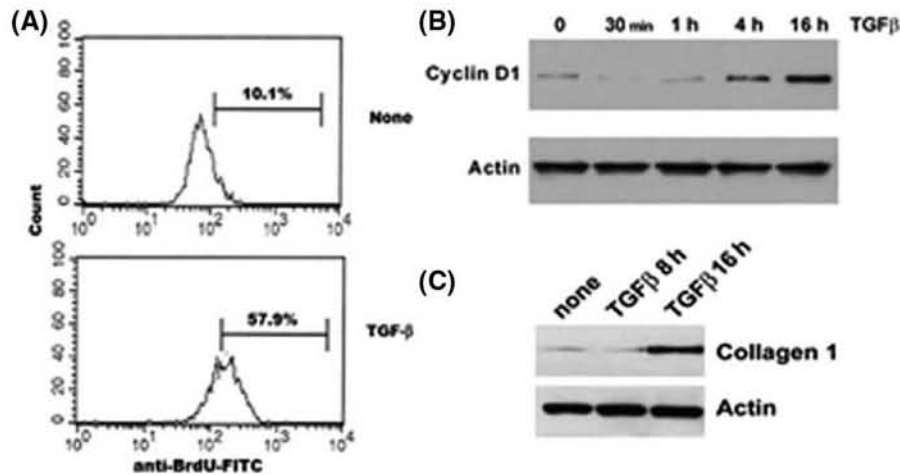
Figure 1 Transforming growth factor-β stimulates vascular smooth muscle cell proliferation and collagen production. (*A*) Flow cytometric histograms of BrdU incorporation in vascular smooth muscle cells. Cells were cultured with and without 10 ng/mL transforming growth factor-β. After incubation for 3 days, 10 µM BrdU was added to the cultures and 4 h later cells were collected, fixed with ethanol, and incubated with anti-BrdU-FITC monoclonal antibody. The bar indicates the per cent of cells incorporating BrdU in their DNA. The data presented are representative of five different experiments, each performed in triplicate. (*B*) Western blot assay of cyclin D1 levels in whole-cell lysates (30 µg) of vascular smooth muscle cells incubated with 10 ng/mL transforming growth factor-β for 0, 30 min, 3, 4, and 16 h. Similar results were obtained in other two different experiments. (*C*) Western blot assay of collagen type I levels in whole-cell lysates (30 µg) of vascular smooth muscle cells treated with 10 ng/mL transforming growth factor-β for 0, 8, and 16 h. The data of collagen upregulation was confirmed in another two independent experiments.

absence or presence of different doses of FK506 or 10 ng/mL TGF-β. After incubation for 3 days, 10 µM BrdU was added to the cultures, and, after a further 4 h, cells were collected, fixed with ethanol, and incubated with anti-BrdU monoclonal antibody. The per cent of BrdU incorporation was measured in flow cytometry (FACScan Becton Dickinson, San Diego, CA, USA).

2.5 Immunoprecipitation of membranes

Cells harvested after a 2 h incubation with FK506 were osmotically lysed in distilled water and subjected to three cycles of rapid freezing and thawing, after addition of protease inhibitors and phosphatase inhibitors. During thawing, the extract was sonicated for 10 min. After obtaining a homogeneous suspension, protein concentration was determined with the Bradford method and 500 µg of protein extract was pre-cleared for 1 h. For immunoprecipitation, 15 µg anti-TβR-I (rabbit polyclonal H-100) or anti-FKBP12 (goat polyclonal N-19; Santa Cruz Biotechnology) was added together with 25 µL protein A-Sepharose (Santa Cruz Biotechnology), and precipitation took place overnight with rotation at 4°C. Samples were separated by 14% SDS-PAGE together with a molecular weight marker and transferred onto membrane filter.

2.6 Cell transfection and short interfering RNA

Twenty-four hours before transfection of two different short interfering (si)RNAs corresponding to the target sequences GCTTGAA-GATGGAAAGAAA and GAAACAAGCCCTTTAAGTT of the FKBP12 gene (Qiagen, Valencia, CA, USA) or of a scrambled duplex as control, VSMCs were incubated in medium without antibiotics at the concentration of 2.5×10^5/mL to obtain 30–50% confluence at the time of transfection. The siRNA or the scrambled oligo was transfected at the final concentration of 50 nM using Metafectene (Biontex, Munich, Germany) according to the manufacturer's recommendations, and 72 h later, cells were harvested to prepare cell lysates. The effect of siRNA on protein expression was determined by Western blot.

2.7 Statistical analysis

The results reported are the mean and the standard deviation of independent experiments. The statistical significance of differences

between means was estimated using Student's *t*-test. Values of $P \leq 0.05$ were considered statistically significant.

3. Results

3.1 Transforming growth factor-β stimulates DNA and collagen synthesis in vascular smooth muscle cells

TGF-β stimulates proliferation of VSMCs and matrix protein production.[2–6] We confirmed this observation in our experimental model of human VSMCs. Indeed, TGF-β (10 ng/mL) significantly increased VSMC proliferation as measured by BrdU incorporation (*Figure 1A*). In five experiments, each carried out in triplicate, the proportion of cells incorporating BrdU in their DNA was significantly higher ($P = 0.02$) in TGF-β-stimulated cells than in unstimulated cells (*Figure 1A*). In accordance with the results of BrdU assay, Western blot showed enhanced levels of cyclin D1 in TGF-β-cultured cells (*Figure1B*). Furthermore, collagen type I levels were increased in whole-cell lysates prepared from VSMCs cultured with TGF-β (*Figure 1C*). Taken together, these findings support the concept that TGF-β is a promoter of cell proliferation and extracellular matrix formation in VSMCs.

3.2 FK506 activates the transforming growth factor-β signalling

FK506 activates receptor I transphosphorylation, which is important for kinase activity and signal transduction.[15] We investigated whether FK506 activates the TGF-β signal in VSMCs. Using Western blot assay, we studied the kinetics of pSmad2 levels in whole-cell lysates prepared from VSMCs cultured with 10 ng/mL TGF-β or 100 ng/mL FK506. We found that the levels of pSmad2 in VSMCs cultured with TGF-β increased as early as 2 min after incubation and persisted for 3–4 h, after which they decreased (*Figure 2A*). Similar results were obtained with cells
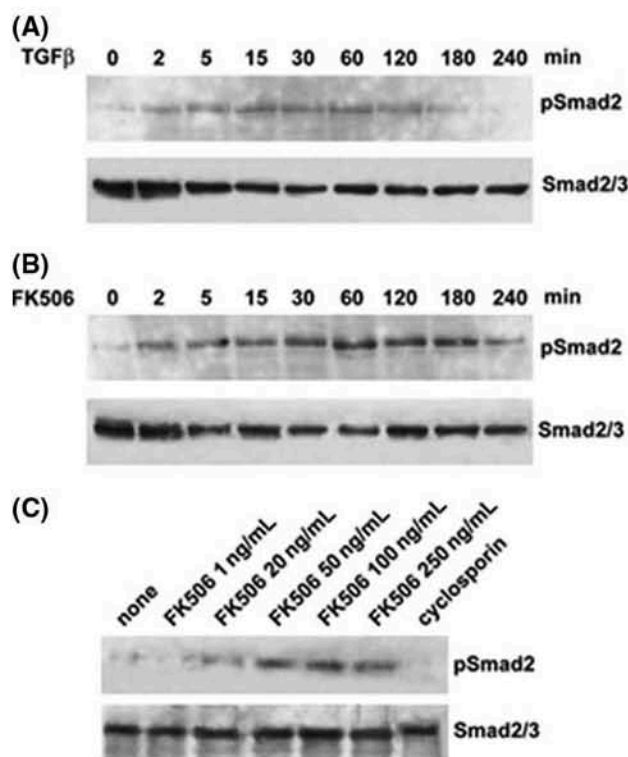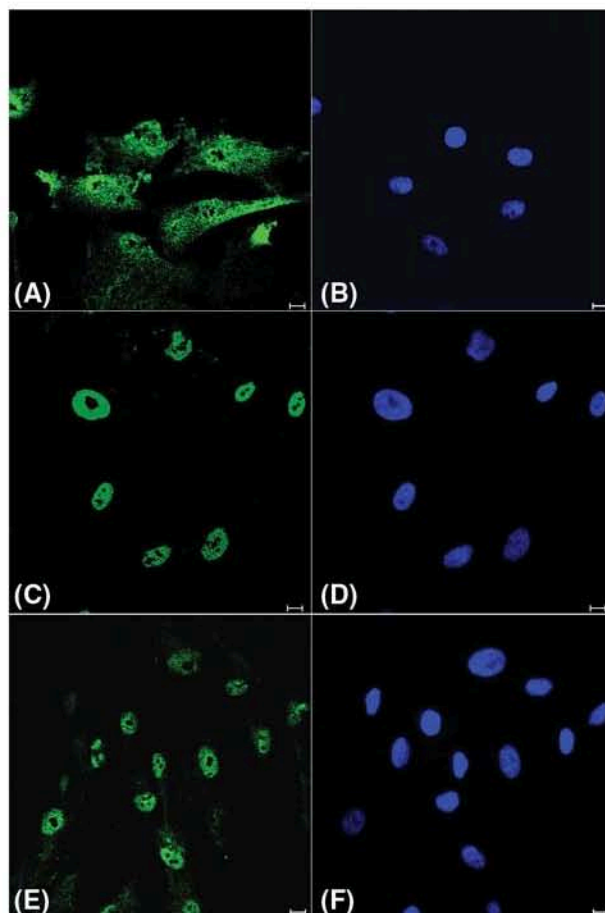
Figure 2 FK506 activates the transforming growth factor-β receptor I kinase activity in vascular smooth muscle cells. (*A*) Kinetics of transforming growth factor-β-induced Smad 2 phosphorylation. Western blot assay of pSmad 2 (Ser 465 467) levels in whole-cell lysates (30 μg) of vascular smooth muscle cells incubated with 10 ng/mL transforming growth factor-β for 0, 2, 5, 15, 30, 60, 120, 180, and 240 min. (*B*) Kinetics of FK506-induced Smad 2 phosphorylation. Western blot assay of pSmad 2 (Ser 465 467) levels in whole-cell lysates (30 μg) of vascular smooth muscle cells incubated with 100 ng/mL FK506 for 0, 2, 5, 15, 30, 60, 120, 180, and 240 min. (*C*) Dose/response effect of FK506 on Smad 2 phosphorylation. Western blot assay of pSmad 2 (Ser 465 467) levels in whole-cell lysates (30 μg) of vascular smooth muscle cells incubated with 1, 20, 50, 100, and 250 ng/mL FK506 and 300 ng/mL cyclosporin, as control, for 1 h. Smad 2/3 was used as loading control. Each experiment presented was performed at least three times.

Figure 3 FK506 induces Smad nuclear translocation. Cells were incubated with control medium (*A* and *B*) or treated with 10 ng/mL transforming growth factor-β (*C* and *D*) or 100 ng/mL FK506 (*E* and *F*). After incubation for 1 h, cells were stained with Smad 4 (*A*, *C* and *E*) to visualize protein localization, or Hoechst 33258 (*B*, *D*, and *F*) to visualize nuclei. Localization of Smad4 was both cytosolic and nuclear in control cells (*A*), whereas it was clearly nuclear in cells treated with transforming growth factor-β (*C*) or FK506 (*E*). Bar 10 μm. The data were confirmed at least in five different experiments.

cultured with FK506 (*Figure 2B*). We investigated whether the effect of FK506 was dose-dependent. As shown in *Figure 2C*, the optimal dose of FK506 for Smad2 activation was >50 ng/mL. Smad phosphorylation was not found in VSMCs cultured with another calcineurin inhibitor, cyclosporine, which binds to cyclophilin A.[14] This finding confirms the specificity of the effect observed with FK506. Receptor-mediated phosphorylation increases the affinity of Smad2 for Smad4 and rapid accumulation of the complex in the nucleus.[11,12] Immunofluorescence of VSMCs stained with anti-Smad4 and confocal microscopy showed that FK506 induced nuclear translocation of Smad (*Figure 3*). Taken together, these results suggest that FK506 activates TGF-β signalling in VSMCs.

3.3 FK506 removes FKBP12 from TβR-1 thereby activating the signal

Displacement of FKBP12 from its binding to the GS region of TβR-1 is essential for the activation of the kinase activity.[13] To investigate whether FK506 displaces FKBP12 binding, we incubated the cells with or without 100 ng/mL FK506 and prepared whole-cell lysates for co-immunoprecipitation experiments. As shown in *Figure 4A*,

TβR-1 co-immunoprecipitated with FKBP12 in unstimulated VSMCs but not in FK506-stimulated VSMCs, suggesting that the drug removed FKBP12. To determine whether this effect was sufficient to activate the kinase activity, we depleted the cells of FKBP12 using two different siRNAs and measured the levels of phosphorylated Smad2. We found that pSmad levels were remarkably increased in FKPB12-depleted cells (*Figure 4B*). Taken together these findings suggest that FKBP12 controls activation of the TGF-β signal in VSMCs.

3.4 FK506 promotes vascular smooth muscle cell growth

We next studied the effect of FK506 on VSMC growth. Cells were incubated with FK506 and proliferation was investigated by measuring BrdU incorporation in cell DNA. As shown in *Figure 5A*, the proportion of cells incorporating BrdU dose-dependently increased in FK506 cultures. The levels of β-catenin, Erk, protein kinase B (PkB/Akt), and the mammalian target of rapamycin (mTOR) were increased (*Figure 5B*), which indicates that FK506 activated the
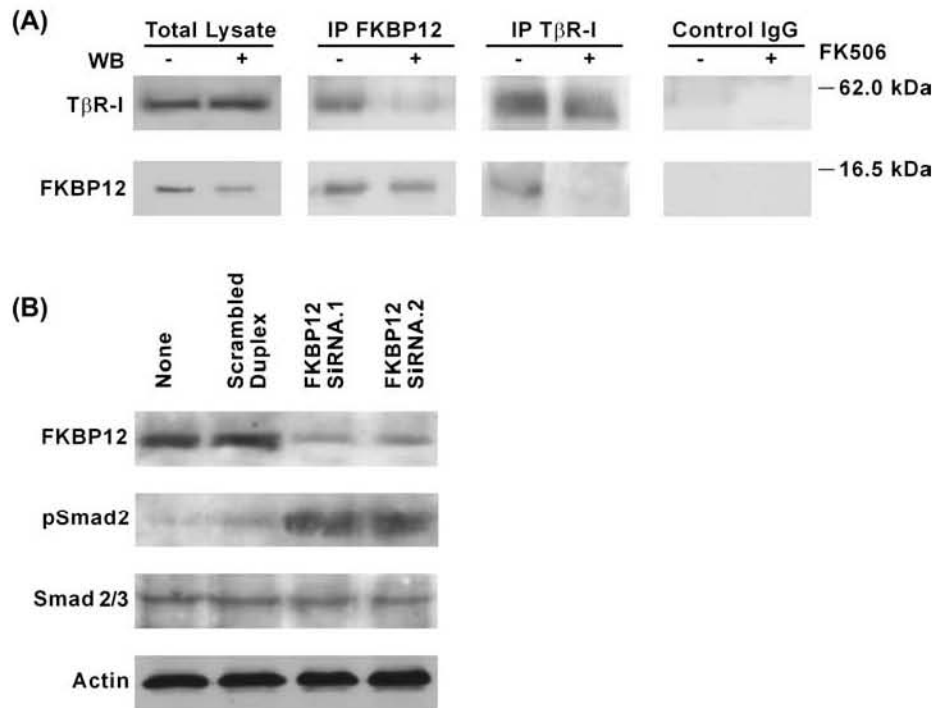
Figure 4 FK506 activates TβR-I by removing FKBP12. (*A*) FKBP12/TβR-I interaction in vascular smooth muscle cells. Total lysates, prepared from cells incubated with and without FK506 (100 ng/mL) for 2 h, were subjected to immunoprecipitation (IP) with anti-TβR-I or FKBP12 antibody. Immunoprecipitated and total lysates were then subjected to Western blot with anti-TβR-I or -FKBP12. The data were confirmed in another independent experiment. (*B*) Western blot assay of FKBP12 and pSmad 2 levels in total lysates prepared from non-transfected vascular smooth muscle cells, from vascular smooth muscle cells transfected with a scrambled duplex or with two different FKBP12 siRNAs, 3 days after transfection. Smad 2/3 and actin were used as loading control. The data were representative of three different experiments.

signalling pathways governing cell proliferation. Consistent with this finding, the cell cycle regulator cyclin D1 was induced in FK506-treated cells. Similar to TGF-β, FK506 increased collagen type I synthesis (*Figure 5C*). FK506 strikingly stimulated VSMC proliferation even in condition which does not favour cell adhesion, as it occurs in the case of metal surface.[26] *Figure 5D* shows results of a 9 day culture of cells seeded onto plates containing a metal stent and incubated with or without 100 ng/mL FK506. The metal stent was not invaded by proliferating cells in culture dishes without FK506. In fact, very few nuclei were visualized on stents removed by such dishes. Normally, once the cells reach the confluence, they detach from the plate and die. But, in the presence of FK506, cell growth continued on the metal support, suggesting that cells were refractory to death. Although the finding of growth on bare stents has no translational implication, it strengthens the hypothesis that FK506 exerts a pro-survival and proliferative effect. Stents were stained with Hoechst 33258 and examined by microscopy and fluorimetrically to evaluate DNA concentrations in the nuclei. Results of absorbance from three different experiments were 32.121 ± 2.001 and 77.126 ± 1.691 OD for cells cultured with and without FK506, respectively.

3.5 Selective inhibition of transforming growth factor-β type I receptor kinase prevents FK506-induced proliferation of vascular smooth muscle cells

To verify that the proliferative response to FK506 depended on activation of the TGF-β signal, we used SB431542, which

is a selective inhibitor of TGF-β type I ALK receptors. This compound efficiently inhibited receptor kinase activity, as indicated by the reduced levels of pSmad in VSMCs cultured with FK506 plus SB431542 compared with the levels of cells cultured with FK506 alone (*Figure 6A*). Treatment of the cells with SB431542 dramatically inhibited proliferation in FK506 cultures (*Figure 6B*), which suggests that Smad 2 phosphorylation is essential for transduction of the proliferative signal stimulated by FK506.

4. Discussion

Here we demonstrate that the immunosuppressant FK506 or 'tacrolimus' acts as a growth factor for VSMCs. This compound is structurally related to rapamycin, which significantly prevents the incidence of in-stent restenosis[27] when administered coated to eluting stents in angioplastic procedures. FKBP12 is the intracellular ligand of both FK506 and rapamycin.[18-20] Although both drugs bind to the same immunophilin receptor, the resulting immunophilin–drug complexes interfere with distinct intracellular signalling pathways. The interaction between FKBP12 and FK506 results in a complex that inhibits calcineurin phosphatase,[18] which controls lymphocyte activation,[19] whereas the binding of FKBP12 to rapamycin produces a complex that inhibits mTOR[28] downstream from the phosphatidyl-inositol 3 kinase (PI3k)/Akt-PkB survival pathway.[29] There is great interest in therapeutically targeting VSMC growth with agents delivered by stents implanted in coronary vessels.[27] As a step in this direction, polymer-free stents coated with FK506 have been developed.[25]
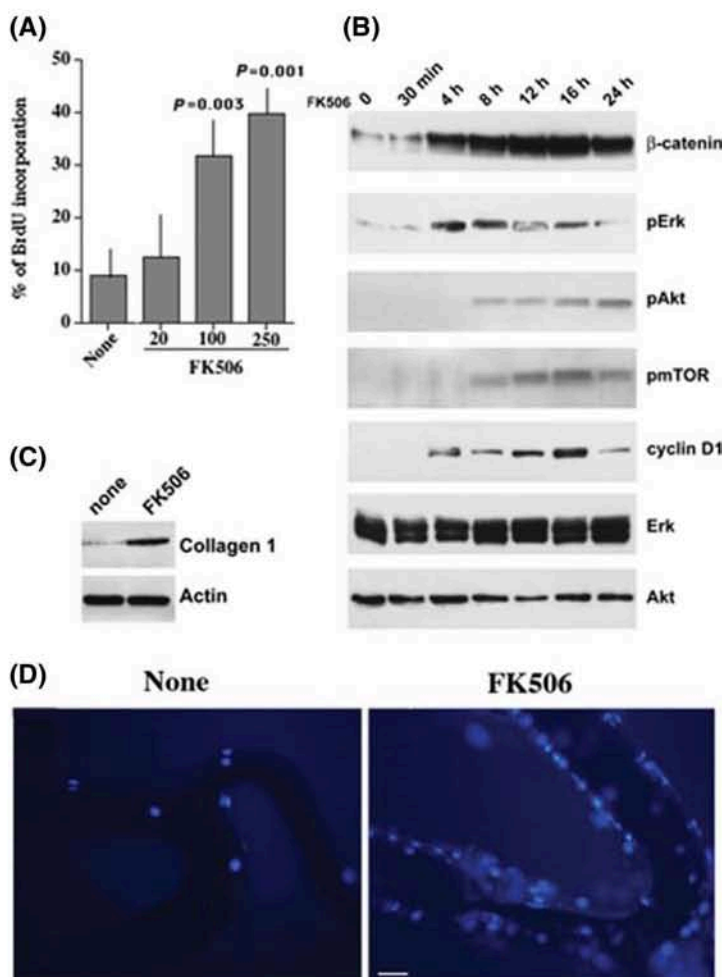
Figure 5 FK506 stimulates vascular smooth muscle cell proliferation. (*A*) Dose/response effect of FK506 on vascular smooth muscle cell proliferation. Graphic representation of mean values and standard deviations of per cent of cells incorporating BrdU in their DNA, in five different experiments, each performed in triplicate. Cells were cultured with and without 20, 100, and 250 ng/mL FK506. After incubation for 3 days, 10 μM BrdU was added to the cultures and 4 h later cells were collected, fixed with ethanol, and incubated with anti-BrdU monoclonal antibody. The per cent of BrdU incorporation, measured by flow cytometry, was significantly increased by FK506 at the doses of 100 ng/mL ($P = 0.003$) and 250 ng/mL FK506 ($P = 0.001$), compared with that found in cells cultured with medium alone. (*B*) FK506 activates signalling kinases involved in cell proliferation. Western blot assay of β-catenin, pErk, pAkt, pmTOR, and cyclin D1 levels in vascular smooth muscle cell lysates prepared from cells cultured with 100 ng/mL FK506, for 0, 30 min, 4, 8, 12, 16, and 24 h. Erk 1/2 and Akt were used for loading control. Comparable results were obtained in two other different experiments. (*C*) Western blot assay of collagen type I levels in whole-cell lysates of vascular smooth muscle cells treated with 100 ng/mL FK506 for 16 h. The result confirmed two other independent experiments. (*D*) FK506 stimulates vascular smooth muscle cell growth on a metal stent. Vascular smooth muscle cells were cultured in dishes containing a metal stent with and without 100 ng/mL FK506. After 9 days of culture, the stent was removed from the dish and nuclei were stained with Hoechst 33258 and visualized with a Zeiss Axioscop 2. Bar 25 μm. In three different experiments, the mean absorbance was 32.121 ± 2.001 and 77.126 ± 1.691 OD for cells cultured with and without FK506, respectively.

It is noteworthy that migration and proliferation of smooth muscle cells in injured vessels are stimulated by cytokines released by infiltrating mononuclear cells.[24] Therefore, FK506, which is a potent inhibitor of lymphocyte activation,[19,20,30] appeared to be a good candidate to counteract this phenomenon. Nevertheless, contrary to rapamycin, which exerts immunosuppressant,[20,30] anti-proliferative,[29] and pro-apoptotic[31] effects, little is known about the effect of FK506 on cell growth. Here we show that FK506 activates the TGF-β signal in VSMCs. In fact, FK506 increased levels of phosphorylated Smad and nuclear translocation of the Smad complex in VSMCs.

This finding is in accordance with studies showing that FKBP12 ligands, i.e. FK506 and rapamycin, promote TGF-β receptor transphosphorylation.[15] We found that FK506 provoked FKBP12 release from the cytoplasmic tail of the TGF-β receptor. This displacement was apparently sufficient to trigger the receptor kinase activity, as suggested by the appearance of phosphorylated Smad in cells depleted of FKBP12.

TGF-β plays an important role in promoting excess intimal hyperplasia after vascular injury, thereby concurring in restenosis after coronary angioplasty.[1-6] Consistent with this notion, TGF-β enhanced proliferation and extracellular matrix production in our specific cellular context of human VSMCs, as indicated by increased BrdU incorporation, cyclin D1 upregulation, and induction of collagen type 1 synthesis.

We found that, similar to TGF-β, FK506 stimulated cell growth. We thus investigated the pathways governing vascular remodelling and VSMC proliferation in cells cultured with FK506. Our data show that FK506 increased the levels of β-catenin, a key regulatory molecule of the highly conserved Wnt pathway[32] that controls the dynamic process of vascular remodelling.[33] Several lines of evidence implicate β-catenin in the development of intimal thickening.[33-35]

(A)

(B)
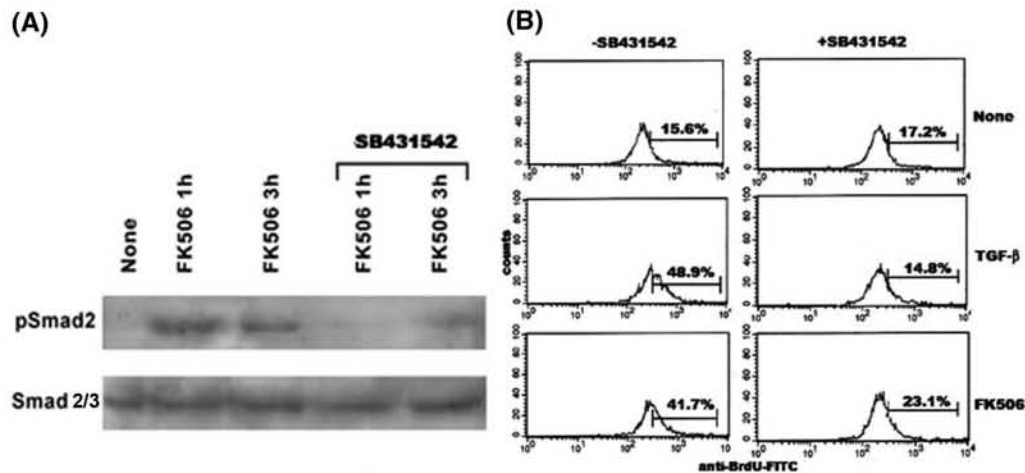
Figure 6 Effect of transforming growth factor-β type I receptor kinase inhibition on FK506-induced proliferation of vascular smooth muscle cell. (A) Western blot assay of pSmad2 levels in whole-cell lysates prepared from vascular smooth muscle cells incubated with 100 ng/mL FK506 for 1 and 3 h in the absence or the presence of 5 μM SB431542. Comparable results were obtained in two other different experiments. (B) Flow cytometric histograms of BrdU incorporation in vascular smooth muscle cells. Cells were cultured with 10 ng/mL transforming growth factor-β or with 100 ng/mL FK506 in the absence or the presence of 5 μM SB431542. After incubation for 3 days, 10 μM BrdU was added to the cultures and 4 h later cells were collected, fixed with ethanol, and incubated with anti-BrdU-FITC monoclonal antibody. The bar indicates the per cent of cells incorporating BrdU in their DNA. The experiment was representative of three independent experiments, each performed in triplicate. The per cent of BrdU incorporation was significantly decreased by SB431542 both in FK506 ($P = 0.05$) and in transforming growth factor-β ($P = 0.003$) cultures.

In an *in vivo* model of intimal thickening, β-catenin expression co-localized in proliferating VSMC within the developing intima.[34] β-catenin regulates VSMC proliferation in response to stimulation by growth factors via the regulation of the cell cycle genes cyclin D1 and p21.[34] Interestingly, the Wnt/β-catenin pathway can be activated in response to various stimuli,[36] including TGF-β.[32,37,38] In agreement with this concept, we found that FK506-induced proliferation was prevented when the TGF-β type I receptor kinase was inhibited. The increase in β-catenin levels was accompanied by the activation of Erk and Akt, which are important mediators of β-catenin signalling.[39,40] Furthermore, consistent with reports that mTOR can be activated through tuberin phosphorylation by both Erk[41] and Akt,[42] mTOR levels were also increased in FK506-treated VSMCs.

It is noteworthy that all these signalling kinases drive biochemical networks that directly regulate the expression of genes responsible for cell cycle progression.[41] In accordance with this finding, we found that the expression of cyclin D1 was enhanced in FK506 cultures. The Akt pathway also exerts a primary role, synergistically driven by mTOR, in cell survival.[41,43] Indeed, stimulation of Akt produces phosphorylation of downstream targets involved in apoptosis control.[43] Phosphorylation of FOXO3A, a member of the forkhead family of transcription factors, leads to inhibition of its transcription activity. This results in the downregulation of the pro-apoptotic BH3-only molecule, Bim.[43] Moreover, Akt-induced phosphorylation of another pro-apoptotic Bcl-2 family member protein, namely Bad, causes its dissociation from the complex with Bcl-xL, thereby allowing cell survival.[43] Therefore, Akt activation may result in resistance to death-inducing signals possibly released in the site of vascular injury.

Although rapamycin also activates TGF-β receptor signalling because of the binding to FKBP12 (not shown), it did not increase the levels of cyclin D1 and collagen type 1 (not shown). This finding suggests that the proliferative and pro-fibrotic stimuli are inhibited downstream the pathway

consequent to mTOR blockage by FKBP12/rapamycin complex itself. Also in the case of immunosuppression, rapamycin acts on the signalling pathway of T-cell activation downstream to FK506. In fact, while FK506 blocks transcription of the IL-2 gene, rapamycin has no effect on gene transcription but rather has a potent inhibitory effect on growth factor-induced proliferation.

Our findings support the conclusion that FK506 is a potential stimulus of neointima formation when administered coated to intravascular stents. This implies that, although FK506 dampens cytokine-induced VSMC migration and proliferation through its immunosuppressant mechanism, it exerts a direct proliferative effect on these cells. Therefore, the clinical outcome of patients receiving FK506-eluting stents depends on the balance between these opposite effects. Curiously, the stent name, 'Janus', who is the Roman god with two faces looking in opposite directions, reflects our conclusions.

Acknowledgements

Funding

References

1. Majesky MW, Lindner V, Twardzik DR, Schwartz SM, Reidy MA. Production of transforming growth factor β1 during repair of arterial injury. *J Clin Invest* 1991;**88**:904 910.
2. Kanzaki T, Tamura K, Takahashi K, Saito Y, Akikusa B, Oohashi H et al. In vivo effect of TGF-β1. Enhanced intimal thickening by administration of TGF-β1 in rabbit arteries injured with a balloon catheter. *Arterioscler Thromb Vasc Biol* 1995;**15**:1951 1957.

3. Nabel EG, Shum L, Pompili VJ, Yang Z-Y, San H, Shu HB *et al.* Direct transfer of transforming growth factor β1 gene into arteries stimulates fibrocellular hyperplasia. *Proc Natl Acad Sci USA* 1993;**90**:10759–10763.
4. Schulick AH, Taylor AJ, Zuo W, Qiu C-B, Dong G, Woodward RN *et al.* Overexpression of transforming growth factor β1 in arterial endothelium causes hyperplasia, apoptosis, and cartilaginous metaplasia. *Proc Natl Acad Sci USA* 1998;**95**:6983–6988.
5. Wolf YG, Rasmussen LM, Ruoslahti E. Antibodies against transforming growth factor-β1 suppress intimal hyperplasia in a rat model. *J Clin Invest* 1994;**93**:1172–1178.
6. Smith JD, Bryant SR, Couper LL, Vary CPH, Gotwals PJ, Koteliansky VE *et al.* Soluble transforming growth factor-b type II receptor inhibits negative remodeling, fibroblast transdifferentiation, and intimal lesion formation but not endothelial growth. *Circ Res* 1999;**84**:1212–1222.
7. Massague J. How cells read TGF-beta signals. (Review). *Nat Rev Mol Cell Biol* 2000;**1**:169–178.
8. Massague J, Blain SW, Lo RS. TGFbeta signaling in growth control, cancer, and heritable disorders. (Review). *Cell* 2000;**103**:295–309.
9. Massague J, Wotton D. Transcriptional control by the TGFβ/SMAD signaling system. *EMBO J* 2000;**19**:1745–1754.
10. Cheifetz S, Weatherbee JA, Tsang ML, Anderson JK, Mole JE, Lucas R *et al.* The transforming growth factor-beta system, a complex pattern of cross-reactive ligands and receptors. *Cell* 1987;**48**:409–415.
11. Janknecht R, Wells NJ, Hunter T. TGF-beta-stimulated cooperation of smad proteins with the coactivators CBP/p300. *Genes Dev* 1998;**12**:2114–2119.
12. Xu L, Chen YG, Massague J. The nuclear import function of SMAD2 is masked by SARA and unmasked by TGFbeta-dependent phosphorylation. *Nat Cell Biol* 2000;**2**:559–562.
13. Wang T, Li BY, Danielson PD, Shah PC, Rockwell S, Lechleider RJ *et al.* The immunophilin FKBP12 functions as a common inhibitor of the TGF beta family type I receptors. *Cell* 1996;**86**:435–444.
14. Dornan J, Taylor P, Walkinshaw MD. Structures of immunophilins and their ligand complexes. *Curr Top Med Chem* 2003;**3**:1392–1409.
15. Chen YG, Liu F, Massague J. Mechanism of TGFbeta receptor inhibition by FKBP12. *EMBO J* 1997;**16**:3866–3876.
16. Aghdasi B, Ye K, Resnick A, Huang A, Ha HC, Guo X *et al.* FKBP12, the 12-kDa FK506-binding protein, is a physiologic regulator of the cell cycle. *Proc Natl Acad Sci USA* 2001;**98**:2425–2430.
17. Tanaka H, Kuroda A, Marusawa H, Hashimoto M, Hatanaka H, Kino T *et al.* Physicochemical properties of FK-506, a novel immunosuppressant isolated from *Streptomyces tsukubaensis*. *Transplant Proc* 1987;**19**:11–16.
18. Sewell TJ, Lam E, Martin MM, Leszyk J, Weidner J, Calaycay J *et al.* Inhibition of calcineurin by a novel FK-506-binding protein. *J Biol Chem* 1994;**269**:21094–21102.
19. Crabtree GR. Calcium, calcineurin, and the control of transcription. *J Biol Chem* 2001;**276**:2313–2316.
20. Abraham RT, Wiederrecht GJ. Immunopharmacology of rapamycin. *Annu Rev Immunol* 1996;**14**:483–510.
21. Rao A, Luo C, Hogan PG. Transcription factors of the NFAT family: regulation and function. *Annu Rev Immunol* 1997;**15**:707–747.
22. Dumont FJ, Staruch MJ, Fischer P, Dasilva C, Camacho R. Inhibition of T cell activation by pharmacologic disruption of the MEK1/ERK MAP kinase or calcineurin signaling pathways results in differential modulation of cytokine production. *J Immunol* 1998;**160**:2579–2589.
23. Sigal NH, Lin CS, Siekierka JJ. Inhibition of human T-cell activation by FK506, rapamycin, and cyclosporine A. *Transplant Proc* 1991;**23**(Suppl. 2):1–5.
24. Davis C, Fischer J, Ley K, Sarembock IJ. The role of inflammation in vascular injury and repair. *J Thromb Haemost* 2003;**1**:1699–1709.
25. Bartorelli AL, Trabattoni D, Fabbiocchi F, Montorsi P, de Martini S, Calligaris G *et al.* Synergy of passive coating and targeted drug delivery: the tacrolimus-eluting Janus CarboStent. (Review). *J Interv Cardiol* 2003;**16**:499–505.
26. Gristina AG, Giridhar G, Gabriel BL, Naylor PT, Myrvik QN. Cell biology and molecular mechanisms in artificial device infections. *Int J Artif Organs* 1993;**16**:755–763.
27. Woods TC, Marks AR. Drug-eluting stents. *Ann Rev Med* 2004;**55**:169–178.
28. Sabatini DM, Erdjument-Bromage H, Lui M, Tempst P, Snyder SH. RAFT1: a mammalian protein that binds to FKBP12 in a rapamycin-dependent fashion and is homologous to yeast TORs. *Cell* 1994;**78**:35–43.
29. Schmelzle T, Hall MN. TOR, a central controller of cell growth. *Cell* 2000;**103**:253–262.
30. Siekierka JJ. Probing T-cell signal transduction pathways with the immunosuppressive drugs, FK-506 and rapamycin. (Review). *Immunol Res* 1994;**13**:110–116.
31. Giordano A, Avellino R, Ferraro P, Romano S, Corcione N, Romano MF. Rapamycin antagonizes NF-kappaB nuclear translocation activated by TNF-alpha in primary vascular smooth muscle cells and enhances apoptosis. *Am J Phys Heart Circ Phys* 2006;**290**:H2459–H2465.
32. Cadigan KM, Nusse R. Wnt signaling: a common theme in animal development. *Genes Dev* 1997;**11**:3286–3305.
33. Wang X, Xiao Y, Mou Y, Zhao Y, Blankesteijn WM, Hall JL. A role for the beta-catenin/T-cell factor signaling cascade in vascular remodeling. *Circ Res* 2002;**90**:340–347.
34. Quasnichka H, Slater SC, Beeching CA, Boehm M, Sala-Newby GB, George SJ. Regulation of smooth muscle cell proliferation by beta-catenin/T-cell factor signaling involves modulation of cyclin D1 and p21 expression. *Circ Res* 2006;**99**:1329–1337.
35. Wang X, Adhikari N, Li Q, Hall JL. LDL receptor-related protein LRP6 regulates proliferation and survival through the Wnt cascade in vascular smooth muscle cells. *Am J Physiol Heart Circ Physiol* 2004;**287**:H2376–H2383.
36. Huang HC, Klein PS. The frizzled family: receptors for multiple signal transduction pathways. *Genome Biol* 2004;**5**:234.
37. Kloth JN, Fleuren GJ, Oosting J, de Menezes RX, Eilers PHC, Kenter G *et al.* Substantial changes in gene expression of Wnt, MAPK and TNFa pathways induced by TGF-β1 in cervical cancer cell lines. *Carcinogenesis* 2005;**26**:1493–1502.
38. Zhou S, Eid K, Glowacki J. Cooperation between TGF-beta and Wnt pathways during chondrocyte and adipocyte differentiation of human marrow stromal cells. *J Bone Miner Res* 2004;**19**:463–470.
39. Almeida M, Han L, Bellido T, Manolagas SC, Kousteni S. Wnt proteins prevent apoptosis of both uncommitted osteoblast progenitors and differentiated osteoblasts by beta-catenin-dependent and -independent signaling cascades involving Src/ERK and phosphatidylinositol 3-kinase/AKT. *J Biol Chem* 2005;**280**:41342–41351.
40. Yun MS, Kim SE, Jeon SH, Lee JS, Choi KY. Both ERK and Wnt/beta-catenin pathways are involved in Wnt3a-induced proliferation. *J Cell Sci* 2005;**118**:313–322.
41. Shaw RJ, Cantley LC. Ras, PI(3)K and mTOR signalling controls tumour cell growth. (Review). *Nature* 2006;**441**:424–430.
42. Tee AR, Fingar DC, Manning BD, Kwiatkowski DJ, Cantley LC, Blenis J. Tuberous sclerosis complex-1 and -2 gene products function together to inhibit mammalian target of rapamycin (mTOR)-mediated downstream signaling. *Proc Natl Acad Sci USA* 2002;**99**:13571–13576.
43. Hennessy BT, Smith DL, Ram PT, Lu Y, Mills GB. Exploiting the PI3K/AKT pathway for cancer drug discovery. *Nat Rev Drug Discov* 2005;**4**:988–1004.

The effect of FK506 on transforming growth factor β signaling and apoptosis in chronic lymphocytic leukemia B cells

Simona Romano,[1] Maria Mallardo,[1] Federico Chiurazzi,[1] Rita Bisogni,[1] Anna D'Angelillo,[1] Raffaele Liuzzi,[2] Giovanna Compare[1] and Maria Fiammetta Romano[1]

[1]Department of Biochemistry and Medical Biotechnologies, Federico II University, Naples; [2]Institute of Biostructure and Bio-Imaging-National Research Council (CNR), Naples, Italy

ABSTRACT

Background
Loss of response to transforming growth factor-beta (TGF-β) is thought to contribute to the progression of chronic lymphocytic leukemia. Recent findings of over-activation of the TGF-β signal in FKBP12-knockout mouse prompted us to investigate whether FK506, the canonical ligand of FKBP, can activate the TGF-β signal in chronic lymphocytic leukemia.

Design and Methods
We studied 62 chronic lymphocytic leukemia samples from patients with Rai/Binet stage 0 to 4 disease. The TGF-β signal was investigated by western blotting and flow cytometry. The levels of Bcl2-family members and death-associated-protein kinase were also investigated by western blotting, whereas apoptosis was studied in flow cytometry. Down-modulation of FKBP12 was obtained by gene silencing with short interfering RNA.

Results
Twenty-two out of 62 chronic lymphocytic leukemia samples were sensitive to TGF-β-induced apoptosis. All but two of the responsive samples underwent apoptosis also when cultured with FK506, but not with cyclosporine. Thirteen samples that were not sensitive to TGF-β were sensitive to FK506. Overall, response to FK506 occurred in 33 samples. FK506 induced Smad2 phosphorylation and nuclear translocation. Accordingly, death-associated-protein kinase, a transcriptional target of Smad, was induced. At the same time, Bcl-2 and Bcl-xL levels decreased whereas the levels of Bim and Bmf increased. A loss of mitochondrial membrane potential preceded caspase activation and cell death. FK506 removed FKBP12 from its binding to the TGF-β-receptor. FKBP12 release activated the receptor-kinase activity as suggested by the enhanced levels of phospho-Smad found in cells depleted of FKBP12.

Conclusions
Our study shows that most chronic lymphocytic leukemia cells escape the homeostatic control of TGF-β and that FK506 restores the TGF-β signal in a proportion of non-responsive samples. We demonstrated that FK506 activates TGF-β receptor I kinase activity in chronic lymphocytic leukemia, which transduces apoptosis by a mitochondrial-dependent pathway.

Key words: FK506, chronic lymphocytic leukemia, TGF-β, apoptosis.

Introduction

Transforming growth factor-beta (TGF-β) is a pleiotropic cytokine important in the control of cell growth and differentiation.[1-3] In normal cells, TGF-β acts as a tumor suppressor by inhibiting cell proliferation or promoting cellular differentiation or apoptosis.[2,4] Several lines of evidence support the view that the loss of sensitivity to TGF-β promotes leukemic transformation[5-7] and contributes to the clinical and biological progression of chronic lymphocytic leukemia (CLL).[8-10] This hematologic malignancy is a slowly progressing leukemia characterized by the gradual expansion of morphologically small, functionally inactive clonal B cells due to defective apoptosis.[11]

TGF -β signals to the nucleus by binding to a specific pair of membrane receptors, type I (TGFBR1) and type II (TGFBR2), which contain a cytoplasmic serine-threonine kinase domain.[2,12] Binding of the ligand to TGFBR2 results in the formation of a TGFBR1/TGFBR2 heteromeric complex and activation of TGFBR2 kinase.[2,12] Activation of TGFBR1 requires phosphorylation of the GS (glycine, serine) region by TGFBR2. Activated TGFBR1 specifically recognizes and phosphorylates signaling molecules that act downstream receptors (Smad) 2 and 3 or R-Smad.[2,12,13] In the basal state, R-Smad are retained in the cytoplasm. In the case of Smad2, this retention is mediated by interactions with the Smad anchor for receptor activation (Sara).[13] In addition to limiting Smad movements, contact with Sara occludes a region of Smad2 that mediates nuclear import.[13] Receptor-mediated phosphorylation not only increases the affinity of Smad2 for Smad4[12] but also decreases its affinity for Sara. Smad4 functions as a shared partner or Co-Smad and is required for the assembly of transcriptional complexes.[2,12] This process results in the release of Smad2 and unmasking of its nuclear import function thereby leading to rapid accumulation of the activated Smad complex in the nucleus.[2,12,13] Once in the nucleus, both R- and Co-Smad are able to activate transcription.[2,12-14]

TGF-β is apoptotic for hematopoietic cells.[15] Although the mechanism involved in TGF-β-induced apoptosis is not well known, mitochondria appear to be important mediators of this process.[16]

Identification of molecules able to restore the TGF-β response in B-CLL can have important implications in the treatment of this disease.[8-10] A network of regulatory inputs controls the TGF-β signaling pathway.[2] A recent study of fibroblasts from FK506 binding protein (FKBP) 12-knockout mice showed that the TGF-β pathway is overactive in cells lacking this protein.[17] FKBP12 is a common inhibitor of the TGF-β family type I receptors,[18-20] it binds to part of the GS region towards the N-terminal end of the serine-threonine kinase domain of *TGFBR1*[2,12] thereby blocking access to activators. Ligand binding induces the release of FKBP12, which is essential for propagating the signal.[2,12,17,18,20] The finding that FKBP12-binding molecules, such as FK506 and rapamycin, are able to promote receptor transphosphorylation,[18,20] prompted us to investigate whether FK506, the canonical ligand of FKBP12,[19,21] could restore TGF-β response and stimulate apoptosis of CLL cells.

Design and Methods

Cell culture and reagents

CLL cells were isolated from the heparinized blood taken from 62 out-patients, after informed consent, by differential centrifugation through a Ficoll-Hypaque density gradient (ICN Flow, Opera, Italy). The study was approved by the Ethics Committee of Federico II University of Naples. Only CLL patients who had >80% CD19 cells co-expressing CD5 were included in the study. Cells were cultured in RPMI 1640 medium supplemented with 10% heat-inactivated fetal calf serum (FCS; ICN Flow). FK506, cyclosporine and TGF-β (Sigma Aldrich, St. Louis, MS, USA) were used at the doses indicated in the Results section. The peptide caspase 3 inhibitor Z-Asp-Glu-Val-Asp fluoromethyl ketone (Z-DEVD-fmk, Sigma Aldrich) was used at the dose of 20 μM. Table 1 shows the clinical profiles of the patients studied, related to the time of blood sampling. The patients did not receive any therapy in the 6 months, at least, preceding blood collection. Peripheral blood lymphocytes were isolated from the heparinized blood of healthy donors by differential centrifugation through a Ficoll-Hypaque density gradient; B lymphocytes were sorted from peripheral blood lymphocytes with a BD FACSAria™ (BD Biosciences, San Jose, CA USA). The purified population was ≥ 97% $CD20^+$.

Cell lysates and western blot assay

Whole cell lysates were prepared by homogenization in modified RIPA buffer [150 mM sodium chloride, 50 mM Tris-HCl, pH 7.4, 1 mM ethylenediamine tetraacetic acid (EDTA), 1 mM phenylmethylsulfonyl fluorite (PMSF), 1% Triton X-100, 1% sodium deoxycholic acid, 0.1% sodium dodecylsulfate (SDS), 5 μg/mL aprotinin and 5 μg/mL leupeptin]. Cell debris was removed by centrifugation. Cell fractionation was obtained as described elsewere[22] with small changes. Briefly, cells were washed twice with phosphate-buffered saline (PBS) and resuspended in 200 μL buffer A [10 mM TRIS HCl pH 7.4, 10% glycerol, 1mM $MgCl_2$, 1 mM PMSF, 5 μg/mL aprotinin and 5 μg/mL leupeptin] for 15 min on ice, before adding 2 μL of 10% Nonidet P-40. The cells were vortexed for 20–30 sec and spun for 10 min at 3000 rpm to spin down the nuclei. The cytoplasmic fraction was saved, and the nuclear pellet was washed once with buffer A. Nuclei were resuspended in modified RIPA buffer and extracted at 4°C for 30 min. Cell lysates were run in 10% SDS in polyacrylamide gel electrophoresis (PAGE) along with a molecular weight marker and transferred onto a membrane filter (Cellulosenitrate, Schleider and Schuell, Keene, NH, USA), which was incubated with the primary antibody.

The rabbit polyclonal antibodies against phospho-Smad2 (Ser 465/467) (Chemicon Temecula, CA, USA), caspase3 (Pharmigen/Becton Dickinson, San Diego, CA, USA), Smad 2,3 (H-465) and Bim (H-191) (Santa

Cruz Biotechnology, Santa Cruz, CA, USA); the mouse monoclonal anti-Bcl-xL (H-5), Bcl-2 (100), Smad4 (B-8), histone H1 (AE-4) (Santa Cruz Biotechnology), death-associated potein kinase (DAPK-55) (Sigma Aldrich), EF-1· (Upstate, Charlottesville, Virginia, USA) and the goat polyclonal anti-Bmf (Santa Cruz Biotechnology), were used diluted 1:500-1:1000. The blots were developed with an electrochemiluminescence system (Supersignal West Pico, Celbio, PIERCE, Rockford, IL, USA).

Immunofluorescence

For nuclear immunofluorescence, nuclei were purified from CLL cells by hypotonic lysis of plasma membrane and sucrose gradient. Briefly, cells were washed twice with PBS and resuspended in 200 µL buffer A [10 mM TRIS HCl pH 7.4, 10% glycerol, 1 mM MgCl$_2$, 1 mM PMSF, 5 µg/mL aprotinin and 5 µg/mL leupeptin] for 15 min on ice, before 2 µL of 10% Nonidet P-40 were added. The cells were vortexed for 20-30 sec and spun for 10 min at 3000 rpm to spin down the nuclei. The pellet was washed once with buffer A, resuspended in buffer A and a cushion carefully laid beneath it (30% sucrose w/v in buffer A). After centrifugation at 6000 rpm for 15 min (4° C), the supernatant was removed and the final pellet washed with buffer B [20 mM TRIS HCL pH 8.0, 75 mM NaCl, 0.5 mM EDTA pH 8.0, 0.85 mM dithiothreitol (DTT), 0.125 mM PMSF]. Nuclei isolated from 10-20×10^6 BCLL cells were subjected to immunostaining for 30 min at 4°C and analyzed by a FACScan 30 (BD) flow cytometer.

For intracellular staining with anti-phosphoSmad 2 antibody, B cells were fixed with 2% paraformaldehyde in Tris buffered saline (TBS) (10× TBS = 0.5M Tris Base, 9% NaCl, pH 7.6) for 20 min and permeabilized with 0.2%TRITON ×100 in TBS for 3 min in ice. Afterwards, cells were incubated with anti-phosphoSmad2 for 30 min at 4°C. After the cells had been washed, phosphoSmad2 was detected by immunostaining with a secondary fluorescein isothiocyanate (FITC) -conjugated anti-rabbit antibody and measured in flow cytometry.

Immunoprecipitation of membranes

Cells were osmotically lysed in distilled water and subjected to three cycles of rapid freezing and thawing. During thawning, extract was sonicated for 10 min. After obtaining a homogeneous suspension, protein concentration was determined using the Bradford method and 500 µg of protein extract were precleared for 1 hour. For immunoprecipitation, 15 µg anti-TGFBR1 (rabbit polyclonal H-100) or anti-FKBP12 (goat polyclonal N-19), (Santa Cruz Biotechnology) were added together with 25 µL protein A-Sepharose (Santa Cruz Biotechnology) and precipitation took place overnight with rotation at 4°C. Samples were separated by 14% SDS-PAGE along with a molecular weight marker and transferred onto a membrane filter.

Cell transfection and short interfering (si)RNA

Twenty-four hours before transfection of siRNA corresponding to the target sequence GCGGCTAGGTGT-

TATCTGA of the FKBP12 gene (Qiagen, CA, USA) or of a scrambled duplex as a control, cells were incubated in medium without antibiotics at the concentration of 5×10^5/mL. The siRNA or the scrambled oligo was transfected at the final concentration of 50 nM using

Table 1. Patients' profiles and response of samples.

	BINET/RAI	LDT[a]	Bulky disease	R TGF-β[b]	R FK506[c]
1.	0/A	Low	-	-	Yes
2.	0/A	Low	-	-	Yes
3.	0/A	Low	-	-	Yes
4.	0/A	Low	-	-	Yes
5.	0/A	Low	-	-	-
6.	I/A	Low	-	-	Yes
7.	0/A	Low	-	-	-
8.	0/A	Low	-	-	-
9.	0/A	Low	-	-	-
10.	0/A	Low	-	Yes	Yes
11.	0/A	Low	-	Yes	Yes
12.	0/A	Low	-	Yes	Yes
13.	0/A	Low	-	Yes	Yes
14.	0/A	Low	-	Yes	Yes
15.	0/A	Low	-	Yes	Yes
16.	I/A	Low	-	Yes	Yes
17.	I/A	Low	-	Yes	Yes
18.	I/A	Low	-	Yes	Yes
19.	I/A	Low	-	-	Yes
20.	I/A	Low	-	-	-
21.	I/A	Low	-	-	-
22.	I/A	Low	-	-	-
23.	I/A	Low	-	-	-
24.	I/A	Low	-	-	-
25.	I/B	Low	-	-	Yes
26.	I/B	Low	-	-	-
27.	I/B	Low	-	-	-
28.	I/B	Low	-	-	-
29.	I/B	Low	-	-	-
30.	I/B	Low	-	Yes	Yes
31.	I/B	Low	-	Yes	Yes
32.	II/A	Low	-	Yes	Yes
33.	II/B	Low	-	Yes	-
34.	II/B	Low	-	Yes	Yes
35.	II/B	Low	-	Yes	Yes
36.	II/B	n/a	-	Yes	Yes
37.	II/B	Low	-	Yes	Yes
38.	II/B	Low	-	Yes	Yes
39.	II/B	Low	-	-	Yes
40.	II/B	High	-	-	Yes
41.	II/B	Low	-	-	Yes
42.	II/B	Low	-	-	-
43.	II/B	Low	-	-	Yes
44.	II/B	High	-	-	Yes
45.	II/B	Low	-	-	-
46.	II/B	Low	-	-	-
47.	II/B	Low	-	-	-
48.	II/B	Low	-	-	-
49.	II/C	Low	-	Yes	-
50.	III/C	n/a	-	-	-
51.	III/C	Low	-	-	-
52.	III/C	High	Yes	-	-
53.	III/C	Low	-	Yes	Yes
54.	III/C	Low	-	Yes	Yes
55.	IV/C	Low	-	Yes	Yes
56.	IV/C	n/a	-	-	-
57.	IV/C	Low	-	-	-
58.	IV/C	Low	-	-	-
59.	IV/C	High	Yes	-	-
60.	IV/C	High	Yes	-	Yes
61.	IV/C	High	Yes	-	-
62.	IV/C	High	Yes	-	-

[a]LDT: lymphocyte doubling time (Low: >12 months); [b]R TGF-β: in vitro response to TGF-β; [c]R FK506: in vitro response to FK506.

Metafectene (Biontex, Munich, Germany) according to the manufacturer's recommendations and after 48 days, cells were harvested to prepare cell lysates. The effect of siRNA on protein expression was confirmed by western blotting.

Analysis of apoptosis

Phosphatidylserine externalization was investigated by annexin V staining. Briefly, 1×10^5 cells were resuspended in 100 μL of binding buffer (10 mM Hepes/NaOH pH 7.5, 140 mM NaCl, 2.5 mM CaCl₂) containing 5 μL of annexin V-FITC (Pharmigen/Becton Dickinson, San Diego, CA, USA) for 15 min at room temperature in the dark. Then 400 μL of the same buffer were added to each sample and the cells were analyzed with a Becton Dickinson FACScan flowcytometer. The lipophilic cation 5,5,6,6 tetrachloro-1,1,3,3 -tetraethylbenzimidazol-carbocyanine iodide (JC-1) was utilized to study mitochondrial membrane potential. In this procedure, the color of the dye changes from orange to green as the membrane potential decreases, due to JC-1 aggregates dissolving in monomers. Briefly, 5×10^5 cells were incubated for 10 minutes at 37°C with 10 μg/mL JC-1 (Molecular Probes, Leiden, The Netherlands), washed, and analyzed by flow cytometry.

Statistical analysis

The results of continuous variables are reported as medians and interquartile ranges. Frequencies are used for categorical data. The statistical significance of differences between groups of continuous data was estimated using the Mann-Whitney non-parametric unpaired test. Fisher's exact test was used to assess differences between categorical variables. p values ≤0.05 were considered statistically significant. The statistical analysis was performed using SPSS statistical package (SPSS Inc. Chicago, IL, USA).

Results

FK506 induces death of B-CLL cells

To investigate the effect of FK506 on CLL cell apoptosis, we cultured the cells with TGF-β (10 ng/mL), FK506 (100 ng/mL) or the cyclophilin A inhibitor cyclosporine (300 ng/mL) and measured cell death by annexin V staining and flow cytometry, after 24 h of incubation. As expected, we found spontaneous apoptosis of CLL cells after their *in vitro* culture.[23] TGF-β increased basal apoptosis by at least 20% in 22 of 62 samples. Figure 1A is a graphic representation of median values and interquartile ranges of apoptosis in samples that were and were not responsive to TGF-β. The median apoptosis in non-responsive samples was 22.0% (range 16.0-27.7%) and 22.0% (range 17.2-26.0%) in the absence and presence of TGF-β, respectively. The median apoptosis in responsive samples was 26.0% (range 20.7-29.2%) and 35.5% (range 30.7-43.7%) in the absence or presence of TGF-β ($p<0.001$), respectively.

Table 1 shows the CLL patients' profiles in relation to the response of the samples. Interestingly, the proportion of patients with low (>12 months) lymphocyte doubling time (LDT) was statistically higher ($p=0.04$) in TGF-β responders (100% low LDT) than in non-responders (81% low LDT). LDT is defined as the time needed for lymphocytes to double in number from the amount present at diagnosis.[24] This finding supports the concept that TGF-β inhibits cell growth. Regarding response to FK506, basal apoptosis was increased in 33 samples (Figure 1B). All but two of the samples sensitive to TGF-β were also sensitive to FK506. Median apoptosis in FK506-non-responsive samples was 22.0% (range 17.5-27.5%) and 22.0% (range 16.5-28.0%) in the absence or presence of the macrolide, respectively. The median apoptosis in FK506-responsive samples was 26.0% (range 21.5-30.0%) and 39.5% (range 29.7-42.2%) in the absence or presence of the drug ($p<0.001$), respectively. Interestingly, FK506 and TGF-β induced a similar degree of apoptosis in responsive samples. Cyclosporine did not induce cell death suggesting that the mechanism responsible for immunosuppression, i.e. calcineurin inhibition, was not involved in activation of the apoptotic machinery. FK506-induced apoptosis was remarkable at doses ≥10 ng/mL (Figure 1C) and reached the maximum level as early as 16 h after incubation (Figure 1D).
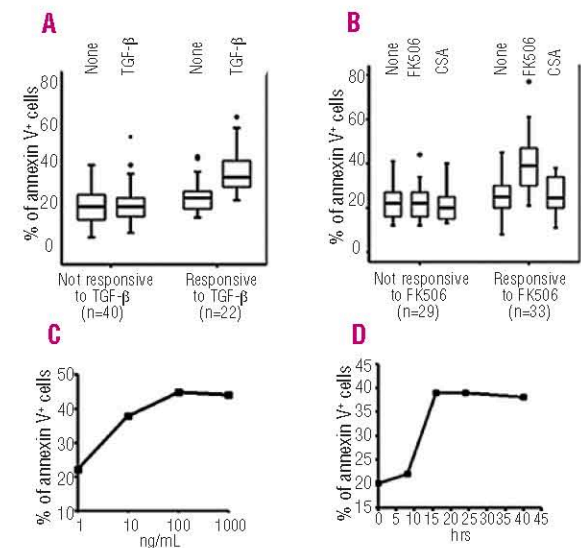


Figure 1. FK506 induces apoptosis of cells from patients with CLL. Graphic representation of median values and interquartile ranges of apoptosis measured by annexin V staining and flow cytometry. Cells were cultured with or without TGF-β (10 ng/mL). (A) With and without FK506 (100 ng/mL) or cyclosporine (300 ng/mL). (B) After 24 h cells were harvested, incubated with annexin V-FITC and analyzed in a flow cytometer. Each experiment was performed in triplicate. (C) Dose/response curve of FK506-induced apoptosis in a responsive sample. Cells were cultured with FK506 at the indicated doses. After 24 h of incubation, cells were harvested and apoptosis was determined by annexin V staining and flow cytometry. The experiment was performed in triplicate; the graphic shows the mean values of the triplicate experiments. (D) Kinetics of FK506-induced apoptosis. Cells were cultured with 100 ng/mL FK506 and were harvested at different times (8, 16, 24 and 40 h) and analyzed for apoptosis with annexin V staining and flow cytometry. The experiment was performed in triplicate and the mean results are reported.

FK506 activates the Smad complex

To test our hypothesis that the apoptotic response to FK506 of BCLL cells resulted from activation of the TGF-β signal, we investigated activation of Smad proteins by measuring the levels of phospho-Smad2 in cells incubated with FK506. Figure 2 shows western blot assays of three different samples, the first of which responded to both FK506 and TGF-β, the second one to FK506 but not to TGF-β and the third one did not respond to FK506. Phospho-Smad2 levels were increased in samples undergoing apoptosis, suggesting that activation of the TGF-β signaling pathway promoted cell death in FK506 cultures. To determine whether this response to TFG-β by CLL cells corresponded to a physiological effect, we studied the response of normal peripheral B lymphocytes to the cytokine. As shown in Figure 3A, phospho-Smad2 levels were increased after 1 h of incubation of purified B lymphocytes with TGF-β. Similarly, FK506 activated Smad in the same cells. Apoptosis analysis showed a slight increase of cell death in both TGF-β- and FK506-cultures.

The levels of phospho-Smad2 in CLL cells cultured with FK506 increased as early as 10 min after incubation, peaked at 3 h and decreased after 4 h (Figure 4A). Nuclear translocation of Smad-complex was found in isolated nuclei stained with anti Smad4 and analyzed by flow cytometry (Figure 4B). Smad nuclear translocation was confirmed by western blot assay of lysates obtained by cell fractionation. As shown in Figure 4C, the increase of Smad4 in nuclei was accompanied by its decrease in the cytoplasm. We used anti-histone H1 as a nuclear loading control and monoclonal antibody against the protein synthesis elongation factor, EF-1α,[25] as a cytosolic loading control.
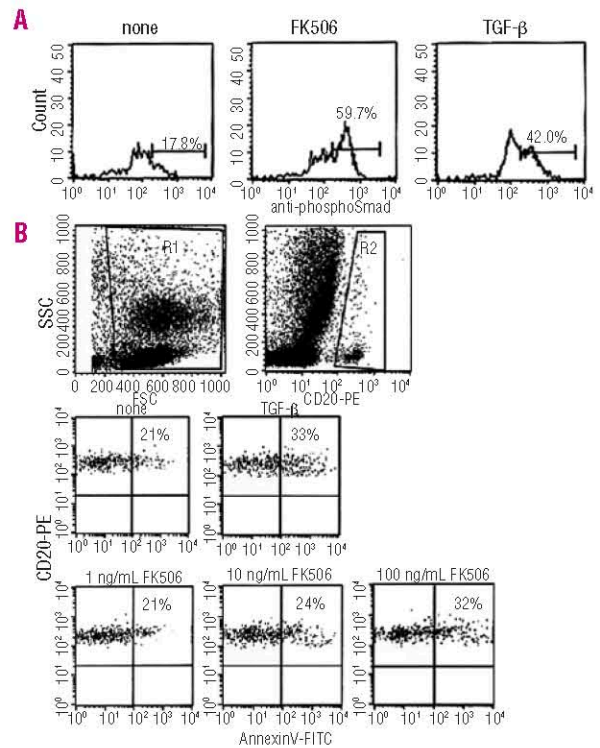
Figure 3. Effect of TGF-β and FK506 on normal B lymphocytes. (A) Flow cytometric analysis of phospho-Smad levels in purified B lymphocytes (CD20+≥97%) cultured in the absence or presence of 10 ng/mL TGF-β or 100 ng/mL FK506 for 1 h. (B) Flow cytometric analysis of apoptosis of B lymphocytes cultured with 10 ng/mL TGF-β and FK506 at different doses. Total peripheral blood lymphocytes were incubated with the indicated doses of the reagents for 48 h. Then, analysis of apoptosis was performed in double staining with annexin V-FITC and CD20-PE. Lymphocytes were identified using a FSC/SSC dual parameter dot plot (gate R1). All events in R1 were sent to a second display of CD20/SSC in which CD20+ cells (gate R2) were easily distinguished from non-B cells. Annexin V expression was measured using a logical gate (R1 and R2) which allows only the events which are in both R1 and R2 to be analyzed. The data presented are representative of three independent experiments.
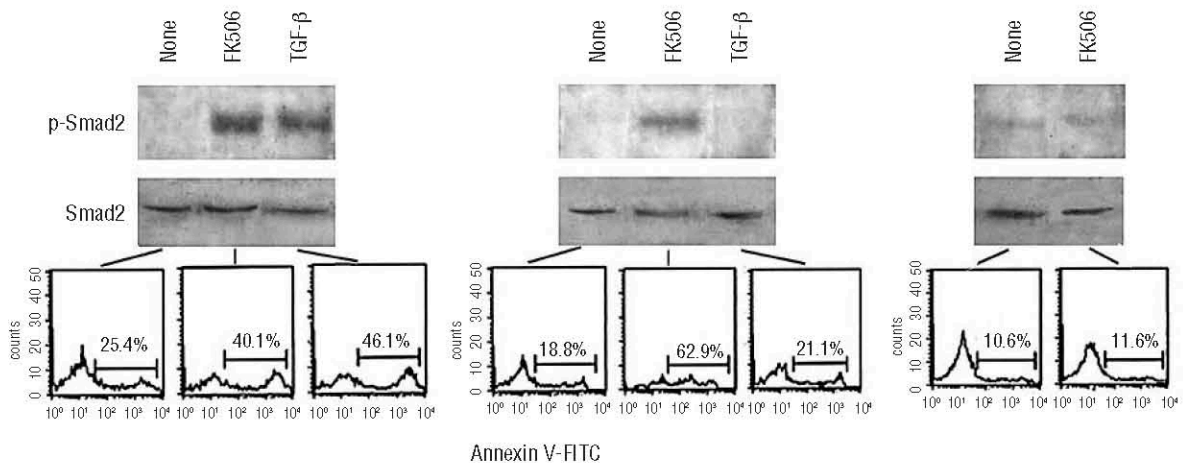
Figure 2. FK506-induced apoptosis is preceded by Smad2-phosphorylation. Western blot assay of phospho-Smad2 at Ser 465-467 in whole cell lysates (30 μg) from three different CLL samples. The samples used were, in order, n. 30 (TGF-β responsive) and n. 60 and 45 (TGF-β non-responsive). Five other samples analyzed did respond to FK506 and showed phosphorylation of Smad2. Cells were cultured with the indicated reagents (100 ng/mL FK506, 10 ng/mL TGF-β) and, after 3 h, a portion of cells was harvested for whole cell lysate preparation, whereas the remaining cells were harvested after a further 21 h and analyzed for apoptosis with annexin V staining and flow cytometry.

FK506 modulates the expression levels of both pro- and anti-apoptotic members of the Bcl-2 family of proteins

Death-associated protein kinase is a transcriptional target of Smad[16] that links Smad to TGF-β mitochondrial events.[16] We used western blot assays to investigate whether FK506 increased the levels of this protein in CLL cells. We also evaluated the expression levels of the anti-apoptotic Bcl-2 and Bcl-xL, and the pro-apoptotic BH3-only molecules, Bim and Bmf, which are implicated in commitment to TGF-β-induced apoptosis.[26-28] We found that the appearance of death-associated protein kinase was accompanied by a decrease of Bcl-2 and Bcl-xL and an increase of Bim (Figure 5A). Bim is an essential regulator of lymphoid system homeostasis and appears to be essential for induction of B-cell apoptosis. All the three Bim isoforms, Bim$_{EL}$, Bim$_L$ and Bim$_S$, which exert comparable activity,[27,28] were upregulated by FK506 in two different samples (Figure 5B). Similarly, the levels of expression of Bcl-2 modifying factor or Bmf were also increased (Figure 5C).

FK506 induces mitochondrial depolarization and activation of caspase 3

In accordance with the modulation of Bcl-2 family member proteins, the study of mitochondrial membrane potential with the lipophilic cation JC-1 showed depolarization in FK506 cultures, whereas this did not occur when cyclosporine was added to the culture medium (Figure 6A). A dose-response effect was observed by stimulating the cells with different FK506 doses (Figure 6B). Figure 6C shows the kinetics of FK506-induced mitochondrial depolarization in a responsive sample. More than 70% of cells depolarized after 8 h. Activation of caspase3 is a hallmark of apoptosis and represents the converging point of both intrinsic (downstream mitochondria) and extrinsic (downstream death receptors) pathways. Previous reports implicate caspase3 in TGF-β-induced apoptosis;[29] we, therefore, investigated whether the active form of caspase3 appeared in cells incubated with FK506. Western blot assay of whole cell lysates prepared after 16 h of incubation revealed the presence of activated caspase3, which resulted from cleavage adjacent to Asp175 (Figure 7).

FK506 activates TGFBR1 by removing FKBP12 from TGFBR1

Displacement of FKBP12 from its binding to the GS region of TGFBR1 is essential for activation of the kinase activity.[20] By co-immunoprecipitation studies, we found that FK506 interfered with the FKBP12/TGFBR1 interac-
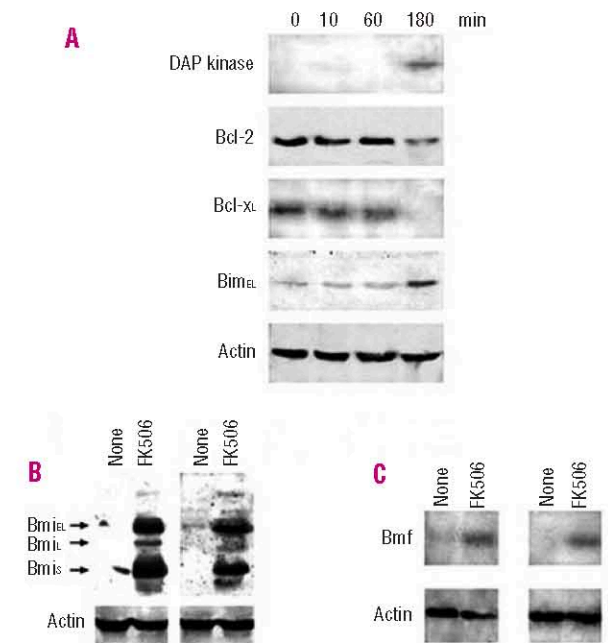

Figure 4. FK506 activates nuclear translocation of Smad complex. Kinetics of FK506-induced Smad2 phosphorylation. **(A)** Western blot assay of phospho-Smad2 (Ser 465-467) levels in whole cell lysates (30 μg) of CLL cells (sample #30,TGF-β responsive) incubated with 100 ng/mL FK506 for the indicated times. **(B)** Flow cytometric histograms of Smad4 expression in purified CLL nuclei. Cells (sample #30,TGF-β responsive) were incubated with 100 ng/mL FK506. After 3 h, cells were harvested and purified nuclei were subjected to indirect immunofluorescence with anti-Smad4. Nuclear autofluorescence was localized between 10²–10³ decades of the logarithmic scale, whereas Smad4-positive nuclei appeared in the 10⁴ decade. Staining with anti-histone or anti EF-1α served as a control of nuclear purification. **(C)** Western blot assay of Smad4 levels in cell lysates (20 μg) obtained by CLL cell fractionation (sample #60, not responsive to TGF-β) after 3 h incubation with 100 ng/mL FK506. Anti-histone H1 or anti EF-1α served as a loading control for nucleus and cytosol, respectively.

Figure 5. FK506 induces death-associated protein (DAP) kinase and modulates several members of the Bcl-2 protein family. **(A)** Western blot assay of DAP kinase, Bcl-2, Bcl-XL and Bim levels in whole cell lysates (30 μg) of CLL cells (sample #30, TGF-β responsive) incubated with 100 ng/mL FK506 for 3 h. **(B)** Western blot assays of the three Bim isoform levels in whole cell lysates (30 μg) of CLL cells from two samples (#30, responsive to TGF-β and #39, not responsive to TGF-β) incubated with 100 ng/mL FK506 for 10 h. **(C)** Western blot assay of Bmf levels in whole cell lysates (30 μg) of CLL cells from two different samples (#30, responsive to TGF-β and #39, not responsive to TGF-β) incubated with 100 ng/mL FK506 for 10 h.

tion. As shown in Figure 8A, TGFBR1 co-immunoprecipitated with FKBP12 in unstimulated- but not in FK506-stimulated peripheral blood lymphocytes, suggesting that the drug removed FKBP12. In order to investigate whether this effect was sufficient to activate the kinase activity, we depleted the cells of FKBP12 and measured the levels of phosphorylated Smad2. Figure 8B shows that a remarkable increase in phosphoSmad levels was associated with reduced levels of FKBP12. Consistent with the activation of the TGF-β signal, enhanced levels of Bim$_{EL}$ were also found. The effect of FKBP12 down-modulation on activation of the TGF-β signal was also confirmed in CLL. Figure 9 shows results from a sample responsive to FK506. Panel A shows flow cytometric histograms of annexin V staining of CLL cells after culture for 24 h in the absence or presence of 100 ng/mL FK506 and with or without the caspase3 inhibitor Z-DEVD-fmk. The percentage of FK506-induced cell death appeared remarkably reduced by the caspase inhibitor. In the experiments whose results are shown in panel B, the same cells were transfected with FKBP12 siRNA or a scrambled duplex as a control. After 48 h, total lysates were prepared and analyzed in western blot assays to measure the levels of FKBP12 and pSmad. Reduced levels of FKBP12 were accompanied by enhanced levels of pSmad. After a further 24 h, apoptosis was measured by annexin V staining (panel C). FKBP12 down-modu-

lation produced levels of apoptosis comparable to those induced by FK506. Similarly to FK506 cultures, Z-DEVD-fmk decreased apoptosis of cells transfected with FKBP12 siRNA. These results were confirmed in two other independent experiments.

Discussion

There is growing interest in understanding and therapeutically targeting TGF-β-mediated processes in cancer[3-5] including hematologic malignancies.[1] Herein, we show that FK506 activates TGF-β-signaling in CLL. FK506, or fujimycin, the canonical ligand of FKBP12,[19] is a 23-membered macrolide lactone mainly used to prevent organ rejection after allogeneic transplants.[21] B lymphocytes from subjects with CLL show heterogenous responses to TGF-β;[10] accordingly, our results indicated that 35.4% of the CLL samples analyzed (22/62) were sensitive to the TGF-β apoptotic effect. FK506 restored response to TGF-β in a further 17.7% of samples, thereby increasing the percentage of responses to 53.2%. Our data show that normal B lymphocytes also responded to TGF-β with low levels of apoptosis, which is in accordance with the notion that TGF-β is an important regulator of hematopoietic homeostasis. The response to TGF-β, found in some of the CLL samples, appeared, therefore, to be a conserved physiological effect.
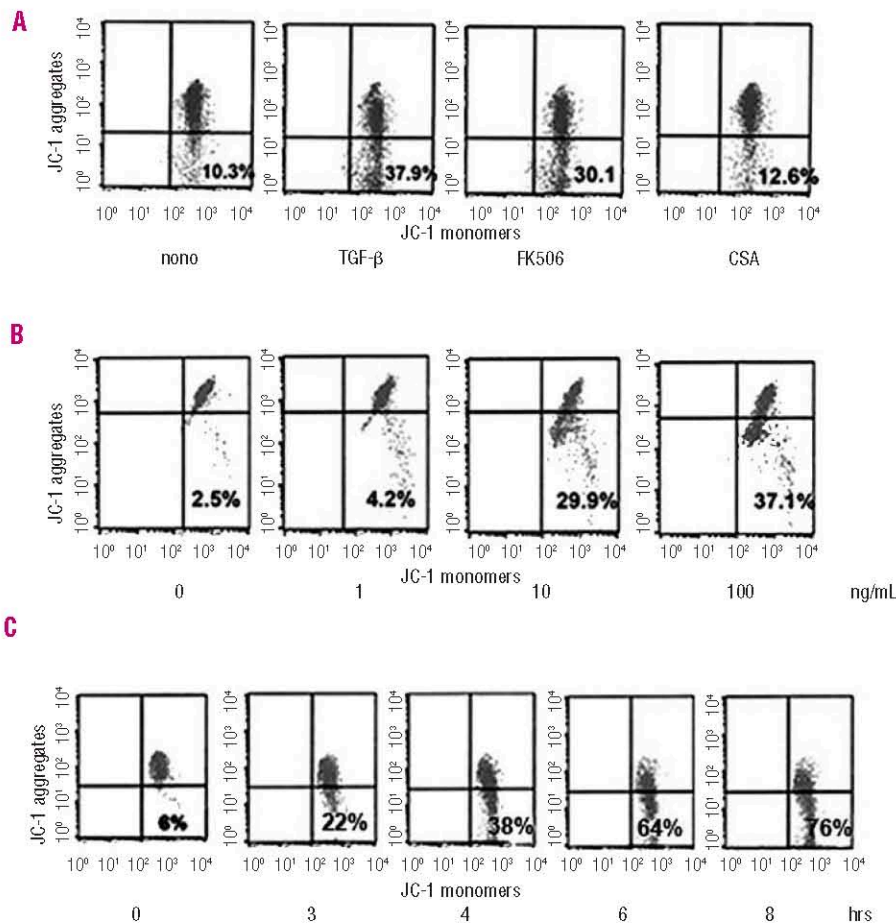
Figure 6. FK506 provokes mitochondrial depolarization. Analysis of mitochondrial membrane potential in three chronic lymphocytic leukemia samples with the lipophilic cation JC-1. The samples used were, in order, #10, #17 and #12 (TGF-β responsive). The percentage of depolarized cells was determined by calculating the amount of JC-1 monomers in flow cytometry. (A) Cells were incubated with or without 10 ng/mL TGF-β, 100 ng/mL FK506, and 300 ng/mL cyclosporine for 8 h. (B) Cells were incubated with the indicated doses of FK506 for 8 h. (C) Cells were incubated with 100 ng/mL FK506 for the indicated times.

FK506 activates TGF-β receptor kinase activity.[18,20] In CLL cells cultured with FK506, the appearance of phosphorylated Smad2 was detected as early as 10 min after incubation. The level of phosphorylated Smad2 peaked after 3 h and disappeared after 4 h. Smad complexes were found in the nucleus after 3 h of incubation with FK506. At the same time, there was an increase in levels of death-associated protein kinase, which is a target of transcriptional activation by Smad.[16] In accordance with reports that Bim is activated and functions as an important initiator of TGF-β-induced apoptosis in both a human gastric carcinoma cell line[26] and a B-cell line,[28] Bim was upregulated in CLL cells cultured with FK506. Bmf is another BH3-only protein implicated in TGF-β-induced apoptosis[27] which plays a role in regulating the growth and survival of B cells[28] and CLL cells.[29] Bim and Bmf are activators of Bax-Bak,[28] which are pro-apoptotic Bcl-2 members that are the downstream effectors controlling the mitochondrion-dependent cell death program. It is now well established that the role of anti-apoptotic Bcl-2 members correlates with their ability to sequester BH3-activators, thereby preventing the acti-
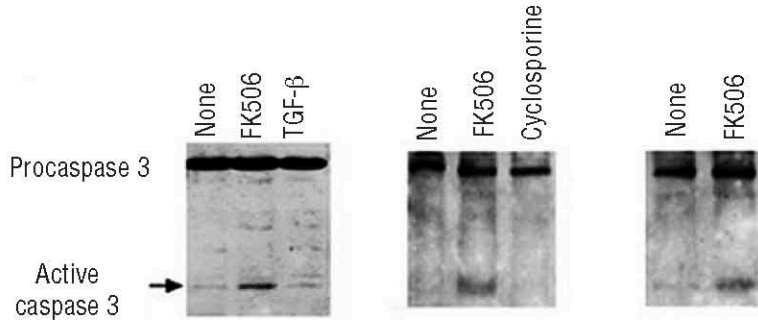
Figure 7. FK506 activates caspase 3. Western blot assay of active caspase 3 in whole cell lysates (30 μg) obtained from chronic lymphocytic leukemia cells of three different samples incubated with the indicated reagents (100 ng/mL FK506, 10 ng/mL TGF-β, 300 ng/mL cyclosporine) for 16 h. The samples used were, in order, #60, #3, and #43 (not responsive to TGF-β). The primary antibody used in this assay recognizes procaspase 3 and the activated caspase3 resulting from cleavage adjacent to Asp175.
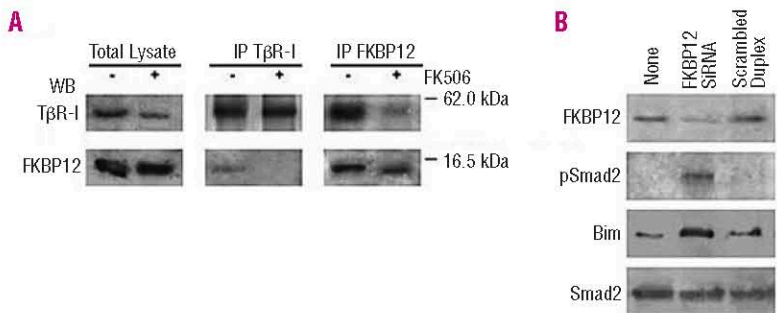
Figure 8. FK506 activates TβR-I by removing FKBP12. (A) FKBP12/TβR-I interaction in peripheral blood lymphocytes. Cell lysates were subjected to immunoprecipitation (IP) with anti-TβR-I or FKBP12 antibody. Immunoprecipitated and total lysates were then subjected to western blotting with anti-TβR-I or -FKBP12. (B) Western blot assay of FKBP12, phosphoSmad2 and Bim levels in total lysates prepared from non-transfected peripheral blood lymphocytes and from peripheral blood lymphocytes transfected with FKBP12 siRNA or a scrambled duplex as a control. Smad2 was used as the loading control.
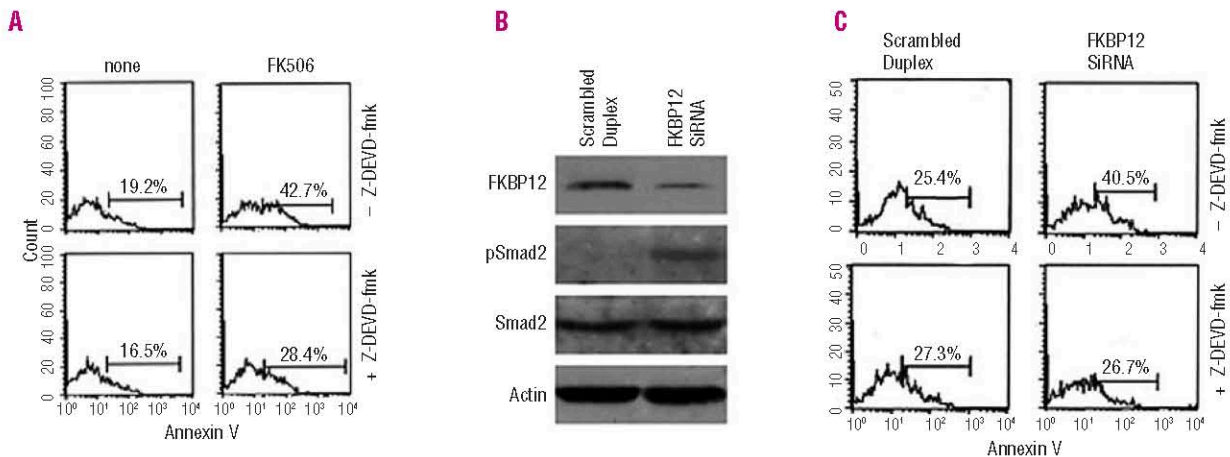
Figure 9. FKBP12 down-modulation causes apoptosis of CLL cells. (A) Flow cytometric histograms of annexin V staining. Chronic lymphocytic leukemia cells were cultured in the absence or the presence of 100 ng/mL FK506 and with or without the caspase3 inhibitor Z-DEVD-fmk (20 μM), then apoptosis was measured after 24 h. (B) The same cells were transfected with FKBP12 siRNA or a scrambled duplex as a control. After 48 h, total lysates were prepared and analyzed by western blotting to measure the levels of FKBP12 and pSmad. (C) Flow cytometric histograms of annexin V staining of chronic lymphocytic leukemia cells transfected with FKBP12 siRNA or a scrambled duplex as a control. Forty-eight hours after transfection, 20μM Z-DEVD-fmk was added to the cultures and, after a further 24 h, apoptosis was measured.

vators from triggering the lethal action of Bax-Bak.[30] FK506-induced apoptosis was preceded by a rapid decrease of Bcl-2 and Bcl-xL. In such condition, it is feasible that Bim caused loss of mitochondrial membrane potential and apoptosis in CLL because of lack of the neutralizing action of Bcl-2 and BclxL.

FK506 removed FKBP12 from the cytoplasmic tail of the TGF-β receptor. This displacement was apparently sufficient to activate the receptor kinase activity, as suggested by the appearance of posphoSmad in cells depleted of FKBP12. An inhibitory effect of TGFBR1 function was observed in FKBP12-overexpressing cells by Chen and colleagues.[18] The increased expression of FKBP12, that we found in some cases (*data not shown*) may, therefore, be one of the reasons for a lack of or no response to TGF-β. Reduced expression of TGFBR1 has been found by several authors in CLL[8-10] and suggested as a cause of insensitivity to TGF-β. It is feasible that in a condition of low receptor level, even normal levels of FKBP12 may be inhibitory and, possibly, the signal might be enhanced by FK506 also in these cases. Moreover, receptor mutations that affect binding but not the kinase domain might also account for response to FK506 but not TGF-β. The absence of response to both TGF-β and FK506 is in accordance with the findings of recurrent mutations in the signal sequence of TGFBR1, which are responsible for defective kinase activity.[31]

Taken together, these findings suggest that FK506 induced activation of the TGF-β signal transduction pathway. In accordance with several reports suggesting that loss of response to TGF-β might provide a selective advantage to CLL B lymphocytes and contribute to the expansion of neoplastic clone,[8-10] our study showed an association between response to TGF-β and a LDT greater than 12 months, suggesting that the cytokine inhibited tumor cell growth. Therefore, rescue of TGF-β response in CLL by FK506 could represent a breakthrough in the treatment of this common hematologic malignancy.

Previous studies have shown that FK506 can reverse the multidrug resistance phenotype[32] and does not suppress bone marrow activity, whereas it apparently stimulates very early hematopoietic progenitor cells.[33] Consequently, FK506 appears to be a promising agent that deserves future investigation in combined chemotherapy.

Immunosuppressive agents have recently been used in anti-cancer therapy with rapamycin and its analogs.[34] However, our study indicates that the apoptotic effect of FK506 occurs irrespectively of an immunosuppressive mechanism. Consequently, it is feasible that derivatives of FK506 that have the same FKBP12-binding properties as FK506 but lack the calcineurin binding domain, and thus lack functional immunosuppressant activity, could exert the same effect as FK506 in CLL.

In conclusion, our study shows that most CLL cells escape the homeostatic control of TGF-β. This finding is common to many tumors[3-5] in which mutations of components of the TGF-β response pathway hamper restoration of the signal. We demonstrate that FK506 can re-activate the TGF-β signal in CLL, thereby increasing the proportion of responsiveness.

Authorship and Disclosures

SR, MM, RB, AD'A, GC performed the experimental work, acquired, analyzed and interpreted data and critically revised the article giving their final approval; FC provided samples and informed consent, performed the experimental work, acquired, analyzed and interpreted data and critically revised the article giving his final approval; RL provided analytical tools and statistical analysis, performed the experimental work, acquired, analyzed and interpreted data and critically revised the article giving his final approval; MFR designed and performed the experimental work, analyzed and interpreted data and wrote the article, revising it critically for important intellectual content. The authors reported no potential conflicts of interest.

References

1. Dong M, Blobe GC. Role of transforming growth factor-beta in hematologic malignancies. Blood 2006; 107:4589-96.
2. Massagué J. How cells read TGF-beta signals. Nat Rev Mol Cell Biol 2000; 1:169-78.
3. Massagué J, Blain SW. TGFbeta signaling in growth control, cancer, and heritable disorders. Cell 2000;103: 295-309.
4. Pasche B. Role of transforming growth factor beta in cancer. J Cell Physiol 2001;186:153-68.
5. Siegel PM, Massagué J. Cytostatic and apoptotic actions of TGF-beta in homeostasis and cancer. Nat Rev Cancer 2005;3:807-21.
6. Lucas PJ, McNeil N, Hilgenfeld E, Choudhury B, Kim SJ, Eckhaus MA, et al. Transforming growth factor-beta pathway serves as a primary tumor suppressor in CD8+ T cell tumorigenesis. Cancer Res 2004;64: 6524-9.
7. Wolfraim LA, Fernandez TM, Mamura M, Fuller WL, Kumar R, Cole DE, et al. Loss of Smad3 in acute T-cell lymphoblastic leukemia. N Engl J Med 2004;351:552-9.
8. Douglas RS, Capocasale RJ, Lamb RJ, Nowell PC, Moore JS. Chronic lymphocytic leukemia B cells are resistant to the apoptotic effects of transforming growth factor-b. Blood 1997;89:941-7.
9. DeCoteau JF, Knaus PI, Yankelev H, Reis MD, Lowsky R, Lodish HF, et al. Loss of functional cell surface transforming growth factor beta (TGF-beta) type 1 receptor correlates with insensitivity to TGF-beta in chronic lymphocytic leukemia. Proc Natl Acad Sci USA 1997;94:5877-81.
10. Lagneaux L, Delforge A, Bron D, Massy M, Bernier M, Stryckmans P. Heterogenous response of B lymphocytes to transforming growth factor-beta in B-cell chronic lymphocytic leukaemia: correlation with the expression of TGF-b receptors. Br J Haematol 1997;97:612-20.
11. Hamblin TJ, Oscier DG. Chronic lymphocytic leukaemia: the nature of the leukaemic cell. Blood Rev 1997; 11:119-28.
12. Cheifetz S, Weatherbee JA, Tsang ML, Anderson JK, Mole JE, Lucas R, Massagué J. The transforming growth factor-beta system, a complex pattern of cross-reactive ligands and receptors. Cell 1987;48:409-15.
13. Xu L, Chen Y-G, Massagué J. The nuclear import function of Smad2 is masked by SARA and unmasked by TGFbeta-dependent phosphorylation. Nature Cell Biol 2000;2:559-62.
14. Janknecht R, Wells NJ, Hunter T. TGF-beta-stimulated cooperation of

smad proteins with the coactivators CBP/p300. Genes Dev 1998;12: 2114-9.

15. Chaouchi N, Arvanitakis L, Auffredou MT, Blanchard DA, Vazquez A, Sharma S. Characterization of transforming growth factor-beta 1 induced apoptosis in normal human B cells and lymphoma B cell lines. Oncogene 1995;11:1615-22.

16. Jang CW, Chen CH, Chen CC, Chen JY, Su YH, Chen RH. TGF-beta induces apoptosis through Smad-mediated expression of DAP-kinase. Nat Cell Biol 2002;4:51-8.

17. Aghdasi B, Ye K, Resnick A, Huang A, Ha HC, Guo X, et al. FKBP12, the 12-kDa FK506-binding protein, is a physiologic regulator of the cell cycle. Proc Natl Acad Sci USA 2001; 98:2425-30.

18. Chen YG, Liu F, Massague J. Mechanism of TGFbeta receptor inhibition by FKBP12. EMBO J 1997; 16:3866-76.

19. Dornan J, Taylor P, Walkinshaw MD. Structures of immunophilins and their ligand complexes. Curr Top Med Chem 2003;3:1392-409.

20. Wang T, Li BY, Danielson PD, Shah PC, Rockwell S, Lechleider RJ, et al. The immunophilin FKBP12 functions as a common inhibitor of the TGF beta family type I receptors. Cell 1996;86:435-44.

21. Tanaka H, Kuroda A, Marusawa H, Hashimoto M, Hatanaka H, Kino T, et al. Physicochemical properties of FK-506, a novel immunosuppressant isolated from Streptomyces tsukubaensis. Transplant Proc 1987;

19 (5 Suppl 6):11-6.

22. Gobeil F Jr, Dumont I, Marrache AM, Vazquez-Tello A, Bernier SG, Abran D, et al. Regulation of eNOS expression in brain endothelial cells by perinuclear EP(3) receptors. Circ Res 2002;90:682-9.

23. Collins RJ, Verschuer LA, Harmon BV, Prentice RL, Pope JH, Kerr JF. Spontaneous programmed death (apoptosis) of B-chronic lymphocytic leukaemia cells following their culture in vitro. Br J Haematol 1989; 71:343-50.

24. Molica S, Alberti A. Prognostic value of the lymphocyte doubling time in chronic lymphocytic leukemia. Cancer 1987;60:2712-6.

25. Bohnsack MT, Regener K, Schwappach B, Saffrich R, Paraskeva E, Hartmann E, Görlich D. Exp5 exports eEF1A via tRNA from nuclei and synergizes with other transport pathways to confine translation to the cytoplasm. EMBO J 2002;21:6205-15.

26. Ohgushi M, Kuroki S, Fukamachi H, O'Reilly LA, Kuida K, Strasser A, Yonehara S. Transforming growth factor beta-dependent sequential activation of Smad, Bim, and caspase-9 mediates physiological apoptosis in gastric epithelial cells. Mol Cell Biol 2005;25:10017-28.

27. Ramjaun AR, Tomlinson S, Eddaoudi A, Downward J. Upregulation of two BH3-only proteins, Bmf and Bim, during TGFbeta-induced apoptosis. Oncogene 2007;26:970-81.

28. Wildey GM, Patil S, Howe PH.

Smad3 potentiates transforming growth factor beta (TGFbeta)-induced apoptosis and expression of the BH3-only protein Bim in WEHI 231 B lymphocytes. J Biol Chem 2003;278:18069-77.

29. Morales AA, Olsson A, Celsing F, Osterborg A, Jondal M, Osorio LM. Expression and transcriptional regulation of functionally distinct Bmf isoforms in B-chronic lymphocytic leukemia cells. Leukemia 2004;18: 41-7.

30. Kim H, Rafiuddin-Shah M, Tu HC, Jeffers JR, Zambetti GP, Hsieh JJ, Cheng EH. Hierarchical regulation of mitochondrion-dependent apoptosis by BCL-2 subfamilies. Nat Cell Biol 2006;8:1348-58.

31. Schiemann WP, Rotzer D, Pfeifer WM, Levi E, Rai KR, Knaus P, et al. Transforming growth factor-beta (TGF-beta)-resistant B cells from chronic lymphocytic leukemia patients contain recurrent mutations in the signal sequence of the type I TGF-beta receptor. Cancer Detect Prev 2004;28:57-64.

32. Arceci RJ, Stieglitz K, Bierer BE. Immunosuppressants FK506 and rapamycin function as reversal agents of the multidrug resistance phenotype. Blood 1992;80:1528-36.

33. Hirao A, Kawano Y, Takaue Y. Effects of immunosuppressants, FK506, deoxyspergualin, and cyclosporine A on immature human hematopoiesis. Blood 1993;81:1179-83.

34. Dutcher JP. Mammalian target of rapamycin inhibition. Clin Cancer Res 2004;10:6382S-7S.

Role of FK506-binding protein 51 in the control of apoptosis of irradiated melanoma cells

S Romano[1], A D'Angelillo[1], R Pacelli[2], S Staibano[3], E De Luna[1], R Bisogni[1], E-L Eskelinen[4], M Mascolo[3], G Calì[5], C Arra[6] and MF Romano*,[1]

FK506-binding protein 51 (FKBP51) is an immunophilin with isomerase activity, which performs important biological functions in the cell. It has recently been involved in the apoptosis resistance of malignant melanoma. The aim of this study was to investigate the possible role of FKBP51 in the control of response to ionizing radiation (Rx) in malignant melanoma. FKBP51-silenced cells showed reduced clonogenic potential after irradiation compared with non-silenced cells. After Rx, we observed apoptosis in FKBP51-silenced cells and autophagy in non-silenced cells. The FKBP51-controlled radioresistance mechanism involves NF-κB. FKBP51 was required for the activation of Rx-induced NF-κB, which in turn inhibited apoptosis by stimulating X-linked inhibitor of apoptosis protein and promoting authophagy-mediated Bax degradation. Using a tumor–xenograft mouse model, the *in vivo* pretreatment of tumors with FKBP51-siRNA provoked massive apoptosis after irradiation. Immunohistochemical analysis of 10 normal skin samples and 80 malignant cutaneous melanomas showed that FKBP51 is a marker of melanocyte malignancy, correlating with vertical growth phase and lesion thickness. Finally, we provide evidence that FKBP51 targeting radiosensitizes cancer stem/initiating cells. In conclusion, our study identifies a possible molecular target for radiosensitizing therapeutic strategies against malignant melanoma.
Cell Death and Differentiation advance online publication, 21 August 2009; doi:10.1038/cdd.2009.115

Malignant melanoma is an aggressive neoplasm. The prognosis is bad in the advanced stages of the disease because of resistance to conventional anticancer treatments and the high metastatic potential of this tumor. Currently, no efficient therapeutic strategies are available to control the advanced disease.[1] The use of radiotherapy, the most common antitumor treatment, is controversial for advanced melanoma; it serves mainly as a palliative treatment because of the tumor's radioresistance. In an attempt to elucidate the mechanism protecting malignant melanoma against the killing effect of ionizing radiation (Rx), we investigated the cellular response to Rx in different human melanoma cell lines.

The DNA damage response is complex and relies on the simultaneous activation of different networks. The response involves DNA damage recognition, repair, and the induction of signaling cascades leading to cell cycle checkpoint activation and stress-related responses.[2,3] Apoptosis is a common biological mechanism for eliminating damaged cells involving the activation of enzymes known as caspases, and leading to endonuclease-mediated internucleosomal fragmentation of DNA.[4] Type II cell death, induced by stress-inducing agents, is autophagy,[5,6] which is a process of intracellular bulk degradation in which cytoplasmic components, including organelles, are sequestered within double-membrane vesicles that deliver the contents to the lysosome/vacuole for degradation.[7] It is controversial whether this recently discovered process causes death or, instead, protects cells.[8] In fact, the products derived from autophagy are recycled to maintain essential cellular processes. However, there are several lines of evidence that support a role for autophagy in increasing the threshold for apoptosis, thereby sustaining cell survival under conditions of stress.[9]

Recently, our studies implicated the large immunophilin FK506-binding protein 51 (FKBP51) in the control of apoptosis induced in malignant melanoma by DNA-damaging agents, such as anthracyclin compounds.[10] We previously showed that FKBP51 is essential for the NF-κB activation induced by doxorubicin. It is noted that NF-κB controls apoptosis at the genetic level and has been implicated in the radioresistance of melanoma.[11,12] It is widely known that the NF-κB transcription complex belongs to the Rel family, which comprises five mammalian Rel/NF-κB proteins: RelA (p65), c-Rel, RelB, NF-κB1 (p50/p105), and NF-κB2 (p52/100).[13] The activity of NF-κB is controlled by cytoplasmic shuttling to

[1]Department of Biochemistry and Medical Biotechnology, Federico II University of Naples, Naples, Italy; [2]Institute of Biostructure and Bio-Imaging, National Research Council (CNR), Naples, Italy; [3]Department of Biomorfological and Functional Sciences, Pathology Section, Federico II University of Naples, Naples, Italy; [4]Division of Biochemistry, Department of Biological and Environmental Sciences, University of Helsinki, Helsinki, Finland; [5]Institute of Endocrinology and Experimental Oncology, Italian National Research Council (CNR), Naples, Italy and [6]Italian National Cancer Institute, G. Pascale Foundation, Naples, Italy
*Corresponding author: MF Romano, Department of Biochemistry and Medical Biotechnologies, Federico II University, via Pansini, 5, 80131, Naples, Italy.
Tel: + 39 081 746 3125; Fax: + 39 081 746 3205; E-mail: romano@dbbm.unina.it

the nucleus in response to cell stimulation. The NF-κB dimers containing RelA or c-Rel are retained in the cytoplasm through interaction with inhibitors (IκBs).[14] In response to a variety of stimuli, IκBs are phosphorylated by the activated IκB kinase (IKK) complex, ubiquitinated, and degraded by the 26S proteosome.[13,14] This process allows NF-κB dimers to translocate to the nucleus, where they stimulate the expression of multiple target genes.[13–15]

In this study, we attempted to investigate the role of FKBP51 in the activation of NF-κB by Rx and in the protection of tumor cells against Rx-induced killing, using different cell lines. Though we detected very low levels of apoptosis, we observed cellular events consistent with autophagy after cell irradiation. By downmodulating the FKBP51 level, we obtained the induction of massive apoptosis after irradiation, both *in vitro* and *in vivo*. We investigated the mechanism of apoptosis regulation and found that FKBP51 controlled radioresistance through the activation of NF-κB. These results suggest that FKBP51 is a promising candidate target for radiosensitizing strategies against malignant melanoma. The translational implication of our findings is reinforced by the clinical evidence of clear immunoreactivity for FKBP51 in all skin samples of cutaneous malignant melanomas (CMMs) from 80 patients. Finally, our study provided evidence that silencing FKBP51 also radiosensitized cancer cells bearing stem markers, which is considered predictive of tumor radiocurability.[16]

Results

FKBP51 downmodulation sensitizes melanoma cells to Rx-induced apoptosis. To investigate the role of FKBP51 in the cellular response to Rx, melanoma cells were transfected with a short interfering (si) RNA previously shown to efficiently downmodulate the protein.[10] Figure 1 shows representative results of the effect of FKBP51 gene silencing in the SAN melanoma cell line. The downmodulating effect of FKBP51 siRNA was specific because it could not be reproduced by a siRNA for FKBP12[17] (Figure 1a). A clonogenic assay was performed using cells transfected with FKBP51 siRNA, non-silencing (NS) RNA, or nothing. Knocking down FKBP51 in melanoma cells produced a sensitizer enhancement ratio[18] of 1.5 (7.2 Gy/ 4.8 Gy). This ratio was calculated on the basis of the radiation dose necessary to obtain the end point of a 90% inhibition of colony formation. As shown in Figure 1b, the line corresponding to 10% survival intercepts the dose response curve of control cells (not transfected or transfected with NS RNA) at 7.2 Gy, whereas that of FKBP51-depleted cells occurred at 4.8 Gy. This result suggests that decreased levels of FKBP51 remarkably increase the cytotoxic effect of radiation in melanoma cells. To investigate the cellular response to Rx in cells depleted of FKBP51, the light chain 3 (LC3)-I to LC3-II conversion and levels of cleaved caspase-3, hallmarks of autophagy[19] and apoptosis,[4] respectively, were investigated by western blot. Whole cell lysates were prepared from cells transfected with the specific siRNA or NS RNA. At 48 h after transfection, cells were exposed to 4 Gy dose Rx and harvested at 0, 2, 4, 6, and 9 h. Figure 1c

shows that the presence of the autophagosome membrane recruited the LC3-II isoform in non-irradiated cells, both transfected and not transfected with FKBP51 siRNA, which is consistent with a basal level of autophagy. The isoform disappeared 6 h after Rx exposure in FKBP51-depleted cells but not in NS RNA-transfected cells. An increase in Beclin-1 (Becn-1) levels was detected in non-silenced cells after 4 h, suggesting that this increase had a role in sustaining the LC3-I to LC3-II conversion. In contrast, the appearance of the active fragment of the execution caspases-3 and -7[20] in FKBP51-depleted cells, as early as 4 h after Rx exposure, suggests the activation of apoptosis. Interestingly, Bax levels decreased in irradiated non-silenced cells, concomitant to increase of Becn-1 levels and LC3-I to LC3-II conversion. Autophagy was confirmed by transmission electron microscopy; a quantitation analysis of autophagic profiles/cell area showed a clear increase in autophagosomes 6 h after Rx exposure (Figure 1d). Apoptosis was confirmed by flow cytometry. Figure 1e shows the flow cytometric histograms of caspase-9 and -3 activation, annexin V binding, and propidium iodide incorporation in irradiated cells. A measure of cell death by annexin V binding in 15 independent experiments clearly showed that Rx induced a remarkable increase in the cell death of FKBP51-depleted cells (48.7 $\pm$ 11.8) compared with that of non-silenced cells (26.7 $\pm$ 8.1) ($P = 0.000$). The mean values of cell death for non-irradiated, non-silenced or silenced cells were 18.0 $\pm$ 4.4 and 27.9 $\pm$ 8.5, respectively ($P = 0.022$). This finding suggests that knocking down FKBP51 reduces the threshold for cell death. The induction of apoptosis in FKBP51-depleted cells was confirmed using the pan-caspase inhibitor z-Valine–Alanine–Aspartic Acid (zVAD), which clearly inhibited Rx-induced cell death (Figure 1f). The sensitizing effect of FKBP51 siRNA on Rx-induced apoptosis was observed also in G361, A375, and SK-MEL-3 melanoma cell lines (not shown).

FKBP51 downmodulation prevents the Rx-induced activation of NF-κB. Rx induces NF-κB activation.[21] We found that the kinetics of IκB degradation showed a decrease in IκBα levels and the complete disappearance of IκBβ as early as 4 h after irradiation, with a return to the basal level after 20 h (Figure 2a). The activation of NF-κB was confirmed by electrophoretic gel mobility shift assay (EMSA) (Figure 2b). According to our earlier findings, the treatment of cells with FKBP51 siRNA prevents both IκB degradation and the nuclear translocation of the transcription factor. In line with NF-κB activation, an increase in the level of the caspase inhibitor X-linked inhibitor of apoptosis protein (xIAP) was observed. As expected, such an increase was not observed in FKBP51-silenced cells (Figure 2c). Consistent with the notion that *xIAP* transcription is under NF-κB control,[15] reduced levels of *XIAP* mRNA, both basal and Rx-induced, were found in p65-silenced cells compared with those in non-silenced cells (Figure 2d). The upregulation of xIAP had a role in the inhibition of irradiated melanoma cell apoptosis. In fact, when xIAP expression was silenced with siRNA, the Rx stimulated caspase activation and cell death (Figure 2e). Taken together, these findings suggest that FKBP51-silenced cells fail to activate NF-κB-controlled anti-apoptotic genes when irradiated.
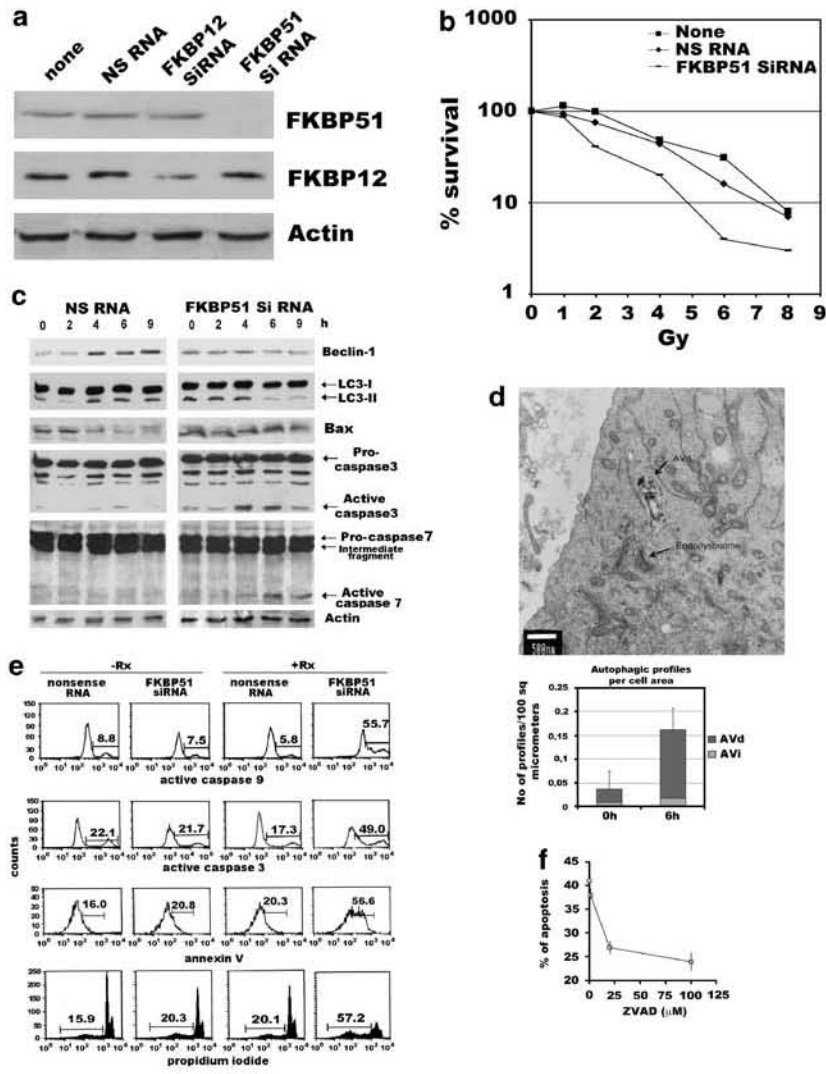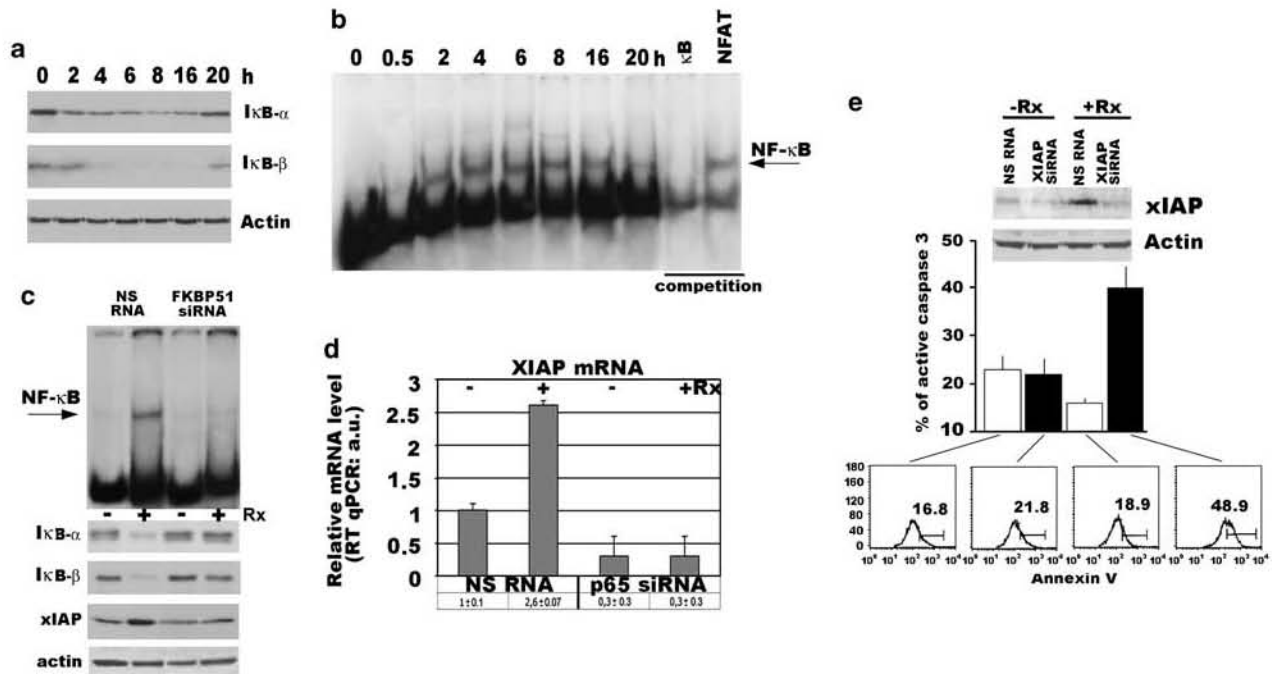
Figure 1 Activation of apoptosis in irradiated melanoma cells depleted of FKBP51. (**a**) Western blot assay of FKBP51 in cell lysates obtained from the melanoma cell line SAN transfected with FKBP51 siRNA, FKBP12 siRNA, or a non-silencing (NS) oligoribonucleotide as control. (**b**) Clonogenic assay of irradiated cells transfected with FKBP51 siRNA, NS RNA, or not transfected. Cells were irradiated with the indicated doses of ionizing radiation (Rx), harvested, and plated in triplicate. After 10 days, the colonies were stained with crystal violet and counted. (**c**) Western blot assay of Becn-1, LC3-II, Bax, caspase-3 and -7 in cell lysates prepared from melanoma cells transfected with FKBP51 siRNA or NS RNA. Cells were irradiated with 4 Gy Rx and harvested at the indicated times. (**d**) Transmission electron microscopy image of an irradiated melanoma cell, 6 h after exposure at a 4 Gy dose. Scale bar, 500 nm. Graphic representation of autophagic profiles/cell area in non-irradiated (0 h) and irradiated (6 h) cells. AVd, degradative autophagic compartment; AVi, initial autophagosome. (**e**) Flow cytometric histograms of active caspases-9 and -3, annexin V binding, and the propidium iodide incorporation of SAN melanoma cells transfected with NS RNA or FKBP51 siRNA. Cells were irradiated with 4 Gy Rx and harvested after 6, 48, and 72 h to measure caspase activity, annexin V binding, and propidium iodide incorporation, respectively. (**f**) Graphic representation of the apoptosis of melanoma cells transfected with FKBP51 siRNA. At 48 h after transfection, cells were incubated with the indicated doses of zVAD and irradiated with 4 Gy Rx. After another 48 h, cells were harvested and apoptosis was determined by annexin V staining

Rx-induced NF-κB sustains autophagy. To investigate whether the enhanced levels of Becn-1 were because of NF-κB activation, we attempted to downmodulate the p65 subunit of NF-κB. A supershift assay provided evidence that p65 represents the main component of the NF-κB complex activated by Rx in our cell system. As shown in Figure 3a, the Rx-induced NF-κB band was supershifted by anti-p50 and anti-p65 antibodies. Melanoma cells transfected with p65 siRNA or a NS RNA control were irradiated and, after 6 h, total cell lysates were prepared. A western blot assay showed that p65 siRNA, but not NS RNA,

downmodulated the protein (Figure 3b). Radiation treatment enhanced the levels of Becn-1 in non-silenced cells, but this was not observed in cells depleted of p65 (Figure 3b). An increase in the levels of the LC3-II isoform was found in irradiated cells but not when p65 was downmodulated (Figure 3b). The Rx-induced increase in Becn-1 protein was associated to increase in *BECN*-1 mRNA levels (Figure 3c). Such increase was not observed in p65-silenced cells (Figure 3c). This result suggests that p65 was essential for Becn-1 expression. Our finding is in accordance with the very recent demonstration that p65

Figure 2 Lack of NF-κB activation and xIAP induction in melanoma cells depleted of FKBP51. (a) Western blot assay of IκBα and IκBβ levels in cytoplasmic extracts prepared from irradiated SAN melanoma cells harvested at the indicated times. (b) An electrophoretic mobility shift assay (EMSA) using nuclear extracts prepared from irradiated melanoma cells harvested at the indicated times. The last two lanes show a competition assay performed with the same κB cold oligonucleotide or an unrelated cold oligonucleotide (NFAT) that was added to the incubation mixture. (c) EMSA using nuclear extracts and western blot assay of whole cell lysates obtained from melanoma cells transfected with non-silencing (NS) RNA or FKBP51 siRNA. At 48 h after transfection, cells were irradiated with 4 Gy ionizing radiation (Rx) and, after an additional 6-h incubation, harvested for the preparation of both nuclear extracts and whole cell lysates. (d) Normalized expression rates of *XIAP* mRNA (a.u., arbitrary units) in melanoma cells SAN, which were transfected with p65 siRNA or a non-silencing RNA, and irradiated or not with a 4 Gy dose. Vertical bars indicate standard deviations. Values were obtained from three independent experiments. (e) Effect of xIAP downmodulation on Rx-induced apoptosis. Western blot assay of xIAP levels in melanoma cells transfected with NS RNA or xIAP siRNA. At 48 h after transfection, cells were irradiated with 4 Gy Rx. Cells were harvested after 6 h for whole cell lysate preparation. At the same time, a flow cytometric analysis of caspase-3 activation was performed. The graph represents the mean values and standard deviations of active caspase-3 from three different experiments, each performed in triplicate. Apoptosis was measured 48 h after irradiation by annexin V binding. A representative result of three independent experiments, performed in triplicate, is shown

exerts transcriptional control on *BECN*-1 gene expression.[22] To investigate whether Becn-1, an important component of the autophagic machinery,[7–9] has a role in the apoptosis inhibition of irradiated cells, we used specific siRNA to downmodulate Becn-1. A western blot assay of whole cell extracts prepared from cells 6 h after irradiation showed an increase in the level of LC3-II isoform in cells transfected with NS RNA but not those depleted of Becn-1 by specific siRNA (Figure 3d). This finding is in accordance with the concept that Becn-1 is essential for the activation of autophagy.[7–9] An analysis of cell death after an additional 40-h incubation showed that the percentage of annexin V-positive cells clearly increased in Becn-1-depleted cells (Figure 3d). This finding was confirmed in two other independent experiments. To investigate the mechanism by which Becn-1 inhibits apoptosis, we investigated the levels of Bax, which is an important component of the permeability transition pore in mitochondrion-dependent apoptosis.[23] Western blot showed reduced Bax levels in irradiated melanoma cells, which is consistent with its degradation. In Becn-1-silenced cells, Bax levels were higher compared with those in non-silenced cells after irradiation (Figure 3e). Bax localization was investigated by confocal microscopy, in double fluorescence with LC3.

Bax was mostly localized in the nucleus, in basal conditions, and to some extent in the cytosol. After irradiation, nuclear Bax apparently translocated to the cytosol. The presence of colocalization areas in LC3 aggregates (see enlarged detail) suggests a possible inclusion of Bax in autophagic vacuoles (Figure 4a). A semi-quantitative western blot analysis of Bax levels in cells irradiated in the absence or presence of inhibitors of lysosomal proteolysis showed a decrease in Bax levels in irradiated cells, but not when inhibitors of lysosomal proteases were added to the cell culture (Figure 4b). This finding supports the hypothesis of an Rx-induced autophagic degradation of Bax.

Taken together, these findings suggest that Becn-1 expression is controlled by NF-κB, and that autophagy may be an additional mechanism through which such transcriptional activity represses apoptosis.

FKBP51 is expressed in malignant melanoma-initiating cells. Normal stem cells have a high drug efflux capability because of the expression levels of ATP-binding cassette (ABC) transporters, which actively pump drugs out of the cell. The ABC, subfamily G, member 2 (ABCG2) is a member of this superfamily of ABC transporter proteins, and it is known
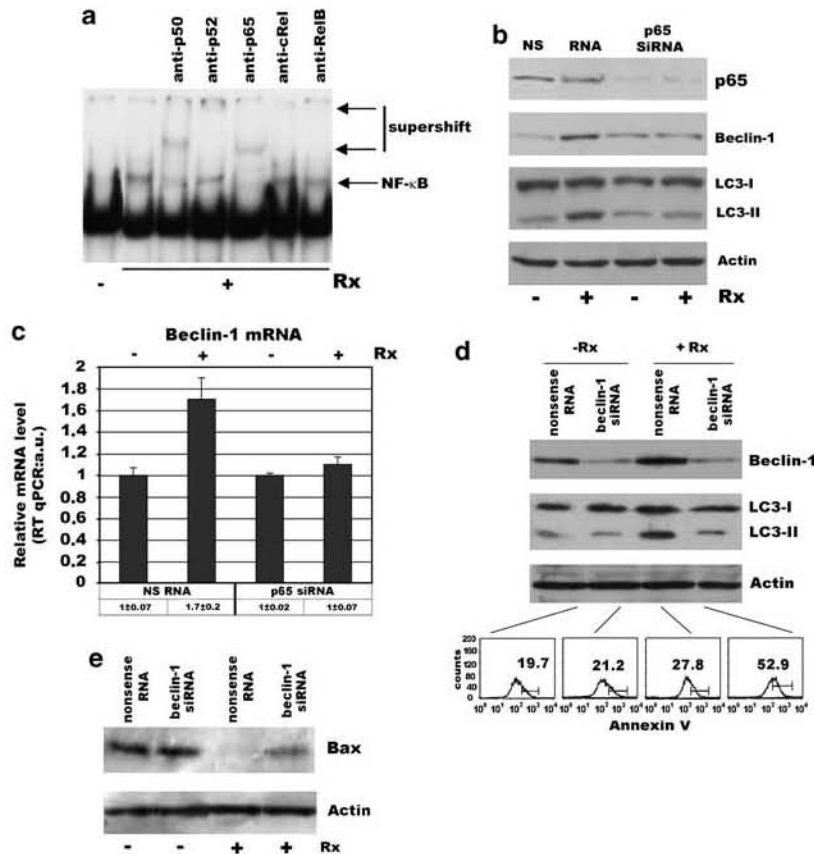
Figure 3 NF-κB promotes cell survival by enhancing the expression of the autophagic protein beclin-1. (**a**) Supershift assay of a nuclear extract prepared from SAN melanoma cells 6 h after a 4 Gy dose of ionizing radiation (Rx). The extract was incubated with [γ-^{32}P] ATP end-labeled NF-κB consensus oligonucleotide in the absence or presence of the indicated antibodies against NF-κB and run in a 6% acrylamide gel electrophoresis. (**b**) Western blot assay of p65, Becn-1, and LC3-II levels in melanoma cells transfected with non-silencing (NS) RNA or p65 siRNA. At 48 h after transfection, cells were irradiated with 4 Gy Rx. Cells were harvested after 6 h for whole cell lysate preparation. (**c**) Normalized expression rates of *BECN*-1 mRNA (a.u., arbitrary units) in melanoma cells SAN, which were transfected with p65 siRNA or a non-silencing RNA, and irradiated or not with a 4 Gy dose. Vertical bars indicate standard deviations. Values were obtained from three independent experiments. (**d**) The effect of Becn-1 depletion on Rx-induced apoptosis. A representative western blot of Becn-1 levels in melanoma cells transfected with NS RNA or Becn-1 siRNA is shown. At 48 h after transfection, cells were irradiated with 4 Gy Rx. A portion of cells was harvested after 6 h for whole cell lysate preparation. After an additional 42 h, the remaining cells were harvested and apoptosis was measured by annexin V binding. A representative result of three independent experiments, each performed in triplicate, is shown. (**e**) The effect of Rx on Bax levels in Becn-1-depleted cells. A representative western blot of Bax levels in melanoma cells transfected with NS RNA or Becn-1 siRNA is shown. At 48 h after transfection, cells were irradiated with 4 Gy Rx. Cells were harvested after 4 h for whole cell lysate preparation

to be not only a member of the membrane transporters implicated in multidrug resistance but also a molecular determinant of cancer stem/initiating cells,[24] including melanoma.[25] To find whether FKBP51 targeting can overcome radioresistance in such cells with enhanced tumorigenic potential, we investigated whether they expressed this immunophilin. The FKBP51 expression was determined by flow cytometry and immunohistochemistry. After the acquisition of 1×10^6 cells with a flow cytometer, a gate was placed for ABCG2$^+$ cells (0.5% of total cells), according to ABCG2-PE/SSc parameters (Figure 5a). The expression of FKBP51 in gated cells was then analyzed in the FL-1 channel. The percentage of FKBP51$^+$ events was comparable in ABCG2$^+$ and ABCG2$^-$ cells, whereas the mean fluorescence intensity (MFI) was clearly higher in ABCG2$^+$ cells compared with that in ABCG2$^-$ cells, suggesting an increased production of FKBP51 in cells with enhanced tumorigenic potential. These data were confirmed in two

other different experiments. The expression of FKBP51 in ABCG2$^+$ cells was confirmed by immunohistochemistry of cells sorted with the BD FACSAria cell sorting system (BD Biosciences, San Jose, CA USA)(Figure 5b). We then investigated the effect of Rx on the apoptosis of ABCG2$^+$ cells. At 48 h after irradiation, melanoma cells transfected with NS RNA or FKBP51 RNA were harvested and stained with ABCG2-PE and annexin V-FITC. The percentage of annexin V-positive events in ABCG2 gated cells clearly indicated a radiosensitizing effect of FKBP51 siRNA on these cells. These data were confirmed in two other independent experiments.

Pretreatment with FKBP51-siRNA promotes apoptosis in irradiated tumor xenografts. We confirmed that the down-modulation of FKBP51 radiosensitized melanoma *in vivo*. To investigate apoptosis in tumor xenografts, the activation of caspase-3 was determined by the immunohistochemistry of
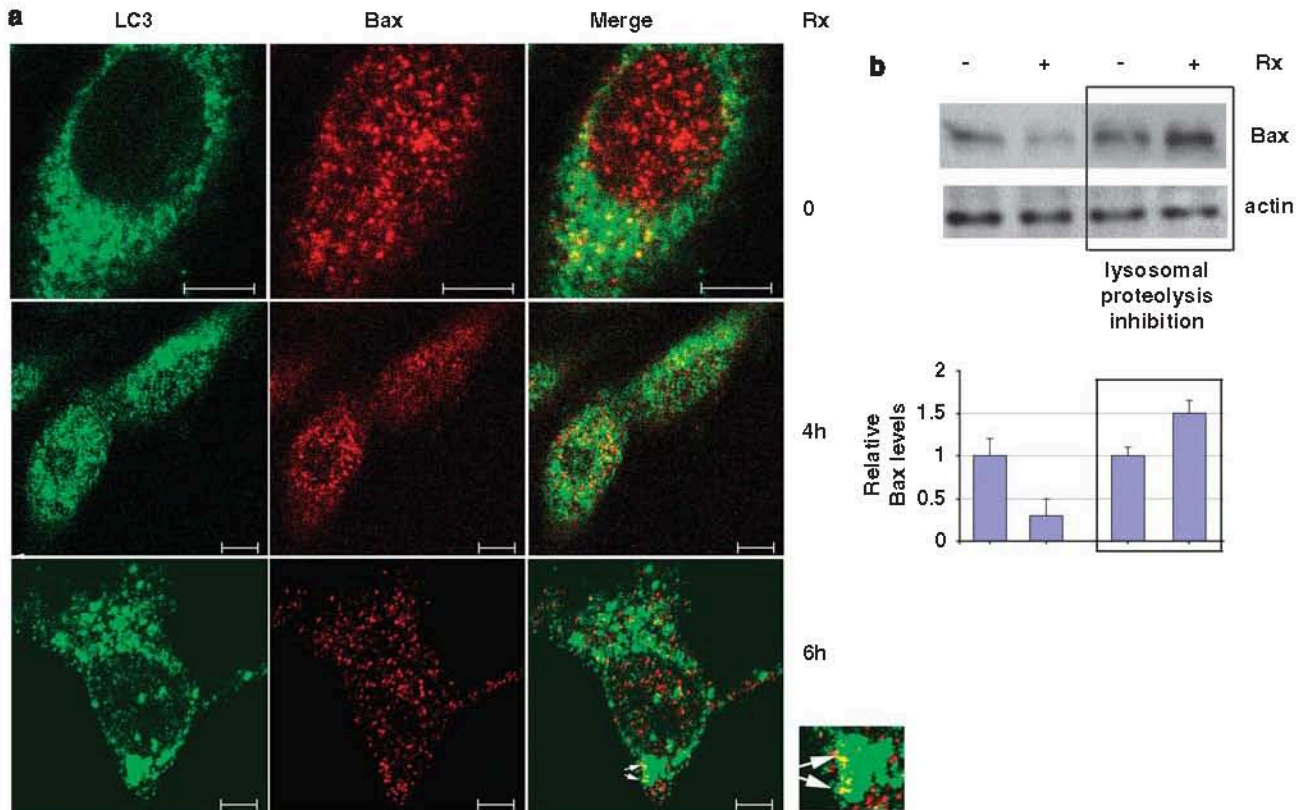
Figure 4 Rx induces Bax delocalization and degradation. (a) Confocal images of cells fixed after 0, 4 h, and 6 h from irradiation with 4 Gy and stained with anti-Bax (red fluorescence) and anti-LC3 (green fluorescence). Enlarged detail of colocalization areas. Bar 5 μm. The data were confirmed in two further experiments. (b) Western blot of Bax levels in melanoma cells irradiated for 6 h with 4 Gy, in the absence or presence of 0.25 mM leupeptin + 10 μg/ml pepstatin. Protease inhibitors were added to the culture medium 1 h before cell harvest. Bax expression levels were quantified by densitometry using NIH Image 1.61 for Macintosh. Integrated optical densities, normalized to actin, were expressed *versus* baseline level[1]

tumor sections and western blot of tumor lysates. Strong immunoreactivity for cleaved caspase-3 was found in the tumor tissues from xenografts pretreated with FKBP51 siRNA before irradiation. The apoptosis was more notable in tumors excised 48 h after irradiation compared with those excised after 24 h (not shown). Only a few apoptotic cells were detected in both non-irradiated (Figure 6a) and irradiated (Figure 6b) non-silenced tumors in which most of the melanocytes were viable and considerable mitotic activity was present. Few melanocytes showing the morphological signs of apoptosis and caspase-3 immunoreactivity were found in non-irradiated silenced tumors (Figure 6c). In contrast, a prevalence of apoptotic melanocytes with clear caspase-3 immunopositivity was present in irradiated silenced tumors (Figure 6d). Western blot confirmed the prominent activation of caspase-3 in tumors pretreated with FKBP51 siRNA.

FKBP51 is a marker of malignant melanocytes. Specimens of cutaneous melanoma from 80 patients and 10 samples of normal skin stored in the archive of the Pathology section (Department of Biomorphological and Functional Sciences, University Federico II of Naples, Italy) were examined for FKBP51 expression. In normal skin, no immunopositive

melanocytes were found. Table 1 presents the patient profiles relative to the cases studied. In most patients (58/80, 72%), a low (+) immunopositivity was found in melanocytes during the radial growth phase. Melanocytes in the vertical growth phase displayed a stronger immunopositivity (+ +) compared with radial melanocytes ($P<0.001$, Pearson $\chi^2 = 62.082$). A significant correlation was found between FKBP51 expression and the thickness of the tumor lesion (Spearman's $\rho = 0.646$, $P<0.001$). Moreover, metastatic melanoma was associated with the highest immunoreactivity (+ + +) (Spearman's $\rho = 0.538$, $P<0.001$). Figure 7 shows representative immunohistochemical stains for FKBP51 in skin specimens from patients with primitive and metastatic lesions. A definite brown cytoplasmic immunostaining for FKBP51 is visible in tumor, but not normal, melanocytes. The immunoreactivity of the metastatic cutaneous lesion was impressive. In conclusion, our findings unequivocally show that FKBP51 is overexpressed in melanoma lesions of all the patients studied and that FKBP51 expression correlates with malignity of the lesions.

Discussion

Among cancers, malignant melanoma is one of the most resistant to treatment.[1] Approximately 80% of melanomas are diagnosed at a localized stage, and the 5-year survival rate
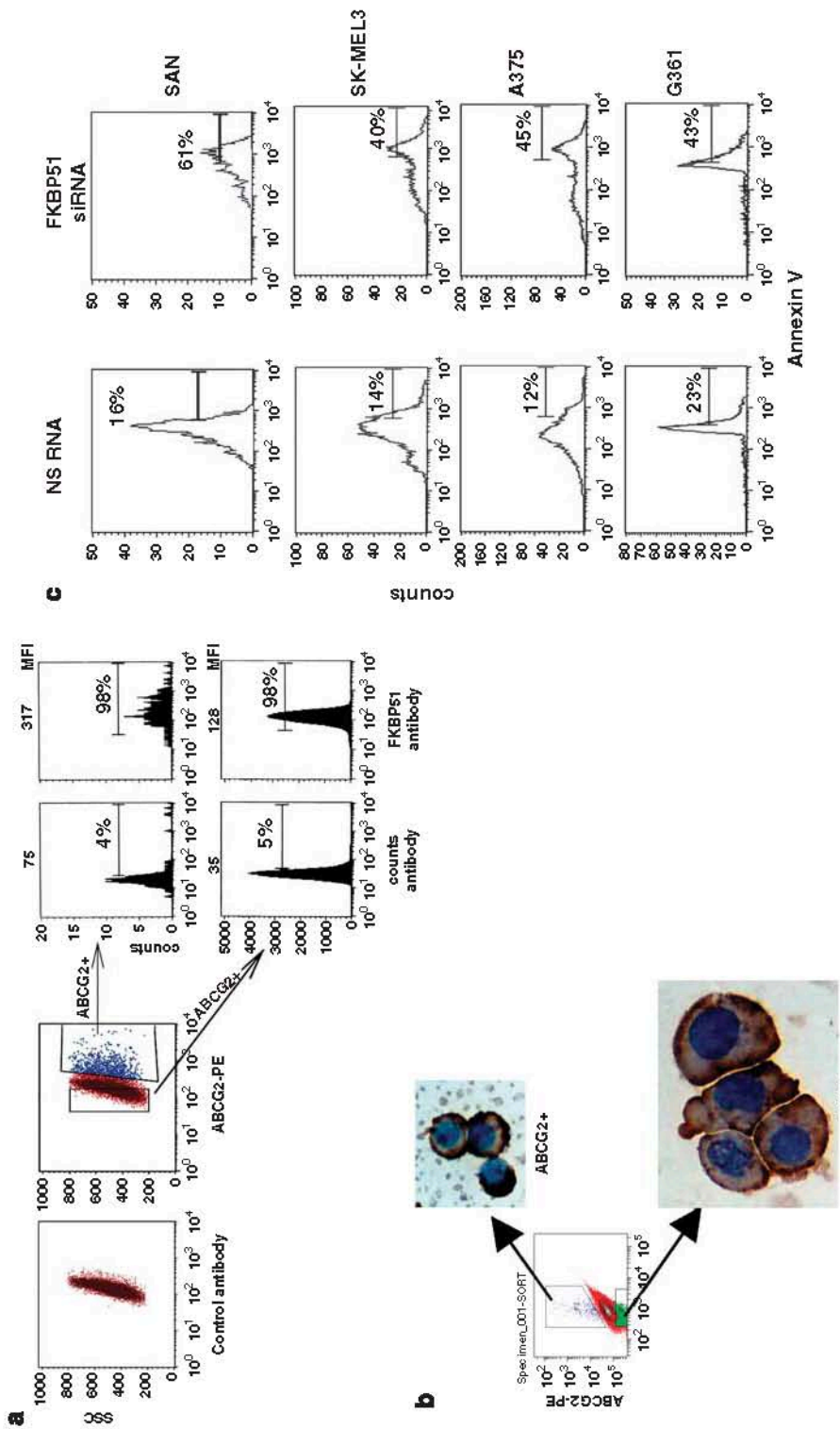
Figure 5 FKBP51 is expressed in ABCG2 + cells. (**a**) Flow cytometric histograms of the ABCG2 gating strategy and FKBP51 expression in SAN melanoma cells. Cells were stained with PE-conjugated isotype control antibody or mouse monoclonal ABCG2-PE. The cells were then fixed, permeabilized, and incubated with or without rabbit anti-FKBP51. After a second staining with anti-rabbit FITC, cells were analyzed by flow cytometry. ABCG2 marked a subpopulation of melanoma cells. According to ABCG2/SSc parameters, two gates were placed, one for ABCG2⁻ cells (red) and another for ABCG2 + cells (blue). The expression of FKBP51 was measured in the gated populations in the FL1-channel. Bars indicate the percentage of FL1-positive events, and the values of mean fluorescence intensity (MFI) are also indicated. (**b**) Detection of FKBP51 by immunohistochemistry. SAN melanoma cells expressing ABCG2 were separated from the whole population by BD FACSaria cell sorting, fixed, and subjected to the immunohistochemical examination of FKBP51. (**c**) Effect of FKBP51 depletion on the ionizing radiation (Rx)-induced apoptosis of ABCG2 + melanoma cells. Flow cytometric histograms of the annexin V binding of ABCG2 + melanoma cells gated as in **a**. Melanoma cells from SAN, SK-MEL3, A375, and G361 cell lines were transfected with non-silencing (NS) RNA or FKBP51 siRNA and irradiated with 4 Gy Rx. After 48 h, cells were harvested and stained with ABCG2-PE and annexin V-FITC to measure apoptosis
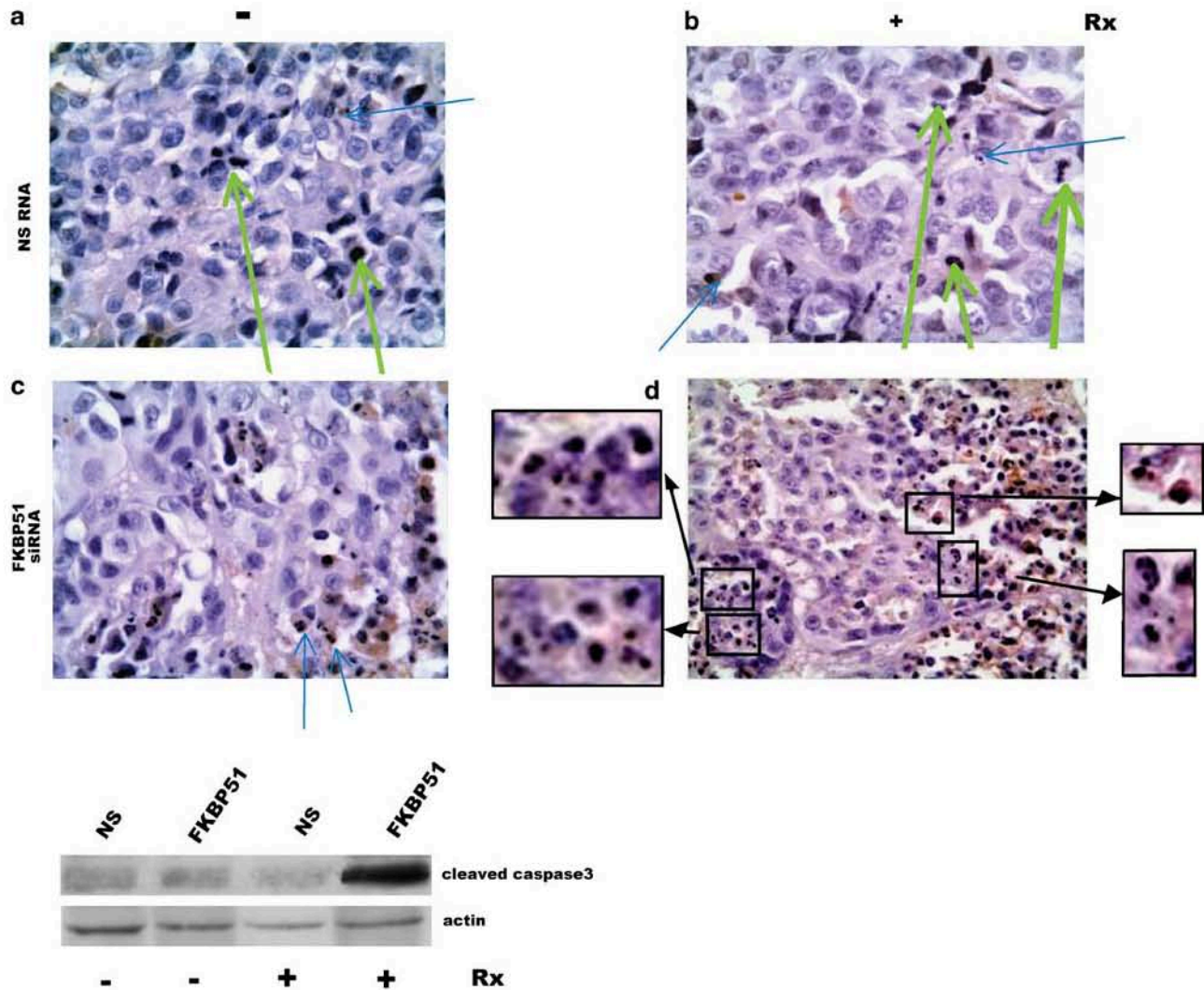
Figure 6 Ionizing radiation (Rx)-induced apoptosis in tumor xenografts pretreated with FKBP51 siRNA. Immunohistochemistry and western blot assay of cleaved caspase-3 in tumor sections. Tumors were excised 48 h after irradiation. For immunohistochemistry, the avidin–biotin complex technique was used. Original magnification, × 250 (**a, b, c**); × 150 (**d**). The morphology of apoptotic nuclei was indicated by blue arrows; green arrows indicate mitosis. Enlarged details of apoptotic nuclei from panel **d**. Whole tissue lysates prepared from the same tumors were run in SDS-PAGE for the western blot assay

associated with this form of the disease is roughly 99%. In contrast, the 5-year survival rates for regional and distant stages of the disease are much lower (65 and 15%, respectively).[1] Patients diagnosed with advanced stage melanoma have a very poor prognosis and relatively few treatment options. These patients continue to pose a significant challenge for clinicians. Although many therapeutic regimens for metastatic melanoma have been tested, very few achieve response rates > 25%.[26] Given the rising incidence of melanoma and the paucity of effective treatments, there is much hope for targeted therapies and promising agents, including those that act on apoptosis-regulating molecules.[11,27] Herein, we showed a novel role for FKBP51 as a marker of melanocyte malignancy and involvement in the protection of melanoma against Rx-induced apoptosis. FKBP51 is a large immunophilin that exerts important biological functions in the cell, among which is the regulation of the steroid hormone response as a component of

the steroid hormone receptor complex[28] and the control of NF-κB activation as a cofactor of the IKKα subunit in the IKK complex.[29] Our data showed that FKBP51 has a relevant role in counteracting apoptotic processes stimulated by Rx. Cellular events were consistent with autophagy, such as an increase in Becn-1 levels and the autophagosome membrane-associated LC3-II isoform, but very few with cell death were observed in irradiated melanoma cells, suggesting that autophagy supports the survival of the tumor cells. Transmission electron microscopy showed an increased number of autophagic vacuoles in irradiated cells. In contrast, typical biochemical markers of apoptosis, such as cleaved caspase-9 and -3, phosphatidylserine externalization on the plasma membrane, and hypodiploid DNA in melanoma cell nuclei, were observed in irradiated melanoma cells pretreated with FKBP51 siRNA. In accordance with our earlier findings,[10] FKBP51 was required for NF-κB activation; in fact, FKBP51 silencing prevented the Rx-induced nuclear translocation of

Table 1 FKBP51 expression in cutaneous malignant melanoma (CMM) and patients' profiles

Case	Age (years)	Sex	Breslow	FKBP51r	FKBP51v	Follow-up (years)
1	58	F	≤1.00	+	+	12
2	36	M	≤1.00	+	+	12
3	67	M	≤1.00	+	+	12
4	45	F	≤1.00	+	+	12
5	50	F	≤1.00	++	++	11
6	49	F	≤1.00	+	+	11
7	42	M	≤1.00	+	+	10
8	43	F	≤1.00	+	+	9
9	43	M	≤1.00	+	++	9
10	49	M	≤1.00	+	+	7
11	40	M	≤1.00	++	++	7
12	41	M	≤1.00	+	+	7
13	39	M	≤1.00	+	++	6R
14	37	F	≤1.00	+	+	6
15	66	F	1.01–2.00	++	++	12N
16	65	F	1.01–2.00	+	++	12
17	56	M	1.01–2.00	+	++	12
18	49	M	1.01–2.00	+	++	12
19	48	M	1.01–2.00	+	++	12
20	39	F	1.01–2.00	+	++	12
21	47	F	1.01–2.00	++	+++	12N,M,D
22	51	M	1.01–2.00	+	++	11
23	53	M	1.01–2.00	+	++	11
24	56	M	1.01–2.00	+	++	11
25	51	F	1.01–2.00	++	++	10
26	45	F	1.01–2.00	+	++	10
27	53	M	1.01–2.00	+	++	10
28	67	M	1.01–2.00	+	++	10
29	54	M	1.01–2.00	+	++	10
30	34	M	1.01–2.00	+	++	9
31	44	F	1.01–2.00	+	++	9
32	43	F	1.01–2.00	+	++	9
33	71	F	1.01–2.00	++	+++	9
34	34	M	1.01–2.00	++	++	9
35	43	F	1.01–2.00	+	++	9
36	51	F	1.01–2.00	+	++	9
37	50	M	1.01–2.00	+	++	9
38	39	F	1.01–2.00	+	++	9N
39	29	F	1.01–2.00	+	++	9
40	42	M	1.01–2.00	+	++	7
41	37	F	1.01–2.00	++	++	7R,N
42	65	M	1.01–2.00	+	++	7
43	43	M	1.01–2.00	++	++	7N
44	44	F	1.01–2.00	+	++	6
45	18	F	1.01–2.00	+	++	4
46	22	M	1.01–2.00	+	++	4
47	24	M	1.01–2.00	+	++	4
48	32	M	1.01–2.00	++	++	4
49	30	F	1.01–2.00	+	++	4
50	38	F	1.01–2.00	+	++	4
51	37	M	1.01–2.00	+	++	3
52	40	M	1.01–2.00	+	++	3
53	40	M	2.01–4.00	++	+++	12
54	36	M	2.01–4.00	+	++	12
55	39	M	2.01–4.00	+	++	11
56	50	F	2.01–4.00	+	+++	11
57	48	F	2.01–4.00	++	++	11
58	45	M	2.01–4.00	++	+++	11N,M,D
59	43	F	2.01–4.00	+	++	10
60	53	F	2.01–4.00	+	++	10
61	47	M	2.01–4.00	++	+++	10N
62	54	M	2.01–4.00	++	+++	10
63	50	M	2.01–4.00	+	++	10
64	69	F	2.01–4.00	+	++	10
65	54	M	2.01–4.00	+	++	10
66	53	M	2.01–4.00	+	++	9
67	42	F	2.01–4.00	++	+++	9N,M,D
68	37	F	2.01–4.00	++	++	9N,M
69	45	F	2.01–4.00	+	++	9
70	49	F	2.01–4.00	++	+++	9N,M,D

Table 1 (Continued)

Case	Age (years)	Sex	Breslow	FKBP51r	FKBP51v	Follow-up (years)
71	32	M	2.01–4.00	+	++	7N
72	38	F	2.01–4.00	+	++	6N
73	38	M	2.01–4.00	+	++	3
74	32	M	2.01–4.00	++	+++	3N,M
75	40	M	2.01–4.00	++	+++	3
76	46	F	2.01–4.00	++	+++	3N
77	50	M	2.01–4.00	+	++	2
78	24	F	2.01–4.00	+	++	2
79	30	M	2.01–4.00	++	++	2
80	32	F	2.01–4.00	+	++	2

Abbreviations: D, tumor death; FKBP51r, FKBP51 radial growth; FKBP51v, FKBP51 vertical growth; M, metastasis; N, lymph node; R, recidivation.

this transcription factor. Among the apoptosis-regulating proteins under NF-κB control, the IAP family of proteins has been widely involved in the resistance of human cancers to apoptosis induced by both radiotherapy and chemotherapy.[30] Our data confirmed the important role for xIAP in melanoma radioresistance. A clear enhancement in the expression of xIAP was found after Rx exposure. By using siRNA specific for xIAP silencing, we found caspase-3 activation and cell death after irradiation. Apparently, xIAP was not the only factor contributing to the resistance to apoptosis. Becn-1-silenced cells were also found to be sensitive to Rx. As expected, any increase in the autophagosome-recruited LC3-II isoform was not observed, suggesting the inhibition of autophagy. Reduced Bax levels in irradiated non-silenced cells but not in Becn-1-silenced cells suggest a role for autophagy in Bax degradation. It is noted that Bax is an important mediator of mitochondrion-dependent apoptosis; therefore, its reduced level may represent an additional mechanism for cell death inhibition.[23] Using siRNA to silence the p65 subunit of the NF-κB transcription complex, we showed that Becn-1 induction also depended on NF-κB. Taken together, these findings suggest that the activation of NF-κB in irradiated melanoma inhibits apoptosis by upregulating the caspase inhibitor xIAP and autophagic protein Becn-1. A scheme of the proposed mechanism is illustrated in Figure 8. This study identifies a protein that acts upstream of NF-κB, and whose knocking down efficiently overcomes the apoptotic machinery block provoked by this transcription factor, thus permitting Rx-induced killing. The relevant role for FKBP51 in radioresistance has also been documented in vivo. The study of tumor sections from melanoma xenografts implanted in nude mice showed unequivocal and extensive apoptosis provoked by a single dose of FKBP51 siRNA before irradiation.

It is a rapidly emerging concept that the radiocurability of a tumor implicates that the cancer stem or initiating cell is killed.[16] A cancer stem cell is defined as a cell within a tumor that possesses the capacity to self-renew and generate the heterogeneous cancer cells that comprise the tumor.[16] Tumor stem or initiating cells have been proposed to exist for melanoma.[31] The ABC transporter, ABCB5, was recently shown to be a marker of cells capable of recapitulating melanomas in xenotransplantation models.[32] The ABCG2

NORMAL SKIN

**PRIMARY MELANOMA
SPINDLE CELLS**

**PRIMARY MELANOMA
EPITHELIOID CELLS**

**CUTANEOUS METASTASIS
FROM MALIGNANT MELANOMA**
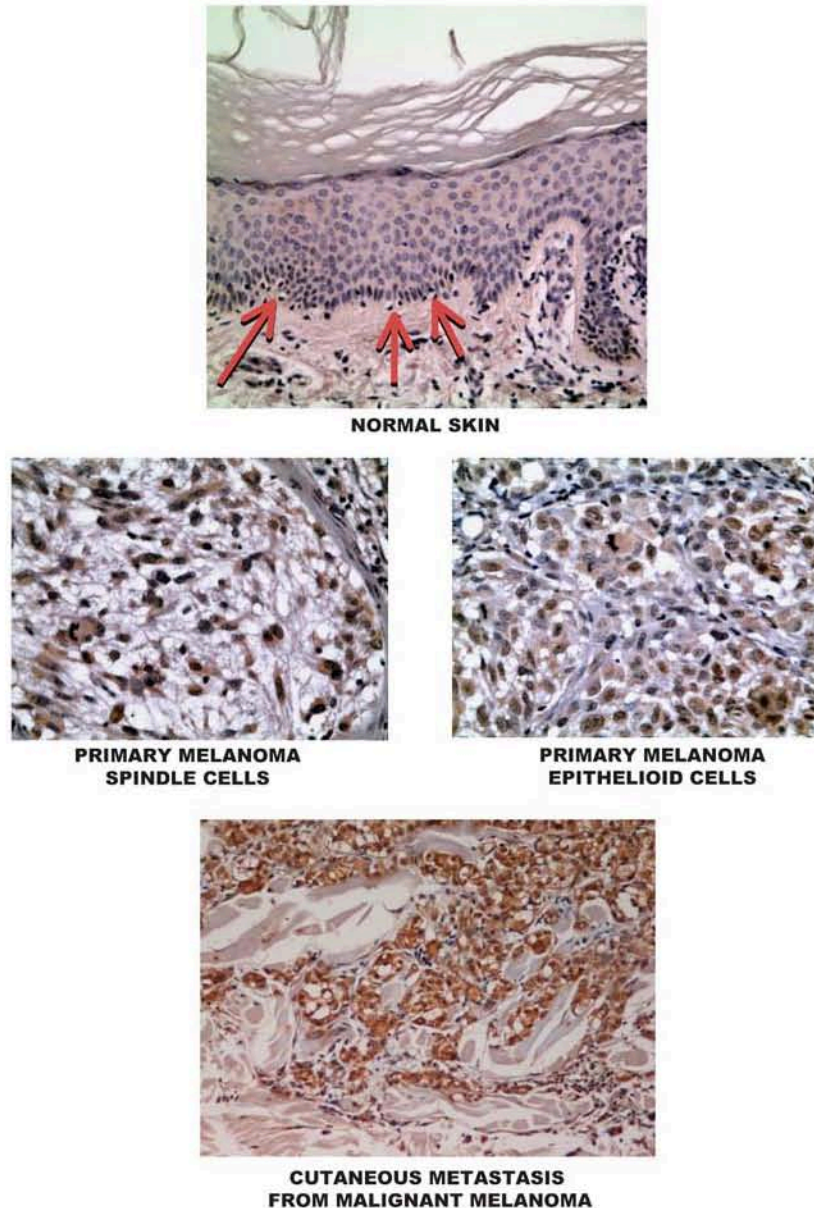
Figure 7 FKBP51 expression in normal skin and cutaneous malignant melanoma (CMM). FKBP51 immunochemical staining of normal skin (red arrows indicate melanocytes, original magnification, ×200); primary malignant melanoma spindle cells (original magnification, ×250); primary malignant melanoma epithelioid cells (magnification, ×250); and dermal metastasis from malignant melanoma (original magnification, ×150), using the avidin–biotin complex technique

and CD133 proteins have been identified as stemness markers in clinical melanomas.[25] Using flow cytometric techniques, we showed that ABCG2$^+$ melanoma cells contain intracytoplasmic FKBP51 at higher levels than do ABCG2 cells, as determined by the MFI values. The presence of FKBP51 was confirmed by an immunohisto-chemical study of ABCG2-sorted cells. Moreover, a flow cytometry analysis of cells double-stained with ABCG2 and annexin V allowed us to verify that ABCG2$^+$ cells are also killed by Rx after pretreatment with siRNA. Taken together, these findings suggest that FKBP51 may be a suitable target for eliminating cancer stem/initiating cells in melanoma.

The translational implication of our findings was reinforced by data obtained from a study on 80 melanoma patients. The protein expression was investigated in CMM both primitive and metastatic. The relevant data from this analysis are that FKBP51 (i) was expressed in all CMMs analyzed but not in normal skin; (ii) expression was higher in melanocytes during the vertical growth phase compared with the radial growth phase; (iii) expression correlated with the thickness of the tumor lesion; (iv) expression was maximal in metastatic melanoma. In conclusion, we show that FKBP51, a protein with important biological roles in normal cells,[28,29,33] acquires a pro-oncogenic potential when its expression is deregulated,
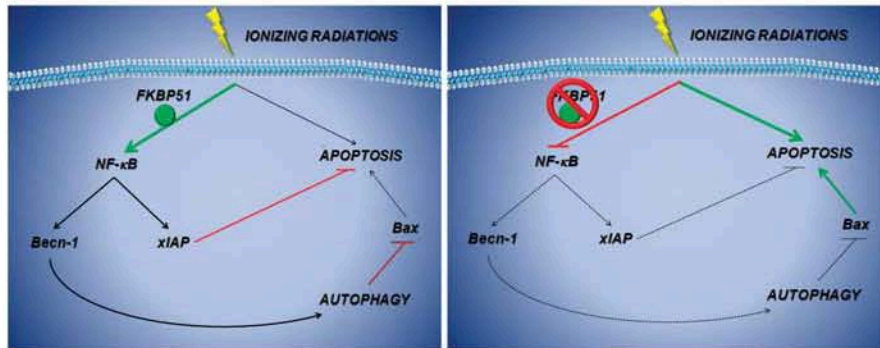
Figure 8 Schematic representation of the proposed mechanism for the FKBP51 suppression of ionizing radiation (Rx)-induced apoptosis. Rx triggers both the apoptotic and NF-κB pathways. FKBP51 is required for the activation of NF-κB, which in turn inhibits apoptosis by stimulating xIAP and promoting authophagy-mediated Bax degradation. In FKBP51-silenced cells, the lack of NF-κB induction permits the activation of apoptotic machinery, leading to cellular suicide

which is what occurs in melanoma. Such deregulation might sustain survival networks that protect the melanoma against killing. Our finding, that FKBP51 controls Rx-induced apoptosis in melanoma and correlates with malignity of the lesions, provides a novel potential target for signaling therapies of advanced disease and opens the door to the development of diagnostic and prognostic tools for FKBP51 expression profile, which can provide important insights into melanoma biology and progression.

Materials and Methods

Cell culture. The melanoma cell line SAN[10,34] was established from a patient's tumor lymphonodal metastasis and was provided by Dr. Gabriella Zupi (Experimental Preclinic Laboratory, Regina Elena Institute for Cancer Research, Roma, Italy). Cells were cultured in RPMI (Roswell Park Memorial Institute) 1640 medium (Lonza, Braine-l'Alleud, Belgium) supplemented with 10% heat-inactivated fetal bovine serum (FBS) (Lonza), 200 mM glutamine (Lonza), and 100 U/ml penicillin-streptomycin (Lonza) at 37°C in a 5% CO_2 humidified atmosphere. The melanoma cell lines G361 and SK-MEL-3[35] (derived from a primary tumor and a lymphonodal metastasis, respectively) were cultured in McCoy's modified medium (Sigma Aldrich, Saint Louis, MO, USA) supplemented with 10% heat-inactivated FBS, 200 mM glutamine and 100 U/ml penicillin-streptomycin at 37°C in a 5% CO_2 humidified atmosphere. The melanoma cell line A375,[36] derived from a metastatic tumor, was cultured in Dulbecco's Modified Eagle's Medium (Lonza) supplemented with 15% heat-inactivated FBS, 200 mM glutamine, and 100 U/ml penicillin-streptomycin at 37°C in a 5% CO_2 humidified atmosphere. G361, SK-MEL-3, and A375 were kindly provided by Dr. Rosella Di Noto (CEINGE, Naples, Italy).

Cell transfection. At 24 h before transfection, cells were seeded into six-well plates at a concentration of 2×10^5 cells/ml to obtain 30–60% confluence at the time of transfection. Then, the cells were transfected with specific short interfering oligoribonucleotide (siRNA) or with a non-silencing oligoribonucleotide (NS RNA) as control, at a final concentration of 50 nM using Metafectene (Biontex, Munich, Germany) according to the manufacturer's recommendations. NS RNAs and siRNAs corresponding to human cDNA sequences for FKBP51, FKBP12, RelA, xIAP, and Becn-1 were purchased from Qiagen (Germantown, Philadelphia, PA, USA). The siRNA sequences were:

5'-ACCUAAUGCUGAGCUdAU-3' for FKBP51;
5'-GCTTGAAGATGGAAAGAAA-3' for FKBP12;
5' AAGATCAATGGCTACACAGGA-3' for RelA (p65);
5'-AAGTGCTTTCACTGTGGAGGA-3' for Birc4 (xIAP);
5'-AGGGTCTAAGACGTCCAACAA -3' for Becn-1.

At 48 h after transfection, cells were irradiated with a 6 MV X-ray of a linear accelerator (Primus, Siemens, München, Deutschland) and processed according to the different experimental procedures.

Clonogenic assay. This assay was performed as described earlier.[37] Briefly, melanoma cells, not transfected and transfected with FKBP51 siRNA or with NS RNA, were irradiated at Rx doses between 1 and 8 Gy, harvested and plated in triplicate at a density of 500 cells/plate. After 10 days, the formed colonies were stained with crystal violet and counted. The mean colony count was calculated for each treatment (both Rx dose and type of cell transfection). The number of colonies in the irradiated dishes was divided by the number of colonies in the non-irradiated dishes and expressed as a percentage. The graph of percent survival (*y* axis) against Rx dose (*x* axis) was performed in semilogarithmic scale.

Cell lysates and western blot assay. Whole cell lysates were prepared by homogenization in modified RIPA buffer (150 mM sodium chloride, 50 mM Tris-HCl, pH 7.4, 1 mM ethylenediamine tetraacetic acid (EDTA), 1 mM phenylmethylsulfonyl fluorite (PMSF), 1% Triton X-100, 1% sodium deoxycholic acid, 0.1% sodium dodecylsulfate (SDS), 5 μg/ml aprotinin, and 5 μg/ml leupeptin). For IκBα and IκBβ detection, cytosolic extracts were obtained from 1×10^6 cells resuspended in 50 μl of lysing buffer (10 mM HEPES, pH 7.9, 1 mM EDTA, 60 mM KCl, 1 mM dithiothreitol, 1 mM PMSF, 50 μg/ml antipain, 40 μg/ml bestatin, 20 μg/ml chymostatin, and 0.2% v/v Nonidet P-40) for 15 min in ice. Cell debris was removed by centrifugation. Protein concentration was determined using the Bradford protein assay. Cell lysates were equalized for total protein, run in 10–14% SDS in polyacrylamide gel electrophoresis (PAGE) and transferred onto a methanol-activated polyvinylidene difluoride membrane (Millipore, Tokyo, Japan), which was incubated with the primary antibody. The goat polyclonal antibodies against FKBP51 (F-13), FKBP12 (N-19), and Actin (I-19) (Santa Cruz Biotechnology, Santa Cruz, CA, USA); the rabbit polyclonal antibodies against Becn-1 (H-300), IκBα (C-21), IκBβ (C-20) (Santa Cruz Biotechnology), LC3 (Novus Biologicals, Littleton, CO, USA), caspase-7 (C7724, Sigma, Saint Louis, MO, USA), and cleaved caspase-3 (Asp175) (Cell Signaling, Danvers, MA, USA) were used diluted 1:500. The mouse monoclonal antibodies against caspase-3 (specific for both pro-caspase and cleaved caspase-3) (Sigma Aldrich), xIAP (Stressgene, San Diego, CA, USA) and Bax (B-9, Santa Cruz Biotechnology) were used diluted 1:1000. The blots were developed with an electrochemiluminescence system (ECL) (GE Healthcare-Amersham, Buckinghamshire, UK).

Transmission electron microscopy. Melanoma cells, irradiated or non-irradiated, were plated on 60-mm dishes. At 30–50% confluence, the cells were fixed with 2% glutaraldehyde in 0.2 M Hepes, pH 7.4, at room temperature for 30 min. The cells were scraped and pelleted, and the fixation was continued for 2 h. The cells were then dehydrated in ethanol and embedded in epoxy resin. Thin sections were cut and stained with uranyl acetate and lead citrate, and examined under a Jeol JEM1200 EX2 Transmission Electron Microscope (Jeol, Tokyo, Japan).

Nuclear extracts, EMSA, and oligonucleotides. Cell nuclear extracts were prepared from 1×10^6 cells by homogenization of the cell pellet in two volumes of 10 mM HEPES, pH 7.9, 10 mM KCl, 1.5 mM $MgCl_2$, 200 mM EDTA, 0.5 mM DTT, 0.5 mM PMSF, and 10% glycerol (v/v). Nuclei were centrifuged at $1000 \times g$ for 5 min, washed, and resuspended in two volumes of the above-specified solution. KCl (3 M) was added until the concentration reached 0.39 M. Nuclei were extracted at 4°C for 1 h and centrifuged at $10\,000 \times g$ for 30 min. The

supernatants were clarified by centrifugation and stored at $-80°C$. Protein concentrations were determined using the Bradford method. The NF-κB consensus 5'-CAACGGCAGGGGAATCTCCCTCTCCTT-3' oligonucleotide[3] was end-labeled with $[\gamma^{32}P]$ ATP using a polynucleotide kinase (Roche, Basel, Switzerland). End-labeled DNA fragments were incubated at room temperature for 20 min with 5 μg of nuclear protein, in the presence of 1 μg poly(dI–dC), in 20 μl of a buffer consisting of 10 mM Tris-HCl, pH 7.5, 50 mM NaCl, 1 mM EDTA, 1 mM DTT, and 5% glycerol (v/v). In supershifting experiments, rabbit antibodies against p105/p50 (N-19), p65 (F-6), cRel (N), RelB (C-19) (Santa Cruz Biotechnology), and against p52 (kindly provided by Professor Shao-Cong Sun, Department of Microbiology and Immunology, Pennsylvania State University College of Medicine, Hershey, PA, USA) were added to the incubation mixture. In competition assays, a 50 $\times$ molar excess of NF-κB or NFAT cold oligo was added to the incubation mixture. Protein–DNA complexes were separated from the free probe on a 6% polyacrylamide (w/v) gel run in 0.25 $\times$ Tris borate buffer at 200 mV for 3 h at room temperature. The gels were dried and exposed to X-ray film (Fuji film, L.E.P., Naples, Italy).

Analysis of apoptosis. Caspase-3 and -9 activity was determined using the Carboxyfluorescein Fluorochrome Inhibitor of Caspases Assay (FLICA) Kits (B-Bridge International, San Jose, USA,) according to the instructions of the manufacturer. Cells are permeable to the fluorochrome inhibitor that binds covalently to the activated caspase, thereby inhibiting enzymatic activity. Briefly, 4 h after exposure to a 4 Gy Rx dose, the cells were harvested and resuspended in 300 μl PBS containing FLICA reagent, for 1 h at 37°C in a 5% CO_2 atmosphere, in the dark. During the incubation, cells were gently resuspended twice to ensure an optimal distribution of the FLICA reagent among all cells. Then, the cells were washed twice in wash buffer by centrifugation at 400 $\times$ g for 5 min, resuspended in 300–400 μl of PBS, and analyzed by flow cytometry. The green fluorescent signal was a direct measure of the number of active caspase enzymes. Phosphatidylserine externalization was investigated by annexin V staining. Briefly, 1 $\times$ 10^5 cells were harvested 48 h after Rx exposure (4 Gy) and resuspended in 100 μl of binding buffer (10 mM Hepes/NaOH pH 7.5, 140 mM NaCl, and 2.5 mM $CaCl_2$) containing 5 μl of annexin V-FITC (Pharmingen/Becton Dickinson, San Diego, CA, USA) for 15 min at room temperature in the dark. Then, 400 μl of the same buffer was added to each sample and the cells were analyzed with a Becton Dickinson FACScan flow cytometer (Becton Dickinson). The peptide caspase-3 inhibitor Z-Asp-Glu-Val-Asp fluoromethyl ketone (Z-DEVD-fmk) was provided by Sigma Aldrich.

Analysis of DNA content by propidium iodide incorporation was performed in permeabilized cells by flow cytometry. Cells (2 $\times$ 10^4) were harvested 72 h after Rx exposure (4 Gy), washed in PBS, and resuspended in 500 μl of a solution containing 0.1% sodium citrate w/v, 0.1% Triton X-100 v/v, and 50 μg/ml propidium iodide (Sigma Chemical Co, Gallarate, Italy). After incubation at 4°C for 30 min in the dark, cell nuclei were analyzed with a FACScan flow cytometer. Cellular debris was excluded from the analysis by raising the forward scatter threshold, and the DNA content of the nuclei was registered on a logarithmic scale. The percentage of the elements in the hypodiploid region was calculated.

Real-time PCR. Total RNA was isolated by Trizol (Invitrogen, Carlsbad, CA, USA) from cells harvested 6 h after Rx, according to the instructions of the manufacturer. A total of 1 μg of each RNA was used for cDNA synthesis with Moloney Murine Leukemia Virus Reverse Transcriptase (Invitrogen). Gene expression was quantified by real-time PCR using the iQSYBR Green Supermix (Biorad, Hercules, CA, USA) and specific real-time-validated QuantiTect primers for Bax, Becn-1, and XIAP (Qiagen) and specific primers for β-actin: Fw 5'-CGACA GGATGCAGAAGGAGA-3', Rev 5'-CGTCATACTCCTGCTTGCTTGCTG-3'.

Confocal microscopy. Cells were fixed in 4% paraformaldehyde in PBS for 20 min, washed twice for 5 min each time, with 50 mM NH_4Cl in PBS permeabilized for 5 min in 0.1% Triton X-100 in PBS. The cwere then blocked in 1% bovine serum albumin (BSA) in PBS for 1 h and washed twice in PBS. Mouse monoclonal anti-Bax (Santa Cruz Biotechnology) and rabbit polyclonal LC3 (Novus Biologicals), diluted 1 : 40 in PBS 0.5% BSA for 1 h in a humidified atmosphere, served as the primary antibody. The cells were then extensively washed in PBS before staining with secondary goat anti-mouse Alexa Fluor 546 and anti-rabbit Alexa Fluor 488 (Molecular Probe, Invitrogen Corporation, Carlsbad, CA, USA). Nuclei were counterstained with Hoechst 33258 (0.5 μg/ml in PBS) (Sigma Aldrich) for 10 min. Finally, the cells were washed in PBS and mounted on glass slides with PBS containing 50% glycerol.

The analysis of immunofluorescence was performed with a confocal laser scanner microscopy Zeiss 510 LSM (Carl Zeiss Microimaging GmbH, München, Germany), equipped with Argon ionic laser (Carl Zeiss Microimaging GmbH, München, Germany) whose I was set up to 488 nm, a HeNe laser whose I was set up to 546 nm, and an immersion oil objective, 63 $\times$ /1.4f. Emission of fluorescence was shown by a BP 505–530 band pass filter for Alexa-488 and 560 long pass for Alexa-546. Images for the double-staining immunofluorescence were acquired by sequential scanning to eliminate the cross talk of chromophores in the green and red channels and then saved in TIFF format to prevent the loss of information. They had been acquired with a resolution of 1024 $\times$ 1024 pixel with the confocal pinhole set to one Airey unit.

Cell sorting and immunostaining of ABCG2$^+$ cells. SAN melanoma cells were harvested, centrifuged for 5 min at 400 $\times$ g, and incubated with a monoclonal antibody against human ABCG2-pycoerythrin (PE) conjugated (R&D Systems, Minneapolis, MN, USA). After incubation at 4°C for 30 min in the dark, cells were fixed with 2% paraformaldehyde in PBS for 1 h and permeabilized with 0.1% Triton X-100 and 0.1% sodium citrate in PBS for 3 min in ice. Afterward, intracellular indirect immunostaining was performed with anti-FKBP51 (H-100) (Santa Cruz Biotechnology) and a secondary fluorescein isothiocyanate (FITC)-conjugated antibody. Expression of FKBP51 in both ABCG2$^+$ and ABCG2$^-$ cells was analyzed in flow cytometry by using the ABCG2-PE/SSc gating strategy. For the immunohistochemistry of ABCG2$^+$ cells, these were sorted from the whole cells of the melanoma cell line SAN with a BD FACSAria (BD Biosciences). The ABCG2$^+$ population was $>77\%$ in purified cells. The sorted cells were immediately fixed with 2% paraformaldehyde in PBS. Then, the cells were deposited on a slide (Cytoslide Shandon, Waltham, MA, USA) by spinning in a cytocentrifuge (Cytospin 3, Shandon) at 600 r.p.m. for 5 min, and subjected to FKBP51 immunohistochemical staining.

Immunohistochemistry. Serial sections of 4-μm thickness from routinely formalin-fixed, paraffin-embedded blocks were cut for each case of CMM and normal skin, and mounted on poly-l-lysine-coated glass slides, as described earlier.[36] Briefly, deparaffinized sections were boiled thrice for 3 min in a 1 mM sodium citrate buffer (pH 6.0), as an antigen retrieval method. To prevent a non-specific binding of the antibody, sections were preincubated with a non-immune mouse serum (1 : 20; Dakopatts, Hamburg, Germany) diluted in PBS–BSA (1%) for 25 min at room temperature. After quenching of endogenous peroxidases with 0.3% hydrogen peroxide in methanol, followed by two rinses with Tris-HCl buffer, the sections were incubated with the anti-FKBP51 primary antibody (F-13) (Santa Cruz Biotechnology) diluted 1 : 50 overnight at 4°C. The standard streptavidin–biotin–peroxidase complex technique, using sequential 20 min incubation with biotinylated linking antibody and peroxidase-labeled streptavidin (labeled streptavidin—biotin complex kit horseradish peroxidase, DAKO, Carpinteria, CA, USA), was performed. 3,3V-diaminobenzidine (3-3V diaminobenzidine tetrachloride; Vector Laboratories, Burlingame, CA) was used as a substrate chromogen solution for the development of the peroxidase activity. Hematoxylin was used for nuclear counterstaining; then, the sections were mounted and coverslipped with a synthetic mounting medium (Entellan, Merck, Darmstadt, Germany). As control, an antibody with irrelevant specificity, but with the same isotype as the primary antibody, was used in each staining run. Only cells with a definite brown cytoplasmic immunostaining were judged as positive for FKBP51 antibody. The immunohistochemical expression of FKBP51 in CMM was evaluated semiquantitatively as the percentage of positive tumor cells among the total melanoma cells present in at least 10 representative fields and scored according to an arbitrary scale (Staibano et al.[38]) as follows: 0 (no immunopositive cells); $+$ ($<5\%$ of positive cells); $++$ ($>5\%$ and $<25\%$ of positive cells); $+++$ ($>25\%$ of positive cells).

Animal studies. SAN melanoma cells, 3 $\times$ 10^6 in a volume of 100 μl PBS, were injected s.c. into one flank of 24 6-week-old athymic nu/nu mice (Charles River Laboratory, Wilmington, MA, USA). Mice were maintained under specific pathogen-free conditions in the Laboratory Animal Facility of the National Cancer Institute, G Pascale Foundation, Naples, Italy. All studies were conducted in accordance with Italian regulations for experimentations on animals. Mice were observed daily for the visual appearance of tumors at the injection sites. Tumor diameters were measured using calipers and calculated as the mean value between the shortest and the longest diameters. When tumors reached $\sim$ 10 mm in mean diameter, 3–4 weeks post-injection of cells, 12 mice were subjected to a single intratumor injection of FKBP51 siRNA and 12 to an injection of NS RNA. After 48 h, 12 mice (six treated with

FKBP51 siRNA and six with NS RNA) were subjected to tumor irradiation. A total of six irradiated animals (three injected with NS RNA and three with FKBP51 siRNA) and six non-irradiated animals (three injected with NS RNA and three with FKBP51 siRNA) were killed 24 h after irradiation. The remaining 12 animals were killed a day later. Each tumor was divided into two parts: one portion was formalin-fixed and paraffin-embedded for immunohistochemistry and the other was processed for the preparation of whole cell lysates. For immunohistochemical assays, 5-μm-thick paraffin-embedded sections were incubated with Tris-buffered saline (TBS)/BSA for 10 min to reduce unspecific staining. Tissue sections were then exposed to rabbit polyclonal antibody against cleaved caspase-3 (Asp175) (Cell Signaling) or isotype-matched control antibody for 1 h. After two washes in TBS, sections were exposed to anti-rabbit biotinylated antibody, washed again, and incubated with peroxidase-labeled streptavidin. 3,3V-diaminobenzidine was used as a substrate chromogen solution for the development of peroxidase activity. Counterstaining of tumor sections was performed using aqueous hematoxylin. Lysates of excised tumors were prepared by homogenization in modified RIPA buffer. Homogenization was conducted in a Dounce Homogenizer, before incubation for 1 h at 4°C. Preparations were subsequently clarified by centrifugation at 14 000 × g for 30 min at 4°C. The protein content of the supernatants was determined using the Bradford method. Samples were equalized for total protein and run in SDS-PAGE electrophoresis. Western blot filter was incubated with the rabbit polyclonal antibody for cleaved caspase-3 (Asp175) (Cell Signaling).

Statistical analysis. The results reported are the mean and standard deviation of independent experiments. The statistical significance of differences between means was estimated using Student's t-test. The χ^2-test was used to assess the difference between categorical variables. The Spearman's rank correlation coefficient was used for non-parametric data. Values of $P \leqslant 0.05$ were considered statistically significant. The statistical analysis was performed using the SPSS statistical package (SPSS Inc., Chicago, IL, USA).

1. Norris LB, Beam S. Multidisciplinary perspectives on melanoma treatment. *Updates from the 44th Annual Meeting of the American Society of Clinical Oncology, The Oncology Nurse* 2008; 1: 1–7.
2. Dewey WC, Ling CC, Meyn RE. Radiation-induced apoptosis: relevance to radiotherapy. *Int J Radiat Oncol Biol Phys* 1995; 33: 781–796.
3. Wallace SS. DNA damages processed by base excision repair: biological consequences. *Int J Radiat Biol* 1994; 66: 579–589.
4. Hengartner MO. The biochemistry of apoptosis. *Nature* 2000; 407: 770–776.
5. Elliott A, Reiners Jr JJ. Suppression of autophagy enhances the cytotoxicity of the DNA-damaging aromatic amine p-anilinoaniline. *Toxicol Appl Pharmacol* 2008; 232: 169–179.
6. Ogata M, Hino S, Saito A, Morikawa K, Kondo S, Kanemoto S et al. Autophagy is activated for cell survival after endoplasmic reticulum stress. *Mol Cell Biol* 2006; 26: 9220–9231.
7. Eskelinen EL. New insights into the mechanisms of macroautophagy in mammalian cells. *Int Rev Cell Mol Biol* 2008; 266: 207–247. Review.
8. Baehrecke EH. Autophagy: dual roles in life and death? *Nat Rev Mol Cell Biol* 2005; 6: 505–510. Review.
9. Mathew R, Karantza-Wadsworth V, White E. Role of autophagy in cancer. *Nat Rev Cancer* 2007; 7: 961–967.
10. Romano MF, Avellino R, Petrella A, Bisogni R, Romano S, Venuta S. Rapamycin inhibits doxorubicin-induced NF-kappaB/Rel nuclear activity and enhances the apoptosis of melanoma cells. *Eur J Cancer* 2004; 40: 2829–2836.
11. Johnson GE, Ivanov VN, Hei TK. Radiosensitization of melanoma cells through combined inhibition of protein regulators of cell survival. *Apoptosis* 2008; 13: 790–802.
12. Munshi A, Kurland JF, Nishikawa T, Chiao PJ, Andreeff M et al. Inhibition of constitutively activated nuclear factor-kappaB radiosensitizes human melanoma cells. *Mol Cancer Ther* 2004; 3: 985–992.
13. Ghosh S, May MJ, Kopp EB. NF-κB and Rel proteins: evolutionarily conserved mediators of immune response. *Annu Rev Immunol* 1998; 16: 225–260.
14. Baldwin Jr AS. The NF-κB and IκB proteins: new discoveries and insights. *Annu Rev Immunol* 1996; 14: 649–681.
15. Karin M, Cao X, Greten FR, Li Z-W. NF-kappaB in cancer: from innocent bystander to major culprit. *Nat Rev Cancer* 2002; 2: 301–310.
16. Baumann M, Krause M, Hill R. Exploring the role of cancer stem cells in radioresistance. *Nat Rev Cancer* 2008; 8: 545–554. Review.
17. Romano S, Mallardo M, Chiurazzi F, Bisogni R, D'Angelillo A, Liuzzi R et al. The effect of FK506 on transforming growth factor beta signaling and apoptosis in chronic lymphocytic leukemia B cells. *Haematologica* 2008; 93: 75–84.
18. Chen AY, Okunieff P, Pommier Y, Mitchell JB. Mammalian DNA topoisomerase I mediates the enhancement of radiation cytotoxicity by camptothecin derivatives. *Cancer Res* 1997; 57: 1529–1536.
19. Kabeya Y, Mizushima N, Ueno T, Yamamoto A, Kirisako T, Noda T et al. LC3, a mammalian homologue of yeast Apg8p, is localized in autophagosome membranes after processing. *EMBO J* 2000; 19: 5720–5728.
20. Chandler JM, Cohen GM, MacFarlane M. Different subcellular distribution of caspase-3 and caspase-7 following Fas-induced apoptosis in mouse liver. *J Biol Chem* 1998; 273: 10815–10818.
21. Habraken Y, Piette J. NF-kappaB activation by double-strand breaks. *Biochem Pharmacol* 2006; 72: 1132–1141. Review.
22. Copetti T, Bertoli C, Dalla E, Demarchi F, Schneider C. p65/RelA modulates BECN1 transcription and autophagy. *Mol Cell Biol* 2009; 29: 2594–2608.
23. Kim H, Rafiuddin-Shah M, Tu HC, Jeffers JR, Zambetti GP, Hsieh JJ et al. Hierarchical regulation of mitochondrion-dependent apoptosis by BCL-2 subfamilies. *Nat Cell Biol* 2006; 8: 1348–1358.
24. Zhou S, Schuetz JD, Bunting KD, Colapietro AM, Sampath J, Morris JJ et al. The ABC transporter Bcrp1/ABCG2 is expressed in a wide variety of stem cells and is a molecular determinant of the side-population phenotype. *Nat Med* 2001; 7: 1028–1034.
25. Monzani E, Facchetti F, Galmozzi E, Corsini E, Benetti A, Cavazzin C et al. Melanoma contains CD133 and ABCG2 positive cells with enhanced tumourigenic potential. *Eur J Cancer* 2007; 43: 935–946.
26. Hocker TL, Singh MK, Tsao H. Melanoma genetics and therapeutic approaches in the 21st century: moving from the benchside to the bedside. *J Invest Dermatol* 2008; 128: 2575–2595.
27. Poeck H, Besch R, Maihoefer C, Renn M, Tormo D, Morskaya SS. 5′-Triphosphate-siRNA: turning gene silencing and Rig-I activation against melanoma. *Nat Med* 2008; 14: 1256–1263.
28. Sinars CR, Cheung-Flynn J, Rimerman RA, Scammell JG, Smith DF, Clardy J. Structure of the large FK506-binding protein FKBP51, an Hsp90-binding protein and a component of steroid receptor complexes. *Proc Natl Acad Sci USA* 2003; 100: 868–873.
29. Bouwmeester T, Bauch A, Ruffner H, Angrand PO, Bergamini G, Croughton K et al. A physical and functional map of the human TNF-alpha/NF-kappaB signal transduction pathway. *Nat Cell Biol* 2004; 6: 97–105.
30. Naumann U, Bähr O, Wolburg H, Altenberend S, Wick W, Liston P et al. Adenoviral expression of XIAP antisense RNA induces apoptosis in glioma cells and suppresses the growth of xenografts in nude mice. *Gene Ther* 2007; 14: 147–161.
31. Zabierowski SE, Herlyn M. Learning the ABCs of melanoma-initiating cells. *Cancer Cell* 2008; 13: 185–187.
32. Schatton T, Murphy GF, Frank NY, Yamaura K, Waaga-Gasser AM, Gasser M et al. Identification of cells initiating human melanomas. *Nature* 2008; 451: 345–349.
33. Baughman G, Wiederrecht GJ, Faith Campbell N, Martin MM, Bourgeois S. FKBP51, a novel T-cell specific immunophilin capable of calcineurin inhibition. *Mol Cell Biol* 1995; 15: 4395–4402.
34. Benassi B, Zupi G, Biroccio A. Gamma-glutamylcysteine synthetase mediates the c-Myc-dependent response to antineoplastic agents in melanoma cells. *Mol Pharmacol* 2007; 72: 1015–1023.
35. Trotta PP, Harrison Jr SD. Evaluation of the antitumor activity of recombinant human gamma-interferon employing human melanoma xenografts in athymic nude mice. *Cancer Res* 1987; 47: 5347–5353.
36. Giard DJ, Aaronson SA, Todaro GJ, Arnstein P, Kersey JH, Dosik H et al. In vitro cultivation of human tumors: establishment of cell lines derived from a series of solid tumors. *J Natl Cancer Inst* 1973; 51: 1417–1423.
37. Franken NAP, Rodermond HM, Stap J, Haveman J, van Bree C. Clonogenic assay of cells in vitro. *Nat Protoc* 2006; 1: 2315–2319.
38. Staibano S, Pepe S, Lo Muzio L, Somma P, Mascolo M, Argenziano G. Poly(adenosine diphosphate-ribose) polymerase 1 expression in malignant melanomas from photo-exposed areas of the head and neck region. *Hum Pathol* 2005; 36: 724–731.

www.nature.com/cddis

Correspondence

FK506-binding protein 51 is a possible novel tumoral marker

S Romano[1], A D'Angelillo[1], S Staibano[2], G Ilardi[2] and MF Romano*[,1]

Dear Editor,

FK506-binding protein (FKBP) 51 is a cochaperone, which belongs to the immunophilin family, a group of proteins with peptidyl-prolyl isomerase activity. FKBPs regulate several biological processes through protein–protein interaction.[1] In particular, FKBP51 is a component of the steroid receptor complex, with a role in steroid resistance;[2] moreover, it is involved in NF-κB activation because of its isomerase activity, which is essential for the function of subunit-α in the IκB kinase complex.[3] According to Baughman et al.,[4] FKBP51 is abundantly expressed in lymphocytes and in several other tissues, but it is expressed at low levels in the pancreas, spleen, and stomach. There is increasing evidence of an association of FKBP51 hyperexpression with cancer[6–8] and a relevant role of this protein in sustaining cell growth,[5] malignancy, and resistance to therapy.[6–8] An immunohisto-chemistry study of expression of FKBP51 in 50 tumoral samples acquired from our pathology section, including breast, lung, pancreas, ovary, and prostate (10 samples for each tumor), and a comparable number of normal tissue samples showed an intense signal in 38 out of 50 tumors analyzed, whereas normal tissues of the same histotypes showed a weak/absent immunohistochemical signal. The 12 tumor samples with low/negative immunohistochemistry were the 10 breast cancer samples and 2 out of 10 pancreatic tumors. Interestingly, these two pancreatic tumors belonged to the well-differentiated histotype (G1). Figure 1a (upper panel) shows representative immunohistochemical findings. Measurement of FKBP51 mRNA levels in deparaffinized tissues using real-time PCR confirmed the immunohisto-chemistry results (representative results in Figure 1a, lower panel). Taken together, these findings support the hypothesis that FKBP51 is a promising novel tumoral marker. The association of FKBP51 overexpression with cancer is in line with the rapidly emerging concept that NF-κB drives tumor-igenesis in the most common genetic alterations associated with cancer.[9,10]

Recently, it has been found, in tumor cell lines, that FKBP51 acted as a scaffold to facilitate the interaction between Akt and PH domain leucine-rich repeat protein phosphatase, which mediates dephosphorylation of pAkt (S473).[11] This raised the question whether FKBP51 may work out as a tumor suppressor by deactivating Akt. As we previously found that intratumoral injection of FKBP51 siRNA followed by irradiation produced extensive apoptosis in melanoma xenografts,[8] we investigated the effect of FKBP51 downmodulation on pAkt (S473) levels in our mouse model of melanoma, in both xenografts and locoregional lymph nodes. Histological examination showed that the mouse lymphatic tissue was not metastatic. Figure 1b shows a representative outcome. On the basis of these results, pAkt (S473) levels were not enhanced with downmodulation of FKBP51 in normal or cancerous tissue.

This observation suggests that pathways upstream from Akt, which are often deregulated in cancer, control activated-Akt levels. This hypothesis is supported by the findings that leukemic lymphocytes often display higher levels of pAkt (S473) in comparison with normal lymphocytes (Figure 1c) even in the presence of similar or higher FKBP51 levels. To assess whether an inverse correlation subsisted between FKBP51 and pAkt (S473) levels, we used western blot to measure these levels in samples of primary lymphatic leukemia and normal peripheral blood lympho-cytes. Expression levels were quantified by densitometry. Spearman's ρ correlation did not indicate any relationship between the two variables (Figure 1d; $P = 0.788$, left; $P = 0.199$, right). Taken together, these findings do not support an essential role of FKBP51 as a factor that controls the phosphorylation status of Akt inside the cell, thereby weakening the hypothesis that the protein may work out as tumor suppressor.

In conclusion, although FKBP51 function is not yet fully elucidated, however, there are clear data suggesting that this immunophilin is often hyperexpressed in tumors and has an active role in pre-neoplastic disorders[5] and cancer.[6–8]

Conflict of interest

The authors declare no conflict of interest.

[1]Department of Biochemistry and Medical Biotechnology, Federico II University of Naples, Naples, Italy and [2]Department Biomorfological and Functional Sciences, Pathology Section, Federico II University of Naples, Naples, Italy
*Corresponding author: MF Romano, Department of Biochemistry and Medical Biotechnology, Federico II University of Naples, Naples 80131, Italy.
Tel: + 39 081 746 3125; Fax: + 39 081 746 3205; E-mail: romano@dbbm.unina.it
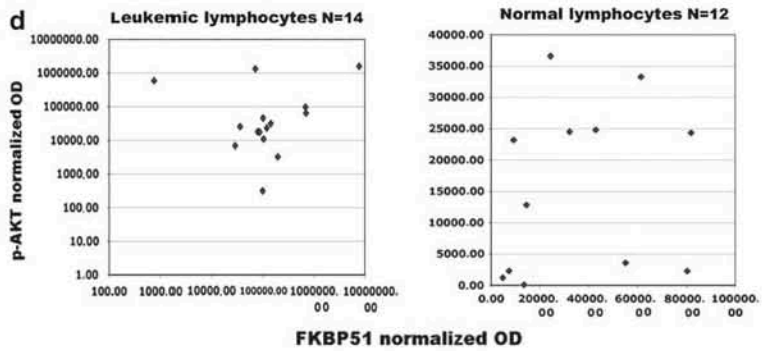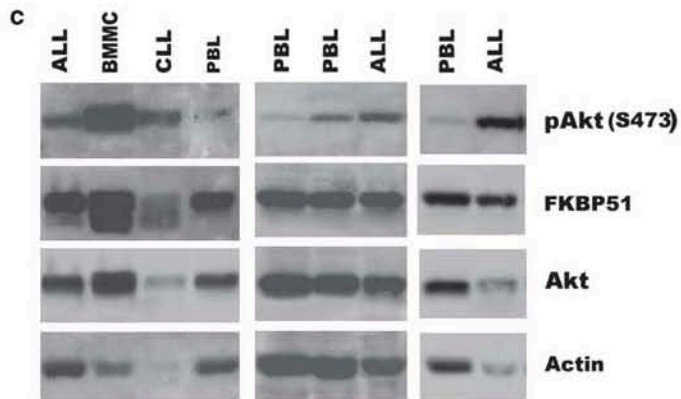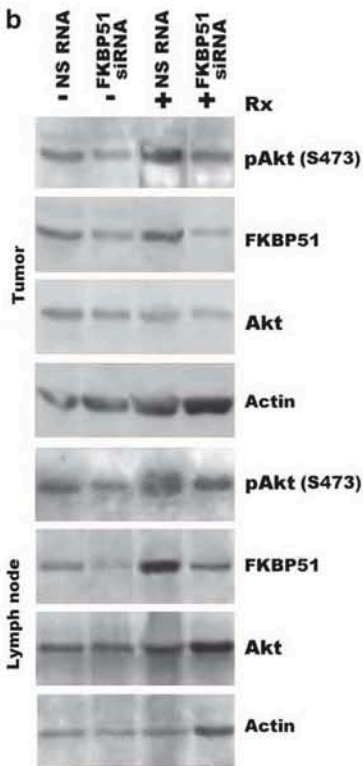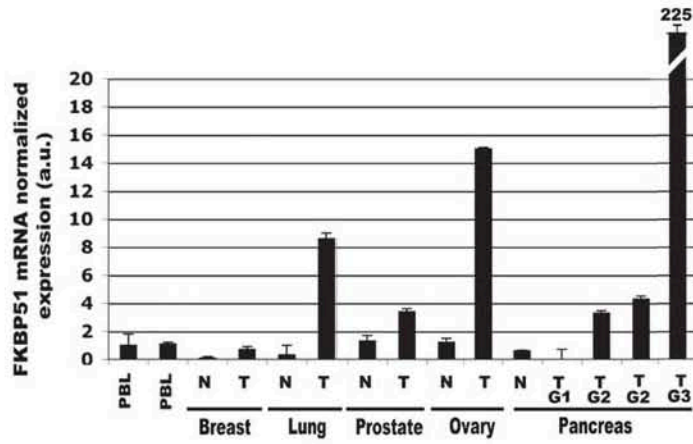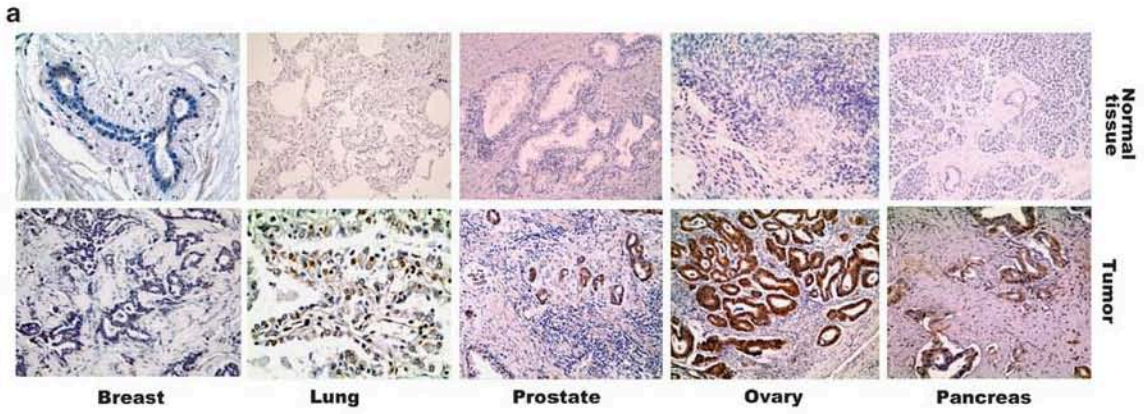
Figure 1 (a) (Upper panel) FKBP51 immunochemical staining of normal and neoplastic tissues. Serial sections of 4 μm from routinely formalin-fixed, paraffin-embedded blocks were cut and mounted on poly-L-lysine-coated glass slides. (Lower panel) Deparaffinized sections were incubated overnight at 4°C with anti-FKBP51 primary antibody (F-13, Santa Cruz Biotechnology, Santa Cruz, CA, USA) diluted 1 : 50. The standard streptavidin–biotin–peroxidase complex technique was performed. Hematoxylin was used for nuclear counterstaining. (Lower panel) Normalized expression rates of FKBP51 mRNA (a.u., arbitrary units) in PBL and deparaffinized tissues; each histogram is referred to a representative normal or tumoral sample. Values represent means and S.D. of arbitrary units from three different real-time experiments, each performed in triplicate. Total RNA was isolated from PBLs with Trizol (Invitrogen, Carlsbad, CA, USA) and from paraffinized tumors using the High Pure RNA Paraffin Kit (Roche Diagnostics GmbH, Mannheim, Germany) according to the manufacturer's instructions. In all, 1 μg of each RNA was used for cDNA synthesis with Moloney Murine Leukemia Virus Reverse Transcriptase (M-MLV RT, Invitrogen). Gene expression was quantified by real-time PCR using the iQ SYBR Green Supermix (Bio-Rad, Foster City, CA, USA) and specific real-time-validated QuantiTect primers for FKBP51 (FW: 5'-GTGGGGAATGGTGAGGAAACGC-3'; REV: 5'-CATGGTAGCCACCCCAATGTCC-3') and specific primers for β-actin. Relative quantitation of FKBP51 transcript across multiple samples was performed by using a coamplified β-actin internal control for sample normalization. The values of each sample were compared to PBL (expression = 1) for an estimate of the relative expression change fold of FKBP51. (b) Western blot assay of pAkt (S473) and FKBP51 levels in lysates prepared from melanoma xenografts and locoregional lymph nodes obtained from athymic nu/nu mice (Charles River Laboratory, Wilmington, MA, USA). For pAkt (S473) detection, the rabbit polyclonal antibody clone D9E (Cell Signaling, Danvers, MA, USA) was used, and for FKBP51, the goat polyclonal antibody F-13 (Santa Cruz Biotechnology) was used. When tumors reached $\sim$ 10 mm in mean diameter, mice received a single intratumoral injection of FKBP51 siRNA (5'-ACCUAAUGCUGAGCUdAU-3') or (nonsilencing) NS RNA. After 48 h, mice were subjected to tumor irradiation, and after a further 48 h, animals were killed and tumors and lymph nodes excised for preparation of lysates. (c) Western blot assays of pAkt (S473) and FKBP51 levels in lysates prepared from different samples of mononuclear cells. Mononuclear cells of acute lymphoblastic leukemia (ALL) were separated by bone marrow; BMMCs were bone marrow mononuclear cells separated from a noninfiltrated bone marrow sample from a lymphoma patient. Mononuclear cells of chronic lymphocytic leukemia (CLL) were separated by peripheral blood. Peripheral blood lymphocytes (PBLs) were from normal donors. (d) Scatterplot of FKBP51 OD *versus* pAkt (S473) OD. FKBP51 and pAkt (S473) expression levels were quantified by densitometry using ImageJ 1.42q (NIH, http://rsb.info.nih.gov/ij/) for Macintosh. Integrated ODs of pAkt were normalized to Akt, whereas integrated ODs of FKBP51 were normalized to actin

◀

1. Kang CB *et al. Neurosignals* 2008; **16**: 318–325.
2. Silverstein AM *et al. J Biol Chem* 1997; **272**: 16224–16230.
3. Bouwmeester T *et al. Nat Cell Biol* 2004; **6**: 97–105.
4. Baughman G *et al. Biochem Biophys Res Commun* 1997; **232**: 437–443.
5. Giraudier S *et al. Blood* 2002; **100**: 2932–2940.
6. Jiang W *et al. Neoplasia* 2008; **10**: 235–243.
7. Periyasamy S *et al. Oncogene* 2010; **29**: 1691–1701.
8. Romano S *et al. Cell Death Differ* 2010; **17**: 145–157.
9. Huang W-C *et al. Molecular Cell* 2007; **26**: 75–87.
10. Meylan E *et al. Nature* 2009; **462**: 104–107.
11. Pei H *et al. Cancer Cell* 2009; **16**: 259–266.

Supplementary Information accompanies the paper on Cell Death and Disease website (http://www.nature.com/cddis)

Stage: Manuscript Approved
Manuscript Reference#: BSP-ACA-MC-2010-55
Manuscript Title: FK506 Binding Proteins as Targets in Anticancer Therapy

Dear Dr. Romano,

This is to notify that your manuscript entitled **"FK506 Binding Proteins as Targets**

 in Anticancer Therapy"

has been approved by the Editor-in-Chief of **"Anti-Cancer Agents In Medicinal Chemistry**

Your manuscript will soon be processed for publication.

Yours sincerely,
Bentham Science Publishers

Visit your work portal (http://bentham-editorial.org) for further information.

FK506 Binding Proteins as Targets in Anticancer Therapy

Simona Romano, AnnaLaura Di Pace, Antonio Sorrentino, Rita Bisogni, Luigi Sivero* and Maria Fiammetta Romano

Department of Biochemistry and Medical Biotechnology, University Federico II, Naples, Italy

*Department of General Surgery, Geriatric, Oncology and Advanced Technology, University Federico II, Naples, Italy

Corresponding author: Maria Fiammetta Romano, Department of Biochemistry and Medical Biotechnology, University of Naples "Federico II". Via S. Pansini 5, 80131 Napoli, Italy. Phone: +39081/7463125. Fax: +39081/7463205. email: romano@dbbm.unina.it

Running title: **FKBP and Cancer**

Abstract

FK506 binding proteins (FKBPs) are the intracellular ligands of FK506 and rapamycin, two natural compounds with powerful and clinically efficient immunosuppressive activity. In recent decades, a relevant role for immunosuppressants as anticancer agents has emerged. Especially, rapamycin and its derivatives are used, with successful results, across a variety of tumors. Of note, rapamycin and FK506 bind to FKBP12, and the resulting complexes interfere with distinct intracellular signaling pathways driven, respectively, by the mammalian target of rapamycin and calcineurin phosphatase. These pathways are related to T-cell activation and growth. Hyperactivation of the mammalian target of rapamycin (mTOR), particularly in cancers that have lost the tumor suppressor gene PTEN, plays an important pathogenetic role in tumor transformation and growth. The signaling pathway involving calcineurin and nuclear factors of activated T-lymphocytes is also involved in the pathogenesis of different cancer types and in tumor metastasis, providing a rationale for use of FK506 in anticancer therapy. Recent studies have focused on FKBPs in apoptosis regulation: Targeting of FKBP12 promotes apoptosis in chronic lymphocytic leukemia, FKBP38 knockdown sensitizes hepatoma cells to apoptosis, and FKBP51 silencing overcomes resistance to apoptosis in acute lymphoblastic leukemia, prostate cancer, melanoma, and glioma. Interestingly, derivatives of FK506 that have the same FKBP12-binding properties as FK506 but lack functional immunosuppressant activity, exert the same apoptotic effect as FK506 in chronic lymphocytic leukemia. These findings suggest that a direct FKBP inhibition represents a further mechanism of immunosuppressants' anticancer activity. In this review, we focus on the role of FKBP members in apoptosis control and summarize the data on the antitumor effect of selective targeting of FKBP.

Keywords: apoptosis, Bcl-2, cancer, FKBP, NF-κB, targeted therapy, TGF-β,

.

Introduction

FKBPs and cyclophilins are the two major subfamilies of immunophilins [1]. Immunophilins are highly conserved proteins endowed with peptidyl-prolyl cis-trans isomerase activity (PPIase), found in abundance in virtually all organisms [1]. The designation "immunophilin" refers to the immunosuppressive character of ligand–protein complexes [2]. Cyclosporine is the natural ligand that binds to cyclophilin A [1], and FK506 and rapamycin are the canonical ligands of FKBPs [1]. FKBP12 is the prototype FKBP [3,4], containing only a single FK506-binding domain (FKBD) comprising 108 amino acids. Human FKBP12 interacts with FK506 and rapamycin with a K_D of 0.4 nM and 0.2 nM, respectively [1, 2, 5]. The complex formations of FKBP with the ligands enhance the stability of FKBP, and the resulting complexes remain more resistant to proteolytic cleavage and create an appropriate binding surface for binding to calcineurin (CaN) and the mammalian target of rapamycin (mTOR) [1, 2, 5]. The FK506/FKBP12 complex interacts with CaN [6] and inhibits its serine–threonine phosphatase, which is important for activating nuclear factors of activated T-lymphocytes [7]. In response to antigenic stimuli, this transcription factor stimulates production of interleukin 2 and other cytokines essential for immune activation [7]. By contrast, the rapamycin/FKBP12 complex inhibits the serine–threonine kinase mTOR [8, 9], which is activated in response to growth factors and nutrients to promote cell-cycle progression [10]. Ultimately, FK506 inhibits the immune response by blocking production of growth factors essential for T-cell clonal expansion, whereas rapamycin suppresses growth factor–induced T-cell proliferation [6]. Both CaN [11, 12] and mTOR [10, 13, 14] are deregulated in various cancer types [10-14] and are responsible for competitive growth advantage, metastatic competence, and therapy resistance, thus providing a rationale for the use of immunosuppressants against cancer [11-17].

FKBPs are defined as canonical or non-canonical immunophilins on the basis of their binding strength to FK506 [2]. Despite an overall structural similarity to that of FKBP12 [18], non-canonical FKBP has multiple substitutions of the aromatic residues in FKBD that unfavorably influence affinity for FK506 [18]. In addition to FKBD, FKBPs possess further domains involved in protein–protein interaction or tetratrico peptide repeat (TPR) motifs, nuclear signaling, calcium binding, protein trafficking, and ATP/GTP-binding sequences [1,2], explaining the wide variety of cellular functions these proteins exhibit [1, 2, 19-22].

Several lines of evidence [23-33] support the concept that FKBP members can regulate programmed cell death through molecular interaction with partners in apoptotic networks. This review focuses on the anti-apoptotic properties of some FKBP members, namely FKBP12, FKBP38, and FKBP51, and summarizes the data that support an antitumor effect of selective targeting of these FKBPs.

Roles of FK506 Binding Proteins in Apoptosis Inhibition

FKBP12 is the guardian of transforming growth factor-β (TGF-β) receptor signaling [22]. TGF-β is a pleiotropic cytokine that regulates a wide range of biological processes [34-36] and that can transduce apoptosis by a mitochondria-dependent pathway [36-38]. In particular, TGF-β is apoptotic for hematopoietic cells and regulates the life span of lymphocytes [39]. The loss of sensitivity to TGF-β promotes leukemic transformation [40, 41]. FKBP12 acts as a natural ligand for the TGF-β type I receptor (TβR-I) [22], binding to a glycine- and serine-rich motif (GS motif) of TβR-I, capping its phosphorylation and stabilizing the inactive conformation of TβR-I [22]. The PPIase core domain of FKBP12 is important for the interaction of the immunophilin with TβR-I. FK506 inhibits this interaction and promotes receptor transautophosphorylation [22, 42]. FK506 activates apoptosis of normal and leukemic lymphocytes through the TGF-β signal [31]. FK506-induced cell death is preceded by: (i) increased levels of phosphorylated Smad2; (ii) translocation of Smad complexes in the nucleus; (iii) induction of the death-associated protein (DAP) kinase, a transcriptional target of Smad; (iv) increased levels of all three Bim isoforms, Bim_{EL}, Bim_L, and Bim_S and of the Bcl-2–modifying factor (Bmf); (v) loss of mitochondrial membrane potential; and (vi) caspase 3 activation [31]. The same apoptotic effect is produced by knocking down FKBP12 [31]. Figure 1 shows a schematic representation of the TGF-β signaling pathway leading to apoptosis and the role of FKBP12 in the control of activation of such a signal.

The non-canonical FKBP38 helps the anti-apoptotic protein Bcl-2 to localize at the mitochondrial membrane and protects cells from apoptosis [23]. FKBP38 interacts with Bcl-2 by binding to the flexible loop of Bcl-2, between Bcl-2 homology 3 and 4 (BH3 and BH4) regions and protects Bcl-2 from degradation [23]. When FKBP38 is knocked down by siRNA, the level of Bcl-2 protein is significantly reduced. Interaction of presenilins (PS) with FKBP38 also results in decreased mitochondrial Bcl-2 and increased susceptibility to apoptosis by antagonizing the anti-apoptotic

function of FKBP38 [26]. PS1/2 molecules are multipass transmembrane proteins localized predominantly in the endoplasmic reticulum and Golgi apparatus [43] and are causative agents in familial Alzheimer's disease [44]. PS1/2 and FKBP38 form macromolecular complexes together with Bcl-2 [26]. PS1/2 proteins sequester FKBP38 and Bcl-2 in the endoplasmic reticulum/Golgi compartments, thereby inhibiting FKBP38-mediated mitochondrial targeting of Bcl-2 and promoting the degradation of FKBP38 and Bcl-2 [26]. Thus, competition between PS1/2 and FKBP38 for subcellular targeting of Bcl-2 regulates mitochondrially mediated apoptosis. Excessive pro-apoptotic activity of PS1/2 through this mechanism is thought to explain its role in the pathogenesis of familial Alzheimer's disease [26,44].

Studies in human fetal liver also confirm the anti-apoptotic role of FKBP38 [27]. The interaction between the hepatitis C virus (HCV) non-structural protein NS5A and FKBP38 is an important mechanism for HCV-infected liver cells to evade apoptosis. NS5A contains three BH domains and mimics the anti-apoptotic function of Bcl-2 [27]. This interaction has been mapped to amino acids 148–236 of NS5A containing a BH domain [27].

The high-molecular-weight FKBP51 is a protein with a specialized role during cell division, exhibiting preferential expression in mitotically active cells [45-47]. The FKBP51-mediated anti-apoptotic mechanism involves activation of the NF-κB transcription complex [24, 25, 28-30]. Of note, NF-κB induces resistance to cancer therapies by modulating the regulation of various anti-apoptotic genes [48], including inhibitors of apoptosis (IAPs) [49], caspase 8 inhibitory protein (cFLIP) [50], A1/Bfl1 [51], tumor necrosis factor (TNF) receptor–associated factors 1 and 2 [52], and others [48]. A proteomic study of mapping of the TNFα/NF-κB signal transduction pathway [53] first identified FKBP51 as an IKKα co-factor, essential for the function of the IKK kinase complex. Subsequent studies [24, 25, 33] from our group also showed that FKBP51 controls NF-κB activation by DNA-damaging agents, including anthracyclin compounds [24, 25] and ionizing radiation [33]. As Figure 2A shows, FKBP51 physically interacts with IKK following treatment of tumor cell with ionizing radiation. This interaction plays a crucial role in the activation of IKK kinase, as suggested by the lack of increase in phospho-IκBα levels after irradiation of FKBP51-depleted cells (Figure 2B). As is already established, IκB phosphorylation, followed by proteolytic degradation of inhibitors, controls cytoplasmic shuttling to the nucleus of NF-κB dimers in response to cell stimulation [23, 24]. FKBP51 plays a relevant role in counteracting apoptotic processes stimulated by radio- and chemotherapy.

Targeting of FKBP51 counteracts NF-κB activation and efficiently overcomes blockage of the apoptotic machinery provoked by this transcription factor, thus permitting cell death [24, 25, 28, 29, 33]. Hyperexpression of the RelA subunit of the NF-κB complex counteracts the pro-apoptotic effect of FKBP51 knockdown [25].

Targeting of FKBP in Cancer

Targeting of FKBP12 with FK506 or siRNA increases TGF-β signaling and stimulates apoptosis of chronic lymphocytic leukemia (CLL) cells [31]. The apoptotic effect of FK506 occurs regardless of the immunosuppressive mechanism [31]. Derivatives of FK506 that have the same FKBP12-binding properties as FK506 but lack the calcineurin binding capability, and thus lack functional immunosuppressant activity, are expected to exert the same pro-apoptotic effect as FK506 in CLL. Consistent with this hypothesis, we showed that three FK506 analogs, FK520, 15-O-demethyl-FK520, and 18-OH-FK520, induce CLL cell death to the same extent as FK506 (Fig. 3). 15-O-demethyl-FK520 and 18-OH-FK520, although bind to FKBP12, have modifications in the composite calcineurin binding surface, thereby display a reduced CaN inhibitory effect compared to FK506 [54, 55]. There is growing interest in therapeutically targeting TGF-β–mediated processes in cancer [56-59], including hematological malignancies [60]. TGF-β, although involved in metastatic processes in advanced tumors, acts as an early tumor suppressor [61]. Loss of response to TGF-β is thought to contribute to tumorigenesis [35, 36, 40, 41] and drug resistance of tumor cells [62]. Targeting of FKBP12 may represent a strategy in cancer chemoprevention or a therapy for early-stage tumors [59].

HCV infection often leads to chronic hepatitis, liver cirrhosis, and hepatocellular carcinoma [63]. A defect of apoptosis, resulting from viral protective strategies, significantly contributes to persistent HCV infection [64] and works together with chronic inflammation [65] to cause tumor transformation. NS5A represents one of these viral anti-apoptotic strategies in HCV infection [27]. Targeting of FKBP38 using RNA interference specifically abrogates resistance to apoptosis of hepatoma cells that hyperexpress the HCV protein NS5A [27]. These results suggest that targeting of FKBP38 may be beneficial in HCV-associated hepatocellular carcinoma.

Targeting of FKBP51 with rapamycin or siRNA sensitizes poor-responsive human melanoma cells to anthracyclin-triggered apoptosis by antagonizing the induction of the anti-apoptotic genes Bcl-2 and c-IAP1 under NF-κB transcriptional control [24]. In addition, FKBP51 targeting enhances the

cytotoxic effect of ionizing radiation in the same tumor [33]. Of greater interest, FKBP51 is expressed at high levels in melanoma cancer stem/initiating cells [33]. These cells are recognizable by the presence of surface markers, including the ATP-binding cassette transporters ABCB5 and ABCG2 [66]. Apparently, melanoma cancer stem cells are killed by ionizing radiation after pre-treatment with FKBP51 siRNA [33], suggesting that FKBP51 may be a suitable target for eliminating such cells responsible for self renewal and recurrence of the tumor. The efficacy of FKBP51 targeting against melanoma has also been documented *in vivo* in a melanoma xenograft mouse model [33]. In addition, targeting of FKBP51 is associated with enhanced apoptosis and reduced proliferation in gliomas [30]. In acute lymphoblastic leukemia, inhibition of FKBP51 overcomes resistance to anthracyclin compounds [25]. In prostate cancer, targeting of FKBP51 dramatically decreases androgen receptor transcriptional activity and tumor growth [32].

Conclusion

FKBPs perform multiple biological functions through specific protein–protein interactions and by acting as chaperones [1, 2]. The molecular interaction with receptors [31, 32], kinases [24, 25, 28, 33], or other proteins [23, 26, 27] that take part in apoptotic signaling cascades also implicates members of this protein family in regulation of programmed cell death [23-33]. Apoptosis plays a crucial role in the control of tissue homeostasis, and defective cell death mechanisms are known to lead to cancer [67]. Furthermore, most cytotoxic anticancer agents induce apoptosis, thus raising the possibility that defects in apoptotic programs contribute to treatment failure [67]. There is much hope for the potential of signaling therapies against cancer, and a greater understanding of the molecular pathways of apoptosis and the causes of their malfunction in cancer is expected to provide new therapeutic targets that may lead to breakthroughs in cancer treatment [68]. Evidence of elevated levels of some FKBP members in tumors [30, 32, 33, 69-71], together with a clear apoptosis sensitizing effect of FKBP inhibition [23-27, 30-33], point to this class of proteins as possible novel targets for cancer therapy. Further studies on the role of this class of proteins in apoptosis dysfunction in cancer may open the door in the near future to developing novel small molecules specifically targeting FKBP. This approach can be achieved by structural studies of FKBP and its partners in apoptotic processes.

List of abbreviations:

Bcl-2 B-cell lymphoma 2, **BH** Bcl-2 homology, **CaN** calcineurin, **CLL** chronic lymphocytic leukemia, **FKBP** FK506 binding protein, **HCV** hepatitis C virus, **IAP** inhibitor of apoptosis, **IKK** Inhibitor κB kinase, **mTOR** mammalian target of rapamycin, **NF-κB** nuclear factor of κ light-chain-enhancer of activated B cells, **PS** presenilins, **TβR-I** transforming growth factor-β type I receptor, **TβR-II** transforming growth factor-β type II receptor, **TGF-β** transforming growth factor-β.

References

[1]   Dornan, J.; Taylor, P.; Walkinshaw, M.D. Structures of Immunophilins and their Ligand Complexes. Curr. Top. Med. Chem., 2003, 3(12), 1392-1409.

[2]   Kang, C.B.; Hong, Y.; Dhe-Paganon, S.; Yoon, H.S. FKBP family proteins: immunophilins with versatile biological functions. Neurosignals, 2008, 16(4), 318-325.

[3]   Siekierka, J.J.; Hung, S.H.; Poe, M.; Lin, C.S.; Sigal, N.H. A cytosolic binding protein for the immunosuppressant FK506 has peptidyl-prolyl isomerase activity but is distinct from cyclophilin. Nature, 1989, 341(6244), 755-757.

[4]   Standaert, R.F.; Galat, A.; Verdine, G.L.; Schreiber, S.L. Molecular cloning and overexpression of the human FK506-binding protein FKBP. Nature, 1990, 346(6285), 671-674.

[5]   Fischer, G.; Aumüller, T. Regulation of peptide bond cis/trans isomerization by enzyme catalysis and its implication in physiological processes. Rev. Physiol. Biochem. Pharmacol., 2003, 148, 105-150. Review.

[6]   Abraham, R.T.; Wiederrecht, G.J. Immunopharmacology of rapamycin. Annu. Rev. Immunol., 1996, 14, 483-510.

[7]   Rao, A.; Luo, C.; Hogan, P.G. Transcription factors of the NFAT family: Regulation and function. Annu. Rev. Immunol., 1997, 15, 707-747.

[8]   Sabatini, D.M.; Erdjument-Bromage, H.; Lui, M.; Tempst, P.; Snyder, S.H. RAFT1: a mammalian protein that binds to FKBP12 in a rapamycin-dependent fashion and is homologous to yeast TORs. Cell, 1994, 78, 35-43.

[9]   Choi, J.; Chen, J.; Schreiber, S.L.; Clardy, J. Structure of the FKBP12-rapamycin complex interacting with the binding domain of human FRAP. Science, 1996, 273(5272), 239-42.

[10]   Schmelzle, T.; Hall, M.N. TOR, a central controller of cell growth. Cell, 2000, 103(2), 253-262.

[11]   Jauliac, S.; López-Rodriguez, C.; Shaw, L.M.; Brown, L.F.; Rao, A., Toker, A. The role of NFAT transcription factors in integrin-mediated carcinoma invasion. Nat. Cell. Biol., 2002, 4(7), 540-544.

[12]   Müller, M.R.; Rao, A. Linking calcineurin activity to leukemogenesis. Nat. Med., 2007, 13(6), 669-671.

[13]   Hennessy, B.T.; Smith, D.L.; Ram, P.T.; Lu, Y.; Mills, G.B. Exploiting the PI3K/AKT pathway for cancer drug discovery. Nat. Rev. Drug. Disc., 2005, 4(12), 988-1004.

[14]   Bjornsti, M.A.; Houghton, P.J. The Tor pathway: a target for cancer therapy. Nat. Canc. Rev., 2004, 4, 335-348.

[15]   Neshat, M.S.; Mellinghoff, I.K.; Tran, C.; Stiles, B.; Thomas, G.; Petersen, R.; Frost, P.; Gibbons, J.J.; Wu, H.; Sawyers, C.L. Sensitivity of PTEN-deficient tumors to inhibition of FRAP/mTOR. Proc. Natl. Acad. Sci. USA., 2001, 98(18), 10314-10319.

[16]   Siamakpour-Reihani, S.; Bandhu-Nepal, D.; Courtwright, A.; Hilliard, E.; Ketelsen, D.; Patterson, C.; Klauber-DeMore N. The calcineurin inhibitor tacrolimus inhibits breast tumor growth in vivo. Cancer Res., 2009, 69 (24 Suppl), Abstract nr 3170.

[17]   Neshat, M.S.; Mellinghoff, I.K.; Tran, C.; Stiles, B.; Thomas, G.; Petersen, R.; Frost, P.; Gibbons, J.J.; Wu, H.; Sawyers, C.L. Sensitivity of PTEN-deficient tumors to inhibition of FRAP/mTOR. Proc. Natl. Acad. Sci. USA., 2001, 98(18), 10314-10319.

[18]   Maestre-Martínez, M.; Edlich, F.; Jarczowski, F.; Weiwad, M.; Fischer, G.; Lücke, C. Solution structure of the FK506-binding domain of human FKBP38. J. Biomol. NMR., 2006, 34(3), 197-202.

[19]   Cameron, A.M.; Steiner, J.P.; Sabatini, D.M.; Kaplin, A.I.; Walensky, L.D.; Snyder, S.H. Immunophilin FK506 binding protein associated with inositol 1,4,5-trisphosphate receptor modulates calcium flux. Proc. Natl. Acad. Sci. USA., 1995, 92(5), 1784-1788.

[20]   Lu, K.P.; Finn, G.; Lee, T.H.; Nicholson, L.K. Prolyl cis-trans isomerization as a molecular timer. Nat. Chem. Biol., 2007, 3(10), 619-629.

[21]   Nelson, C.J.; Santos-Rosa, H.; Kouzarides, T. Proline isomerization of histone H3 regulates lysine methylation and gene expression. Cell, 2006, 126(5), 905-916.

[22]   Wang, T.; Li, B.Y.; Danielson, P.D.; Shah, P.C.; Rockwell, S.; Lechleider, R.J.; Martin, J.; Manganaro, T.; Donahoe, P.K. The immunophilin FKBP12 functions as a common inhibitor of the TGF beta family type I receptors. Cell, 1996, 86(3), 435-44.

[23]   Shirane, M.; Nakayama, K.I. Inherent calcineurin inhibitor FKBP38 targets Bcl-2 to mitochondria and inhibits apoptosis. Nat. Cell. Biol., 2003, 5(1), 28-37.

[24]   Romano, M.F.; Avellino, R.; Petrella, A.; Bisogni, R.; Romano, S.; Venuta, S. Rapamycin inhibits doxorubicin-induced NF-kappaB/Rel nuclear activity and enhances the apoptosis of melanoma cells. Eur. J. Cancer. 2004, 40(18), 2829-2836.

[25]   Avellino, R.; Romano, S.; Parasole, R.; Bisogni, R; Lamberti, A.; Poggi, V.; Venuta, S.; Romano, M.F. Rapamycin stimulates apoptosis of childhood acute lymphoblastic leukemia cells. Blood, 2005, 106(4), 1400-1406.

[26]   Wang, H.Q.; Nakaya, Y.; Du, Z.; Yamane, T.; Shirane, M.; Kudo, T.; Takeda, M.; Takebayashi, K.; Noda, Y.; Nakayama, K.I.; Nishimura, M. Interaction of presenilins with FKBP38 promotes apoptosis by reducing mitochondrial Bcl-2. Hum. Mol. Genet., 2005, 14(13), 1889-1902.

[27]   Wang, J.; Tong, W.; Zhang, X.; Chen, L.; Yi, Z.; Pan, T.; Hu, Y.; Xiang, L.; Yuan, Z. Hepatitis C virus non-structural protein NS5A interacts with FKBP38 and inhibits apoptosis in hepatoma cells. FEBS Lett., 2006, 580(18), 4392-4400.

[28]   Giordano, A.; Avellino, R.; Ferraro, P.; Romano, S.; Corcione, N.; Romano, M.F. Rapamycin antagonizes NF-kappaB nuclear translocation activated by TNF-alpha in primary vascular smooth muscle cells and enhances apoptosis. Am. J. Physiol. Heart. Circ. Physiol., 2006, 290(6), H2459-65.

[29]   Romano, M.F.; Romano, S.; Mallardo, M.; Bisogni, R.; Venuta, S. In: Rapamycin controls multiple signalling pathways involved in cancer cell survival. Cell Apoptosis Research Trends. Nova Publishers, ED.; 2007, 263-276, 40(18), 2829-2836.

[30]   Jiang, W.; Cazacu, S.; Xiang, C.; Zenklusen, J.C.; Fine, H.A.; Berens, M.; Armstrong, B.; Brodie, C.; Mikkelsen, T. FK506 binding protein mediates glioma cell growth and sensitivity to rapamycin treatment by regulating NF-kappaB signaling pathway. Neoplasia, 2008, 10(3), 235-243.

[31]   Romano, S.; Mallardo, M.; Chiurazzi, F.; Bisogni, R.; D'Angelillo, A.; Liuzzi, R.; Compare, G.; Romano, M.F. The effect of FK506 on transforming growth factor beta signaling and apoptosis in chronic lymphocytic leukemia B cells. Haematologica, 2008, 93(7), 1039-1048.

[32]   Periyasamy, S.; Hinds, T.Jr.; Shemshedini, L.; Shou, W.; Sanchez, E.R. FKBP51 and Cyp40 are positive regulators of androgen-dependent prostate cancer cell growth and the targets of FK506 and cyclosporin A. Oncogene, 2010, 29(11), 1691-1701.

[33]   Romano, S.; D'Angelillo, A.; Pacelli, R.; Staibano, S.; De Luna, E.; Bisogni, R.; Eskelinen, E.L.; Mascolo, M.; Calì, G.; Arra, C.; Romano, M.F. Role of FK506-binding protein 51 in the control of apoptosis of irradiated melanoma cells. Cell. Death. Differ. 2010, 17(1), 145-57.

[34]   Massague, J. How cells read TGF-beta signals. Nat. Rev. Mol. Cell. Biol., 2000, 1(3), 169-178. Review.

[35]   Massague, J.; Blain, S.W. TGF beta signaling in growth control, cancer, and heritable disorders. Cell, 2000, 103, 295-309. Review.

[36]   Siegel, P.M.; Massague, J. Cytostatic and apoptotic actions of TGF-beta in homeostasis and cancer. Nat. Rev. Cancer., 2005, 3(11), 807-821. Review.

[37]   Jang, C.W.; Chen, C.H.; Chen, C.C.; Chen, J.Y.; Su, Y.H.; Chen, R.H. TGF-beta induces apoptosis through Smad-mediated expression of DAP-kinase. Nat. Cell. Biol., 2001, 4(1), 51-58.

[38]   Perlman, R.; Schiemann, W.P.; Brooks, M.W.; Lodish, H.F.; Weinberg, R.A. TGF-beta-induced apoptosis is mediated by the adapter protein Daxx that facilitates JNK activation. Nat. Cell. Biol., 2001, 3(8), 708-714.

[39]   Chaouchi, N.; Arvanitakis, L.; Auffredou, M.T.; Blanchard, D.A.; Vazquez, A.; Sharma, S. Characterization of transforming growth factor-beta 1 induced apoptosis in normal human B cells and lymphoma B cell lines. Oncogene, 1995, 11(8), 1615-1622.

[40]   Lucas, P.J.; McNeil, N.; Hilgenfeld, E.; Choudhury, B.; Kim, S.J.; Eckhaus, M.A.; Ried, T.; Gress, R.E. Transforming growth factor-beta pathway serves as a primary tumor suppressor in CD8+ T cell tumorigenesis. Cancer Res., 2004, 64(18), 6524-6529.

[41]   Wolfraim, L.A.; Fernandez, T.M.; Mamura, M.; Fuller, W.L.; Kumar, R.; Cole, D.E.; Byfield, S.; Felici, A.; Flanders, K.C.; Walz, T.M.; Roberts, A.B.; Aplan, P.D.; Balis, F.M.; Letterio, J.J. Loss of Smad3 in acute T-cell lymphoblastic leukemia N. Engl. J. Med., 2004, 351(6), 552-559.

[42]   Chen, Y.G.; Liu, F.; Massague, J. Mechanism of TGFbeta receptor inhibition by FKBP12. EMBO J., 1997, 16(13), 3866-3876.

[43]   Li, X.; Greenwald, I. Membrane Topology of the C. elegans SEL-12 Presenilin. Neuron, 1996, 17(5), 1015-1021.

[44]   St. George-Hyslop, P.H. Molecular genetics of Alzheimer's disease. Biol. Psychiatry, 47(3), 183-199.

[45]   Liu, T.M.; Martina, M.; Hutmacher, D.W.; Hui, J.H.; Lee, E.H.; Lim, B. Identification of common pathways mediating differentiation of bone marrow- and adipose tissue-derived human mesenchymal stem cells into three mesenchymal lineages. Stem cells, 2007, 25(3), 750-760.

[46]   Menicanin, D.; Bartold, P.M.; Zannettino, A.C.; Gronthos, S. Genomic profiling of mesenchymal stem cells. Stem Cell Rev., 2009, 5(1), 36-50. Review.

[47]   Yeh, W.C.; Li, T.K.; Bierer, B.E. McKnight, S.L. Identification and characterization of an immunophilin expressed during the clonal expansion phase of adipocyte differentiation. Proc. Natl. Acad. Sci. USA., 1995, 92(24), 11081-11085.

[48]   Karin, M.; Cao, X.; Greten, F.R.; Li, Z.W. NF-kappaB in cancer: from innocent bystander to major culprit. Nat. Rev. Cancer, 2002, 2(4), 301-310.

[49]   Roy, N.; Deveraux, Q.L.; Takahashi, R.; Salvesen, G.S.; Reed, J.C. The c-IAP-1 and c-IAP-2 proteins are direct inhibitors of specific caspases. EMBO J., 1997, 16(23), 6914–6925.

[50]   Thome, M.; Schneider, P.; Hofmann, K.; Fickenscher, H.; Meinl, E.; Neipel, F.; Mattmann, C.; Burns, K.; Bodmer, J.L.; Schroter, M.; Scaffidi, C.; Krammer, P.H.; Peter, M.E.; Tschopp, J. Viral FLICE-inhibitory proteins (FLIPs) prevent apoptosis induced by death receptors. Nature, 1997, 386(6624), 517-520.

[51]   Wang, C.Y.; Guttridge, D.C.; Mayo, M.W.; Baldwin, A.S.Jr. NF-κB Induces Expression of the Bcl-2 Homologue A1/Bfl-1 To Preferentially Suppress Chemotherapy-Induced Apoptosis. Mol. Cell. Biol., 1999, 19(9), 5923-5929.

[52]   Rothe, M.; Wong, S.C.; Henzel, W.J.; Goeddel, D.V. A novel family of putative signal transducers associated with the cytoplasmic domain fo the 75 kDa tumor necrosis factor receptor. Cell, 1994, 78, 681-692.

[53]   Bouwmeester, T.; Bauch, A.; Ruffner, H.; Angrand, P.O.; Bergamini, G.; Croughton, K.; Cruciat, C.; Eberhard, D.; Gagneur, J.; Ghidelli, S.; Hopf, C.; Huhse, B.; Mangano, R.; Michon, A.M.; Schirle, M.; Schlegl, J.; Schwab, M.; Stein, M.A.; Bauer, A.; Casari, G.; Drewes, G.; Gavin, A.C.; Jackson, D.B.; Joberty, G.; Neubauer, G.; Rick, J.; Kuster, B.; Superti-Furga, G. A physical and functional map of the human TNF-alpha/NF-kappaB signal transduction pathway. Nat. Cell. Biol., 2004, 6, 97-105.

[54]   Kawai, M.; Lane, B.C.; Hsieh, G.C.; Mollison, K.W.; Carter, G.W.; Luly, J.R. Structure-activity profiles of macrolactam immunosuppressant FK-506 analogues. FEBS Lett., 1993, 316(2), 107-113.

[55]   Liu, J.; Albers, M.W.; Wandless, T.J.; Luan, S.; Alberg, D.G.; Belshaw, P.J.; Cohen, P.; MacKintosh, C.; Klee, C.B.; Schreiber, S.L. Inhibition of T cell signaling by immunophilin-ligand complexes correlates with loss of calcineurin phosphatase activity. Biochemistry, 1992, 31(16), 3896-3901.

[56]   Elliot, R.L.; Blobe, G.C. Role of transforming growth factor-β in human cancer. J. Clin. Oncol., 2005, 23(9), 2078-2093.

[57]   Arteaga, C.L. Inhibition of TGFβ signaling in cancer therapy. Curr. Opin. Genet. Dev., 2006. 16(1), 30-37.

[58]   Massagué, J. TGFβ in cancer. Cell, 2008, 134(2), 215-230.

[59]   Romano, M.F. Targeting TGFbeta-mediated processes in cancer. Curr. Opin. Drug. Discov. Devel., 2009, 12(2), 253-63. Review.

[60]   Dong, M.; Blobe, G.C. Role of transforming growth factor-beta in hematologic malignancies. Blood, 2006, 107(12), 4589-4596.

[61]   Bierie, B.; Moses, H.L. Tumour microenvironment: TGFβ: The molecular Jekyll and Hyde of cancer. Nat. Rev. Cancer., 2006, 6(7), 506-520.

[62]   Stoika, R.; Yakymovych, M.; Souchelnytskyi, S.; Yakymovych, I. Potential role of transforming growth factor beta1 in drug resistance of tumor cells. Acta. Biochem. Pol., 2003, 50(2), 497-508.

[63]   Di Bisceglie, A.M. Hepatitis C. Lancet, 1998, 351(9099), 351-355.

[64]   Shimotohno, K. Hepatitis C virus as a causative agent of hepatocellular carcinoma. Intervirology, 1995, 38(3-4), 162-169.

[65]   Coussens, L.M.; Werb, Z. Inflammation and cancer. Nature, 2002, 420(6917), 860-867.

[66]   Zhou, S.; Schuetz, J.D.; Bunting, K.D.; Colapietro, A.M.; Sampath, J.; Morris, J.J.; Lagutina, I.; Grosveld, G.C.; Osawa, M.; Nakauchi, H.; Sorrentino, B.P. The ABC transporter Bcrp1/ABCG2 is expressed in a wide variety of stem cells and is a molecular determinant of the side-population phenotype. Nat. Med., 2001, 7(9), 1028-1034.

[67]   Brown, J.M.; Attardi, L.D. The role of apoptosis in cancer development and treatment response. Nat. Rev. Cancer., 2005, 5(3), 231-237.

[68]   Ghobrial, I.M.; Witzig, T.E.; Adjei, A.A. Targeting Apoptosis Pathways in Cancer Therapy. Cancer J. Clin., 2005, 55,178-194.

[69]   Khatua, S.; Peterson, K.M.; Brown, K.M.; Lawlor, C.; Santi, M.R.; LaFleur, B.; Dressman, D.; Stephan, D.A.; MacDonald, T.J. Overexpression of the EGFR/FKBP12/HIF-2alpha pathway identified in childhood astrocytomas by angiogenesis gene profiling. Cancer Res., 2003, 63(8), 1865-1870.

[70]   Olesen, S.H.; Christensen, L.L.; Sørensen, F.B.; Cabezón, T.; Laurberg, S.; Orntoft, T.F.; Birkenkamp-Demtröder, K. Human FK506 binding protein 65 is associated with colorectal cancer. Mol. Cell. Proteomics., 2005, 4(4), 534-544.

[71]   Romano, S.; D'Angelillo, A.; Staibano, S.; Ilardi, G.; Romano, M.F. FK506-binding protein 51 is a possible novel tumoral target. Cell. Death. Dis., 2010, Published online 15 July 2010.
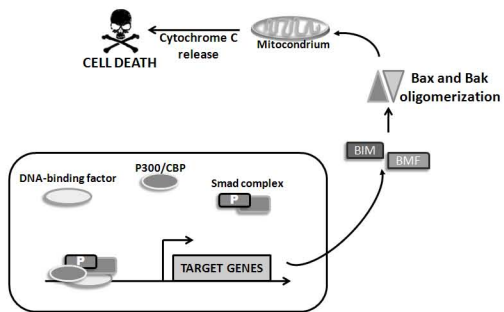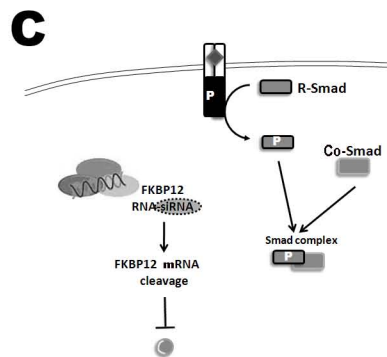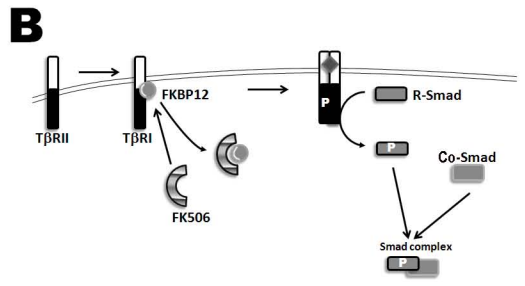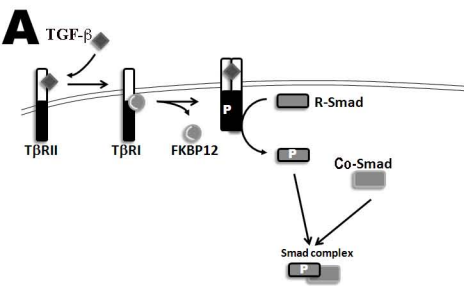
Legends to the figures
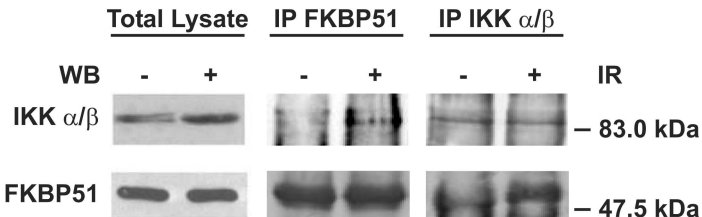
Fig. 1 **Schematic representation of TGF-β signal**. (A) TGF-β binds a specific pair of membrane receptors, type I (TβR1) and type II (TβR2), that contain a cytoplasmic serine–threonine kinase domain. This binding results in the formation of a TβR1/TβR2 heteromeric complex and activation of TβR2 kinase. Activated TβR1 specifically recognizes and phosphorylates signaling molecules that act on downstream receptors, namely R-Smad, which form a complex with other Smad molecules (Co-Smad). This complex translocates into the nucleus and can activate transcription of genes involved in mitochondrial apoptosis. (B) Activation of TβR1 requires phosphorylation of the GS (glycine, serine) region by TβR2. Under basal conditions, this region is capped by FKBP12, blocking the signal progression. FK506 displaces the immunophilin from the GS region, thus permitting TGF-β signaling in the absence of ligand. (C) Activation of such a signal can also be achieved by knocking down FKBP12 with specific siRNA that targets the FKBP12 mRNA, leading to RNA degradation and reduced protein levels.

Fig. 2 **FKBP51 controls ionizing radiation–induced NF-κB activation in melanoma.** (A) FKBP51/IKK interaction in melanoma cells. Whole cell lysates of melanoma SAN cell line [24, 33], not irradiated and 3 h after irradiation with 4 Gy, were prepared by homogenization in modified RIPA buffer. After obtaining a homogeneous suspension, protein concentration was determined and 500 μg of protein extract was precleared for 1 h. For immunoprecipitation, 15 μg anti-FKBP51 or anti-IKKα/β were added together with 25 μL protein A-Sepharose, and precipitation took place overnight with rotation at 4°C. Immunoprecipitated and total lysates were then separated by a SDS/polyacrylamide gel electrophoresis, transferred onto a membrane filter, and incubated with goat polyclonal anti-FKBP51 or rabbit anti-IKKα/β. The immunoprecipitation assay result, that was confirmed in another independent experiment, suggests that FKBP51 directly interacts with IKKα/β after exposure to ionizing radiation (IR), thus activating NF-κB transcriptional factors. (B) Western blot assay of IκBα and phospho-IκBα levels. At 48 h from transfection, melanoma cells were irradiated at 4 Gy and harvested at the indicated times. Cytosolic extracts were obtained from melanoma SAN cells transfected with FKBP51 siRNA or a non silencing (NS) RNA as control, by homogenization in lysing buffer. Cytosolic lysates were then separated using SDS-PAGE gel and transferred onto a membrane filter that was incubated with rabbit

polyclonal anti-IKKα/β and anti–phospho-IKKα/β. These results suggest that in irradiated cells, FKBP51 downmodulation blocks IκBα phosphorylation and degradation, thus avoiding NF-κB activation.

Fig. 3 **Targeting of FKBP12 causes apoptosis of CLL cells**. CLL cells, isolated from heparinized blood, were cultured with FK506, FK520, 15-O-DES-FK520, and 18-OH-FK520 at a dose of 100 nM and cyclosporine at a dose of 300 nM. After 24 h, cells were harvested, and phosphatidylserine externalization was investigated by annexin V-FITC staining. Then cells were analyzed by flow cytometry. Numbers reported in the dot plots represent the percentages of FITC-positive cells. Increased annexin V binding was observed in samples cultured with FK506 or its analogs and not with cyclosporine.

A

	Total Lysate	IP FKBP51	IP IKK α/β
WB	− +	− +	− + IR

IKK α/β — 83.0 kDa

FKBP51 — 47.5 kDa

B

| | 0 | 4 | 6 | 0 | 4 | 6 | h |

IκBα

p-IκB

actin

NSRNA   FKBP51 siRNA

None	FK506	Cyclosporin
14	43	14
FK520	15-O-DES-FK520	18-OH-FK520
47	49	45

counts

Annexin V